Screening Whole-Genome Sequenced Strains to Investigate Genetic Determinants of Gentle Touch Sensitivity in *Caenorhabditis elegans*

Stephanie Terese Lawry

Submitted in partial fulfillment of the
requirements for the degree of
Doctor of Philosophy
under the Executive Committee
of the Graduate School of Arts and Sciences

COLUMBIA UNIVERSITY

2020

Abstract

Screening Whole-Genome Sequenced Strains to Investigate Genetic Determinants of Gentle Touch Sensitivity in *Caenorhabditis elegans*

Stephanie Terese Lawry

Genetic screens have laid much of the groundwork for our current understanding of biology, and mutagenesis screens in *Caenorhabditis elegans* have proven to be a particularly useful tool in determining the molecular components of biological processes. The Million Mutation Project (MMP) is a collection of mutagenized *C. elegans* strains that have been clonally propagated and whole-genome sequenced. Utilizing the MMP, I have performed a screen for touch insensitive mutants to assess the phenotypic coverage of the set, to obtain new alleles of known genes, and to potentially identify touch phenotype-causing mutations in genes that have not yet been linked to the touch response.

In this thesis I first present my rationale for screening the MMP set for touch phenotypes, then review what has already been learned about genes required for the function of the neurons that sense gentle touch in *C. elegans*. I describe my approach to phenotyping the MMP set and present statistics on response distributions. As expected, most of the MMP strains that I determined to have strong touch insensitive phenotypes had mutations in genes identified in previous touch phenotype mutageneses. However, some of the phenotype-causing MMP alleles cause protein-coding changes in regions that were not known to be affected by previously characterized alleles. The genomic data from the MMP also allowed me to consider protein-altering mutations in known touch genes that did not result in a detectable phenotype. Finally, I address the set of strains for which we have not identified candidate causative mutations.

Although I have not discovered any previously unknown touch genes through my screen of the MMP, it is still quite possible that the touch insensitive mutants I have identified will lead us to identify additional genes needed for gentle touch sensation. Ultimately, my screen has successfully demonstrated the utility of the MMP set and provided new insights as to the structure and function of the genetic determinants of gentle touch sensation in *C. elegans*.

Table of Contents

List of Tables and Figures

Acknowledgments

I thank my advisor Martin Chalfie, first for welcoming me to come work in his lab and also for the great deal of freedom he has allowed me in my day to day work. Mistakes were made, mostly by me, but I'm glad to have been able to make them and am grateful for Marty's trust in my abilities. Of course, I also thank him for his guidance and assistance, particularly in conceiving the project presented here.

I thank my thesis committee members that have been working with me since my qualifying exam, Oliver Hobert and Stuart Firestein. In addition to the supervision and recommendations they have given me throughout my graduate work, I appreciate the time they have invested in me.

I am grateful to the past and present Chalfie lab members who have assisted me. I thank former lab members Xiaoyin Chen for helping get oriented in the lab during my rotation and Chaogu Zheng for often being the person most likely to have a helpful answer. I thank Matt Walker for his work in performing complementation tests, and Hieu Hoang for help in performing injections. I would also like to thank Francess Kamara for helping with freezing of strains and Ana Maria for her fundamental role in organizing the lab.

I thank Chi Chen in Oliver Hobert's lab for the injections she performed, and other Hobert lab members for their assistance with tools and reagents. Thank you to the Piano and Gunsalus lab at NYU for providing the Chalfie lab with Million Mutation Project stocks, and to Mark Edgley for organizing the distribution of most of the Million Mutation Project stocks.

Finally, I would like to thank my husband Jacob for all his support and advice.

Chapter 1: Introduction

1.1 Strategies for Genetic Screening

Establishing relationships between genotypic and phenotypic variations has proven to be a powerful approach to developing our understanding of biological processes. Historically, the identification of heritable phenotypic variations has usually been the first step in linking genotype and phenotype. The earliest genetic studies of this sort relied on the isolation of rare phenotypes caused by spontaneously generated mutations, but systematized genetic screens only became possible after the discovery of environmentally induced mutations (St Johnston, 2002). The *Drosophila* geneticist H. J. Muller was among the first to demonstrate high-energy radiation mutagenesis in 1927 (Muller, 1927), and soon afterwards the technique was being applied across a variety of organisms for the purpose of genetic analysis. Chemical mutagenesis was subsequently developed, with the first successful demonstrations utilizing mustard gas and formaldehyde (Auerbach and Robson, 1946; Rapoport, 1946). Today, the more commonly utilized chemical mutagens are the alkylating agents ethyl methanesulfonate (EMS) and N-ethyl-N-nitrosourea (ENU). These mutagens have proven to provide a workable balance between potency (fewer mutant animals can be screened for phenotypes if each animal carries more mutations) and lethality/sterility (animals that cannot survive and/or reproduce are not amenable to genetic analysis) (Probst and Justice, 2010; Kutscher and Shaham, 2014; Venken and Bellen, 2014). A third method of mutagenesis was developed following the discovery of transposons by Barbara McClintock in the 1940's (McClintock, 1950; Kleckner et al., 1977; Jones, 2005). While genetic alterations caused by transposon activity are less random and significantly more rare than

those induced by radiation or chemical mutagens, they are easier to identify and are more likely to disrupt protein function (Bessereau, 2006).

Mutagenesis screens have been very extensively and successfully utilized in *Caenorhabditis elegans*, *Drosophila melanogaster*, and *Arabidopsis thaliana*. In the first *C. elegans* EMS mutagenesis screens, Sydney Brenner identified 619 mutants with readily visible phenotypes, including animals with uncoordinated movement, abnormal body proportions, blistered cuticles, and misshapen heads (Brenner, 1974). Brenner's 1974 paper reporting on these screens and subsequent initial analyses proved to be the landmark publication that established *C. elegans* as a model organism. Not long after, *Drosophila* geneticists Christiane Nüsslein-Volhard and Eric Wieschaus published the results of their mutagenesis screen for defects in embryonic development, which later earned them a Nobel Prize (Nusslein-Volhard and Wieschaus, 1980; Jurgens et al., 1984; Nusslein-Volhard et al., 1984; Wieschaus et al., 1984). The screen conducted by Nüsslein-Volhard and Wieschaus, often referred to as the Heidelberg screen after the university town where it was performed, is considered to be the first saturation screen (a screen attempting to identify all genes that can be mutated to give a particular phenotype) completed in *Drosophila* (St Johnston, 2002; Wieschaus and Nüsslein-Volhard, 2016). The most bountiful mutagenesis screens to further our understanding of plant biology have utilized *Arabidopsis thaliana* (Koornneef and Meinke, 2010). While the technique for mutagenizing the flowering plant *Arabidopsis thaliana* was first described in the 1940's, the species did not become a popular model organism until the early 1980's. The eventual widespread adoption of *A. thaliana* as a plant model was in part due to the relatively increased likelihood of achieving saturation in mutagenesis screens utilizing the species (Meyerowitz, 2001). Among higher plants, *A. thaliana* has one of the smallest known genomes with the fewest repetitive sequences.

Therefore, the chances of obtaining marked phenotypic changes through mutagenesis are increased, and map-based cloning is simplified (Page and Grossniklaus, 2002).

Genetic screens are often categorized as either “forward” or “reverse” depending on whether the steps of analysis go from phenotype to genotype or from genotype to phenotype. The mutagenesis screens I have hereto described are considered forward screens, since mutagenized animals are selected on the basis of their phenotype before being genetically characterized. Alternatively, geneticists can obtain animals with known genotypes and test them for phenotypes in reverse genetic approaches. The last few decades have provided many spectacular new tools for performing reverse genetics, including the discovery of RNAi knockdown (Fire et al., 1998) and the development of targeted genome editing techniques, most notably the CRISPR-Cas9 system which allows genomic changes to be made with unprecedented ease and precision (Jinek et al., 2012; Doudna and Charpentier, 2014).

Reverse screens can be advantageous in that they allow for investigation of a smaller subset of candidate genes. Forward mutagenesis screens are by nature untargeted, so that alleles of known phenotype-causing genes are just as likely to be identified in any given round of screening. Reverse genetics can accelerate the process of gene discovery by targeting genes that have not already been characterized. Furthermore, reverse genetic screens using RNAi have the major advantage of allowing the study of genes that result in lethal or sterile phenotypes when mutated. Although RNAi knockdown can also induce lethal and sterile phenotypes, strategically timed knockdown of essential genes can allow animals to develop and reproduce as normal (Calixto et al., 2010b). However, incomplete knockdown by RNAi is at times a disadvantage, since the reduction in gene expression might not be enough to result in a detectable phenotype (Fraser et al., 2000). RNAi knockdown may also be associated with off-target effects, meaning

that resulting phenotypes might not be due to knockdown of the intended target (Echeverri et al., 2006).

Genetic screens can also be performed to study interactions between genes by applying either forward or reverse genetic screening techniques to previously characterized mutant animals. In this way, mutations that either suppress or enhance a mutant phenotype can be identified. Modifier screens can reveal functional relationships between proteins and identify the roles for genes that do not mutate to cause phenotypes in wild-type backgrounds (Jorgensen and Mango, 2002; St Johnston, 2002). They have proved especially useful for determining the components of signaling pathways (Wang and Sherwood, 2011; Mackay, 2014).

Approaches to genetic screening often depend on the qualities of the organism being utilized. To give some examples, yeast are particularly amenable to high-throughput library screening in which a collection of identified mutants are exposed to a particular treatment due to the ease of storing and treating strains in 96-well plates (Cohen and Schuldiner, 2011). RNAi screens are commonly used by both *C. elegans* and *Drosophila* geneticists, but systemic RNAi is more commonly used for screens in *C. elegans* whereas tissue-specific RNAi is more common in *D. melanogaster* (Mohr et al., 2014). Forward genetic screens have historically been far less prevalent in mouse genetics, but advances in sequencing technology have improved the feasibility of such screens (Moresco et al., 2013).

1.2 *C. elegans* as a Model Organism

A number of qualities make *C. elegans* an ideal organism for use in genetic research. Some of these qualities are intrinsic to the species. *C. elegans* has a generation time of about three days when grown at 25°C, and each self-fertilizing hermaphrodite produces about 300

offspring. Their small size makes the worms very easy to culture, and they tend to be quite hardy, being able to survive in a dormant state without food for months. They can survive being frozen and thus can be kept for long-term storage with minimal maintenance. *C. elegans* have a transparent cuticle that allows for observation of internal systems, which include various tissue types and organs. Additionally, they have an invariant number of somatic cells that arise from consistent lineages (Corsi et al., 2015).

The other major advantages to working with *C. elegans* arise from our existing knowledge of its morphology, behavior, and genetics. Developmental lineages of the somatic cells are well described, which has allowed for identification of mutant animals in which developmental lineages are altered (Horvitz and Sulston, 1980; Sulston and Horvitz, 1981). The hermaphrodite nervous system contains 302 neurons of 118 neuronal classes plus 56 glial cells (Sulston, 1983), and *C. elegans* was the first organism for which all neurons and synaptic connections between them were mapped (White et al., 1986; Jarrell et al., 2012; Cook et al., 2019). Additionally, *C. elegans* was the first multicellular animal for which a complete genome sequence was published. Even with much being known about *C. elegans*, the worm is still a complex system with many mysterious features. However, existing knowledge of a system can facilitate the obtainment of further knowledge, providing context for additional observations.

A third set of advantages conferred by study of *C. elegans* is the vast amount of tools and resources available to the research community. A number of online resources exist for access to general information (WormBook), anatomical information (WormAtlas), and extensive genetic, phenotypic, and scholarly references (WormBase). Several collections of strains are available to order for research purposes, including the Caenorhabditis Genetics Center, the National Bioresource Project, and the Million Mutation Project.

1.3 The Million Mutation Project

The Million Mutation Project (MMP) is a set of 2006 whole-genome sequenced mutagenized strains (Thompson et al., 2013). It should be noted that many previous reports refer to 2007 MMP strains, but one strain (VC40667) was removed from the official set due to sequencing data discrepancies (Mark Edgley, personal communication). The set includes over 800,000 unique single nucleotide substitutions and over 16,000 indels and chromosomal rearrangements. Although the majority of these mutations do not affect protein coding regions, the set includes about 183,000 protein-affecting mutations in over 19,000 genes. Considering that the *C. elegans* genome contains about 20,000 protein-coding genes, the mutational coverage of the MMP is quite remarkable. With the exception of strong alleles (nonsense, frameshift, or splice site mutations) affecting essential genes, the MMP strains contain mutations spread somewhat evenly throughout the genome (Thompson et al., 2013).

The MMP strains were generated by mutageneses followed by growth of F1 animals on 1% nicotine to allow for the selection of heterozygous *unc-22* mutants (Thompson et al., 2013). *unc-22* is a large gene with a dominant loss of function phenotype for animals grown on nicotine (Moerman and Baillie, 1979), so the selection step allowed for identification of successfully mutagenized animals that might still produce *unc-22* homozygous wild-type offspring. The *unc-22* phenotype was selected against in F2 animals to ensure that not all strains carried *unc-22* mutations, and subsequent generations were clonally propagated through F10 before being prepared for storage and sequencing (Thompson et al., 2013). The clonal propagation served to increase the number of homozygous mutant alleles that would then be stably maintained through subsequent generations (Figure 1-1).

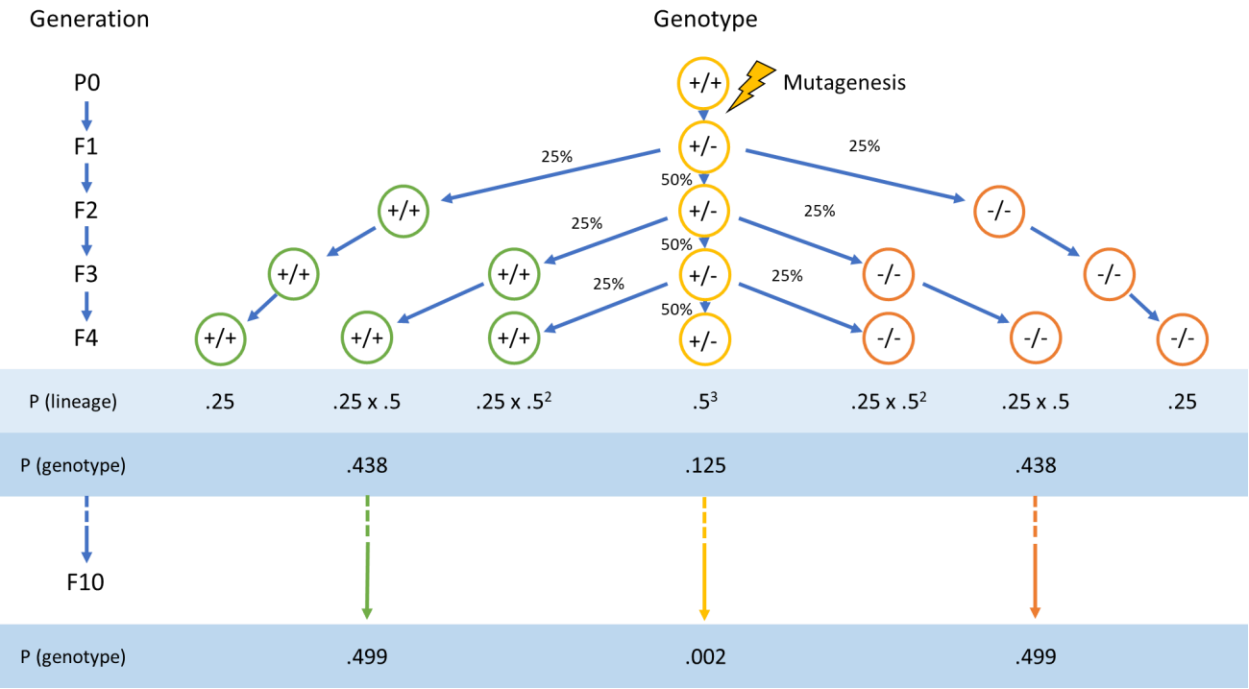

Figure 1-1: Drive to homozygosity by independent clonal propagation. If one independent lineage is maintained, by F4 about 12.5% of alleles are expected to be in the heterozygous state, and by F10 only 0.2% of alleles are expected to be in the heterozygous state.

Following clonal propagation, the MMP strains were whole-genome sequenced and mutations were identified (Thompson et al., 2013). Based on a set of alleles verified by Sanger sequencing, the MMP variant calls should have less than a 1% false positive rate. Around 5% of genome sequences had too little coverage for any variant calls to be made, and lower-coverage areas are predicted to have a false negative call rate of about 2% based on comparison of variant call frequencies between high and low coverage regions, giving a total false negative rate of about 7%. Additionally, around 25,000 of the mutations identified appeared to be present in a heterozygous state. The mutations were included among the MMP variant calls but can be distinguished by allele name: alleles numbered between gk100000 and gk962522 are

homozygous; alleles numbered gk962523 up may be non-homozygous or prone to loss by genetic drift (Thompson et al., 2013).

Genomic data from the set allowed for precise estimations of the quantity and qualities of mutations caused by treatment with different mutagens. The MMP strains were mutagenized with either UV radiation following trimethylpsoralen treatment (UV/TMP, 10 strains) or exposure to EMS (737 strains), ENU (260 strains), or a mix of both EMS and ENU (999 strains) (Thompson et al., 2013). EMS is considered to be a more potent mutagen that ENU, but is also more biased towards specific base-pair alterations (Brenner, 1974; Flibotte et al., 2010). The single-nucleotide substitution mutations in MMP strains mutagenized with EMS alone were found to be about 90% GC to AT transitions (Thompson et al., 2013). In contrast, the MMP strains mutagenized with ENU contained roughly (rounded to the nearest 5^{th}) 45% GC to AT transitions, 20% AT to GC transitions, and 35% combined transversions (GC to CG, GC to TA, AT to AT, or AT to CG). The combination of EMS and ENU not only produced more mutations, but did so in a manner that was slightly less biased towards GC to AT transitions (80% of substitutions) than EMS alone (Thompson et al., 2013). For a summary of the MMP mutation types caused by each treatment, see Figure 1-2.

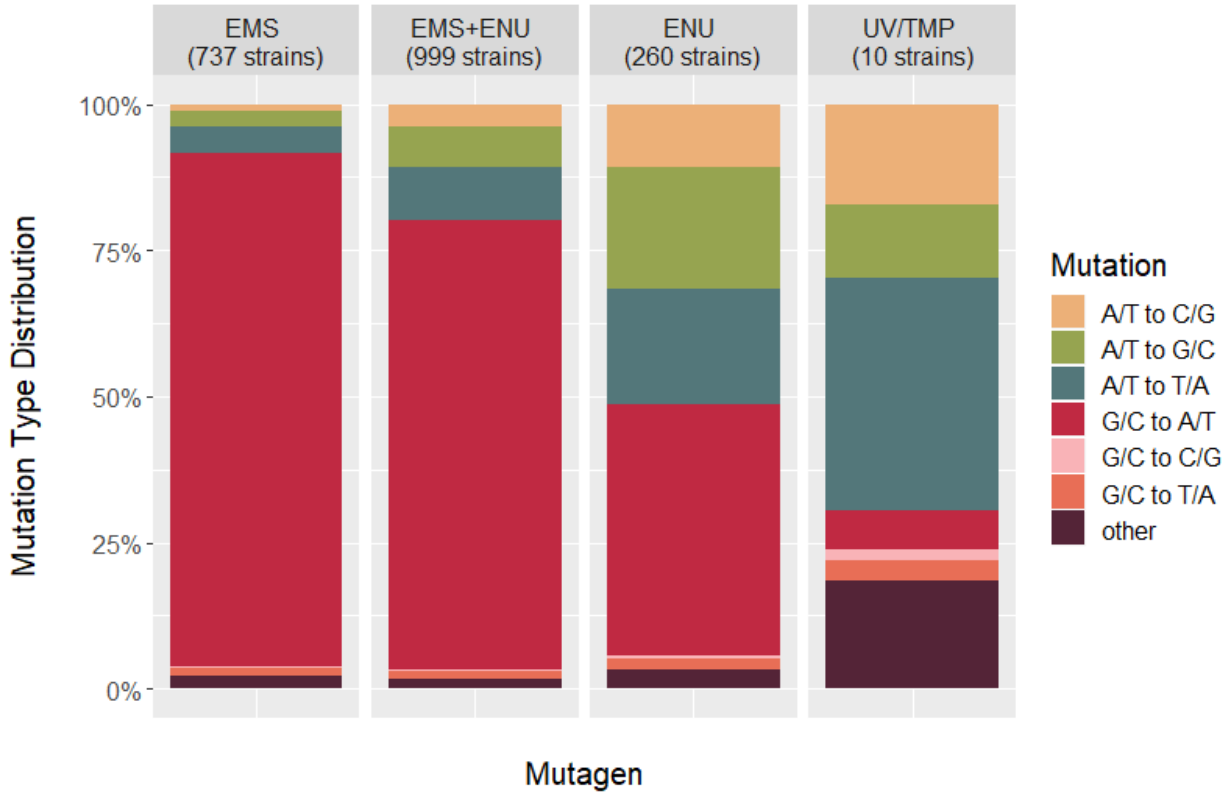

Figure 1-2: MMP mutations by mutagen and mutation type. Single-nucleotide point substitutions are grouped by wild-type to mutant base pair identity; other mutations including indels and complex substitutions are grouped together. Figure is based on the mutation dataset provided by Thompson et al. (2013).

Since the completion of the MMP, several groups have utilized the set to investigate the effects of different alleles within one or more genes of interest. After isolating anthelminthic drug-resistant strains from a forward mutagenesis and determining candidate phenotype causing genes, Mathew et al. (2016) tested MMP strains carrying mutations in candidate genes and were able to identify additional alleles conferring resistance. 20 *pink-1* (predicted serine/threonine kinase) MMP strains were tested and six of them proved to have the drug resistance phenotype. Additionally, two out of five MMP strains with *mev-1* (mitochondrial complex II subunit) mutations also gave a phenotype. The group then went on to test 26 other MMP strains with

mutations in other genes encoding subunits of the mitochondrial complex II, and found six alleles of three genes conferring drug resistance (Mathew et al., 2016).

In a report published by Bulger et al. (2017), 40 MMP alleles affecting the insulin-like receptor DAF-2 were analyzed for phenotypic effects. 35 of the alleles were found to have no effect, and 5 alleles proved to be novel dauer-enhancing mutations. The effects of all 5 phenotype-causing alleles were verified in a wild-type background through CRISPR editing. One of the phenotype-causing mutations was a missense allele affecting a region of the protein with unclear function where no previously identified *daf-2* alleles were localized to. Therefore, by testing 40 MMP strains, the group was able to confirm the importance of regions where mutations had already been mapped, confirm the lesser importance of regions where MMP mutations had no detectable effects, and identify a new region of previously unknown importance (Bulger et al., 2017).

Chen et al. (2019) utilized MMP strains for structure/function analysis of the lipid-transporting ATPase TAT-1. The group analyzed vacuolar phenotypes in 16 MMP strains carrying mutations in *tat-1*, and were surprised to find that even though most of the MMP mutations affected conserved amino acids and were predicted to be deleterious by bioinformatics programs, only three resulted in phenotypes. Two of the mutants had significantly stronger phenotypes, and their *tat-1* mutations were found to affect the conserved PISL and DKTGT motifs. The authors conclude discussion of their results by stressing the importance of verifying bioinformatics predictions in vivo (Chen et al., 2019).

The MMP has also been used for gene discovery in the form of accelerated forward screens. Wang et al. (2015) crossed fluorescent markers into MMP strains to visualize Q neuroblast migration. After examining 90 strains, the group identified two strains in which Q cell

descendants were mislocalized and mapped the causative mutation in one strain to a region of chromosome III. After RNAi knockdown of several candidate genes, they identified the phenotype-causing gene as *hse-5*, encoding a heparan sulfate-modifying enzyme. The effect was confirmed in a *hse-5* deletion mutant, and cell-specific rescue experiments determined that HSE-5 affected Q cell polarization in a non-cell autonomous manner. Wang et al. (2015) do not elaborate on anything that happened regarding the second Q cell migration MMP mutant they identified.

Timbers et al. (2016) performed a larger forward screen of MMP strains, testing 480 strains for dye-filling defects that indicate disfunctions in ciliated sensory neurons. The group combined their phenotypic results with the genotypic information on the tested strains using the Sequence Kernel Association Test (SKAT), a rare-variant association analysis (Wu et al., 2011). The SKAT results were then used to prioritize candidate genes that had not already been linked to dye-filling defects (Timbers et al., 2016). Most of the MMP strains with severe dye-filling defects had mutations in genes already known to cause the phenotype, but the authors were able identify three strains with severe dye-filling defects that all had mutations in a previously unstudied glycosyltransferase gene, *bgnt-1.1*. Rescue experiments with a fosmid containing *bgnt-1.1* were successful, and CRISPR-generated *bgnt-1.1* knockout alleles also displayed dye-filling defects (Timbers et al., 2016).

1.4 Research Goals and Summary

Particularly after reading about the success others have had in using the MMP set as a tool for genetic screening, we were inspired to consider how we might use the MMP to further our own studies of mechanosensation. We also saw an opportunity to interrogate the usefulness

of using the MMP strains as a set. Gentle body touch is a relatively well studied system in *C. elegans,* and we wondered to what extent the MMP set would demonstrate the range of touch insensitive phenotypes we have already observed. We wondered how many of the genes we knew to mutate to cause touch insensitivity would be represented as phenotype-causing in the set, and if we could find any interesting new MMP alleles of previously identified touch genes. Furthermore, we saw that the homozygous state of the mutant animals would allow us to test for more subtle phenotypic effects that might be difficult to isolate in a screen of mixed genotype animals.

In this thesis, I describe our forward screen of the entire MMP set for mechanosensory phenotypes. In Chapter 2, I introduce the neuronal basis of gentle touch sensation in *C. elegans* and review our knowledge of the molecular components involved in mechanosensory neuron function. These include genes identified through forward mutagenesis screens for touch insensitive animals and numerous additional regulating and modifying factors. As the number of genes we know to mutate to cause touch insensitivity is now quite large, I was unable to describe the importance of every one of such genes but have provided an accompanying list of additional factors. In Chapter 3 I go on to describe our screen of the MMP, explaining how we decided on the extent of phenotypic testing to perform and how we structured the retesting of strains we deemed potentially insensitive. I discuss the results of some preliminary analyses we performed using the Sequence Kernel Analysis Test (SKAT) applied by Timbers et al. (2016), then consider our results and summary statistics as a whole. I explain our approach to determining candidate causative mutations and verifying phenotype-causing mutations in known touch genes, providing a summary of verification results. In Chapter 4 I present what we learned about known touch genes by considering the types and locations of previously identified and MMP alleles that did

and did not result in touch phenotypes. I discuss factors we might use to predict the phenotypic effects of mutations, ultimately demonstrating that scores for chemical differences between amino acid substitutions and scores indicating degrees of evolutionary conservation fail to provide strong and direct correlations. In Chapter 5, I address the touch insensitive MMP strains for which we do not have candidate causative mutations by describing the phenotypic characterization of some particular strains and summarizing our progress towards mapping and verifying unknown causative mutations. In Chapter 6 I then conclude by summarizing what we have learned from our screen of the MMP, laying out plans for future experiments, and providing recommendations for further studies utilizing the MMP.

Chapter 2: The Molecular Components of Gentle Touch Sensation in *C. elegans*

One of my goals in screening the Million Mutation Project for touch insensitive mutants was to further expand our knowledge regarding the molecular basis of gentle touch sensation. In this chapter, I discuss our current understanding of the gentle touch response in *C. elegans* with a focus on the molecular components of touch receptor neuron physiology. These include the mechanoreceptor complex subunits and regulators of the mechanoreceptor complex, determinants of some of the unique physical characteristics of touch receptor neurons, and proteins involved in signaling pathways downstream of mechanically activated membrane depolarization. I also consider a number of other genes associated with reduced gentle touch response rates, including essential genes that were originally implicated in touch sensitivity through RNAi screens, genes with alleles linked to more subtle reductions in gentle touch sensitivity, and genes that mutate to give phenotypes that interfere with gentle touch response assays.

2.1 Basic Neurology of the Gentle Touch Response

Laser ablation studies have identified five sensory neurons required for response to gentle body touch, consisting of three anteriorly located neurons (ALMR, ALML, and AVM) and two posteriorly located neurons (PLMR and PLML). One additional posteriorly located neuron (PVM) shares morphological characteristics that are otherwise unique to the five critical sensory neurons but does not appear to be necessary for normal gentle touch response (Chalfie and Sulston, 1981). Collectively, these six neurons are referred to as touch receptor neurons (TRNs).

The TRNs have a relatively simple morphology, with long anteriorly directed neurites that run along about half the body length and form limited synaptic branches towards their distal ends. The PLMs also have shorter posteriorly directed neurites that extend towards the tip of the tail (Figure 2-1). TRN processes are uniquely identifiable in EM cross-sections due to an abundance of large-diameter microtubules not seen in any other cells and a relatively thick layer of surrounding extracellular matrix. The large-diameter microtubules are arranged in partially overlapping bundles, consistently oriented with one microtubule end situated towards the interior of the process and the opposing side of microtubule ends terminating near the plasma membrane (Chalfie and Thomson, 1979). The extracellular matrix (ECM), originally called the extracellular mantle, generally separates the TRN processes from the hypodermis in which they are embedded, although the processes are also anchored to the hypodermis through hemi-desmosome-like structures (Chalfie and Sulston, 1981).

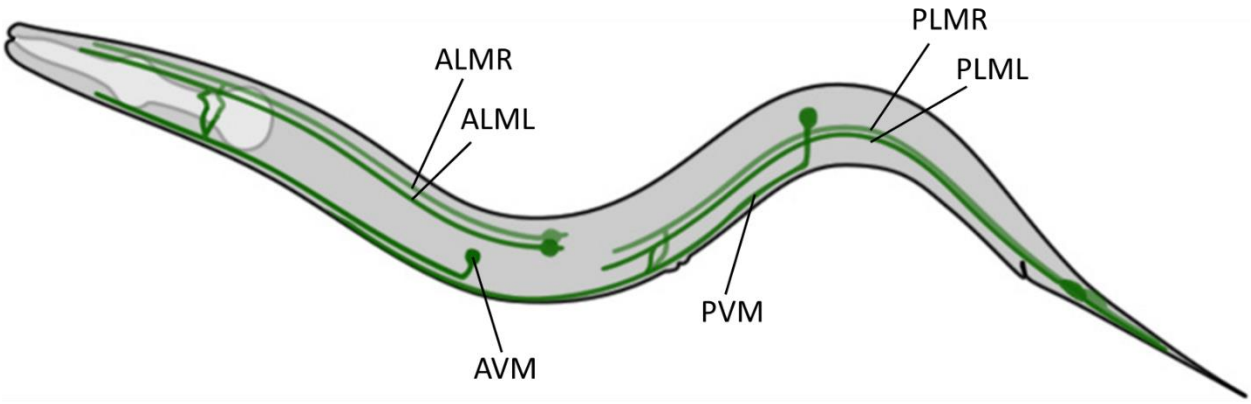

Figure 2-1: Diagram of the six gentle body touch receptor neurons. Neurons are depicted in green. Based on figure provided by Chalfie et al. (2014).

Proteins essential for TRN development and function were identified through mutagenesis screens for animals that failed to respond to touch but had no other obvious

abnormalities (Chalfie and Sulston, 1981; Chalfie and Au, 1989). Constituents of both the TRN large-diameter microtubules and extracellular matrix are required for touch sensation (MEC-7, MEC-12, MEC-1, MEC-5, and MEC-9), as are the subunits and regulators of the mechanically activated ion channels found in the TRNs (MEC-4, MEC-10, MEC-2, MEC-6, and MEC-14). Pre- and post-translational regulators of proteins necessary for TRN identity and function were also identified (MEC-15, MEC-8, and MEC-3). These and other proteins involved in TRN development and function are discussed in the following sections.

The TRNs do not appear to receive any direct synaptic inputs, but form gap junctions and outgoing chemical synapses to the premotor interneurons AVA, AVD, AVB, and PVC. The electrical gap junction synapses are presumed to be excitatory, as the anterior TRNs (which promote backwards movement in response to stimulation) form gap junctions with AVD (which stimulates motor circuits for backwards movement) and the posterior TRNs (which promote forwards movement in response to stimulation) form gap junctions with PVC (which stimulates motor circuits for forwards movement). Conversely, the chemical synapses are presumed to be inhibitory, as the anterior TRNs synapse onto PVC and AVB (which drives forwards movement along with PVC), and the posterior TRNs synapse onto AVA and AVD (which drives backwards movement along with AVA). The premotor interneurons synapse onto excitatory motor neurons (forward motor neurons VA and DA, and reverse motor neurons VB and DB) that innervate the body wall muscles (Chalfie et al., 1985).

Simply put, the gentle touch response can be separated into three separate stages: sensation (occurring at the level of TRN activity), signal integration (occurring at the level of interneuron activity), and locomotory response (occurring at the level of motor neuron and muscle activity). In our gentle touch response assays, we apply stimuli and observe the resulting

locomotory response, so a lack of locomotory response can indicate disruption at any of the three stages. Here I have chosen to focus on the stage of sensation and TRN signal transmission, with only passing acknowledgement of mutations that appear to affect more downstream processes or act as indirect confounders. In the original set of screens for touch insensitive mutants, such narrowing of focus was achieved by excluding mutants that exhibited additional visible phenotypes or were also defective for harsh touch response (which is sensed and mediated by a partially overlapping set of neurons but is primarily driven by a distinct set of sensory neurons) (Chalfie and Sulston, 1981; Li et al., 2011). In our screen of the Million Mutation Project, we did not take these same measures in our initial determination of response rates, leading us to identify some causative mutations with pleiotropic and/or indirect effects on TRN function and/or response rates. In the review that follows, genes known to directly affect TRN function but that also have pleiotropic effects are discussed along with genes more primarily associated with TRN function, whereas genes associated with phenotypes that otherwise interfere with gentle touch response assays are more briefly mentioned in the last section.

2.2 The Mechanoreceptor Complex and its Regulators

Mechanoreceptor complex subunits: MEC-4 and MEC-10

Rapid mechanosensory responses are thought to rely largely on force-gated ion channels, since second messenger signaling pathways could not account for the observed speed of signal relay (Corey and Hudspeth, 1979). The major mechanosensory channel complex present in TRNs is composed of degenerin epithelial sodium channel (DEG/ENaC) subunits MEC-4 and MEC-10 (Figure 2-2). MEC-4 was one of the first DEG/ENaC proteins identified (Driscoll and

Chalfie, 1991), but the superfamily is now thought to be ubiquitous across animal genomes (Ben-Shahar, 2011). The DEG/ENaC superfamily includes degenerins (deg) in nematodes, pickpocket (ppk) genes in arthropods, Hydra sodium channels (HyNaC) in cnidarians, FMRFamide-activated sodium channels (FaNaC) in mollusks, and ENACs and acid-sensing ion channels (ASIC) in vertebrates (Hanukoglu and Hanukoglu, 2016). DEG/ENaCs are trimeric, sodium-selective, non-voltage-gated transmembrane channels that serve a wide range of functions across organisms but share a high degree of sequence conservation and overall primary structure similarity (Gessmann et al., 2010; Eastwood and Goodman, 2012). Invariably, DEG/ENaC subunits have extracellular cysteine-rich domains between two transmembrane domains and cytoplasmic N- and C-termini. Both transmembrane helices are highly conserved, with the first membrane spanning domain (MSDI) being hydrophobic, and the second (MSDII) being amphipathic and implicated in pore function (Gessmann et al., 2010). The region preceding MSDII contains the degenerin (d) site, at which the introduction of large-side chain residues can increase channel open probability and lead to necrotic cell death (Driscoll and Chalfie, 1991; Brown et al., 2008). Although neurotoxic DEG/ENaC mutants were first identified in *C. elegans*, hyperactive ASICs have also been found to cause cell death in various mammalian models, suggesting a conserved mechanism of necrosis (Xiong et al., 2004; Yermolaieva et al., 2004; Pan et al., 2013).

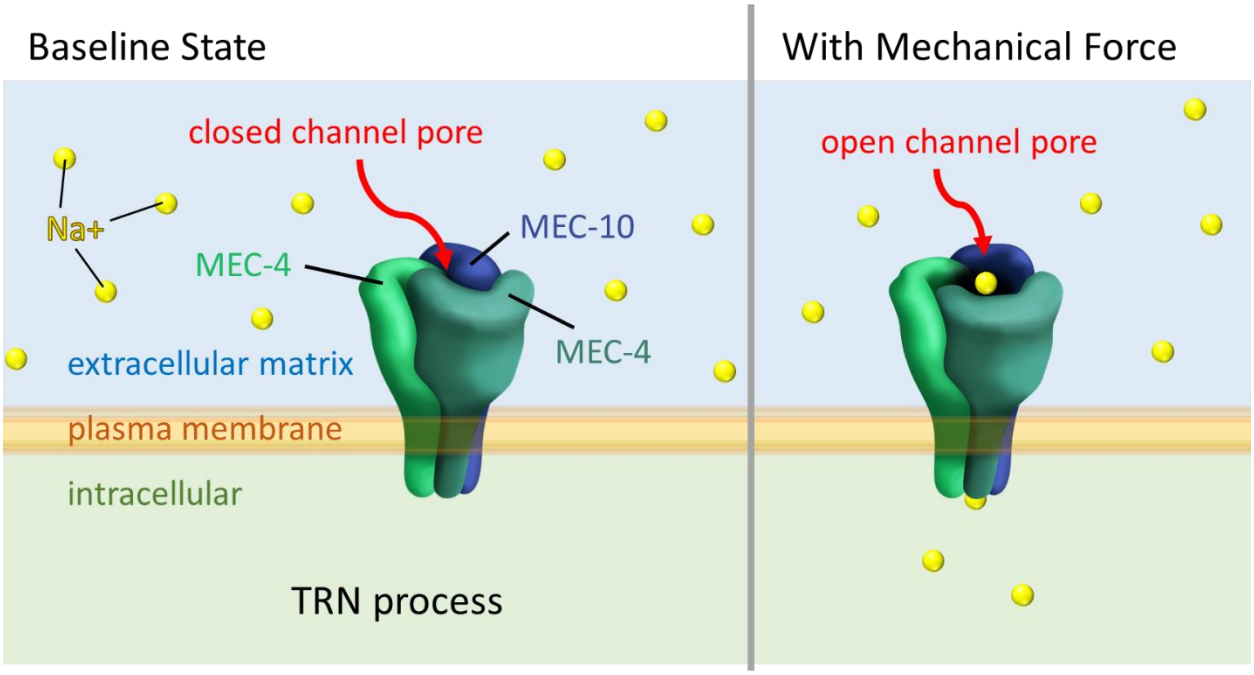

Figure 2-2: Illustration of the TRN mechanosensory complex. The channel complex is composed of three subunits which may include MEC-4 (depicted in dark and light green) and MEC-10 (depicted in blue). In response to mechanical stimuli, the channel pore (indicated with a red arrow) opens and allows an influx of sodium ions (depicted in bright yellow). The plasma membrane, intracellular region, and extracellular matrix of a TRN process appear in light yellow, light green, and light blue, respectively.

Between MEC-4 and MEC-10, MEC-4 appears to be the more critical DEG/ENaC subunit involved in mechanosensation. Although MEC-4 and MEC-10 are 48% identical in amino acid sequences and are predicted to have nearly indistinguishable topologies, early genetic evidence made it clear that the two proteins are not interchangeable (Huang and Chalfie, 1994). Firstly, the original mutagenesis screens for touch-insensitive mutants produced 59 *mec-4* alleles, with mutations distributed throughout the gene, but only six *mec-10* alleles, four of which were within a 25 nucleotide stretch of sequence within MSDII (Chalfie and Sulston, 1981; Chalfie and Au, 1989; Huang and Chalfie, 1994). These results were later explained by demonstrating that five of the six previously identified *mec-10* alleles were recessive gain-of-function mutations, and that *mec-10* null alleles produced a subtler effect on touch sensitivity than *mec-4* null or loss-

of-function alleles (Arnadottir et al., 2011). Additionally, *mec-4* loss-of-function mutations completely suppressed the effect of *mec-10*(d) expressed through an extragenic array, suggesting that MEC-10 activity is dependent on MEC-4 (Huang and Chalfie, 1994).

Expression experiments in Xenopus oocytes provided more clarity to the nature of interaction between MEC-4 and MEC-10. Many of these experiments made use of degenerin (d) alleles, since wild-type DEG/ENaCs alone could not be made to produce a detectable current through the oocyte cell membrane, whereas (d) mutant proteins produce a constitutive whole-cell current that allows for the study of current altering conditions. MEC-4(d) can produce a current in the absence of MEC-10, suggesting the formation of a functional homomeric channel. In contrast MEC-10(d) cannot produce a current alone or in combination with wild-type MEC-4, and wild-type MEC-10 significantly decreased the current conducted by MEC-4(d) (Goodman et al., 2002). Interestingly, the effect of MEC-10 on MEC-4(d) does not seem to result from changes in channel surface expression or from changes in single-channel properties (Brown et al., 2007; Arnadottir et al., 2011).

Imaging experiments with fluorophore-tagged proteins expressed in Xenopus oocytes showed that MEC-4 forms homotrimers alone and along with MEC-10 creates a heterotrimeric channel that has two MEC-4 subunits and one MEC-10 subunit (Chen et al., 2015b). Whereas MEC-4 has been observed to localize all along the TRN processes, MEC-10 localization is relatively more abundant in the TRN cell body and proximal neurites. Chatzigeorgiou et al. (2010a) reported that in *mec-10* null mutants, response to gentle touch was significantly more disrupted when stimulus was applied closer to either ALM or PLM cell bodies. It is unclear why this might be the case.

mec-4 expression is specific to the TRNs, whereas *mec-10* is expressed in both the TRNs and other sensory neurons (Huang and Chalfie, 1994; Lai et al., 1996; Chatzigeorgiou et al., 2010b). Since the MEC-10 subunit does not seem to be able to form a functional channel on its own, it's believed that MEC-10 associates with other DEG/ENaC subunits outside of the TRNs (Chelur et al., 2002; Goodman et al., 2002). The in vivo fluorescent signal from fluorophore-tagged MEC-4 is much greater than that of MEC-10, so most studies on TRN mechanosensory channel complex localization have utilized tagged MEC-4. Fluorophore-tagged MEC-4 localizes to regularly spaced spots of bright fluorescence, termed puncta, along the TRN processes (Chelur et al., 2002). The puncta are aligned with cuticular annuli, hemidesmosome attachments to the hypodermis, and other MEC proteins, which will be discussed in more depth further on. Although each puncta appears to contain many channels, in vivo electrophysiology recordings of TRNs suggest that the number of puncta and the number of functional mechanoreceptor channels is about the same (O'Hagan et al., 2005). Thus, the puncta may represent reservoirs of inactive channels, but this is unclear particularly since MEC-4 puncta overlap with puncta of extracellular matrix proteins thought to be necessary for channel function (Emtage et al., 2004). Immunogold labeling of MEC-4 in electron micrographs showed about half of labeled MEC-4 associated with 15-protofilament microtubules (Cueva et al., 2007). Intracellular reservoirs of MEC-4 could represent a recycling pool of inactive channels, as Butterworth et al. (2005) suggested for mammalian ENaCs.

MEC-10 appears to localize in a slightly different manner than MEC-4. Chatzigeorgiou et al. (2010a) reported that fluorophore-tagged MEC-10 does not form puncta in the TRNs, and instead described a diffuse fluorescent signal seen within TRN cell bodies and proximal neurites. Chen et al. (2015b) confirmed the observation that fluorophore-tagged MEC-10 predominantly

localizes to the cell body and proximal neurite in a diffuse manner, but also found MEC-10 puncta in about 10% of cells. Interestingly, Chen et al. (2015b) also found that co-expression of fluorophore-tagged MEC-10 along with either tagged or untagged copies of MEC-4 resulted in the reliable formation of MEC-10 puncta throughout the TRN neurite. In the case where both proteins were tagged, MEC-4 and MEC-10 puncta were seen to overlap, consistent with the formation of heteromeric channel complexes observed in Xenopus oocytes.

The usual lack of fluorescent MEC-10 puncta in the TRN distal neurites does not necessarily indicate the complete absence of the subunit, since fluorescent signals from singular proteins are generally too weak to be detected in vivo by confocal microscopy (Chen et al., 2015b). The presence of a limited amount of MEC-10 in the distal neurites is supported by that loss of *mec-10* disrupts the punctate distribution of fluorophore-tagged MEC-2, a mechanosensory channel complex associated membrane protein that normally localizes to puncta throughout the TRN process (Zhang et al., 2004).

Beginning with the greater number of *mec-4* mutations identified through mutagenesis screens for touch insensitivity, more has been revealed about the relationship between structure and function in MEC-4 as compared to MEC-10. Structure-function analysis of MEC-4 has provided information on regions all throughout the protein, highlighting that even non-conserved sequences and regions not covered by identified channel-disrupting substitutions play critical roles in channel function (see Figure 2-3 for a 3D representation of MEC-4 protein structure). The cytoplasmic N-terminal domain of MEC-4, most of which is not conserved across DEG/ENaCs, is likely involved in interactions with other channel complex subunits and may act to inhibit channel activity, although its role does not appear to be strictly inhibitory since disruptions to the sequence have been shown to decrease channel activity (Hong et al., 2000).

The more conserved region of the N-terminal intercellular domain spans only a short sequence of amino acids just prior to MSDI, which has been shown to affect ion permeation and selectivity in mammalian DEG/ENaCs (Gründer et al., 1999). On the extracellular side of MSDI, there is a highly conserved domain of unknown function containing multiple residues common to almost all known DEG/ENaCs (Zhang et al., 2008). No touch-insensitive alleles have been identified within this region, and it is not mutated in any Million Mutation Project strains, but was found to be a region of subunit interaction in the solved structure of a vertebrate ASIC (Jasti et al., 2007). In partial support for the hypothesis that this is also a site of subunit interaction in MEC-4, an amino acid substitution just prior to the region increased *mec-10*(d) toxicity but had no detectable effect on its own (Zhang et al., 2008).

Most of the MEC-4 protein is situated on the extracellular side of the membrane. This region contains three cysteine rich domains (CRDI, II, and III), which may tether MEC-4 to the extracellular matrix, and perhaps serve to open the channel in response to forces acting on the extracellular matrix in a "tether" or "spring" model (Gu et al., 1996; Hong et al., 2000; Tavernarakis and Driscoll, 2000). CRDI and an adjacent region called the extracellular regulatory domain (ERD) are unique to nematode degenerins (Garcia-Anoveros et al., 1995). Mammalian DEG/ENaC subunits contain only one CRD, corresponding to MEC-4 CRDIII (Bianchi, 2007). Identified channel-disrupting missense mutations cluster just before and within CRDIII, suggesting critical importance to channel function (Hong et al., 2000). Intriguingly, CRDIII includes a region with significant sequence similarity to scorpion venom neurotoxins; the region is sometimes referred to as the neurotoxin-related domain (NTD). The homologous venom neurotoxins are known to bind sodium channels with high affinity, suggesting that the

NTD might be involved in high-affinity interactions, perhaps as in a tether or spring model of channel gating (Tavernarakis and Driscoll, 2000).

The specific amino-acid sequence of MEC-4 MSDII appears to be more critical to channel function than that of MSDI. Mutageneses for phenotypes indicating altered channel function (including touch insensitivity and suppression of (d)-induced cell death) have identified 15 SNP missense alleles causing substitution of 7 amino acids within the 21 amino acid MSDII, but none within the 21 amino acid MSDI (Hong and Driscoll, 1994; Hong et al., 2000; Royal et al., 2005). Substitutions of the pore-lining resides within MSDII have been reported to affect ion selectivity, and channel gating response to mechanical force (Matthewman et al., 2016; Shi et al., 2018). The region is highly conserved among DEG/ENaC channels. Swapping the rat lung α-rENaC MSDII for MEC-4 MSDII maintains MEC-4 channel function in *C. elegans*, despite the two proteins functioning in different cell types (Hong and Driscoll, 1994).

Although screens for touch insensitive mutants have not identified any mutations within the intracellular C-terminal region of MEC-4 and the region is not highly conserved among DEG/ENaCs, it is not dispensable for protein function and likely plays a role in protein trafficking and surface maintenance. For one, both a truncated version of MEC-4 lacking amino acids 740-768 and a version with four C-terminal lysines substituted by alanines were shown to interfere with wild-type MEC-4 in vivo and failed to rescue the phenotype of touch insensitive *mec-4* mutants (Hong et al., 2000). Furthermore, two *mec-4* C-terminal mutations were identified in a mutagenesis screen for suppression of MEC-4(d) induced cell death: one causing a read-through adding 7 amino acids to the end of the protein, and the other resulting in an amino acid substitution with increased volume and polarity. The mutation causing an amino acid substitution was found to have no effect on single-channel conductance properties in Xenopus oocytes, but

resulted in significantly fewer MEC-4::GFP puncta seen along the TRN process when expressed in vivo, suggesting disruptions in channel trafficking (Royal et al., 2005).

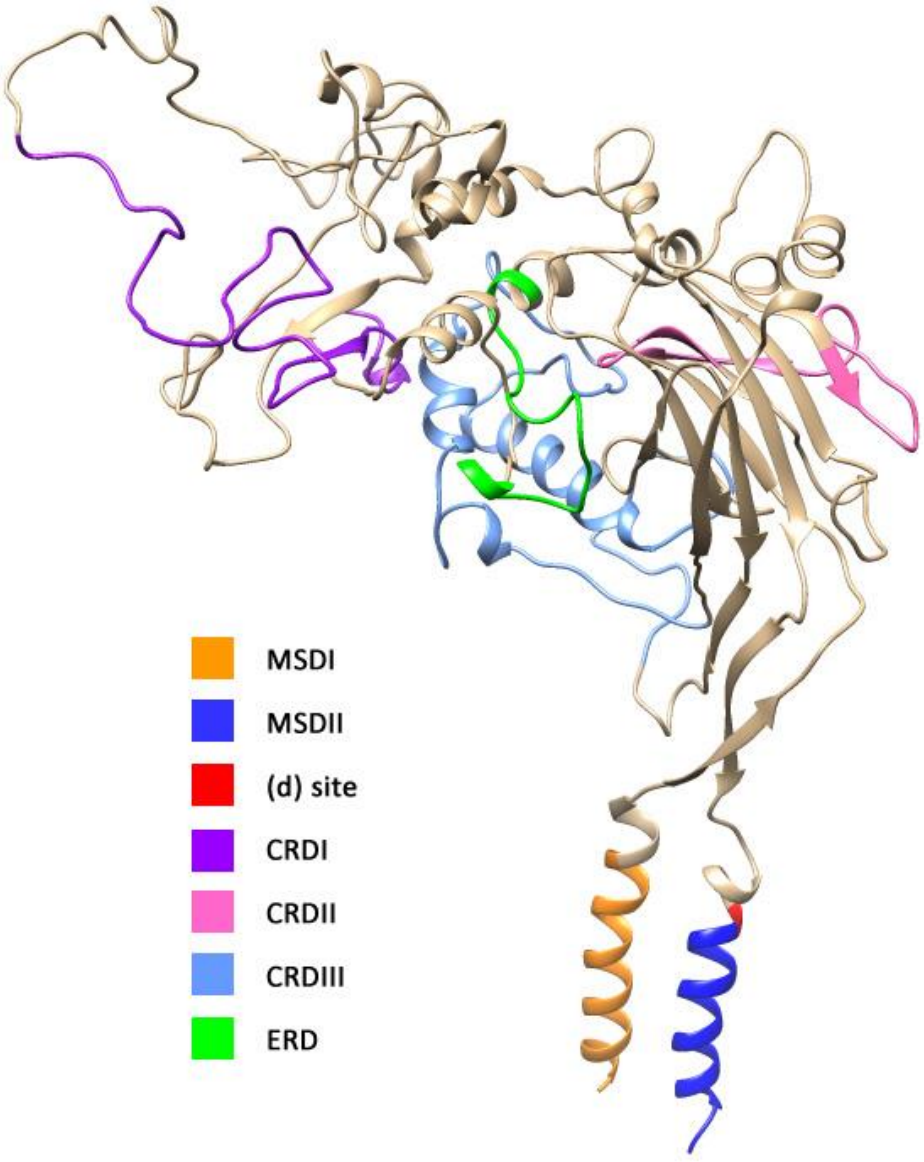

Figure 2-3: Ribbon model of MEC-4 structure. The modeled structure is based on homology to human ENaC (Noreng et al., 2018) and does not include the MEC-4 N and C-terminal domains. The model includes MEC-4 aa 114 to 729 (the full protein is 768 aa). Some regions of note are indicated by ribbon color (see figure key).

The similarities between the amino acid sequences of MEC-4 and MEC-10 allow much of what is known about the structure and function of MEC-4 to be applied to MEC-10. However, it is much more interesting to consider which sequences account for the functional differences between the two proteins. As has already been mentioned, MEC-10 is different from MEC-4 in that it cannot form a functional channel on its own and is not localized throughout the cell in the same manner as MEC-4, but the reasons for these differences are largely unclear. However, it was recently found that MEC-10 is necessary for a response to laminal sheer stress (LSS, a type of mechanical stimulus) in Xenopus oocytes. Without MEC-10, the MEC-4(d) channel does not produce significant changes in whole-cell current in response to LSS, but the incorporation of MEC-10 results in demonstrably mechanosensitive channels (Shi et al., 2016). Experiments with chimeric proteins in which domains were swapped between MEC-4 and MEC-10 demonstrated that the MEC-10 N-terminal and MSDI domains are necessary to confer response to LSS (Shi et al., 2016). Further experiments showed that similar substitutions in MEC-4 and MEC-10 MSDII resulted in different alterations to LSS response. Notably, the specific amino acids critical to LSS response in MEC-10 MSDII are predicted to neighbor the critical residues in MSDI (Shi et al., 2018).

In addition to the six TRNs, MEC-10 is expressed in FLP, PVD, and PVM. Its role in these neurons is less well understood but is likely to also be mechanosensory. The role of MEC-10 in harsh touch sensitivity is debated. Chatzigeorgiou et al. (2010b) reported that *mec-10* null (*tm1552*) mutants lacked detectable calcium transients in response to harsh touch, which could be rescued by expression of MEC-10 with a PVD-specific promoter. In a similar set of experiments, Chatzigeorgiou and Schafer (2011) demonstrated that harsh head touch response also required *mec-10*. However, Arnadottir et al. (2011) reported no significant loss of harsh

touch sensitivity using the same *mec-10* null (*tm1552*) mutation used by Chatzigeorgiou et al. (2010b). Also using *mec-10* (*tm1552*), Li et al. (2011) found that loss of *mec-10* did not alter harsh touch invoked mechanoreceptor currents in PVD. More recently, Tao et al. (2019) also reported that behavioral and calcium imaging experiments showed normal response to harsh touch in *mec-10* (*tm1552*) animals. Altogether, it seems more likely that *mec-10* is not necessary for the response to harsh touch.

MEC-10 is involved in proprioception in PVD. *mec-10* null mutants have altered posture and lack body bend induced calcium transients in PVD (Albeg et al., 2011). It was also shown that *mec-10* null mutants move with reduced sinusoidal amplitude and wavelength, which could be rescued by *mec-10* expressed under a PVD-specific promoter. Similar locomotion defects were observed for deletion mutants of DEG/ENaC subunit genes *unc-8* and *del-1*, and double or triple mutants for the three genes showed no change in phenotype as compared to animals with a single mutation, indicating that MEC-10, UNC-8, and DEL-1 may assemble to form a heteromeric channel (Tao et al., 2019).

Two other membrane proteins are necessary for TRN mechanoreceptor function: MEC-2 and MEC-6. Although these proteins were originally thought to be part of the channel complex, recent work indicates that they are not. First, fluorophore-tagged MEC-2 and MEC-6 were observed to colocalize with MEC-4 in puncta along the TRN processes, and epitope-tagged versions of all four proteins (MEC-2, MEC-4, MEC-6, and MEC-10) co-immunoprecipitated from expression in Chinese hamster ovary cells (Chelur et al., 2002). Additionally, null mutations in either *mec-2*, *mec-4*, or *mec-6* were found to eliminate MRCs in vivo, consistent with a model in which the three proteins are core channel components (O'Hagan et al., 2005). More recent evidence has indicated that MEC-2 and MEC-6 do not contribute to the

mechanoreceptor complex: in Xenopus oocytes, fluorophore-tagged MEC-2 and MEC-6 were observed to localize independently of MEC-4 and MEC-10 channel complexes, and co-immunoprecipitation experiments indicated strong interactions between MEC-4 and MEC-10 but only weak interactions between MEC-4 and MEC-2 or MEC-6. These results suggest that the in vivo association between MEC-2, MEC-6, and the mechanoreceptive ion channel complex are mediated by other protein factors and that MEC-2 and MEC-6 are not core channel components (Chen et al., 2015b). Instead, MEC-2 and MEC-6 play significant roles in regulating the mechanoreceptor complex. Other *mec* genes that affect the channel complex either directly or indirectly are discussed below.

Mechanoreceptor complex regulating membrane proteins: MEC-2, UNC-24, and MEC-19

MEC-2 is embedded in the cytosolic surface of the plasma membrane and is similar to human stomatin, which is found in red blood cells, and podocin, which is found in blood-filtering kidney cells (Huang et al., 1995; Goodman et al., 2002; Huber et al., 2006). Both stomatin and podocin are associated with cholesterol-rich membrane fractions (Snyers et al., 1999; Schwarz et al., 2001). Similarly, MEC-2 has been shown to bind cholesterol, which appears to be necessary for touch sensitivity (Huber et al., 2006). Although MEC-2 does not contribute to the mechanoreceptor ion channel pore, many lines of evidence indicate that it affects channel activity. For one, *mec-2* alleles can suppress or enhance the effect of gain-of-function *mec-10*(d) and *mec-4*(d) alleles that cause cell death by keeping the channel in an open state (Huang and Chalfie, 1994; Huang et al., 1995; Gu et al., 1996). It has also been demonstrated that co-expression of MEC-2 with constitutively active forms of MEC-4/MEC-10 ion channels in Xenopus oocytes caused a 40-fold increase in sodium current amplitude without altering the

surface expression of the channels. Additionally, while wild-type MEC-4/MEC-10 channels did not produce a detectable current when expressed alone or together in Xenopus oocytes, currents were detected when MEC-2 was co-expressed (Goodman et al., 2002). When changes in membrane potential and current were measured in vivo by whole-cell patch clamp recording of TRNs, it was found that loss of *mec-2* resulted in the elimination of mechanoreceptor currents (O'Hagan et al., 2005). When MEC-4/MEC-10 channel properties were measured in Xenopus oocytes, it was found that co-expression of MEC-2 increased single-channel conductance, though not by enough to explain the 40-fold increase in current previously described. The more notable effect of MEC-2 on whole-cell current could be due to facilitating transition between inactive and active channel states (Brown et al., 2007).

Full MEC-2 activity requires both its N and C-terminal cytoplasmic domains (Goodman et al., 2002), but the central stomatin-like prohibitin (PHB) domain appears to most critical (Bianchi, 2007). Mutations in the PHB domain were found to disrupt the punctate distribution of MEC-2 (Zhang et al., 2004). Since MEC-4 is also required for the punctate distribution of MEC-2, the interaction between MEC-4 and MEC-2 is likely to occur directly or indirectly through the MEC-2 PHB domain (Emtage et al., 2004). Interestingly, co-expression of either human stomatin or the PHB domain of MEC-2 along with full-length MEC-2 reduced the effect of MEC-2 on MEC-4/MEC-10 channel current in Xenopus oocytes, which may indicate that MEC-2 forms multimer complexes through its PHB domain (Goodman et al., 2002). While MEC-2 interaction with mechanoreceptor channels and multimerization do not require cholesterol, the PHB domain is also necessary for the cholesterol binding activity of MEC-2 (Huber et al., 2006). MEC-2 cholesterol binding is necessary for touch sensitivity, and may be key for activating mechanoreceptor channels (Huber et al., 2006; Brown et al., 2007). MEC-2 may act on MEC-

4/MEC-10 channels by modifying the lipid environment around the channels, either by recruiting the complex to cholesterol-rich membrane fractions or by increasing the local amount of cholesterol (Huber et al., 2006).

Until recently, mutations in *mec-2* were only associated with touch sensitivity phenotypes and *mec-2* expression was thought to be exclusive to the TRNs (Zhang et al., 2004). However, in a screen for mutants with abnormal thermotaxis behavior, Nakano et al. (2020) discovered a gain-of-function *mec-2* mutation that interfered with normal activity of the thermosensory neuron AFD. The team then went on to show that although expression of the *mec-2*a isoform was restricted to the TRNs, *mec-2*c was expressed in AFD and the olfactory neuron AWC. *mec-2* loss of function mutations appeared have no effect on thermotaxis or AFD activity, suggesting redundancy with one or more of the nine other *C. elegans* stomatin genes expressed in AFD. Because the mutation isolated by Nakano et al. (2020) affects the coding sequence of all *mec-2* isoforms, the mutants should also be tested for touch response phenotypes in the future.

A second stomatin-like protein, UNC-24, is also expressed in the TRNs and is thought to influence mechanoreceptor channel activity (Zhang et al., 2004). In addition to the PHB domain found in MEC-2, UNC-24 has a sterol-carrier protein domain which may function to insert cholesterol and other sterols into the plasma membrane (Barnes et al., 1996; Sedensky et al., 2004). Compared to MEC-2, UNC-24 only has minor effects on the touch response, with *unc-24* null mutants exhibiting a slightly reduced anterior touch response probability and a normal posterior response (Zhang et al., 2004). Whereas the expression of MEC-2 along with MEC-4(d) in Xenopus oocytes increases channel activity by about 40-fold, the addition of UNC-24 has no effect on MEC-4(d) current alone and decreases current by about 30% when expressed with both MEC-2 and MEC-4(d). Even so, the in vivo effect of UNC-24 on MEC-4 does not appear to be

inhibitory since loss of UNC-24 enhances the touch insensitive phenotypes of temperature-sensitive *mec-6* and *mec-4* alleles. Immunoprecipitation experiments using epitope-tagged proteins expressed in Xenopus oocytes suggest that UNC-24 interacts with both MEC-2 and MEC-4(d) and does not affect the interactions between MEC-2 and MEC-4(d). Furthermore, fluorophore-tagged UNC-24 colocalizes with fluorophore-tagged MEC-2 puncta in vivo (Zhang et al., 2004).

Another membrane protein thought to regulate the mechanoreceptor complex is MEC-19. *mec-19* was identified in a screen for genes that may normally inhibit MEC-4(d) activity (Chen et al., 2016a). MEC-19 is a relatively small protein with 129 amino acids and one predicted transmembrane domain. It was found to affect the amount of fluorophore-tagged MEC-4 visible in TRN neurites, and to regulate the surface expression of fluorophore-tagged MEC-4 in Xenopus oocytes. Epitope-tagged MEC-19 and MEC-4(d) reciprocally coimmunoprecipitate from expression in Xenopus oocytes, suggesting that MEC-19 may regulate MEC-4 by direct physical interaction. MEC-19 could potentially either inhibit the insertion or promote the removal of MEC-4 from the membrane, but the mechanisms of MEC-19 activity have been difficult to guess at, in part because no homologs have been identified outside of Caenorhabditis species (Chen et al., 2016b).

Proteins thought to influence mechanoreceptor lipid environment: MEC-18, ELO-1, and others

The fact that MEC-2 cholesterol binding is necessary for touch sensitivity suggests that the mechanoreceptor complex lipid environment has significant effects on channel function. Several other genes that mutate to cause reduced touch sensitivity are also suspected to affect

mechanoreceptor channel function through changes in the composition of surrounding lipid environments. These include *mec-18, elo-1, fat-1, fat-3, fat-4,* and *mboa-6*.

mec-18 is only expressed in the TRNs and encodes a protein similar to firefly luciferase and acetyl-CoA-synthase (also known as long-chain-fatty-acyl-CoA ligase) (Gu, 1998). This family of enzymes appears to function through ATP-dependent binding of AMP to their substrate. Null mutations in *mec-18* enhance TRN degeneration in *mec-10*(d) mutants (Huang and Chalfie, 1994), suggesting that MEC-18 activity modulates DEG/ENaC activity. Although it's been hypothesized that MEC-18 could act directly on the mechanoreceptor complex (Gu, 1998), evidence suggesting that MEC-18 plays a role in fatty-acid metabolism has been building (M. Chalfie, unpublished).

Further evidence for the effects of altered plasma-membrane lipid environments on mechanoreceptor channel function comes from the finding that the loss of enzymes involved in the production of polyunsaturated fatty acids (PUFAs) can significantly reduce touch sensitivity. Vasquez et al. (2014) found that mutations in *elo-1*, *fat-1*, *fat-3*, and *fat-4* cause reduced touch sensitivity. The supplementation of growth medium with arachidonic acid (AA) and/or eicosapentanoic acid (EPA), two large PUFAs, increased touch sensitivity of *fat-1*, *fat-3*, *fat-4*, and *fat-1*; *fat-4* mutants but did not have similar effects on wild-type animals. The reduction in touch sensitivity caused by mutations in PUFA synthetases is likely to be upstream of mechanoreceptor channel function since light stimulation of optogenetically engineered TRNs produced similar responses in *fat-1*; *fat-4* mutant and wild-type animals. Furthermore, the team demonstrated that neuronally-enhanced RNAi knockdown of *mboa-6*, a lysophospholipid enzyme responsible for incorporating PUFAs into the plasma membrane, also resulted in reduced touch sensitivity. The effect could be rescued by supplementation of growth medium with AA-

containing phospholipids. Additionally, TRN membranes lacking PUFAs had altered mechanical properties suggesting increased membrane bending stiffness (Vasquez et al., 2014).

Mechanoreceptor complex regulating chaperones: MEC-6, POML-1, and others

As mentioned above, MEC-6 was once thought to be part of the mechanoreceptor complex in part due to its dramatic effect on channel function. It has since been found that while MEC-6 is a membrane-spanning protein, it is probably localized to the ER rather than to the cell membrane. In the ER, MEC-6 is involved in the maturation of DEG/ENaC proteins. Similar roles were discovered for two other chaperone-like proteins, POML-1 and CRT-1 (Chen et al., 2016a). A fourth ER-resident chaperone, NRA-2, does not appear to be necessary for normal DEG/ENaC protein folding but may serve as a quality-control mechanism prior to export from the ER (Kamat et al., 2014).

Mutations in MEC-6 can cause severe reductions in touch sensitivity, and its complete loss eliminates MRCs in TRNs (O'Hagan et al., 2005). It has long been suspected that the effect of MEC-6 on touch sensitivity is through MEC-4, since mutations in *mec-6* disrupt the punctate localization of MEC-4 and prevent cell death in *mec-4*(d) animals (Chalfie and Wolinsky, 1990; Huang and Chalfie, 1994; Chelur et al., 2002). Experiments with *mec-4*(d) in Xenopus oocytes often include coexpression of MEC-6, since MEC-6 was found to increase channel activity, particularly in combination with MEC-2 (Chelur et al., 2002; Goodman et al., 2002). Early evidence from Chelur et al. (2002) suggested that the effect of MEC-6 on channel activity was not due to a change in MEC-4 surface expression, hinting that it might instead play a role in activating the channels. This was somewhat in contrast to a finding within the same study that *mec-6* null mutations greatly reduced the appearance of fluorophore-tagged MEC-4 in vivo.

More recently, it was shown that MEC-6 does alter surface expression of MEC-4 in Xenopus oocytes (Chen et al., 2016a). Chen et al. (2016a) suggested that the effect had not been detected in previous experiments due to MEC-4 achieving a maximum steady-state amount of membrane expression 5 days after injection with or without MEC-6.

MEC-6 is similar to mammalian paraoxonases, which are most well known for their role in protecting low-density lipoprotein from oxidation by hydrolyzing organic esters and phosphates (Chelur et al., 2002; Précourt et al., 2011). Several of the residues believed to be necessary for the enzymatic activity of human paraoxonase are not conserved in MEC-6, so it is unclear whether MEC-6 has any enzymatic activity (Brown et al., 2008). It has been hypothesized that MEC-6, like paraoxonase, might associate with high-density lipoprotein particles on the plasma membrane and thus affect MEC-4 by modulating the lipid environment of the channel (Brown et al., 2008), but more recent experiments have demonstrated that MEC-6 localizes to the ER (Chen et al., 2016a). Some mammalian paraoxonases are also ER resident proteins, where they are thought to protect against ER stress and prevent activation of the unfolded protein response (Horke et al., 2007). The human paraoxonase PON-2 has been shown to regulate ENaC activity, suggesting an evolutionarily conserved relationship between paraoxonase-like chaperones and DEG/ENaC subunits. However, it should be noted that while MEC-6 serves to increase mechanoreceptor channel activity, PON-2 negatively regulates ENaC activity (Shi et al., 2017).

MEC-6 has a single membrane spanning domain near the N-terminus, with the majority of the protein likely extending into the ER lumen. The C-terminus includes multiple potential glycosylation sites, which are known to be used in the mammalian homolog PON-2, but lacks the calcium binding domain and calcium binding residues found in mammalian PONs (Chen et

al., 2016a). Although enzymatic activity has not been demonstrated for MEC-6, most of the identified *mec-6* missense mutations disrupt the domain associated with enzymatic activity in homologous proteins (see Chapter 4).

MEC-6 expression is not restricted to the TRNs in *C. elegans*, as it also appears to be expressed in many other neurons, muscles, and the canal cell (Chelur et al., 2002). MEC-6 may be required for the function of other DEG/ENaC channels in these cells, as is suggested by genetic interactions with *deg-1* and *unc-8*. Just as mutations in *mec-6* can prevent cell death in *mec-4*(d) and *mec-10*(d) mutants, *deg-1*(d) and *unc-8*(d) mutant phenotypes also require MEC-6 (Chalfie and Wolinsky, 1990; Huang and Chalfie, 1994; Shreffler et al., 1995). However, the effects of MEC-6 on different DEG/ENaC subunits varies somewhat, as has been demonstrated by expression experiments in Xenopus oocytes. Whereas MEC-4(d) currents are greatly increased by coexpression with MEC-6, the same effect is not observed with UNC-8(d) (Matthewman et al., 2016). The difference appears to be mediated by interactions between MEC-6 and the DEG/ENaC extracellular domains, as chimeric proteins with part of the UNC-8(d) extracellular domain replaced with that of MEC-4 were strongly affected by coexpression with MEC-6 (Matthewman et al., 2018).

Like MEC-6, POML-1 is expressed in the ER and appears to be involved in DEG/ENaC maturation. POML-1 was first investigated in relation to the touch response due to its similarity to MEC-6 and other paraoxonases. Null mutations in *poml-1* do not produce touch insensitivity except for when combined with certain sensitizing mutations. These sensitizing mutations include hypomorphic alleles of *mec-6* that do not result in touch insensitivity on their own but almost completely abolish the touch response in combination with a *poml-1* null allele, suggesting partial redundancy between POML-1 and MEC-6. *poml-1* null mutations also

dramatically reduce touch sensitivity in a temperature sensitive *mec-4* mutant background and suppress cell death in *mec-4*(d) mutants. However, unlike with MEC-6, loss of POML-1 does not suppress the neuronal phenotypes caused by any other (d) mutant DEG/ENaC genes. This is true even in neurons that express both POML-1 and DEG/ENaC genes other than MEC-4. Expression of POML-1 is generally more restricted that that of MEC-6, with fluorophore-tagged POML-1 being observed in the six TRNs, IL1, AIM, ALN, and BDU neurons. Both MEC-6 and POML-1 are likely to affect relatively few proteins, since their loss does not induce the general ER stress response (Chen et al., 2016a).

CRT-1 (calreticulin) is a third protein thought to act as a chaperone in the maturation of MEC-4, with partial redundancy with MEC-6 and POML-1 (Chen et al., 2016a). Mutations in *crt-1* decrease MEC-4 protein levels and slightly reduce touch sensitivity (Xu et al., 2001). Furthermore, *crt-1* mutations in combination with a *poml-1* null allele cause greatly reduced touch sensitivity (Chen et al., 2016a). As with MEC-6 and POML-1, the loss of CRT-1 suppresses cell death in *mec-4*(d) mutants (Xu et al., 2001). However, CRT-1 is thought to have a more general role than either MEC-6 or POML-1, as it is expressed widely and has been shown to be induced by the unfolded protein response pathway and by more general environmental stressors including exposure to high temperatures and ethanol (Park et al., 2001; Lee et al., 2007). In addition to its role as a chaperone, calreticulin is well known to bind calcium and regulate calcium levels in both the ER lumen and the cytoplasm (Michalak et al., 2009). The calcium-regulating activity of CRT-1 might be an important factor in the genetic interactions between *crt-1* mutations and *mec-4*(d), since pharmacologically increasing intracellular calcium levels in *crt-1*; *mec-4*(d) double mutants significantly restores TRN necrosis (Xu et al., 2001).

Another ER-resident protein shown to affect degenerin-induced necrosis in the TRNs is NRA-2, a homolog of mammalian nicalin (Kamat et al., 2014). Interestingly, mutations in *nra-2* enhance necrosis in *mec-10*(d) mutants but not in *mec-4*(d) mutants. Loss of NRA-2 does not appear to significantly affect the distribution of fluorophore-tagged wild-type MEC-4 or MEC-10, but increases the surface expression of fluorophore-tagged MEC-10(d) (Kamat et al., 2014). This may be due to a requirement for wild-type MEC-4 in assembled channel trimers. When expressed in Xenopus oocytes, NRA-2 reduces the current in cells expressing MEC-4(d) or MEC-10(d) along with wild-type MEC-4 but has no effect on cells expressing only MEC-4(d). Furthermore, *nra-2* mutant animals show decreased localization of fluorophore-tagged MEC-10(d) to the ER, suggesting that wild-type NRA-2 might serve to prevent the release of abnormal channels from the ER (Kamat et al., 2014). Therefore, unlike the chaperones discussed above, NRA-2 does not appear to regulate DEG/ENaC protein folding, but rather serves as a quality-control monitor prior to release. However, *nra-2* mutants are slightly touch insensitive, which is not an obvious consequence of the proposed model (Kamat et al., 2014). NRA-2 might function as a chaperone for channel assembly as was proposed for assembly of acetylcholine receptor pentameters in muscle ER. In the ER of muscle cells, fluorophore-tagged NRA-2 does not colocalize with markers for ER exit sites and secretory vesicles (Almedom et al., 2009). Kamat et al. (2014) suggested that NRA-2 might affect the assembly of mechanoreceptor channels in the TRNs through its calcium-binding EF hand domain, since ER calcium can affect complex formation (Suzuki et al., 1991; Biemesderfer et al., 1993).

TRN extracellular matrix components: MEC-1, MEC-5, and MEC-9

The TRN extracellular matrix (ECM) is believed to play an important role in regulating mechanoreceptor channel localization and may also affect channel function. Mutations resulting in the loss of TRN ECM constituent proteins MEC-1, MEC-5, and MEC-9 abolish gentle touch sensitivity and prevent proper distribution of the mechanoreceptor complex, suggesting some level of interaction between the DEG/ENaC channel and the ECM. MEC-1. MEC-5, and MEC-9 could also be important for determining the mechanical properties of the ECM. It might be that the structural integrity of the ECM is required to translate mechanical force to the plasma membrane. One of these genes might also tether the mechanoreceptor complex to the ECM.

MEC-1 is a presumptive secreted protein necessary for the accumulation and organization of the ECM coating the TRN processes (Emtage et al., 2004). *mec-1* null mutants are touch insensitive, lack the prominent ECM normally associated with the TRNs, and have TRNs that fail to be ensheathed by the hypodermis (Chalfie and Sulston, 1981). The ensheathment phenotype appears to be mostly distinct from the touch phenotype, since C-terminal truncated MEC-1 can restore TRN attachment but not touch sensitivity (Emtage et al., 2004), and mutations in other genes such as *him-4* (which encodes hemicentin) have been found to cause a similar attachment phenotype without abolishing touch sensitivity (Vogel and Hedgecock, 2001). However, it should be noted that *him-4* and other attachment-defective mutants have been found to demonstrate partial touch insensitivity and differences in plate-tap response behavior, indicating that TRN attachment may be necessary for optimal touch sensitivity (Vogel and Hedgecock, 2001; Emtage et al., 2004; Chen and Chalfie, 2014).

Like many ECM proteins, MEC-1 contains multiple copies of disulfide bond domains including Kunitz-like and EGF domains (Emtage et al., 2004). Kunitz domains are relatively

short motifs of about 60 amino acids that form α-β folds constrained by disulfide bonds. They are associated with high-affinity interactions and tight, non-covalent bonds (Ranasinghe and McManus, 2013). The longest isoform of MEC-1, which is required for touch sensitivity, contains 15 Kunitz-like repeats and two EGF domains (Emtage et al., 2004). EGF domains are commonly found in the extracellular domains of membrane-bound proteins or in secreted extracellular proteins, and consist of two β-sheets stabilized by disulfide bonds (Wouters et al., 2005). In MEC-1, only the C-terminal-most EGF domain contains the amino acid sequences associated with calcium-binding. Interestingly, the only two previously identified *mec-1* missense mutations that cause touch insensitivity are located within the 15th Kunitz-like repeat (Emtage et al., 2004).

MEC-1 expression and the phenotypes associated with *mec-1* mutations are not limited to TRNs. Promotor fusion constructs have indicated that *mec-1* is expressed in TRNs, SDQ, PLN, ALN, PVT, and intestinal muscle (Emtage et al., 2004). In addition to TRN and gentle-touch response related phenotypes, *mec-1* mutants have also been found to have defects in amphid and phasmid ciliated neurons (Lewis and Hodgkin, 1977; Perkins et al., 1986; De Vore et al., 2018), male-specific sensory neurons (De Vore et al., 2018), and neurosecretory-motor neurons (Axäng et al., 2008). Male-specific behavioral phenotypes (presumably due to defects in male-specific sensory neurons) have also been reported (De Vore et al., 2018).

In the TRNs, fluorophore-tagged MEC-1 localizes both diffusely and in regularly spaced puncta of bright fluorescence along the processes. Patterns of localization differ between the lateral and ventral processes, with lateral processes displaying both diffuse and punctate fluorescence, and ventral processes lacking diffuse localization but maintaining periodic puncta. Mutations that disrupt the regular distribution of the puncta have been identified in *mec-5* and

mec-9, with null mutations resulting in the loss of puncta without affecting the diffuse localization of MEC-1 in the lateral touch processes. Fluorophore-tagged MEC-5 localizes in a manner similar to MEC-1 and forms puncta that colocalize with MEC-1 puncta. The MEC-1/MEC-5 puncta appear to align with the circumferential ridges of the cuticle called annuli (Emtage et al., 2004). Together, MEC-1 and MEC-5 likely coordinate the localization of DEG/ENaC channel complexes. Fluorophore-tagged MEC-4 puncta colocalize with MEC-1/MEC-5 puncta, and while null mutations in *mec-1* and *mec-5* disrupt the localization of MEC-4, mutations in *mec-4* do not affect the localization of MEC-1 or MEC-5 (Emtage et al., 2004). Thus, the dramatic effect of *mec-1* and *mec-5* mutations on touch sensitivity may be largely due to effects on MEC-4.

MEC-5 is a collagen secreted by the body wall muscle that contributes to the ECM coating the TRNs (Du et al., 1996; Coblitz et al., 2009). MEC-5 is unique amongst collagens in both the number of G-X-Y (a glycine residue followed by two residues of variable identity) repeats and in the sequence of surrounding amino acids (Du et al., 1996). As mentioned previously, fluorophore-tagged MEC-5 appears to colocalize with fluorophore-tagged MEC-1 and is distributed in similar manner, with diffuse uniform fluorescence surrounding more intense puncta that are distributed along the TRN process. The punctate, but not diffuse, pattern of localization is disrupted by mutations in *mec-1* and *mec-9*, whereas the diffuse, but not punctate, pattern is disrupted by mutations in *him-4* (Emtage et al., 2004).

All of the previously identified *mec-5* alleles are recessive, and about half of them are temperature sensitive. This abundance of temperature sensitive alleles could result from changes in the thermostability of the triple helix homotrimerization of collagen, or from affecting interactions with other proteins (Du et al., 1996). Protein-protein interactions critical to the

function of MEC-5 are suggested by that partially insensitive phenotypes caused by a number of other *mec* genes, including *mec-2, mec-4,* and *mec-10,* are dominantly enhanced by a temperature sensitive allele of *mec-5,* and by that phenotypes caused by a number of *mec-5* alleles are dominantly enhanced by temperature sensitive alleles of other *mec* genes including *mec-4* (Gu et al., 1996). Most of the temperature-sensitive *mec-5* alleles have mutations that substitute for glycine in the C-terminal G-X-Y repeats, similar to the pattern of disease-related mutations found in human type I collagen, which may hint that these mutations are more likely to affect triple helix assembly than touch protein interactions. However, the temperature sensitive *mec-5* allele that dominantly enhances phenotypes caused by mutations in other *mec* genes is located in the N-terminal region of G-X-Y repeats and is not common in other collagens (Du et al., 1996; Gu et al., 1996).

Although only the MEC-5 secreted from body wall muscle cells is necessary for touch sensitivity (Coblitz et al., 2009), MEC-5 is probably expressed in a number of other cell types. GFP and LacZ promoter fusions including up to 1.5 Kb of sequence upstream of *mec-5* indicated expression in the seam cells and hypodermal cells (Du et al., 1996), and GFP promoter fusions including up to 3 Kb of sequence upstream of *mec-5* indicated expression in the nervous system, intestine, and ventral nerve cord (McKay et al., 2003; Hunt-Newbury et al., 2007). The role of MEC-5 outside of TRN function has not been well studied, but *mec-5* alleles have been shown to cause defects in ciliated sensory neurons and male-specific behaviors, with particularly penetrant abnormalities in the localization of fluorophore-tagged PKD-2 (encoding polycystin, a transient receptor potential cation channel) in CEM cilia (De Vore et al., 2018).

MEC-9 is a secreted protein with several Kunitz-type serine protease inhibitor (Ku) and epidermal growth factor (EGF) domains. The *mec-9* transcript produces two isoforms: a longer

protein (MEC-9L) encoded in 19 exons and a shorter protein (MEC-9S) transcribed from the 10 C-terminal-most exons of *mec-9L* with an expanded first exon (Du et al., 1996). MEC-9L is only expressed in the TRNs, whereas MEC-9S is found in the TRNs, several ciliated neurons, and the ventral nerve cord (De Vore et al., 2018). Only MEC-9L is required for touch sensitivity. MEC-9L includes 5 Ku domains, 7 EGF repeats (of both Ca^{2+} binding type and non-Ca^{2+} binding type), a glutamic acid-rich region, and 7 putative N-glycosylation sites. The Ca^{2+} binding EGF repeats are not included in MEC-9S, which may reflect a TRN-specific Ca^{2+} interaction (Du et al., 1996).

Like *mec-1* and *mec-5*, *mec-9* was found to affect ciliated sensory neurons and male-specific behaviors, though to a somewhat greater extent. Whereas all three genes affect the localization of PKD-2 in male-specific ray cilia, only *mec-9* affects the other *C. elegans* ortholog of polycystin, LOV-1. In the same study, only *mec-9* was required for all tested male-specific behaviors, including mate searching, response to hermaphrodite contact, and response to the hermaphrodite vulva. Furthermore, *mec-9* was found to be a negative regulator of ciliary extracellular vesicle (EV) biogenesis and release, and to be required for normal CEM dendritic morphology. Interestingly, *mec-9* was found to be a positive regulator of ciliary length in amphid channel neurons, but a negative regulator in IL2 and CEM neurons (De Vore et al., 2018). While all these findings involved MEC-9S rather than MEC-9L, they still might be able to provide hints as to the mechanisms of function for both isoforms.

Additional mechanoreceptor complex regulators: MEC-14, MFB-1, and CAV-1

MEC-14 is one of the less well-studied genes that were identified in the original mutagenesis screens for touch insensitive mutants (Chalfie and Au, 1989). It is hypothesized to

regulate mechanoreceptor channel activity due to that mutations in *mec-14* can reduce *mec-10*(d) neurotoxicity (Huang and Chalfie, 1994) and that mutations in *mec-14* greatly reduce mechanoreceptor currents measured in vivo (R. O'Hagan and M. Chalfie, unpublished). Furthermore, MEC-14 shares weak homology with shaker-type potassium channel β subunits, which regulate the activity of pore-forming α subunits (Li et al., 2006). Like shaker-type potassium channel β subunits, MEC-14 may have oxidoreductase activity, but enzymatic activity has not been demonstrated (McCormack and McCormack, 1994). C-terminal fluorophore-tagged MEC-14 that rescued touch sensitivity in *mec-14* null mutants was only observed in the TRNs and localized to bright puncta along TRN axons. Mutations in *mec-12* disrupted the MEC-14 puncta, which were replaced by a diffuse pattern of localization (G. Caldwell et al., unpublished).

MFB-1 was identified as a modulator of MEC-4 activity through a search for mutations that restored touch sensitivity in insulin-signaling mutants (insulin-signaling genes that reduce touch sensitivity are mentioned in the section on additional genes associated with touch insensitivity). In wild-type animals, MFB-1 negatively regulates mechanoreceptor activity by ubiquitinating MEC-4 (Chen and Chalfie, 2015). MFB-1 is an F-box containing protein, indicating that it is a component of an SCF E3 ubiquitin ligase complex (Aoyama et al., 2004). Although ubiquitination can be a step in targeting proteins for degradation through the ubiquitin-proteasome pathway, ubiquitinated proteins also function in a number of other signaling pathways (Oh et al., 2018). The ubiquitination of MEC-4 by MFB-1 does not appear to reduce MEC-4 activity by targeting it for degradation, since blocking protein degradation does not restore the loss of touch sensitivity caused by upregulation of MFB-1. Rather, touch sensitivity in mutants with increased expression of MFB-1 can be rescued by loss of caveolin/CAV-1 (Chen

and Chalfie, 2015). Caveolin is a membrane scaffolding protein that can induce endocytosis (Fridolfsson et al., 2014). Therefore, the ubiquitination of MEC-4 by MFB-1 likely targets it for removal from the plasma membrane by CAV-1 (Chen and Chalfie, 2015).

2.3 Other Key Components of Touch Receptor Neuron Physiology and Identity

TRN microtubule components: MEC-7 and MEC-12

Although microtubules are generally quite important to neuronal function, the microtubules within the TRNs appear to play an important role in mechanosensation. The TRN microtubules have a particularly wide diameter, due to their being composed of 15 protofilaments (PF) as compared to the 11-PF microtubules seen in other *C. elegans* cells (Chalfie and Thomson, 1982). While the necessity for wider diameter microtubules in the TRNs is unclear, mutants or drug-treated animals that lack 15-PF microtubules have reduced touch sensitivity (Chalfie and Thomson, 1982; Bounoutas et al., 2009a). The 15-PF microtubules have been found to influence the expression and transport of other *mec* genes and proteins, but these effects are not enough to explain the reduction in touch sensitivity that occurs in animals treated with TRN microtubule depolymerizing drugs as adults, which do not show the same defects in protein expression and distribution (Bounoutas et al., 2009a). Therefore, the 15-PF microtubules appear to affect touch sensitivity by altering the structural properties of the TRNs. It is not known to what extent they are directly involved in mechanosensory channel function or signal transduction (Krieg et al., 2015).

Microtubules are tubular structures assembled from heterodimeric protofilaments of α and β-tubulin. Most eukaryotic organisms express multiple partially redundant tubulin isoforms,

which is thought to be required for the diverse range of microtubule functions, including cell division, structuring cell shape or protrusions, intracellular transport, and cell motility (Goodson and Jonasson, 2018). *C. elegans* tubulin genes include 9 α-tubulins and 6 β-tubulins, many of which are only expressed in a subset of cells (Hurd, 2018). The tubulins that form TRN 15-PF microtubules are MEC-7 and MEC-12 (Savage et al., 1989; Fukushige et al., 1999). Both *mec-7* and *mec-12* genes are expressed in other cells lacking 15-PF microtubules, indicating that they are fundamental to but not sufficient for formation of the specialized TRN microtubules (Hamelin et al., 1992; Mitani et al., 1993; Fukushige et al., 1999). Mutations in either gene can touch insensitivity and eliminate the 15-PF microtubules, which are replaced by the more standard 11-PF microtubules (Chalfie and Thomson, 1982; Chalfie and Au, 1989). Although certain *mec-7* mutations have distinct effects, many of the mutant alleles identified confer similar phenotypic effects between the two genes, indicating the importance of their specific cooperative function.

Considering the degree of touch insensitivity conferred by *mec-7* and *mec-12* mutations, it was hypothesized that the TRN microtubules are necessary for mechanosensory channel gating, perhaps by functioning as intracellular tethers affiliated with the mechanoreceptor channel complex (Huang and Chalfie, 1994; Gu et al., 1996). However, in vivo whole-cell patch clamp recording revealed that mechanoreceptor currents (MRCs) were still present in *mec-7* and *mec-12* animals, albeit at reduced amplitudes (O'Hagan et al., 2005; Bounoutas et al., 2009a). One alternate hypothesis posits that the specialized 15-PF microtubules provide necessary mechanical rigidity (Chalfie and Thomson, 1982), but their presence alone does not seem to be sufficient, since *mec-12* alleles that preserve the 15-PF microtubules but still cause touch insensitivity have been identified (Chalfie and Au, 1989). It may be that the structural role of

TRN microtubules is mediated through attachments to the plasma membrane, which are suggested by EM images showing frequent association between distal ends of microtubules and the plasma membrane (Chalfie and Thomson, 1979; Cueva et al., 2007). Bounoutas and Chalfie (2007) suggested that such attachments might slow equilibration of the membrane, allowing channels to remain open for longer. Bounoutas et al. (2009a) noted that the *mec-12* (e1605) mutation, which causes touch insensitivity without eliminating the 15-PF microtubules, alters a residue likely situated near the microtubule exterior. The change could disrupt an interaction with a protein mediating attachment to the plasma membrane (Bounoutas et al., 2009a).

MEC-7 and MEC-12 are necessary for the maintenance of the primary PLM process and its synaptic branch; without either protein, the process and branch are generated as usual, but the process extends beyond its usual length and the synaptic branch is retracted. This was found to be due to the association between the TRN microtubules and a microtubule-associated Rho guanine nucleotide exchange factor, RHGF-1. In the absence of MEC-7 or MEC-12, RHGF-1 activates a DLK-1 neuronal remodeling signaling pathway involved in both Wallerian degeneration and axon regeneration (Chen et al., 2014). In a separate study, DLK-1 signaling resulting from loss of TRN microtubules (caused by loss of either *mec-7*, *mec-12*, or the microtubule depolymerizing drug colchicine) was found to reduce the expression of many proteins including several necessary for touch sensitivity (Bounoutas et al., 2011).

Certain *mec-12* missense alleles and *mec-7* alleles in a sensitized background have been found to cause morphological distortions in the TRNs appearing as bends or kinks in the processes and TRN axonal degeneration (Hsu et al., 2014; Krieg et al., 2017). Similar phenotypes have been observed in mutants for microtubule associated and cytoskeletal proteins (Topalidou et al., 2012; Krieg et al., 2014), and in older animals and mutants with accelerated

aging phenotypes (Pan et al., 2011). No such distortions have been found in mutants lacking 15-PF microtubules, suggesting that they can be caused by defects in microtubules, but not by their absence (Krieg et al., 2017).

Mutations in either *mec-7* or *mec-12* can cause disruption of MEC-2 and MEC-4 localization, defects in synaptic vesicle transport, and aberrant ribosomal distribution (Huang et al., 1995; Emtage et al., 2004; Krieg et al., 2017; Noma et al., 2017). These phenotypes may be due to the role of microtubules in intracellular transport, for which they serve as tracks for cargo-carrying proteins like kinesins and dyneins.

Earlier evidence suggested that the loss of either *mec-7* or *mec-12* eliminated the formation of 15-PF microtubules (Chalfie and Thomson, 1982; Chalfie and Au, 1989; Fukushige et al., 1999), but it has since been found that the *mec-12* mutation previously thought to be a null allele is most likely an antimorphic gain of function allele that interferes with MEC-7 (Zheng et al., 2017). *mec-12* deletion alleles reduced the abundance of microtubules but did not affect the microtubule diameters measured from EM images. Therefore, MEC-7 is necessary for the formation of 15-PF microtubules, and can form 15-PF microtubules with a different α-tubulin isoform in the absence of MEC-12 (Zheng et al., 2017). In the absence of MEC-7, 15-PF microtubules are replaced by the more standard 11-PF microtubules (Chalfie and Thomson, 1982; Zheng et al., 2017). The 11-PF microtubules are sufficient for neurite outgrowth to occur but result in touch insensitivity (Chalfie and Sulston, 1981).

A phenotype particular to some *mec-7* mutants is the extensive growth of an ectopic posterior neurite in ALM (Savage et al., 1994). In wild-type animals, ALM has a long anterior neurite and a very short or absent posterior neurite. *mec-7* neomorphic mutations thought to confer increased microtubule stability result in dramatic extension of the posterior neurite, which

assumes an axon-like identity as implied by mislocalized presynaptic markers and synaptic vesicles (Kirszenblat et al., 2012). The existence of *mec-12* alleles that produce a similar but less extreme phenotype suggest that both tubulins affect the regulation of microtubule stability, but that MEC-7 plays a more significant role (Zheng et al., 2017). The development of the ectopic axon interferes with the growth and function of the anterior neurite, preventing full extension and resulting in lower levels of presynaptic markers (Kirszenblat et al., 2012; Zheng et al., 2017). Furthermore, most or all of the *mec-7* alleles that result in the growth of an ectopic posterior neurite have reduced touch sensitivity (Zheng et al., 2017).

Zheng et al. (2017) grouped the morphological effects of *mec-7* missense mutations into three categories: 1) loss of function mutations that caused effects similar to those associated with the knockout allele, 2) dominant-negative antimorphic alleles that resulted in severely shortened neurites, and 3) neomorphic alleles that caused growth of the ALM posterior neurite. A large set of *mec-7* missense alleles were categorized accordingly and mapped to a predicted structure of MEC-7 using the solved structure of bovine β-tubulin for reference. Loss of function mutations were distributed throughout the protein, but anti and neomorphic alleles had mutations clustered in particular regions. The antimorphic alleles caused changes in regions thought to be important for tubulin polymerization, including the GTP/GDP binding pocket and the interdimer interfaces. Most of the neomorphic alleles had altered residues on the exposed surfaces of the microtubules, suggesting that they may affect interactions with other proteins.

MEC-12 is unique in that it is the only *C. elegans* tubulin with a lysine-40 acetylation site (Fukushige et al., 1999). Acetylated MEC-12 has been detected both in vivo and in cultured TRNs, and at lower levels in other neurons that express MEC-12 (Fukushige et al., 1999; Bianchi et al., 2004; Solinger et al., 2010). Some of the phenotypes associated with mutations in *mec-12*

have been hypothesized to result from changes in or loss of microtubule acetylation (Solinger et al., 2010; Cueva et al., 2012). However, the role of α-tubulin acetylation is unclear, as non-acetylatable MEC-12 has been shown to rescue *mec-12* mutant phenotypes including touch insensitivity and axonal degeneration (Fukushige et al., 1999; Neumann and Hilliard, 2014). Furthermore, phenotypes caused by *mec-12* alleles are not particularly distinct from those caused by *mec-7*, suggesting that mutations in *mec-12* affect TRN morphology through the general disruption of microtubules, rather than by specifically disrupting the acetylation of microtubules. Cueva et al. (2012) proposed that the polymorphic microtubules seen in both α-tubulin acetylase deficient mutants and *mec-12* mutants rescued with non-acetylatable MEC-12 resulted from the absence of acetylated tubulin, but microtubules of varying shape and diameter have also been reported in *mec-7* mutants (Savage et al., 1994). Hsu et al. (2014) reported on a *mec-12* gain-of-function mutation that resulted in axon swelling and neuronal degeneration, similar to a phenotype caused by loss of the α-tubulin acetyltransferase MEC-17, but the *mec-12* mutant was found to retain acetylated tubulin, and a similar phenotype has since been described in a *mec-7*/β-spectrin double mutant (Krieg et al., 2017). The role of tubulin acetylation will be further discussed in relation to MEC-17.

TRN microtubule-associated proteins: MEC-17, ATAT-2, and others

Microtubule-associated proteins (MAPs) are essential for orchestrating the properties and organization of microtubules. MAPs can act to stabilize, destabilize, and bundle microtubules, and some serve as intermediaries for association between the microtubules and other proteins or cellular structures. Some MAPs alter microtubules through post-translational modifications of tubulin, which can include acetylation, polyglutamylation, phosphorylation, and detyrosination.

Post-translational modifications can alter the physical properties of microtubules such as stability and rigidity, but they can also affect the kinetics of proteins that interact with microtubules (Bodakuntla et al., 2019). In the TRNs, MAPs associated with changes in touch sensitivity include the α-tubulin acetylases MEC-17 and ATAT-2, the tau-like protein PTL-1, the microtubule organizing protein ZYG-8, and the less well understood ELP-1.

MEC-17 is a particularly intriguing protein in that its non-enzymatic activity appears to be more important for touch sensitivity than its tubulin acetyltransferase activity (Topalidou et al., 2012). MEC-17 is exclusively expressed in the TRNs, and at higher levels than even MEC-7 or MEC-12 (Zhang et al., 2002; Topalidou and Chalfie, 2011). *mec-17* mRNA is found throughout TRN axonal processes but has been demonstrated to act at the protein level, suggesting a requirement for newly synthesized MEC-17 along the processes. The other *C. elegans* tubulin acetyltransferase, ATAT-2, is redundant with MEC-17 in regards to enzymatic activity, but its mRNA is expressed at relatively lower levels in the TRNs and is localized to the cell body (Topalidou et al., 2012). Even so, *atat-2* mutants have reduced touch sensitivity (Akella et al., 2010; Shida et al., 2010). Unlike *mec-17*, *atat-2* is broadly expressed in other neurons (Shida et al., 2010).

Loss of MEC-17 can cause morphological abnormalities in TRN processes including bends and kinks, beading or swelling, ectopic branching, and axonal degradation. *mec-17* mutants also show variation in TRN microtubule diameter, loss of microtubule luminal material, and disruptions in microtubule organization. Microtubules in the TRNs normally form a single continuous bundle, but in *mec-17* mutants they often dissociate from the main bundle and pack into different arrangements. These phenotypes suggest an important role for MEC-17 in microtubule formation and stability (Topalidou et al., 2012). Neumann and Hilliard (2014) found

that *mec-17* mutants had an increased number of growing microtubules, but with significantly reduced growth rates. No changes in microtubule track length or growth duration were observed.

The effect of tubulin acetylation on touch sensitivity in *C. elegans* is somewhat unclear but appears to be limited. Akella et al. (2010) concluded that non-acetylatable MEC-12 is about 30% less efficient at rescuing touch sensitivity in *mec-12* mutant animals compared to the wild-type protein, and Shida et al. (2010) found an even larger difference between *mec-12* mutants rescued with wild-type and non-acetylatable MEC-12. It's unclear whether these results contradict an earlier report by Fukushige et al. (1999) that non-acetylatable MEC-12 rescues touch insensitivity in *mec-12* mutants, as the authors did not provide experimental data or explicitly compare to rescue with wild-type MEC-12. Shida et al. (2010) reported that *mec-17* mutants rescued with wild-type MEC-17 were more touch sensitive than those rescued with catalytically inactive MEC-17, but their data suggest that introduction of the wild-type MEC-17 did not rescue touch sensitivity and that the catalytically inactive MEC-17 in fact reduced touch sensitivity. Subsequently Topalidou et al. (2012) concluded that MEC-17 acetyltransferase activity is not needed for touch sensitivity after demonstrating that wild-type and two catalytically inactive versions of MEC-17 rescue touch insensitivity in *mec-17* and *mec-17*; *atat-2* mutants to about the same extent. Their data suggest that *mec-17*; *atat-2* mutant animals rescued with catalytically inactive constructs were slightly less touch sensitive than mutants rescued with wild-type MEC-17, but not significantly so. In another attempt to address the controversy, Davenport et al. (2014) tested the ability of variants of human MEC-17 to rescue touch insensitivity in *mec-17*; *atat-2* mutant animals, and found that catalytically active and inactive versions were equally effective. Overall, it appears that α-tubulin acetylation could have some effect on *C. elegans* touch sensitivity but is not essential.

Interestingly, the enzymatic role of MEC-17 orthologs appears to be important for mechanosensation in other organisms. In Drosophila, blocking α-tubulin acetylation through either non-acetylatable α-tubulin alleles or α-tubulin acetyltransferase (dTAT) knockout resulted in loss of gentle touch response. dTAT knockout animals with or without catalytically inactive dTAT showed disruptions in microtubule density and localization, suggesting an effect of tubulin acetylation on microtubule dynamics (Yan et al., 2018). Mice lacking the mammalian *mec-17* ortholog Atat1 showed dramatic defects in response to both gentle and harsh mechanical stimuli, which could not be rescued by catalytically inactive Atat1. However, unlike in *C. elegans* and Drosophila, Atat1 knockout mice did not display changes in the overall organization of the microtubule network. Rather, there appeared to be changes in the mechanical rigidity of the sensory neurons, so that more force was required to activate mechanosensitive ion channels (Morley et al., 2016).

Some of the phenotypes associated with loss of MEC-17 in *C. elegans* are not rescued by catalytically inactive variants, including microtubule abundance, microtubule protofilament number, and axonal morphological defects (Topalidou et al., 2012). Interestingly, this implies that microtubule abundance and protofilament number do not play a significant role in touch sensation. However, they may be necessary for TRN axonal integrity, allowing animals to remain touch sensitive as they age. The effect of MEC-17 and α-tubulin acetylation on microtubule dynamics is not straightforward, since both stabilizing and destabilizing effects have been reported (Kalebic et al., 2013; Yang et al., 2013; Neumann and Hilliard, 2014; Portran et al., 2017). The emerging consensus is that α-tubulin acetyltransferase (αTAT) promotes long-lived microtubules by weakening interactions between protofilaments, rendering microtubules more flexible and more resilient to breakage following repeated mechanical deformation (Eshun-

Wilson et al., 2019). It should be noted that 15-PF microtubules are stiffer than lower PF number microtubules (Gittes et al., 1993), which might make them particularly susceptible to breakage.

Non-catalytic effects of αTAT have also been demonstrated in vitro (Howes et al., 2013) and in mammalian cells (Kalebic et al., 2013), suggesting that the binding of the enzyme has direct effects on microtubule dynamics. There is also evidence to suggest that αTAT binds tubulin at multiple sites, both on the luminal surface (where acetylation takes place) and on the outer surface (which is not associated with any αTAT enzymatic activity) (Howes et al., 2013). Interestingly, the enzymatic activity of αTAT seems to require an unusual amount of substrate interaction. In human MEC-17, a large hydrophobic patch that appears to make extensive contacts with α-tubulin is required for enzymatic activity (Davenport et al., 2014). Given the considerable amount of physical interaction between αTAT and tubulin, it is not surprising that αTAT binding should have structural consequences. Indeed, it's been hypothesized that MEC-17 affects *C. elegans* touch sensitivity regardless of enzymatic activity by acting as a structural component (Topalidou et al., 2012).

Although MEC-17 plays a more important role in microtubule structure than ATAT-2, the other α-tubulin acetyltransferase expressed in TRNs, ATAT-2, has a greater effect on TRN synapse maintenance. *atat-2* mutant animals exhibit normal synapse assembly but fail to retain synaptic branches and boutons, as observed via fluorophore-tagged synaptic vesicle marker RAB-3 and presynaptic active-zone markers UNC-10 and SYD-2. Disrupted synapse maintenance was also observed in *mec-17* mutants, but to a lesser extent. Acetyltransferase-dead ATAT-2 failed to rescue the synaptic maintenance defects seen in *atat-2* mutants, and treatment of *atat-2* mutant animals with the microtubule destabilizing drug colchicine enhanced the phenotype, indicating a necessity for acetylated tubulin. The effect of ATAT-2 on synapse

maintenance appears to occur through a pathway including the signaling protein RPM-1, since *rpm-1* mutants display a similar phenotype to *atat-2* mutants and *rpm-1*; *atat-2* double mutants. Additional genetic interactions suggest that ATAT-2 acts downstream of RPM-1. In contrast, mutations in *mec-17* enhance the synapse maintenance phenotype caused by mutations in *rpm-1* (Borgen et al., 2019).

The chemical synapses formed by the TRNs are not required for touch sensitivity (Chalfie et al., 1985) but affect modulations of the touch response such as habituation (Rankin and Wicks, 2000). In the process of habituation, animals become less likely to respond to stimulation after repeated exposures within an appropriate timeframe. Indeed, *atat-2* and *rpm-1* mutants are slower to habituate to mechanosensory stimuli. Loss of RPM-1 causes greater habituation defects than loss of ATAT-2, but *rpm-1*; *atat-2* double mutants habituate similarly to *rpm-1* mutants (Borgen et al., 2019). The more dramatic habituation phenotype seen in *rpm-1* mutants as compared to *atat-2* mutants is probably due to the large number of RPM-1 downstream targets (Grill et al., 2016). Furthermore, in addition to acting as a signaling hub within the TRNs, RPM-1 is expressed widely throughout the nervous system, including in the interneurons that process and relay input from the TRNs (Park et al., 2009) and in the motor neurons that drive muscle activity (Zhen et al., 2000).

The *C. elegans* MAP PTL-1 was first investigated due to its homology to the human protein tau (Goedert et al., 1996), which plays a role in many human disease states (Morris et al., 2011). In adult *C. elegans*, PTL-1 was found to be expressed in a variety of cells, but with highest expression levels in ALM, PLM, and AVM (Goedert et al., 1996; Gordon et al., 2008). Furthermore, loss of *ptl-1* was shown to cause very slightly reduced touch sensitivity alone and further decreased touch sensitivity in combination with a loss-of-function β-spectrin (*unc-70*)

mutation (Gordon et al., 2008). Since tau is a microtubule binding protein that promotes microtubule assembly and stability, it was hypothesized that PTL-1 affects touch sensitivity through association with the TRN 15-PF microtubules (Goedert et al., 1996). Using light microscopy, Gordon et al. (2008) did not observe any defects in TRN microtubule formation or localization in *ptl-1* null mutants, but subsequent electron microscopy analysis showed that *ptl-1* mutants had fewer, shorter microtubules that were closer together than in wild type animals (Krieg et al., 2017). However, Chew et al. (2013) found that *ptl-1* C-terminal deletion mutants lacking the microtubule binding domain (MBD) were fully touch sensitive. Thus, it is still unclear how PTL-1 affects touch sensitivity.

Even so, the microtubule binding activity of PTL-1 does seem to be necessary for maintaining the morphological integrity of aging TRNs. *ptl-1* null and MBD deletion mutants show hastened accumulation of age-related TRN defects including axon swelling and ectopic branching (Chew et al., 2013). Krieg et al. (2017) suggested that PTL-1 protects the axon from mechanical stress by allowing adjacent microtubules to glide past one another in light of their finding that *ptl-1* mutants had more closely spaced microtubules. It might be interesting to relate the effects of PTL-1 to those of MEC-17, since PTL-1 is thought to increase the rigidity of microtubules (Gordon et al., 2008; Krieg et al., 2017) while α-tubulin acetylation is thought to protect neuronal integrity by decreasing the rigidity of microtubules (Eshun-Wilson et al., 2019).

ZYG-8 is a MAP required for full touch sensitivity but is also necessary for mitotic cell division (Bellanger et al., 2012). Loss of ZYG-8 results in embryonic lethality (Wood et al., 1980), so temperature-sensitive alleles have been used to study its function beyond early development. ZYG-8 is expressed in the germline, gonad, hypodermis, ventral nerve cord motor neurons, amphid neurons, and the six TRNs (Bellanger et al., 2012). The TRNs of *zyg-8* mutants

often have misshapen cell bodies and shortened lateral branches and occasionally have polarity defects. These defects are likely due to disruption of the TRN microtubules, as *zyg-8* mutant TRNs have fewer and shorter microtubules that fail to organize into bundles. Protofilament number is unaffected in *zyg-8* mutants, suggesting that loss of ZYG-8 does not affect initial microtubule polymerization dynamics but is necessary for either the growth or maintenance of longer microtubules (Bellanger et al., 2012). The retention of 15-PF microtubules in *zyg-8* mutants also adds to the evidence that large-diameter microtubules alone are not sufficient to confer wild-type touch sensitivity. The number, length, and organization of microtubules appear to be crucial as well.

ZYG-8 binds directly to microtubules via its doublecortin (DCX) domain. ZYG-8 also contains a kinase domain, which is not necessary for its association with microtubules, but studies of various *zyg-8* alleles in embryo development suggest that efficient ZYG-8 function requires kinase activity (Gönczy et al., 2001). Interestingly, vertebrate doublecortin-like kinase (DCLK) is capable of autophosphorylating its DCX domain (Burgess and Reiner, 2000), but removal of the kinase domain increases the microtubule-binding ability of the DCX domain (Nagamine et al., 2011). It is not known whether phosphorylation of ZYG-8 has similar effects. Nevertheless, ZYG-8 likely influences microtubule stability and organization through binding to microtubules. The TRN microtubules in *zyg-8* mutants were observed to be closer together than in wild-type animals, suggesting that ZYG-8 binding may control the spacing between adjacent microtubules. The reduced length and number of microtubules in *zyg-8* mutants implies that ZYG-8 binding also increases microtubule stability (Bellanger et al., 2012).

ELP-1 is another MAP found to affect touch sensitivity, but its involvement has not been studied in depth. ELP-1 is expressed in the TRNs and other neurons including the ray neurons in

the male tail and the ciliated IL1 neurons, as well as in muscles, intestinal cells, and hypodermal seam cells (Hueston et al., 2008). Fluorophore-tagged ELP-1 localizes to microtubules and to focal adhesion sites throughout the body-wall muscle. A predicted hypomorphic allele and dsRNAi against *elp-1* caused reduced touch sensitivity (Hueston et al., 2008). Hueston et al. (2008) suggest that ELP-1 may act in TRNs to bundle microtubules or to anchor microtubule ends to the plasma membrane, but these hypotheses have yet to be tested.

Additional post-translational touch protein regulators: MEC-15

15-PF microtubule stability is likely to also depend on the activity of MEC-15, albeit indirectly. The loss of *mec-15* has widespread effects on the development and function of the TRNs, including abnormal cell body morphology, shortened processes, defects in chemical synapse formation, loss of microtubules, and reduced touch sensitivity (Bounoutas et al., 2009b; Zheng et al., 2020). Most or all of these mutant phenotypes appear to stem from microtubule disfunction, as is evidenced by that mutations in *mec-7* and *mec-12* can dominantly suppress or enhance all *mec-15* null phenotypes (Bounoutas et al., 2009b).

MEC-15 is an F-box protein with WD40 repeats. The F-box motif is a protein-protein interaction domain that binds to SKP1 proteins in Skp1-Cullin1-F-box (SCF) ubiquitin-ligase complexes, which generally target proteins for degradation. F-box proteins act as the SCF complex substrate-recognition subunit by interacting with the target protein(s), generally through other protein-protein interaction domains such as WD repeats or leucine-rich repeats (Kipreos and Pagano, 2000). Therefore, MEC-15 likely targets microtubule destabilizing proteins for degradation through the ubiquitination-proteasome system (UPS).

To identify the target(s) of MEC-15, Zheng et al. (2020) performed a screen for suppressors of *mec-15* mutant phenotypes. Among the *mec-15* suppressing mutations were lesions in two heat-shock protein (hsp) cochaperone genes, *sti-1* and *pph-5*, and in the dual leucine zipper kinase gene *dlk-1*. While fluorophore-tagged STI-1 and PPH-5 protein levels appeared unchanged in a *mec-15* mutant background, DLK-1 levels were elevated, suggesting that MEC-15 targets DLK-1 but not STI-1 or PPH-5. Furthermore, the loss of *dlk-1* suppressed the effects of loss of *sti-1* or *pph-5*, suggesting that STI-1 and PPH-5 are upstream regulators of DLK-1. Zheng et al. (2020) concluded the hsp chaperones and UPS are likely acting against each other, with chaperones stabilizing proteins that are then degraded by the UPS. Zheng et al. (2020) also found that loss of hsp chaperone pathway components including STI-1 and PPH-5 rescued touch insensitivity in *mec-15* mutants, but loss of DLK-1 did not. Therefore, MEC-15 likely targets proteins other than DLK-1, and hsp chaperones likely act on other proteins that destabilize microtubules in the absence of MEC-15 mediated degradation.

TRN intracellular calcium regulators: EGL-19, UNC-36, and others

Following TRN membrane depolarization by mechanoreceptor channels, a rise in intracellular calcium occurs (Suzuki et al., 2003). Intracellular calcium levels are generally used as a proxy for measuring neuronal activity and measurements of TRN activity have been done as such, but the role of calcium transients in TRN signal transmission is unclear. While there does seem to be a general correspondence between the amplitude of calcium transients and response probability, mutations that reduce the amplitudes of calcium transients do not necessarily cause a proportional decrease in response probability, and vice-versa (Suzuki et al., 2003; Chen and Chalfie, 2014). However, intracellular calcium levels appear to play a key role in TRN

habituation (Kindt et al., 2007). Direct measurements of membrane depolarization in the TRNs showed no changes in mechanoreceptor current following repeated stimuli (O'Hagan et al., 2005), but in vivo calcium indicators have shown calcium transients of decreasing amplitude corresponding to short-term habituation (Suzuki et al., 2003; Kindt et al., 2007).

In investigating the calcium transients invoked by mechanosensory stimuli, Suzuki et al. (2003) tested mutants for several known calcium channels and found that only *egl-19* alleles affected the observed calcium transients. EGL-19 is an α1 subunit of a voltage gated calcium channel (VGCC), a plasma membrane-bound channel that allows relatively long-lasting (L-type) influx of calcium upon activation by high voltage. VGCC α1 subunits independently form a channel pore and are sensitive to voltage; accessory subunits modulate channel kinetics and subcellular targeting (Roca-Lapirot et al., 2018). EGL-19 is expressed in some neurons and widely across muscle types (Lee et al., 1997), where it is a major carrier of inward current and is required for muscle cell action potentials (Liu et al., 2011). *egl-19* null mutants are lethal due to embryonic arrest caused by the inability of body wall muscles to contract, but gain of function and partial loss of function alleles have been isolated (Lee et al., 1997).

In vivo imaging of TRNs demonstrated that an *egl-19* loss of function allele significantly reduced the magnitude of calcium influx, but touch sensitivity assays on animals carrying the same allele only showed a slight reduction in response probability (Suzuki et al., 2003). Cultured mechanoreceptor neurons showed reduced calcium influx due to mutations in *egl-19*, but also in *unc-36*, a VGCC α2/delta subunit. Strangely, *unc-36* mutant animals did not show significant changes in the TRN calcium transients measured in vivo, but *unc-36* mutants were more touch insensitive than *egl-19* mutants. This led to the finding that *unc-36* mutants sometimes have AVM cell migration defects (23% penetrance) and occasional ALM cell migration defects (8%

penetrance). The cell migration phenotypes are too low penetrance to account for the observed reduction in touch sensitivity, but they indicate a functional role for UNC-36 in TRN development (Frøkjær-Jensen et al., 2006). *egl-19* mutants also showed some AVM and ALM migration defects, as did mutants for *unc-2*, a gene encoding a non-L-type VGCC α1 subunit (Tam et al., 2000; Kindt et al., 2002). UNC-36 is thought to form complexes with both EGL-19 and UNC-2 (Schafer et al., 1996; Lainé et al., 2011), but the gentle touch and cell migration phenotypes compared between *unc-2* and *unc-36* are more similar than those between *egl-19* and *unc-36*. Therefore, the defects in *unc-36* mutants are likely tied to the role of UNC-36 as an auxiliary subunit of UNC-2 (Frøkjær-Jensen et al., 2006). Indeed, mutations in *unc-36* often phenocopy mutations in *unc-2*, suggesting that they commonly interact (Caylor et al., 2013).

unpublished

Unlike EGL-19, which is expressed mostly in muscle cells (Lee et al., 1997), UNC-2 is expressed exclusively in the nervous system (Mathews et al., 2003). UNC-2 has been implicated in a variety of nematode behaviors, including locomotion, egg-laying, feeding, and defecation (Brenner, 1974; Avery, 1993; Schafer and Kenyon, 1995; Mathews et al., 2003). The behavioral defects associated with mutations in *unc-2* are largely attributed to its role in synaptic release, but UNC-2 has also been shown to affect cell migration, synapse formation, intrinsic membrane potential oscillation, and asymmetric neuronal fate (Tam et al., 2000; Schumacher et al., 2012; Caylor et al., 2013; Gao et al., 2018). Thus, although *unc-2* null mutations are not lethal, the systemic importance of UNC-2 has likely discouraged straightforward investigation as to its role in TRN development and function. There are few studies addressing the relationship between UNC-2 and touch sensitivity, despite the significant reduction in touch sensitivity cause by mutations in *unc-2* (M. Chalfie, ; Frøkjær-Jensen et al., 2006).

Even so, much has been learned about the structure and function of UNC-2 through mutational analysis in *C. elegans* and by relation to vertebrate homologs, which have been well studied due to their role in human physiology (Dolphin, 2018). Like other VGCC α1 subunits, UNC-2 is a relatively large protein, with its longer isoforms coding for over 2000 amino acids. The protein contains four repeated homologous domains (I-IV) joined by intracellular linkers, with each repeat containing six membrane spanning α-helices (S1-S6) (Mathews et al., 2003). S4 is thought to be most critical for the voltage-sensing properties of the channel, S6 contains most of the pore-lining residues, and a hydrophobic region between S5 and S6 (P-loop) plays a crucial role in the channel's ion selectivity (Pozdnyakov et al., 2018). The domain I-II linker contains G-protein βγ and calcium channel β subunit binding motifs, and the C-terminal domain following domain IV contains calmodulin binding IQ motifs and a calcium binding EF-hand (Mathews et al., 2003). Characterized *unc-2* loss of function missense mutations don't appear to be clustered, but map to S2, S4, between S4 and S5, between S5 and S6, and the C-terminal domain (Mathews et al., 2003; Huang et al., 2019). A gain of function missense mutation thought to decrease the voltage activation threshold has been identified within the intracellular linker following IIIS6, and transgenic animals with substitutions in and near IS4 also appear to have hyperactive channels (Huang et al., 2019). The lack of clustered missense mutations identified in *unc-2* suggests that much of the amino acid sequence is critical for proper channel function. Indeed, most of the coding sequence is highly conserved between homologs and orthologs (Mathews et al., 2003).

Another intracellular calcium regulator found to affect touch sensitivity is MCA-3. MCA-3 is a plasma membrane calcium transport ATPase that pumps excess calcium out of the cytoplasm. Null mutations of *mca-3* are lethal, likely due to toxic increases in cytosolic calcium

levels, which can initiate programmed or degenerative cell death (Bednarek et al., 2007). However, RNAi against *mca-3* and a partial loss of function allele were found to significantly reduce touch sensitivity (Chen et al., 2015a). Interestingly, *mca-3* mutant animals had normal levels of baseline cytoplasmic calcium concentration in ALM neurons and showed reduced calcium level increases in response to touch. The reduced calcium response to touch suggests defects upstream of the components involved in producing touch-evoked calcium transients (Chen, 2013). Since MCA channels are thought to be inactive at resting cytosolic calcium levels (Hegedűs et al., 2020), it may be that the loss of function mutation characterized allows sufficient channel activity to maintain a normal baseline state but leads to longer periods of elevated calcium levels following mechanical stimulation. The temporal increase in calcium levels might cause mechanoreceptor channels to become inactivated, as is hypothesized to occur through post-translational modifications (Chen and Chalfie, 2015).

Pre-translational touch gene regulators: MEC-8, MEC-3, and others

Mutations that result in touch insensitivity have also been found in pre-translational regulators of touch gene expression, including the RNA processing gene MEC-8 and transcription factors involved in TRN cell fate determination. These include MEC-3, UNC-86, and ALR-1, which are involved in the initiation and maintenance of TRN differentiation, and CEH-13, EGL-5, and LIN-32 which are involved in earlier stages of TRN differentiation.

MEC-8 is a nuclear protein that binds mRNA and regulates alternative splicing (Lundquist et al., 1996). Several targets of MEC-8 regulation are known, but it is likely only or mostly through regulation of the *mec-2* mRNA that MEC-8 affects touch sensitivity. In the absence of MEC-8, the ninth intron of *mec-2* is not spliced out and translation terminates before

assembly of the MEC-2 C-terminal domain necessary for interaction between MEC-2 and MEC-4 (Calixto et al., 2010b). MEC-8 is expressed widely in the early embryo and gradually becomes more restricted during larval stages and adulthood, at which point expression occurs in the hypodermis, intestine, vulval cells, chemosensory neurons, and the TRNs (Spike et al., 2002; Calixto et al., 2010b). In addition to touch insensitivity, phenotypes associated with loss of MEC-8 include cold-sensitive embryonic and larval lethality, aberrant chemosensation, defects in ciliated sensory neurons, and deficient attachment of the body wall muscle to the hypodermis (Perkins et al., 1986; Chalfie and Au, 1989; Lundquist and Herman, 1994). In addition to *mec-2*, known targets of MEC-8 regulation include the perlecan proteoglycan gene *unc-52* and the fibrillin glycoprotein gene *fbn-1* (Lundquist et al., 1996; Kelley et al., 2015).

MEC-8 has two RNA recognition motifs (RRM) on either side of a low-complexity sequence high in alanine and glutamine residues (Lundquist et al., 1996). Comparable regions with large proportions of alanine and glutamine (AQ) are found in other RNA-binding proteins such as SUP-12, ASD-1, and FOX-1, but their function is unclear (Mackereth, 2015). It's hypothesized that AQ-rich regions are involved in protein-protein interactions or protein localization (Toba and White, 2008; Mackereth, 2015). MEC-8 is believed to function as a homodimer, as has been demonstrated for homologous vertebrate RNA-binding proteins (Sagnol et al., 2014; Teplova et al., 2016). A homodimerization motif identified in the vertebrate RNA-binding protein for multiple splicing 2 (RBPMS2) is conserved within the first RRM of MEC-8 (Sagnol et al., 2014), and a purified construct containing the first RRM of MEC-8 has been shown to dimerize in vitro (Soufari and Mackereth, 2017).

Some of the genes discussed so far can be considered TRN cell fate markers, since they are only expressed in cells that have differentiated to TRN identity. These include *mec-4*, *mec-7*,

mec-17, and *mec-18*. Other genes expressed in the TRNs including most of those discussed above are considered TRN terminal differentiation genes, since they are expressed in TRNs after the occurrence of terminal differentiation. TRN cell fate markers and many of the TRN terminal differentiation genes are directly regulated by the cooperative binding of two transcription factors, MEC-3 and UNC-86 (Xue et al., 1992; Xue et al., 1993; Duggan et al., 1998; Zhang et al., 2002). Although MEC-3 and UNC-86 cooperatively regulate TRN terminal differentiation genes, their mutant phenotypes are somewhat distinct. In *mec-3* loss-of-function mutants, ALM neurons adopt the identity of their sister cell BDU (Way and Chalfie, 1988; Gordon and Hobert, 2015). Since BDU cell fate requires UNC-86, loss-of-function mutations in *unc-86* do not lead to the same phenotype (Gordon and Hobert, 2015). UNC-86 is generally more widely expressed than MEC-3, being found in 57 adult neurons (Finney and Ruvkun, 1990). MEC-3 expression is found in adult TRNs, FLP, PVD, ventral nerve cord cells, vulval cells, and two neurons that may be AIZL/R (Way and Chalfie, 1989). Both *mec-3* and *unc-86* loss-of-function alleles abolish gentle touch sensitivity (Chalfie and Sulston, 1981; Sze et al., 1997).

The establishment of TRN cell fate certainly necessitates expression of MEC-3 and UNC-86, but additional factors are clearly involved since MEC-3 and UNC-86 are expressed together in other cells that do not share TRN identity (Way and Chalfie, 1988; Finney and Ruvkun, 1990). Additional facilitatory factors expressed only in TRNs have been identified, such as ALR-1. ALR-1 appears to work by reducing the variability of MEC-3 expression levels (a threshold level of MEC-3 expression is required for TRN differentiation, and if *mec-3* transcription is activated but does not exceed the threshold level, MEC-3 expression is not maintained). Indeed, *alr-1* mutant animals are variably touch insensitive (Topalidou and Chalfie, 2011). In contrast, some cells that express both MEC-3 and UNC-86 prevent the adoption of

TRN cell fate via inhibitory factors. Inhibitory/negative regulators of TRN identity include EGL-44, EGL-46, and PAG-3 (Mitani et al., 1993; Jia et al., 1996). However, inhibitory factors have not been identified for most cells that express both MEC-3 and UNC-86.

To provide one example of positive and negative regulators acting in balance to prevent TRN cell fate: FLP and PVD neurons are prevented from differentiating into TRNs by expression of the cooperating transcription factors EGL-44 and EGL-46 (Mitani et al., 1993; Wu et al., 2001). MEC-3 and UNC-86 are necessary for the differentiation of the FLP and PVD neurons, as is demonstrated by the sluggish movement patterns caused by loss of FLP and PVD in *mec-3* mutant animals (Albeg et al., 2011), but the negative regulators EGL-44 and EGL-46 inhibit both expression of TRN-specific genes and expression of the positive regulator ALR-1 (Zheng et al., 2018). Another positive regulator of TRN cell fate that acts subsequent to the activation of *mec-3* by UNC-86 is AHR-1. In AVM, AHR-1 increases MEC-3 expression and blocks the expression of PVD terminal differentiation genes. In *ahr-1* mutant animals, AVM adopts a PVD-like morphology with increased dendritic branching and anterior touch sensitivity is reduced (Smith et al., 2013).

Unlike ALR-1 and AHR-1, the transcription factor ZAG-1 appears to promote TRN cell fate independently of MEC-3 and UNC-86 activity. ZAG-1 is expressed in the six TRNs and is absent in FLP and PVD, but expression of *zag-1* is not affected by mutations in *mec-3* (Zheng et al., 2018). ZAG-1 inhibits the expression of *egl-44* and *egl-46*, and *zag-1* mutants appear to have an extra PVD-like cell as a result of PVM adopting the PVD cell fate (Smith et al., 2013). However, ZAG-1 also appears to be necessary for normal neurite development, since loss-of-function mutations in *zag-1* result in severely shorted ALM and PLM neurites (Zheng et al., 2018). Such defects have not been observed in *mec-3* loss-of-function mutants, further

reinforcing a role for ZAG-1 beyond simply promoting TRN differentiation. *zag-1* loss-of-function mutant animals are touch insensitive (Smith et al., 2013).

Prior to TRN differentiation, the activation of *mec-3* by UNC-86 is facilitated by HOX proteins. Although HOX proteins are not strictly necessary for the adoption of TRN fate, mutations in HOX proteins result in incompletely penetrant TRN differentiation and morphological defects (Zheng et al., 2015). In the anterior cells, the HOX protein CEH-13 is necessary to increase the probability of MEC-3 activation. The autoregulation of CEH-13 requires the TALE cofactor CEH-20, and indeed, *ceh-20* mutant animals display ALM differentiation phenotypes similar to those observed in *ceh-13* mutant animals and exhibit reduced anterior touch sensitivity (Zheng et al., 2015). Additionally, the HOX cofactor UNC-62 appears to affect ALM positioning and axonal guidance in a non-cell-autonomous manner.

In the posterior TRN precursor cells, the HOX protein EGL-5 is necessary to increase the probability of *mec-3* activation. Interestingly, even though EGL-5 is involved in PLM differentiation, it also appears to be necessary for the function of differentiated PLMs. *mec-17*, a TRN fate marker, is expressed in at least one PLM in more than 75% of *egl-5* mutants but 100% of *egl-5* mutant animals are posterior touch insensitive (Zheng et al., 2015). EGL-5 is subject to suppression by the HOX gene regulator SEM-4 in PHC and PLN. Loss of function mutations in *sem-4* cause PHC and PLN to adopt PLM and PVM-like fates, but a gain-of-function allele that causes reduced touch insensitivity has also been identified (Toker et al., 2003). Like *egl-5*, the HOX genes *nob-1* and *php-3* are also necessary for PLM differentiation, but unlike *egl-5* they appear to act prior to the onset of *unc-86* expression, since *nob-1* and *php-3* mutants are generally deficient in *unc-86* expressing cells. A viable loss-of-function allele that decreases posterior touch sensitivity has been identified for *nob-1*, but not *php-3* (Zheng et al., 2015).

LIN-32 and VAB-15 are transcription factors with roles in embryonic development and touch cell precursor differentiation and migration. A *lin-32* allele was identified in the original set of mutagenesis for touch insensitive mutants, where it was found to cause only posterior touch insensitivity (Chalfie and Au, 1989). *lin-32* mutants lack AVM, PVM, and PLM cells (Chalfie and Au, 1989) and have present but displaced ALMs (Hedgecock et al., 1987). It was later found that LIN-32 in fact affects the differentiation of all six TRNs, but is partly functionally redundant with VAB-15 in the ALMs (Du and Chalfie, 2001). *lin-32*; *vab-15* double mutants usually lack one or more ALMs and have more severe defects in ALM migration. As with *lin-32*, *vab-15* mutants lack AVM, PVM, and PLM cells and exhibit ALM positional defects, but also have more severe developmental defects and are likely to be inviable (Du and Chalfie, 2001). Recent evidence suggests that VAB-15 is an upstream regulator of LIN-32 (Zhao et al., 2020), but the enhanced defects in *lin-32*; *vab-15* double mutants as compared to *vab-15* single mutants suggest that expression of LIN-32 is not entirely dependent on VAB-15 (Du and Chalfie, 2001).

2.4 Additional Genes Associated with Gentle Touch Sensitivity

Essential genes that could mutate to cause touch insensitivity

When we started our screen and were identifying insensitive Million Mutation Project (MMP) strains with mutations in known touch genes, we did not look for mutations in any essential genes whose loss results in lethality or sterility. Although we were aware of many essential touch genes that we had previously identified through an RNAi screen (Chen et al., 2015a), we did not expect to find any phenotype causing mutations in these genes through our

MMP screen. However, the mapping of an insensitive strain that lacked mutations in any of the known *mec* genes we searched for narrowed down our candidate mutations to a list that included a mutation in the essential touch gene *mca-3*. The strain failed to complement a partial loss of function *mca-3* reference allele, so going forward we also checked insensitive MMP strains for essential touch genes and performed complementation tests to either partial loss of function or balanced reference alleles. However, we did not end up confirming any additional phenotype-causing mutations in essential touch genes. For this reason, *mca-3* is discussed along with other previously identified touch genes.

In some cases, essential genes determined to affect touch sensitive in an RNAi screen from our lab were genetically confirmed to mutate to cause touch insensitivity following the identification of partial loss-of-function alleles or through phenotyping of mosaic loss-of-function mutants (Chen et al., 2015a). Some of these genes are discussed or listed elsewhere in this chapter according to their determined roles in TRN function. The remaining set of genes is presented in Table 2-1.

Genetically confirmed genes	Unconfirmed genes
cab-1	*C30B5.6*
cdk-1	*cal-2*
cgt-3	*crn-1*
fzy-1	*dmd-5*
goa-1	*eif-2 β-ε*
kin-18	*F19F10.9*
let-502	*unc-11*
let-92	*unc-43*
mog-5	*vha-5*
mps-1	*C30B5.6*
pnk-1	*cal-2*
ptc-1	*crn-1*
sqv-3	*dmd-5*
tom-1	*F19F10.9*
unc-11	*mfap-1*
unc-43	*mrps-10*
vha-5	*mtch-1*
	myo-3
	nars-1
	nsf-1
	pas-4
	pfd-3
	pxl-1
	rpn-1
	saps-1
	spcs-3
	T19B10.2
	T20H4.5
	taf-5
	taf-9
	vha-20

Table 2-1: Essential genes that (could) mutate to cause touch insensitivity.

Genes that mutate to cause partial touch insensitivity

Since we expected our MMP screen to be more sensitive than previous mutagenesis screens for touch insensitivity, we also checked insensitive strains for mutations in genes that mutate to cause weak or partial touch insensitivity. Additionally, we checked for mutations in genes that are involved in structures or pathways we had already found to affect touch

sensitivity, but that have not been demonstrated to mutate to give weak or partial touch phenotypes. As of yet, we have not identified any MMP phenotype-causing mutations in these genes, which are listed in Table 2-2.

Category	Gene	Reference(s)
Cytoskeletal		
	unc-70	Krieg et al. (2014) ; Krieg et al. (2017)
Focal adhesion		
	pat-2 *pat-3* *pat-6* *unc-97* *unc-112*	Chen and Chalfie (2014)
Potassium channel		
	shw-3	Cai et al. (2009)
	twk-10	S. Lawry, unpublished
Insulin signaling pathway		
	daf-2 *age-1* *pdk-1* *akt-1* *ins-10* *ins-22* *che-1*	Chen and Chalfie (2014)
Other neuronal signaling pathways		
	ngl-1 *nrx-1*	Calahorro and Ruiz-Rubio (2012)
	egl-3	Kass et al. (2001)
	fax-1	Gamez-Del-Estal et al. (2014)
Endopeptidase		
	sel-12	Sarasija et al. (2018)

Table 2-2: Genes that mutate to cause partial touch insensitivity. Genes are organized by either protein function or signaling pathway membership. References are to publications in which partially touch insensitive phenotypes are reported for each gene.

2.4 Phenotypes that Interfere with Gentle Touch Response Assays

Certain phenotypes cause non-response in gentle touch assays without indicating any issues in TRN function. One such phenotype, termed twitcher, causes ongoing spasms in the body wall muscles that habituate the TRNs and prevent normal levels of touch response. Additionally, harsh touch phenotypes can result from dysfunctions downstream of TRN activity, interfering with the observed avoidance response. Twitchers and harsh touch insensitive animals were mostly excluded from thorough analysis in the original set of gentle touch mutagenesis screens, but since we were able to check the MMP set for mutations in genes associated with these phenotypes, we included them in our search for known touch genes and yet attempted to determine causality through genetic complementation. Ultimately, we found a significant number of insensitive strains that had phenotype-causing mutations in such genes. Some of the genes associated with twitcher and harsh touch insensitive phenotypes are listed in Table 2-3.

Category	Gene	Reference(s)
Twitcher		
	unc-22	Brenner (1974)
	unc-54	Chalfie and Sulston (1981)
	unc-43	LeBoeuf et al. (2007)
	let-51 *let-52* *let-56* *let-58* *let-59* *let-60*	Moerman and Baillie (1981)
	lev-11	Lewis et al. (1980)
Harsh Touch Insensitive		
	rpm-1	Giles et al. (2015)
	unc-31	Edwards et al. (2008)
	ceh-14	Gordon and Hobert (2015)
	glr-1	Kass et al. (2001)
	jnk-1	Villanueva et al. (2001)
	egl-30	Edwards et al. (2008)
	deg-1	Chalfie and Wolinsky (1990)
	tab-1	L. Carnell et al., unpublished

Table 2-3: Genes associated with twitcher and harsh touch insensitive phenotypes.
References are to publications in which the phenotype was first linked to one or more alleles of the gene.

Chapter 3: Screening the Million Mutation Project for Gentle Touch Phenotypes

The forward screens performed by Chalfie and Sulston (1981) and Chalfie and Au (1989) identified 18 genes required for gentle touch sensation. The screens recovered an average of 21 alleles per gene, strongly suggesting that the screen had reached saturation. However, in the time since, a number of additional genes affecting touch sensitivity have been identified (for a list of 51 empirically demonstrated touch phenotype-causing genes, see section on Identification of known genes in Materials and Methods). Some of these genes may not have been identified during the mutagenesis screens due to pleiotropic effects (animals with obvious physical defects were not regarded), and others are likely to have been missed due to their causing relatively weaker touch defects. In any case, the continuing discovery of genes that mutate to cause touch insensitivity leads us to believe that although the proverbial low-hanging fruits have been depleted, one might yet finish the harvest with a good ladder and a telescope-handled picker.

The Million Mutation Project (MMP) provides us with the opportunity to phenotype mutants with greater accuracy due to the homozygosity of the strains, and furthermore allows for accelerated identification of phenotype-causing mutations due to the whole-genome sequencing data available for each strain (Thompson et al., 2013). By phenotyping sequenced strains, we can even make use of negative results by identifying mutations that fail to cause a detectable phenotype.

There are several reasons why we decided to phenotype the entire set as opposed to considering a portion of the strains. For one, testing a greater number of alleles for any particular gene provides us with greater power to estimate the likelihood of that gene being involved in

touch sensation. Several groups that have tested MMP strains for particular phenotypes have noted that the majority of protein altering mutations in genes already associated with phenotype-causing alleles did not result in detectable phenotypes (Mathew et al., 2016; Bulger et al., 2017; Chen et al., 2019). Therefore, to give an illustrative example, it would be difficult to make assumptions regarding the relevance of a gene for which three missense alleles had been tested and found not to result in a phenotype, but more reasonable to disregard a gene for which ten missense alleles and two nonsense alleles had been tested and found not cause a phenotype. For this reason, Timbers et al. (2016) only considered genes represented by 7 or more MMP alleles in their computational approach to gene discovery. Timbers et al. (2016) charted the number of genes with multiple protein altering alleles in a subset of MMP strains to determine a minimum number of MMP strains to examine and found that the distribution of multiple non-synonymous alleles followed a pattern of exponential decay, with many genes represented by one non-synonymous allele and exponentially fewer genes represented by increased numbers of non-synonymous alleles. With this being the case, examining a larger set of strains greatly increases the number of genes represented by multiple non-synonymous alleles.

We charted the number of protein altering alleles per gene in the full MMP set and found that the number of genes per allele count could be approximated by a gamma distribution (Figure 3-1). To relate our chart to that provided by Timbers et al. (2016), the distribution could also be approximated by exponential decay when considering only genes with six or more protein altering alleles. As mentioned above, Timbers et al. (2016) had only considered genes represented by 7 or more protein altering mutation in their computational analysis. They reported that in their sampling of 480 MMP strains, 1150 genes met this minimum allele requirement. Therefore, we also used our fitted gamma distribution to approximate the number of genes which

met different minimum allele requirements given different portions of the MMP set sampled (Figure 3-2). The line graphs for minimum allele requirements of 5, 10, and 15 resembled sigmoid curves, with inflection points near 700, 1300, and 1700 strains sampled, respectively. The line graphs for minimum allele requirements of 20, 25, and 30 resembled exponential growth curves. Considering that the returns (in terms of genes meeting a minimum allele requirement) were not significantly decreased approaching complete sampling of the MMP set for minimum allele requirements of 10 and up, we decided that it would be worthwhile to phenotype the entire MMP set.

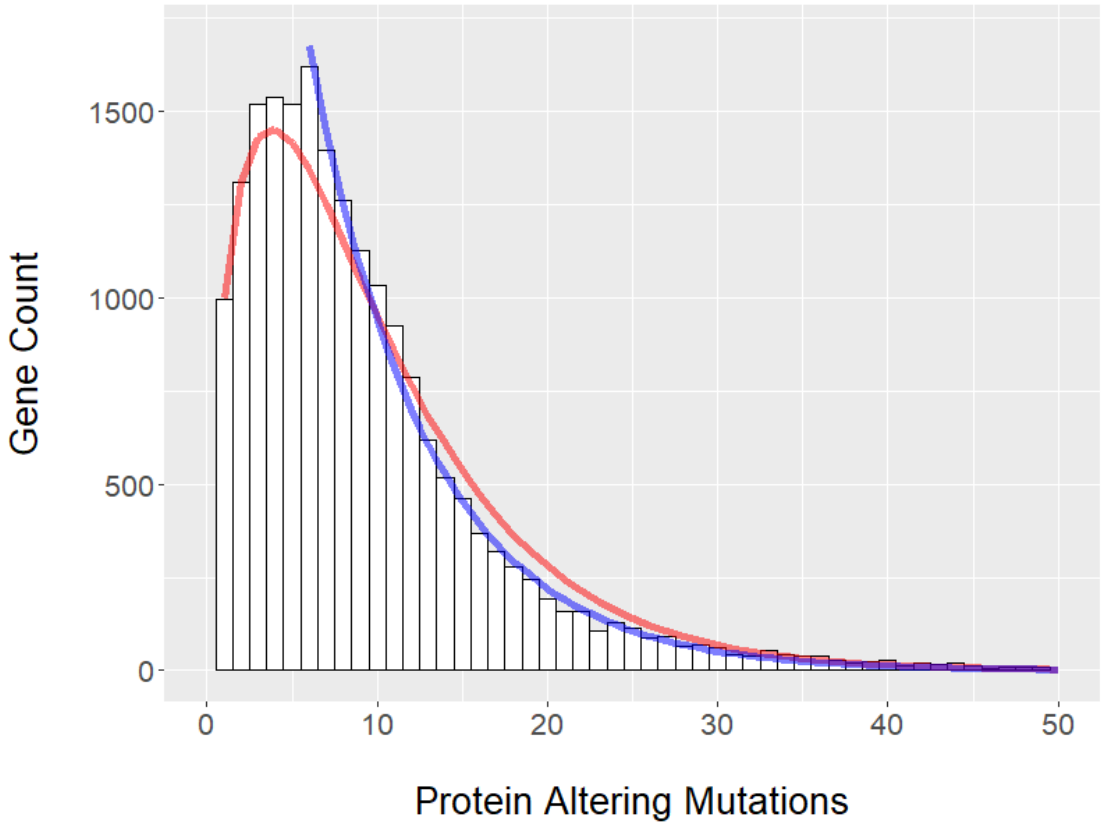

Figure 3-1: Genes with multiple protein altering MMP mutations. Histogram shows number of genes (y-axis) that have a given number of protein altering MMP mutations (x-axis). Chart is cropped at a maximum of 50 protein altering mutations to emphasize distribution shape. Red line shows fitted gamma distribution (shape = 1.63, rate = 0.166). Blue line shows equation for exponential decay ($y = 4000e^{-0.145x}$).

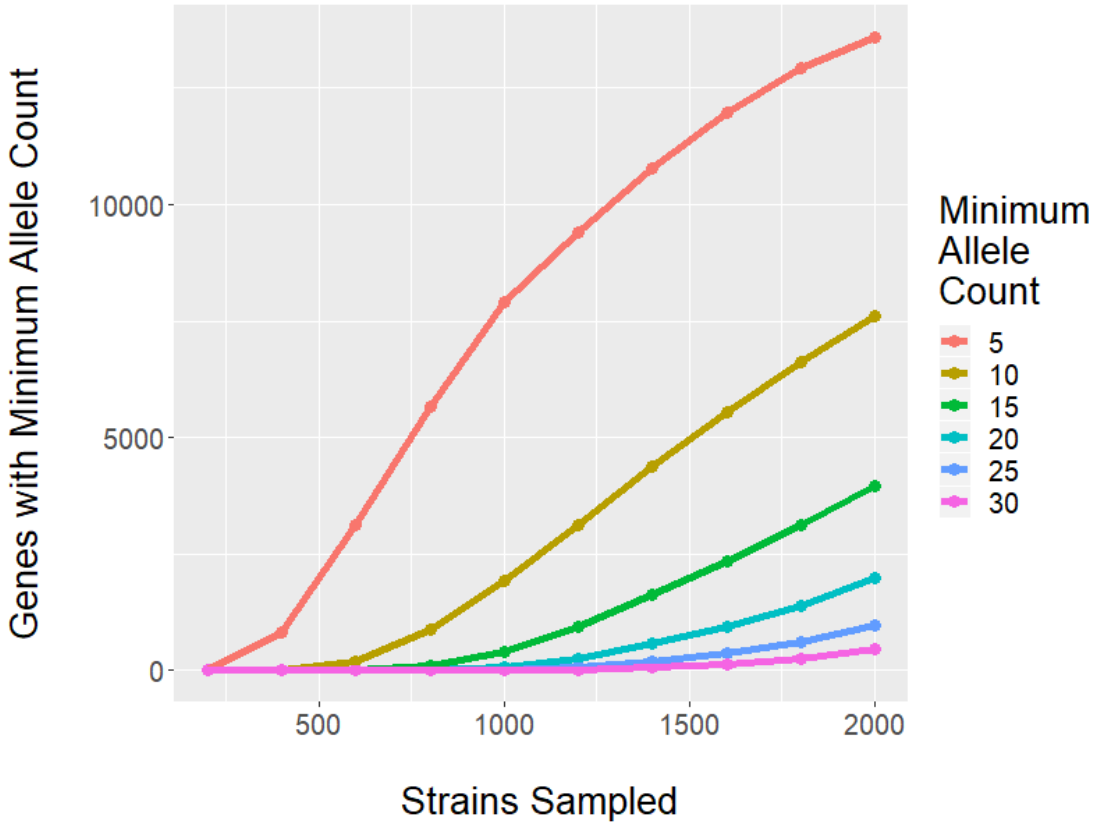

Figure 3-2: Multiple allele counts in MMP strains. Line graphs show the estimated number of genes (y-axis) meeting a given minimum allele count (color key) based on the number of MMP strains sampled (x-axis). Estimates are based on the gamma distribution shown in Figure 3-1.

Another one of our goals in touch phenotyping the MMP set was to evaluate the phenotypic and genetic completeness of the set. That is to ask, what sort of range of phenotypes and genotypes are exhibited by the strains in the MMP set? If we were able to identify a wide range of touch-insensitive phenotypes within the set, it would suggest more value for the set as an exploratory tool. Similarly, if we were able to identify touch insensitive alleles of all the same genes that had been identified in forward mutageneses for touch insensitive animals, it would suggest the value of screening the MMP strains as compared to performing new mutageneses.

In this chapter, I discuss the approaches we took in testing the MMP strains for touch phenotypes and verifying the identity of phenotype-causing alleles for genes that have already

been linked to touch sensitivity. I present several statistical analyses applied to the partial and complete response data sets and make estimations regarding errors and correlation between anterior and posterior response rates. Finally, I provide tables reporting the genes for which we verified phenotype-causing mutations and compare the number of touch gene alleles identified in the MMP to the number of alleles identified through mutagenesis screens.

3.1 Designing the Screen

In order to minimize the time spent testing the touch response phenotype of each strain, I developed specialized variants of previously described touch assays.

Developing specialized touch response assays

Wild-type *C. elegans* move in response to being stroked with an eyebrow hair glued to the end of a toothpick, traveling backwards in response to anterior stimulus and forwards in response to posterior stimulus (Chalfie and Sulston, 1981). Hobert et al. (1999) developed a semi-quantitative touch response assay in which individual worms are tested for response multiple times by alternating the application of anterior and posterior stimuli. For touch sensitive animals, such alternation allows for more rapid testing since changes in direction of locomotion are easy to detect. For example, if a worm is moving forwards, it is difficult to determine response to posterior stimulus (a sensitive worm might respond by either moving more quickly or for a longer duration of time), but easy to determine response to anterior stimulus (a sensitive worm might either stop moving forwards or reverse direction). A fully sensitive worm will halt or change the direction of its locomotion with each alternating stimulus, and therefore can be tested repeatedly with as little as one second between stimuli. However, for worms that are not

fully touch sensitive, the experimenter must wait for spontaneous stops or changes in direction, introducing variance and increasing the duration of the assay.

One way to assay a population for touch sensitivity while avoiding some of the issues associated with using repeated alternating stimuli is to test one response per animal. However, such an approach requires greater number of animals and obscures estimates of variance between individuals. Furthermore, we have found that even relatively insensitive animals are significantly more likely to respond to the first stimulus applied than to subsequent stimuli, so testing only one response per animal might constrain the range of response rates. We expect the range of response rates to already be more constrained in assays for anterior sensitivity since the anterior touch cells are significantly more responsive than the posterior touch cells (Chen and Chalfie, 2014, 2015). An upward shift of response rates leads to more information loss for a range already closer to the ceiling rate of 100% response, so it is not ideal to test for anterior touch sensitivity by observing one response per animal.

As another approach, we also considered generally increasing the duration between stimuli without sacrificing efficiency by testing multiple worms in parallel. This method requires a greater degree of attention but in the case of testing anterior sensitivity it can also alleviate the necessity to apply alternating stimuli, since worms are generally biased against backwards movement and tend to stop or change direction just a few seconds after initiating backwards locomotion.

In order to optimize for both time and information value, we chose to assay anterior and posterior sensitivity using different methods. For the purposes of our screen, I tested anterior sensitivity with multiple stimuli per individual, and posterior sensitivity with one posterior stimulus per individual. In testing for posterior sensitivity, we chose to apply an anterior stimulus

prior to the posterior stimulus in order to reduce the probability of forward locomotion (which is generally high for healthy adult worms away from a food source). Individuals still moving forwards after a single anterior stimulus were not tested for posterior sensitivity.

Planned structure of the testing approach

In order to minimize both the average time spent testing each strain and the probability of false positive results, we decided to conduct the screen using defined rounds of testing. We planned our approach so that all of the MMP strains would undergo an initial round of testing but only strains deemed potentially insensitive would undergo additional rounds of testing. To minimize the amount of time spent within the structure of the screen testing strains with mutations in known touch genes, strains that were identified as potentially insensitive during the initial round of screening and were not deemed false positives after two rounds of testing would be checked for mutations in known touch genes. Strains that did have mutations in known touch genes would then be complemented against reference alleles for verification, and strains that did not have mutations in known touch genes would undergo further retesting for a total minimum of three rounds. To minimize the amount of time spent testing strains with more obvious phenotypes, only strains with weaker phenotypes would be tested for a total minimum of four rounds, and only strains with high variability would be tested for a total minimum of five rounds. The criteria by which strains were categorized are discussed below.

Defining known touch genes

Since the insensitive strains could be easily tested for causative mutations in known touch genes by genetic complementation, we chose to err on the side of being overly inclusive in

compiling a list of known touch genes to check for mutations in. In addition to the genes identified through earlier screens for touch insensitive mutants (Chalfie and Sulston, 1981; Chalfie and Au, 1989), we included all genes we were aware of that could mutate to reduce touch sensitivity. We also included genes that only have synthetic effects on touch sensitivity (meaning that their alleles could only cause touch insensitivity in combination with another mutated gene), genes that had only been implicated in touch response through RNAi knockdown, and genes that had not been directly tested for a role in touch sensitivity but had been implicated through a related phenotype (such as overall reduced plate-tap response). Since certain phenotypes can indirectly interfere with touch sensitivity assays, we also included genes associated with twitcher, tab, harsh touch insensitive, and rapid habituation phenotypes. Finally, we also included some transcription factors known to play a critical role in the establishment of TRN identity. A table of known touch genes is provided in the Materials and Methods section (Table 3-1).

Determining the extent of testing per round and criteria for retesting

Before starting the screen, we were not sure how the response rates of the strains would be distributed, but we wanted to start the process of retesting potentially insensitive strains prior to finishing the screen. We figured this could be done by either setting aside strains with low average response rates relative to the growing set of previously tested strains, or by establishing criteria by which to retest strains that gave response rates below a given threshold. The second method would identify both strains with low average response rates and strains with high variance response rates. Considering that our chosen assays would provide more information about the variance of anterior response rates, we decided to use only the first method for

identifying potentially posteriorly insensitive strains and both methods for identifying potentially anteriorly insensitive strains.

To establish criteria for flagging tested strains as potentially anteriorly insensitive, I modeled response distributions using anterior response data from one wild-type strain and two moderately insensitive strains. I identified values for which the model set of wild-type worms would respond at or below the threshold with a frequency less than 5% and both model sets of partially insensitive worms would respond at or below the threshold with a frequency of more than 95% (Table 3-1). No threshold values satisfied these requirements for 3 or less individuals tested any number of times or for 5 or less individuals tested 5 or less times.

		Tests per Individual					
		5	6	7	8	9	10
Individuals Tested	4		3		4		5
	5	2	2 or 3	3	3 or 4	4	4 or 5

Table 3-1: Modeled threshold response values for identifying potentially touch insensitive strains. Numbers within the bordered cells indicate threshold response values for which the wild-type strain would fall at or below less than 5% of the time and insensitive strains would fall at or below more than 95% of the time given the numbers of individuals tested (rows) and tests per individual (columns). Cells with two values indicate that either threshold response value satisfies the requirements. Blank cells indicate that no threshold response values satisfy the requirements.

For a more generalized categorization of relative sensitivity, we chose to use estimated percentiles. Our methods for estimating percentiles is described in the section on Materials and Methods. To identify potentially insensitive strains after the first round of testing, we chose to use a 5^{th} percentile threshold. If we were to assume zero correlation between anterior and posterior touch sensitivity, we would expect about 200 strains to have an average response below

the 5th percentile of anterior and/or posterior sensitivity. If we were to assume perfect correlation between anterior and posterior touch sensitivity, we would expect about 100 strains to have an average response below the 5th percentile of anterior and/or posterior sensitivity. From our experience, anterior and posterior touch sensitivity tend to be somewhat correlated, leading us to expect around 150 strains to be deemed potentially insensitive in this manner.

We decided that for each round of testing anterior sensitivity, I would test the anterior response of 5 individuals 5 times each, for a total of 25 touch stimuli. After the first round of testing, each strain for which one or more individuals responded 2 or fewer times or for which the average response fell below the 5th percentile of previously tested strains would be flagged as potentially insensitive. Additional strains would be retested as needed if the 5th percentile average response increased after more strains had been tested. Similarly, I would test the posterior response of 25 individuals 1 time each, and flag strains with average responses below the 5th percentile as being potentially insensitive.

Classifying phenotypes

In order to categorize phenotypes for further testing, we chose to continue using estimated percentile thresholds. We expected that after retesting, the average responses of some strains would increase slightly. We decided that if the increase was relatively modest but brought the average response rate over the estimated 5th percentile threshold, we should still consider the strain as being notably insensitive. Thus, for strains that had been retested at least once, we decided to use a 10th percentile threshold for determining false positives. We also wanted to categorize the relative strength of phenotypes, so that strains that had repeatedly proven to have strong phenotypes need not undergo additional rounds of testing. Therefore, we considered

strains with an average response rate below the 5th percentile as having strong phenotypes, and strains with an average response rate above the 5th percentile but below the 10th percentile as having weak phenotypes. A summary of retesting criteria is provided in Figure 3-3.

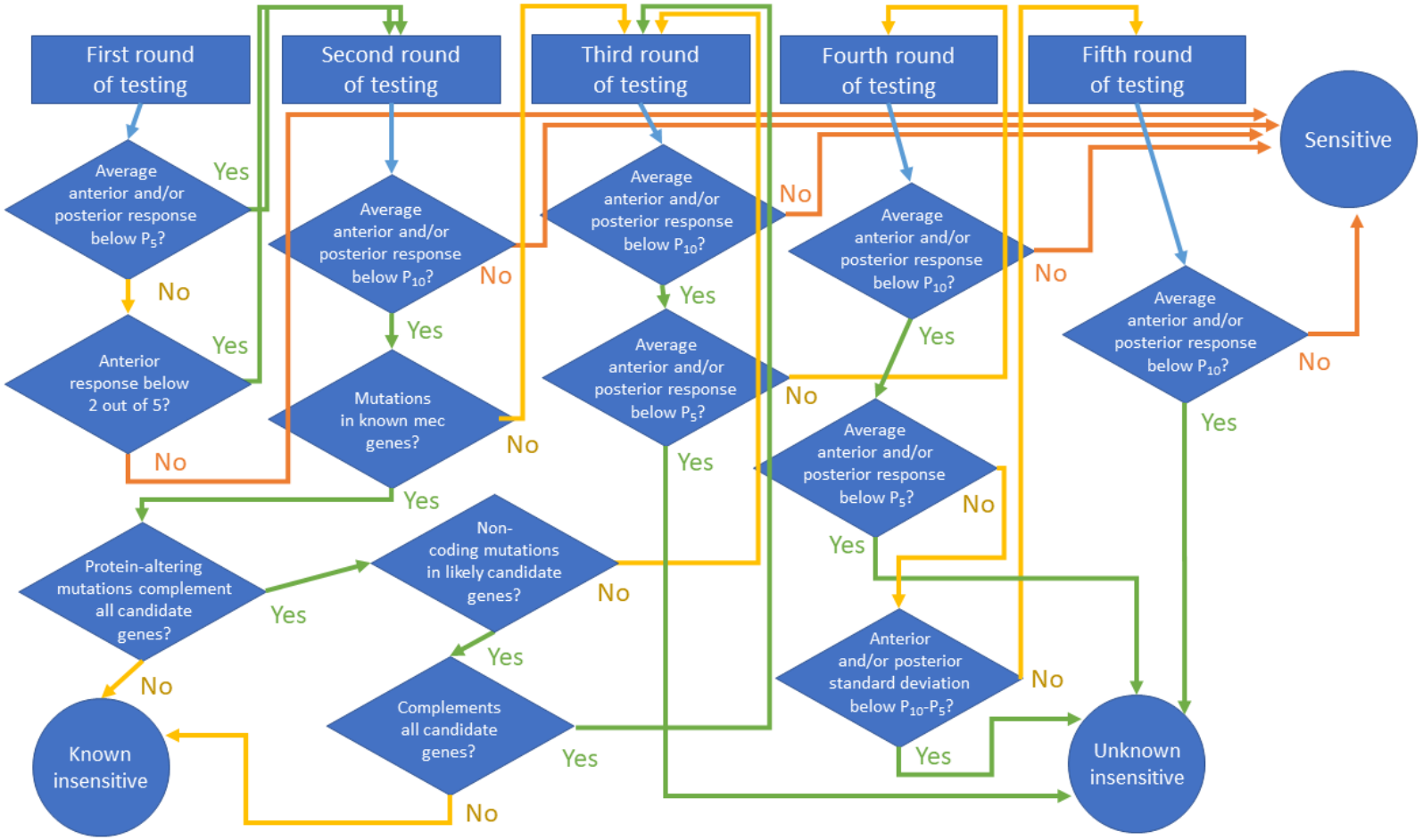

Figure 3-3: Flowchart of screening process. Strains with mutations in previously identified touch genes were subject to fewer rounds of testing (two rounds minimum) than those without. Strains with stronger phenotypes were subject to fewer rounds of testing (three rounds minimum) than those with weaker phenotypes. Strains with more consistent response rates were subject to fewer rounds of testing (four rounds minimum) than those with higher variance.

Prioritizing Candidate Causative Mutations

In order to make the process of verifying candidate causative mutations more efficient, we prioritized protein-altering mutations in genes associated with strong touch insensitive phenotypes. We regarded nonsense, missense, and splice-site mutations as protein-altering, and considered the set of genes identified in previous forward screens for touch insensitivity to be more likely candidates. Protein-altering mutations in other known genes would be considered second tier candidates, meaning that we would only test for complementation against these genes if an insensitive strain had no mutations in or had already complemented against the likely candidates. Non-coding mutations in likely candidate genes were considered third tier candidates, and we chose not to test non-coding mutations in other known genes for complementation as part of our prescribed process.

Other considerations

For the sake of simplicity, we decided not to formally blind the screen. However, we also chose not to check the genotype of strains prior to testing. We decided that in retesting potentially insensitive strains, strains to be retested would not be separated but rather would be mixed in with strains being tested for the first time without any special marking.

Touch response probability is affected by the presence of bacteria, so in order to minimize response variability it is ideal to test worms within a consistent density of bacteria. The simplest way to do this is to only test worms that have travelled off the bacterial lawn, since lawn density can vary both within a lawn (the perimeter of a lawn tends to accumulate increased bacterial densities) and between plates. However, this methodology can lead to certain complications. For one, wild-type animals are much more likely to be found on the bacterial

lawn than off. Therefore, on more sparsely populated plates, it is unlikely that sufficient numbers of animals within the desired age range will be found off the lawn. The required population density can vary between strains of different genotypes since certain mutations can increase or decrease lawn-leaving behavior. In cases where lawn-leaving is particularly infrequent the population can near starvation before a sufficient number of animals can be found off the lawn. In cases where lawn-leaving is particularly frequent, rising population density quickly increases the frequency of interactions between animals off the lawn, which can interfere with assays. To address this, I chose to monitor the population growth and lawn-leaving frequency of plates to be screened so that testing could be completed at an appropriate level of population density. It is also possible that individuals found off the lawn may have biased characteristics within the variabilities of a population. I did not make extensive attempts to control for this possibility but chose to only test worms that appeared to be of relatively average vitality and demonstrated some capability for movement prior to testing.

3.2 Results

Sequence Kernel Analysis Test (SKAT)

Prior to completing the screen, we wondered if our incomplete set of data could be used to start identifying new touch genes. Using the data analysis SKAT pipeline designed by Timbers et al. (2016), we separately analyzed anterior and posterior response data.

Data collected from 1430 strains provided only one statistically significant (Bonferroni adjusted P-value < 0.05) result, which indicated *unc-2*, a gene already known to mutate to touch insensitivity (see Tables 3-2 and 3-3). Nevertheless, we proceeded to test touch sensitivity in

mutants for some of the non-significant results. We prioritized genes that appeared within the top 100 on both lists and for which reference alleles were readily available. Out of 27 reference mutant strains tested for anterior and posterior touch sensitivity, one proved to have slightly reduced posterior touch sensitivity (Figure 3-4). However, the one posterior insensitive MMP strain carrying a protein-altering mutation in the identified gene (*flr-1*) had a significantly stronger phenotype than the *flr-1* reference mutants and complemented the *flr-1* reference allele.

Gene	Bonferroni adjusted P-value	Tested strains with mutations
unc-2	0.022509	45
mab-10	0.143188	13
pes-10	0.54472	8
mec-9	0.54472	11
F52B5.3	0.54472	20
T06D8.10	0.54472	27
R02D5.6	0.54472	11
mec-4	0.628444	20
bre-4	0.628444	9
dpy-8	0.628444	8
dnj-22	0.628444	10
F23D12.2	0.628444	22
egl-45	0.628444	8
mec-2	0.628444	10
C03H12.1	0.628444	15

Table 3-2: Anterior response SKAT results. Top fifteen most significant results from SKAT on anterior response data from 1430 MMP strains. Rows containing previously known touch genes are shaded in grey. Rows containing genes for which reference alleles were tested for anterior and posterior touch sensitivity are shaded in blue.

Gene	Bonferroni adjusted P-value	Tested strains with mutations
Y71G12B.13	0.311587	9
flr-1	0.311587	11
ulp-1	0.311587	7
Y81B9A.1	0.311587	11
mfap-1	0.311587	7
F23B12.1	0.311587	7
T23B12.2	0.311587	7
pdi-2	0.311587	7
aat-5	0.311587	7
hrp-2	0.311587	15
Y65B4BL.3	0.311587	8
unc-122	0.311587	11
F19F10.10	0.311587	13
T26C5.3	0.311587	7
cid-1	0.311587	15

Table 3-3: Posterior response SKAT results. Top fifteen most significant results from SKAT on posterior response data from 1430 MMP strains. There are no previously known touch genes listed. Rows containing genes for which reference alleles were tested for anterior and posterior touch sensitivity are shaded in blue.

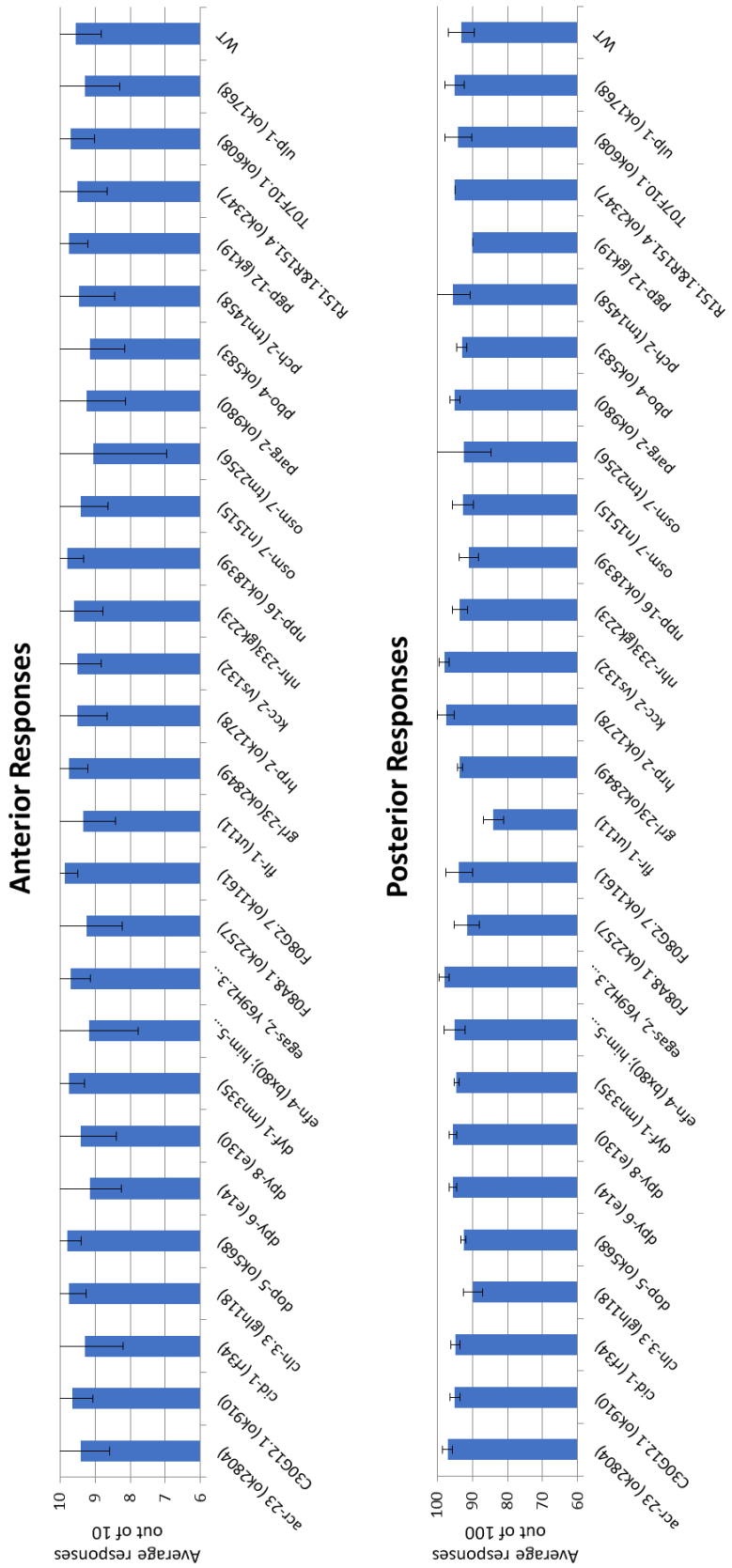

Figure 3-4: Touch response in mutants for SKAT candidate genes. Anterior and posterior touch response in mutants for genes that appeared within the top 100 most significant results from SKAT on anterior and posterior data from 1430 MMP strains. Error bars show sample standard deviation.

Data collected from 1698 strains provided no statistically significant (Bonferroni adjusted P-value < 0.05) results (see Tables 3-4 and 3-5). Since the power of the regression had not improved, and since our prior attempt at using the SKAT results to identify new touch genes had not proved particularly fruitful, we decided not to pursue the approach further.

Gene	Bonferroni adjusted P-value	Tested strains with mutations
unc-2	0.10932	51
mec-1	0.717362	46
mab-10	0.883895	15
R02D5.6	0.883895	12
pes-10	0.883895	9
mec-9	0.883895	13
K06H6.5	0.883895	7
mec-4	0.883895	21
mec-2	0.883895	12
dsh-2	0.883895	13
F58E1.7	0.883895	11
dnj-22	0.883895	10
C03H12.1	0.883895	17
nhr-31	0.883895	7
C36C9.5	0.883895	14

Table 3-4: Anterior response SKAT results. Top fifteen most significant results from SKAT on anterior response data from 1698 MMP strains. Rows containing previously known touch genes are shaded in grey.

Gene	Bonferroni adjusted P-value	Tested strains with mutations
Y53F4B.13	0.353839	17
jph-1	0.353839	8
Y65B4BL.3	0.353839	10
aqp-3	0.353839	10
T11F1.7	0.353839	10
clec-4	0.353839	7
ulp-1	0.353839	7
Y71G12B.13	0.353839	10
col-90	0.353839	10
T28D6.6	0.353839	7
mfap-1	0.353839	7
C23H3.3	0.353839	7
F17A9.4	0.353839	7
rnp-6	0.353839	19
F23B12.1	0.353839	7

Table 3-5: Posterior response SKAT results. Top fifteen most significant results from SKAT on posterior response data from 1698 MMP strains. There are no previously known touch genes listed.

Retesting and estimates of error rates

Upon completion of the screen, I had identified 100 strains with strong touch response phenotypes (anterior and/or posterior response rate(s) at or below 5th percentile), and 32 strains with weak touch response phenotypes (anterior and/or posterior response rates(s) at or below 10th percentile). These values include strains that were found to have phenotypes that interfere with

gentle touch sensitivity assays, such as twitcher or harsh touch insensitive. For a brief summary of the touch response phenotypes identified, see Table 3-6.

Phenotype	Number of Strains
Sensitive	1874
Strong	63
Strong Anterior	21
Strong Posterior	16
Weak	3
Weak Anterior	19
Weak Posterior	10

Table 3-6: Summary of touch response phenotypes identified in MMP strains.

The smaller number of strains we identified as having weak phenotypes is an artifact of our retesting criteria, since I only assigned touch insensitive phenotypes to strains that had undergone multiple rounds of testing. In fact, most of the strains I have deemed to exhibit weak phenotypes had appeared to exhibit strong phenotypes based on the initial round of testing. Had I also retested strains that appeared to exhibit weak phenotypes from the initial round of testing, we would expect our classifications to provide a roughly equal number of strains with strong and weak phenotypes. Thus, an estimated false negative rate for identification of weak phenotypes is:

$$\frac{\text{expected strains with weak phenotypes} - \text{identified strains with weak phenotypes}}{\text{strains that were not retested}} = \frac{100 - 32}{1756}$$

$$= 3.9\%$$

Ultimately, I ended up doing more retesting than necessitated by our original criteria, having chosen to use the original criteria as a minimum requirement (Table 3-7). For example,

after the first round of testing, 176 strains were flagged as being potentially insensitive according to our criteria, but 250 strains were tested at least one additional time. Most of the strains that were not flagged after the first round but retested anyway (74 strains) did not prove to have any detectable phenotype, but two of such strains proved to have strong touch response phenotypes after repeated rounds of testing, and five of such strains proved to have weak touch response phenotypes. We can use these values to estimate a false negative rate for identification of insensitive strains with strong touch phenotypes after the first round of testing. However, the initial response rates of strains that were not deemed potentially touch insensitive after the first round of testing but were retested anyway were skewed towards having lower response rates as compared to the total distribution of response rates. That is, strains that had initial response rates that were above the 5^{th} percentile but lower than average were much more likely to be retested. Therefore, the ratio of the number of strains that were retested despite not being flagged as potentially insensitive and were later determined to have strong touch phenotypes (false negatives) to the total number of strains that were retested despite not being flagged (retested negatives) represents a high estimate of the false negative rate for identification of strains with strong touch phenotypes:

$$\frac{\text{strong phenotype false negatives}}{\text{retested negatives}} = \frac{2}{74}$$

$$= 2.7\%$$

For a potentially more accurate estimate of false negative rate for identifications of strains with strong and weak touch phenotypes, we can consider the likelihood of finding false

negatives within a set of strains retested by chance by weighting false negative rates by their probability of appearing in the set of untested strains:

$$\frac{\sum P(strong\ false\ negative\ given\ initial\ response\ n) \times unretested\ strains\ with\ initial\ response\ n}{unretested\ strains} = \frac{24.7}{1756}$$

$$= 1.4\%$$

$$\frac{\sum P(weak\ false\ negative\ given\ initial\ response\ n) \times unretested\ strains\ with\ initial\ response\ n}{unretested\ strains} = \frac{125}{1756}$$

$$= 7.1\%$$

Calculating the false positive rate for strains flagged as being potentially touch insensitive is a much simpler matter. Out of the 176 strains that were deemed potentially touch insensitive after the first round of testing, 53 were determined to be sensitive after additional testing (53/176 =30%). Out of the 157 strains deemed as potentially touch insensitive following the second round of testing, 124 underwent additional testing, and 30 were later determined to be sensitive (30/124=24%). Similarly, after the third round (15/77 =19%) and fourth rounds (4/45=8.8%), the false positive rate continued to decrease. No strains that were flagged as being insensitive in the fifth round of testing were later determined to be sensitive, but only 4 strains were tested more than five times.

Round of Testing	Number of Strains Tested	Number of Strains Determined to be (Potentially) Insensitive
1	2006	176
2	250	157
3	137	114
4	84	64
5	48	37
6	4	4
7	1	1

Table 3-7: Summary of screening process

Summary statistics

Our final phenotypic categorizations (strong and weak) required us to calculate percentile values for the response rates of the entire MMP set, and we were interested in additional information that might be gathered concerning the distribution of response rates. For these purposes, we only considered responses from the initial round of testing for each strain. Both anterior and posterior response rates were highly skewed towards full responsiveness. As we had predicted, the skew of anterior response rates was more extreme, with a mode of 25 out of 25 responses and a mean of about 23.2 out of 25 responses (Figure 3-5). Posterior response rates were just slightly less, with a mode of 23 and a mean of about 21.9 (Figure 3-6). Both distributions are relatively peaked with semi-heavy tails, appearing more hyperbolic than normal.

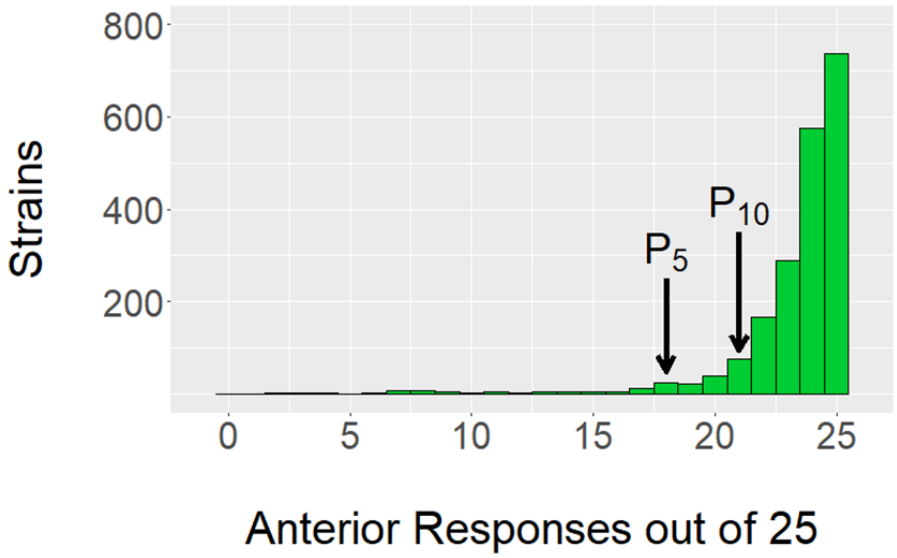

Figure 3-5: MMP anterior response distribution. Distribution of anterior response sums from initial rounds of testing for 2006 MMP strains. The 5th percentile response rate is marked at 18 out of 25 responses. The 10th percentile response rate is marked at 21 out of 25 responses.

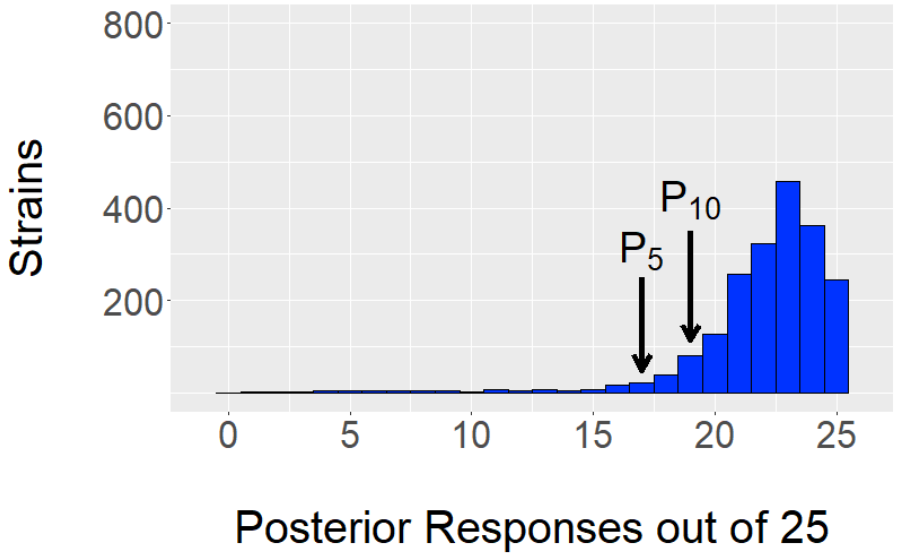

Figure 3-6: MMP posterior response distribution. Distribution of posterior response sums from initial rounds of testing for 2006 MMP strains. The 5th percentile response rate is marked at 17 out of 25 responses. The 10th percentile response rate is marked at 19 out of 25 responses.

As we had predicted, there was a correlation between anterior and posterior response rates (Figure 3-7). The strength of the correlation was fairly weak ($R^2 = 0.38$), but we wondered if this might be due to the inevitably large error margins expected from limited sampling of a variable trait. Thus, we hypothesized that the average response rates from strains that had been tested more extensively would show stronger anterior-posterior correlation. However, this did not appear to be the case. The strength of correlation between average anterior and posterior response rates for strains that underwent at least 3 rounds of testing (n = 137) was indicated by $R^2 = 0.32$. To test if the relatively unchanged strength of correlation was due to the increased variance among strains with reduced sensitivity, we sampled the set of initial test data for responses that fell below the 10th percentile in either anterior or posterior response for comparison (n = 364, $R^2 = 0.24$). To test if the relatively unchanged strength of correlation was due to the smaller sample size of strains that had undergone multiple rounds of testing, we applied linear regressions to 100 randomly sampled sets of n = 137 from the initial test data and found values of R^2 ranging from 0.013 to 0.68, with a mean of 0.37. From these comparisons we conclude that the set of responses from 2006 strains represents an accurate strength of correlation between anterior and posterior response rates due to adequate sampling, and that while the strains with reduced touch sensitivity did indeed provide more variable response rates, repeated testing successfully corrected for the variance.

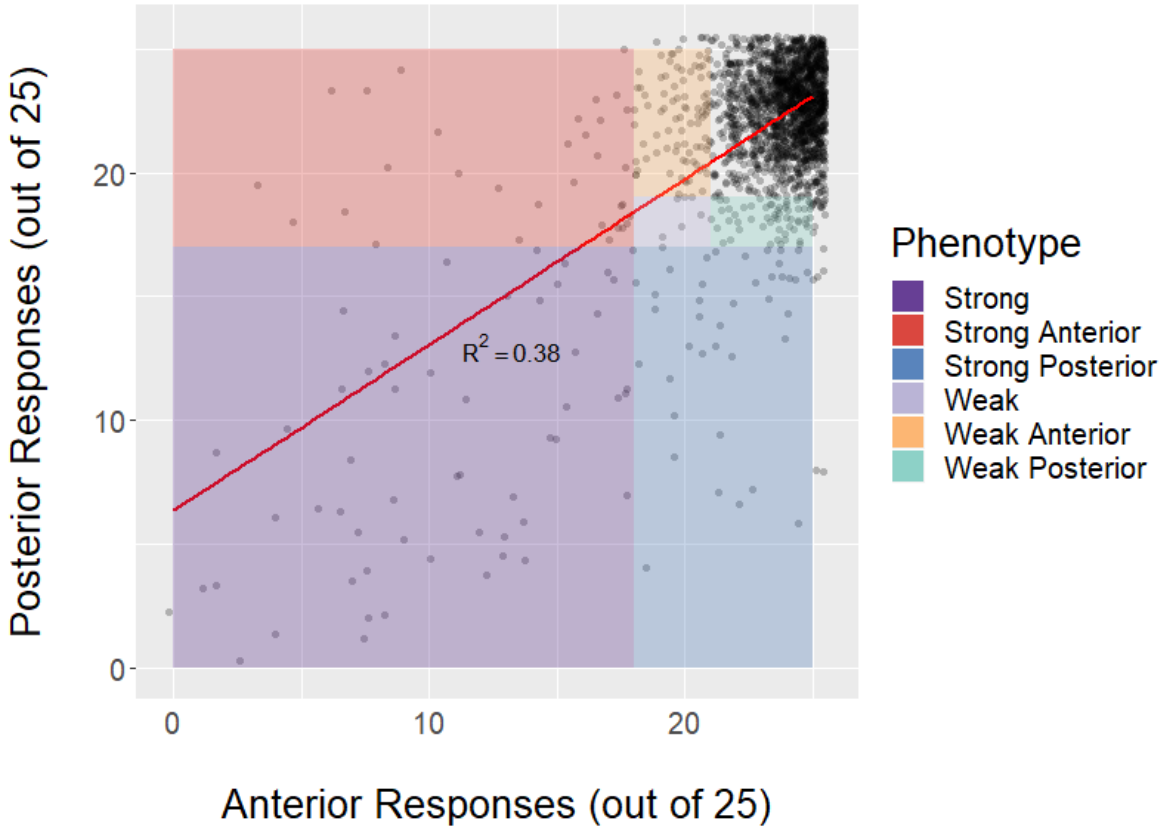

Figure 3-7: Correlation between anterior and posterior responses of all strains. Jittered plot of anterior and posterior response sums from initial round of testing for 2006 MMP strains. Each point represents the initial test data from one strain. The linear regression model (red line) of posterior response as predicted by anterior response provides an estimated coefficient (line slope) of 0.67. R^2 value is shown. Phenotypic categorization is indicated by colored shading.

Verified, unverified, and unknown causative mutations

We decided to begin the process of identifying phenotype causing mutations in MMP strains with touch response phenotypes by checking insensitive strains for mutations in a list of known genes and performing appropriate complementation tests. Partly because our list of known genes contained both genes known to have touch insensitive alleles and genes thought to be otherwise directly or indirectly related to touch response phenotypes (for brevity we will refer to these genes as "known touch genes"), most of the insensitive MMP strains that we identified proved to carry mutations in known touch genes. We also expected that most if not all of the

MMP strains we identified as being touch insensitive would prove to have causative mutations in known touch genes, since previous mutagenesis screens had been repeated to the point of saturation. Furthermore, we expected that strains with stronger phenotypes would be more likely to have mutations in genes identified through the original series of screens for touch insensitive mutants (we will refer to these genes as "original *mec* genes"). Indeed, this proved to be the case (Table 3-8).

We categorized insensitive strains with protein-altering mutations in known touch genes and/or intronic mutations in original *mec* genes as having unverified causative mutations, and the remaining strains as having unknown causative mutations. Strains that failed to complement reference alleles of known touch genes were recategorized as having verified causative mutations. Some strains with unverified causative mutations had candidate causative mutations in known genes but complemented all candidate gene reference alleles. These were recategorized as being strains with unknown causative mutations. A small number of strains with unverified causative mutations proved to mate very poorly, and we were not able to perform complementation tests. Additionally, there are some strains for which we have not finished attempting to verify candidate causative mutations (Table 3-9).

	Strong Phenotypes	Weak Phenotypes
Verified	**70**	**6**
Original mec genes	47	4
Other known gentle touch genes	12	1
Not gentle touch genes	11	1
Unverified	**6**	**9**
Unable to complement	5	0
Yet to complement	1	9
Unknown	**24**	**17**
Complemented candidate known touch genes	18	13
No candidate causative mutations	4	3
Interfering phenotype with unknown causative mutation	2	1

Table 3-8: Categorized insensitive strains. Strains with touch response phenotypes categorized according to causative mutations and phenotype. Major categories and total strains in major categories are in bold.

The nature of the phenotype-causing mutations identified in known touch genes will be discussed in Chapter 4, but here I present the identity of the verified genes along with the number of phenotype causing alleles that we found within the MMP set (Table 3-9). For the set of original *mec* genes, I have also listed the number of alleles identified in the forward screens performed by Chalfie and Sulston (1981) and Chalfie and Au (1989).

Gene	Verified Phenotype-Causing MMP Alleles	Alleles Identified Through Mutagenesis Screens
Original mec		
egl-5	0	1
lin-32	0	1
mec-1	6	63
mec-2	9	54
mec-3	0	15
mec-4	7	59
mec-5	2	37
mec-6	2	9
mec-7	6	54
mec-8	0	7
mec-9	3	33
mec-10	2	6
mec-12	4	15
mec-14	4	9
mec-15	2	5
mec-17	2	1
mec-18	1	6
unc-86	1	9
Other known touch genes		
age-1	1	
alr-1	1	
mca-3	1	
unc-2	7	
unc-36	4	
Non-touch genes		
rpm-1	1	
unc-22	7	
unc-31	2	
unc-42	1	
unc-54	1	

Table 3-9: Verified phenotype causing MMP alleles with reference to alleles of original *mec* genes.

Initial response data from verified insensitive strains

Having plotted the distribution of initial response rates for all strains, we were curious as to where the insensitive strains with phenotype-causing mutations in original *mec* genes would fall among the distribution as compared to insensitive strains with phenotype-causing mutations in other and unknown touch genes. Therefore, we plotted the initial anterior and posterior response rates of a subset of strains, including strains that were determined to have touch phenotypes but excluding strains with additional obvious phenotypes (including Unc, twitcher, and harsh-touch insensitive) and strains for which phenotype-causing mutations in known *mec* genes had not been ruled out (Figure 3-8). As expected, most of the strains found to have phenotype-causing mutations in the original *mec* genes had initial response rates that fell beneath both the anterior and posterior 5th percentiles and were spread throughout the lower left corner of the plot. Having excluded strains with additional phenotypes, response rates from only three strains with phenotype-causing mutations in other known touch genes (*age-1*, *alr-1*, and *mca-3*) were plotted. Two of these three strains (with phenotype-causing mutations in *age-1* and *alr-1*) had initial response rates that fell below both the anterior and posterior 5th percentiles but were relatively closer to the upper right corner of the range. One of the three strains (with a phenotype-causing mutation in *mca-3*) had initial response rates below the 5th percentile for posterior response but above the 5th percentile for anterior response. Unsurprisingly, insensitive strains with phenotype-causing mutations in unknown touch genes tended to have initial response rates that fell relatively closer to the upper right corner of the plot.

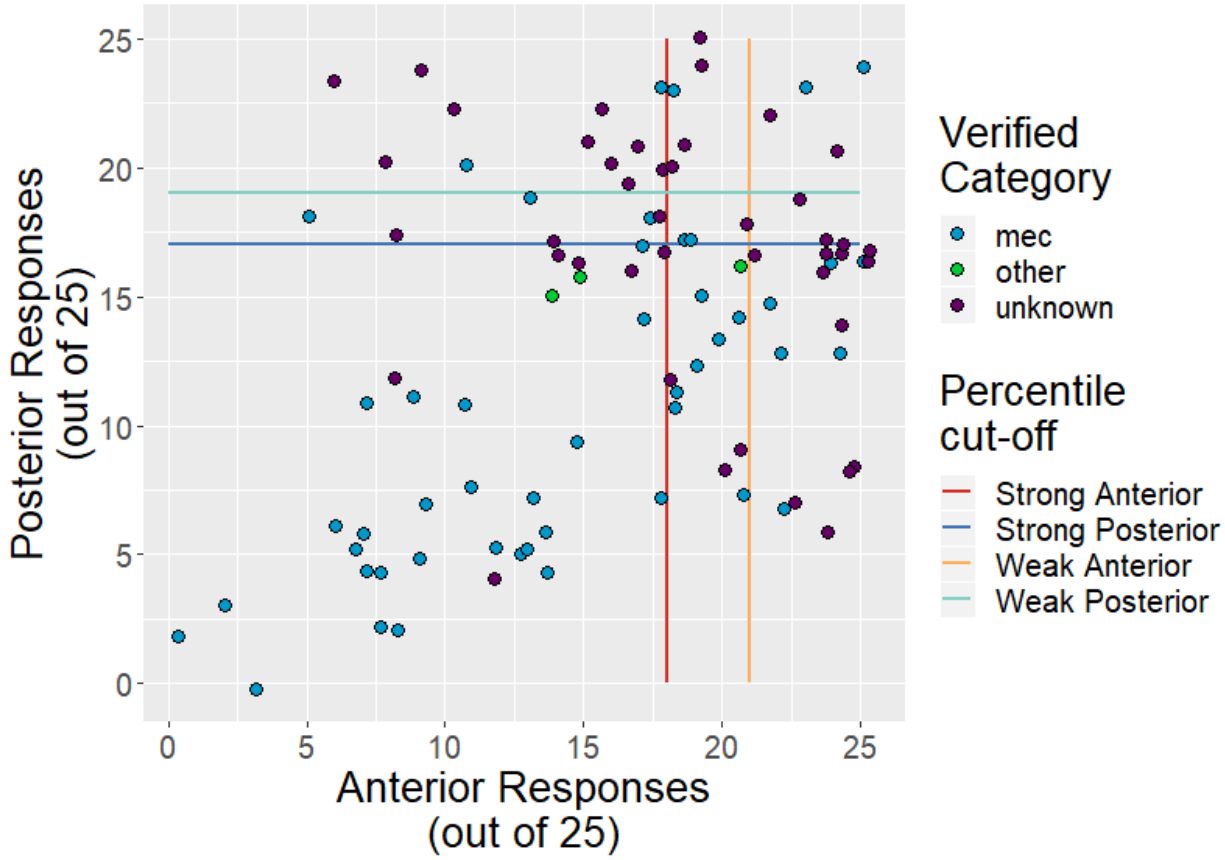

Figure 3-8: Initial response rates of insensitive strains. Strains with additional phenotypes and strains for which phenotype-causing mutations in known touch genes have not been ruled out are excluded. Dot colors indicate if phenotype-causing mutations are in original *mec* genes (mec, blue), in other known touch genes (other, green), or in unknown genes (unknown, purple). Colored lines indicate the 5th (strong) and 10th (weak) percentiles for anterior and posterior responses. Plotted points are jittered to reduce overplotting.

There were 10 strains with unknown phenotype-causing mutations with only either anterior or posterior response rates that fell well below the 5th percentile cut-offs but were not at, below, or near the 5th percentile cut-offs for the opposing response. In fact, there was a general effect where strains with phenotype-causing mutations in the original *mec* genes showed an overall positive correlation between anterior and posterior response rates (slope of 0.61, R^2 = 0.39), but strains with phenotype-causing mutations in unknown touch genes showed an overall negative correlation (slope of -0.27, R^2 = 0.08). This effect suggests that some of the unknown

touch genes may have been overlooked in the original mutagenesis screens due to their being only either anteriorly or posteriorly insensitive. It should be noted here that two of the original *mec* genes were found to cause only either anterior or posterior touch insensitivity (*egl-5* and *lin-32*), but perhaps not coincidentally only one allele for each of these genes was identified though the original screens (Chalfie and Au, 1989).

Additional observations

Since I performed the screen by preparing plates in batches and then monitoring their population densities, I noticed that strains for which plates achieved optimal population density sooner were significantly more likely to be touch sensitive. Unfortunately, I did not record information on how many days passed between plate preparation and testing for each strain, so I cannot make any formal estimates regarding the correlation.

3.3 Discussion

Utility of the Sequence Kernel Analysis Test (SKAT)

Although we identified one gene for which a null reference allele proved to be weakly touch insensitive following our use of the SKAT, in general we did not find the analysis to be helpful for identifying previously unknown touch genes. We believe this may be due in part to the nature of our phenotypic data. For one, the data from manual gentle touch response assays tends to be very noisy. We attempted to compensate for this by performing additional rounds of testing for strains that appeared to be touch insensitive, but the majority of strains were only subjected to 25 anterior and 25 posterior touch tests. Additionally, the analysis pipeline we used

was optimized for data with log-normal distribution. We might have attempted to modify the analysis to fit the more hyperbolic distribution of our data but chose not to.

Response data distributions

One of the weaknesses of our gentle touch response assays is that response data tends to skew heavily towards full responsiveness. If this were not the case, we could make better estimates as to the variance and error represented in the data. For example, since our anterior response data peaks at full responsiveness, we can predict a theoretical response distribution curve, but have limited evidence as to where along the curve the ceiling response rate falls.

Estimated error rates

Given the size of our screen, even our lower estimates of false negative error rates are somewhat high. If our lower estimated rate of false negatives for strong touch response phenotypes is correct, we would expect to identify another 25 strongly touch insensitive strains within the set of strains that were not retested. We are less concerned about the false negative error rates for weakly touch insensitive strains, because the strains with weak touch phenotypes that we have identified have proven to be much more difficult to work with for both complementation testing and reisolation of outcrossed mutants. Ultimately, we are unlikely to invest much more time into characterizing the strains with weak mutations.

Correlation of anterior and posterior response

We were somewhat surprised that there was not a stronger correlation between anterior and posterior touch response rates. Our results may have arisen from the variance within our

data, but the strength of correlation was relatively unchanged when we limited the comparison to strains that had been tested over at least three rounds. It is common practice to pool gentle touch response data from anterior and posterior stimuli, but our results suggest that this may obscure actual phenotypic variations.

We would expect anterior and posterior response rates to be strongly correlated because the anterior and posterior TRNs generally express the same suite of genes at similar levels. There are certain exceptions to this generalization. For example, the relatively decreased responsiveness of the PLMs as compared to the ALMs is thought to be in part due to higher levels of MFB-1 expression in the PLMs (Chen and Chalfie, 2015). Additionally, habituation of anterior and posterior response occurs at different rates and appears to rely on different factors (Chen and Chalfie, 2014).

Verification of causative mutations

It is notable that almost all of the genes we expected to identify (the original *mec* genes) through our screen of the MMP were represented (the information we have gained regarding these genes will be discussed in Chapter 4). We also identified causative mutations in genes that are known to affect the gentle touch response but were not identified through forward screens. These included the HOX genes *alr-1* and *unc-42*, although we do not consider *unc-42* a touch gene because it affects the interneurons of the gentle touch response circuit. We also identified causative mutations in *age-1* and *mca-3*, which were relatively recently identified as playing a role in touch sensitivity (Chen and Chalfie, 2014; Chen et al., 2015a). *mca-3* is essential gene required for viability, and we were somewhat surprised to identify a phenotype-causing loss-of-function allele within the MMP set. Although there is a significant number of essential genes we

know to affect touch sensitivity, we have not yet identified any other such phenotype-causing alleles (Chen et al., 2015a). Strikingly, we identified seven and four touch phenotype-causing alleles of the calcium channel subunits UNC-2 and UNC-36, respectively.

3.4 Materials and Methods

C. elegans strains and culture

C. elegans strains were maintained at 20°C as described by (Brenner, 1974). Million Mutation Project strains were obtained from the Piano and Gunsalus lab, Mark Edgley, and the Caenorhabditis Genetics Center. Additional strains are listed in Appendix I.

Gentle touch response assays

Anterior touch sensitivity alone was assessed by touching each animal five times anteriorly, with at least a three second gap between stimuli and not until the animal ceased backing, turning, or coiling behavior. Posterior touch sensitivity alone was tested by touching each animal once posteriorly about one second after an anterior touch. Animals that remained in a forward locomotory state after an anterior stimulus were not tested for posterior response.

Computational analysis

SKAT analysis was completed using programs provided by Timbers et al. (2016). To match the input type used by Timbers et al. (2016), response data was transformed to reflect the number of non-responses resulting from each touch stimulus. Constants of 0.02 and 0.005 were added to anterior and posterior response values, respectively.

Identification of Known Genes

To check strains for mutations in known touch genes, we used information from both the MMP website and WormBase. From the dataset of MMP variants from the MMP website, we extracted a list of variants within known genes. From WormBase, we downloaded the list of alleles for each known gene and then extracted MMP alleles. We then used Microsoft Excel to reference each insensitive strain against the list of mutations in known genes. A list of known genes, their established connection to touch response, and their associated touch phenotypes is provided in Table 3-10. Phenotype strength of known genes with published reports on the degree of touch sensitivity associated with their alleles was calculated by response percentage relative to reported wild-type response (to correct for differences in methodology) and was categorized in alignment to the response percentage categories used in our MMP screen. Anterior response phenotype was considered strong if the reported response rate fell beneath 72% relative to wild-type (with 18 out of 25 responses being the 5^{th} percentile rate in our screen and 25 out of 25 responses being the most common response rate), weak if the reported response rate fell below 84% (10^{th} percentile rate in our screen), and very weak if the reported response rate was statistically significant compared to wild-type but fell below 88% (15^{th} percentile rate in our screen). Posterior response phenotype was considered strong for rates below 73% (with 17 out of 25 responses being the 5^{th} percentile rate in our screen and 23 out of 25 being the most common response rate), weak for rates below 83%, and very weak for rates below 87%. General response phenotype was considered strong for rates below 73%, weak for rates below 83%, and very weak for rates below 88%. In cases where different alleles of the same gene had different phenotypic strengths, only the strongest allele was considered. All genes identified in the forward screens for touch insensitive mutants (Chalfie and Sulston, 1981; Chalfie and Au, 1989) were assumed to

have strong phenotypes even if a specific response rate has not been published, except in the case of genes reported only to affect either the anterior or posterior response. In most other cases the numerical response rate was inferred from graphically presented data. Graphically presented data was converted to quantitative data for determining phenotypic strength by comparing pixel length of bar heights.

Category	Gene	Phenotypic Strength			Reference(s)
		General	Anterior	Posterior	
Forward Screen					
	unc-86	Strong			Chalfie and Sulston (1981)
	mec-1	Strong			
	mec-2	Strong			
	mec-3	Strong			
	mec-4	Strong			
	mec-5	Strong			
	mec-6	Strong			
	mec-7	Strong			
	mec-8	Strong			
	mec-9	Strong			
	mec-10	Strong			
	mec-12	Strong			
	mec-14	Strong			Chalfie and Au (1989)
	mec-15	Strong			
	mec-17	Strong			
	mec-18	Strong			
	egl-5			Strong	
	lin-32			Strong	
Reported Insensitive					
	atat-2	Strong			Akella et al. (2010) ; Shida et al. (2010) ; Topalidou et al. (2012) ; Davenport et al. (2014)
	unc-42	Strong	Strong	None	Brockie et al. (2001)
	egl-19	Strong	Strong	Strong	Buddell et al. (2019)
	nlg-1	Strong	Strong	Strong	Calahorro and Ruiz-Rubio (2012)
	nrx-1	Strong	Strong	Strong	
	age-1		Strong	None	Chen and Chalfie (2014)
	akt-1		Strong	None	
	daf-2	Strong	Strong	Strong	
	pat-2	Strong	Strong	None	
	pat-3	Strong	Strong	None	
	pat-6	Weak	Strong	None	
	pdk-1	Strong	Strong	Strong	
	cab-1	Strong	Strong	Strong	Chen et al. (2015a)
	cdk-1	Strong	Strong	Strong	
	ceh-20	None	Very Weak	None	
	cgt-3	Strong	Strong	Strong	
	fzy-1	Strong	Strong	Strong	
	goa-1	Strong	Strong	Strong	
	ins-10		Strong		
	ins-22		Strong		
	kin-18	Strong	Strong	Strong	
	let-502	Strong	Strong	Strong	
	let-92	Strong	Strong	Strong	

Category	Gene	Phenotypic Strength			Reference(s)
		General	Anterior	Posterior	
Reported Insensitive					
	mca-3	Strong	Strong	Strong	Chen et al. (2015a)
	mog-5	Strong	Strong	Strong	
	mps-1	Strong	Strong	Strong	
	pnk-1	Strong	Strong	Strong	
	ptc-1	Strong	Strong	Strong	
	sqv-3	Strong	Strong	Strong	
	tom-1	Strong	Strong	Strong	
	unc-11	Strong	Strong	Strong	
	unc-112	Strong	Strong	Strong	
	unc-43	Strong	Strong	Strong	
	vha-5	Strong	Strong	Strong	
	crt-1	Weak			Chen et al. (2016a)
	txdc-9	Strong	Strong	Strong	
	unc-2	Strong			Frøkjær-Jensen et al. (2006)
	unc-36	Strong			
	nra-2	Strong			Kamat et al. (2014)
	egl-3	Strong			Kass et al. (2001)
	unc-70	Strong			Krieg et al. (2014)
	sel-12	Strong			Sarasija et al. (2018)
	ahr-1		Strong		Smith et al. (2013)
	zag-1		Strong		
	sem-4	Strong			Toker et al. (2003)
	alr-1	Strong			Topalidou and Chalfie (2011)
	elo-1	Strong			Vasquez et al. (2014)
	fat-3	Strong			
	fat-4	Weak			
	unc-24	Weak	Strong	None	Zhang et al. (2004)
RNAi					
	pat-4				Calixto et al. (2010a)
	ldb-1				Cassata et al. (2000)
	C30B5.6				Chen et al. (2015a)
	cal-2				
	crn-1				
	dmd-5				
	eif-2βE				
	F19F10.9				
	F26G1.2				
	F55F8.3				
	gfi-2				
	glf-1				
	gtf-2E2				
	hars-1				
	hmr-1				
	knl-1				

Category	Gene	Phenotypic Strength			Reference(s)
		General	Anterior	Posterior	
RNAi					
	lam-2 *let-611* *mfap-1* *mrps-10* *mtch-1* *myo-3* *nars-1* *nsf-1* *pas-4* *pfd-3* *pxl-1* *rpn-1* *saps-1* *spcs-3* *T19B10.2* *T20H4.5* *taf-5* *taf-9* *vha-20* *vha-20*				Chen et al. (2015a)
Synthetic					
	akt-2				Chen and Chalfie (2014)
	poml-1				Chen et al. (2016a)
	ptl-1	None			Gordon et al. (2008)
	lgc-37				Topalidou and Chalfie (2011)
	mtd-1				Zhang et al. (2002)
Twitcher					
	unc-54				Chalfie and Sulston (1981)
	lev-11 *unc-22*				Lewis et al. (1980)
	let-60				Moerman and Baillie (1981)
Touch Abnormal (tab)					
	deg-1				Chalfie and Sulston (1981)
	tab-1				Chalfie, Unpublished
	egl-47			Strong	Desai and Horvitz (1989)
	deg-3				Treinin and Chalfie (1995)

Category	Gene	Phenotypic Strength			Reference(s)
		General	Anterior	Posterior	
Harsh Touch					
	rpm-1	None			Bounoutas et al. (2009b)
	unc-31				Edwards et al. (2008)
	ceh-14				Gordon and Hobert (2015)
	glr-1	None			Kass et al. (2001)
	jnk-1				Villanueva et al. (2001)
Harsh Touch and Habituation					
	egl-30				Kindt et al. (2007) ; Edwards et al. (2008)
Habituation					
	pkc-1				Kindt et al. (2007)
	eat-4				Rankin and Wicks (2000)
	cat-2 *dop-1*				Sanyal et al. (2004)
Initial Tap Response					
	tpa-1	Weak			Kindt et al. (2007)
TRN Identity Transcription Factor					
	vab-15 *mig-21*				Du and Chalfie (2001)
	lin-14				Mitani et al. (1993)
	ceh-13 *nob-1*				Zheng et al. (2015)

Table 3-10: Known touch genes. Genes are categorized by their established connection to touch response. Genes in the Reported Insensitive are also denoted by phenotype strength (Strong, Weak, or Very Weak) and category (General, Anterior, and Posterior). General indicates that reports used combined anterior and posterior response data or the average relative response rates of anterior and posterior responses. Blank cells indicate cases where the particular phenotypic category was not reported on. Genes outside of the Reported Insensitive category also have a phenotypic strength denoted if published reports provided gentle touch response rates. Multiple references are listed in cases where data from multiple groups that reported on gentle touch response rates associated with a gene were considered.

Verification of causative mutations

Complementation tests were implemented as described by Brenner (1974).

Chapter 4: Million Mutation Project Alleles of Genes Known to Affect Gentle Touch

4.1 Introduction

Clusters of phenotype-causing point mutations are often used to infer which parts of a protein are most important to its function. Where only phenotype-causing alleles are identified, which is generally the case for alleles identified through mutageneses, it remains a possibility that regions of a protein lack phenotype-causing alleles not due to their lack of functional significance, but to other factors such as decreased likelihood of mutation or pleiotropic effects that prevent testing for the phenotype of interest. The whole-genome sequencing data from the Million Mutation Project (MMP) identifies new alleles without the same degree of bias towards phenotypic effects, providing a unique opportunity to investigate the "negative space" around previously identified mutations.

To compare alleles of known *mec* genes that do and do not result in a detectable phenotype, we compared the locations and types of MMP mutations confirmed to cause touch insensitivity with mutations that either appeared in touch sensitive strains or else appeared in insensitive MMP strains where a mutation in a different gene had been confirmed to be phenotype-causing. For reference, we also compared these to the collection of previously identified point-mutation alleles provided on WormBase (Harris et al., 2019), which presumably had all been isolated due to phenotype-causing effects, though without limitation to gentle touch response phenotypes. For some of the genes with few or no previously identified alleles mapped on WormBase, we considered additional alleles that we are aware of.

Here, I discuss known touch genes in the order in which they were introduced in Chapter 2 and provide charts showing the transcript and protein coding sequences of each gene along with the location of previously identified and MMP alleles. I mostly limited such consideration to genes that were identified in the mutageneses performed by Chalfie and Sulston (1981) and Chalfie and Au (1989) (which I refer to as the original *mec* genes), in part because these were the genes we considered most likely to have touch insensitive MMP alleles, and also because we generally have more knowledge regarding the function and structure of these genes. Original *mec* genes for which we did not identify any touch insensitive MMP alleles are also considered here, seeing as how we are interested in the nature of MMP mutations that both did and did not result in phenotypes. I also charted and analyzed mutations in *unc-2* due to the relatively large number of *unc-2* alleles identified in our MMP screen. In my discussion of each gene, I provide a brief summary of protein function and structure and consider the nature and location of previously identified alleles in comparison to MMP alleles. I then suggest conclusions about the function and structure of known *mec* genes that one might draw from such comparisons.

4.2 Results

Most of the MMP strains with strong touch insensitive phenotypes proved to have causative mutations in known *mec* genes, as we determined by failure to complement against reference alleles (see Chapter 3). However, there were also many instances in which MMP strains complemented reference alleles for candidate *mec* genes. Quite a few insensitive strains carried protein-altering mutations in more than one known *mec* gene, so verification was necessary to distinguish which of the protein-altering *mec* mutations led to a phenotype. In some cases, we have not yet been able to test candidate *mec* genes for complementation (see Chapter 3,

section on verified, unverified, and unknown causative mutations in Results). Unverified candidate causative mutations were excluded from the charts and analyses that follow.

I chose to chart only point mutations for the sake of straightforward comparison. Previously identified alleles and MMP alleles were categorized as either missense, nonsense, synonymous, splice-site affecting, or other non-coding. In addition, we calculated the Grantham score of substitutions caused by missense alleles (Grantham, 1974). Grantham scores quantify the difference between chemical properties of amino acid residues, and thus can be used to predict which substitutions are likely to be disruptive. Using our sample of MMP missense alleles in known *mec* genes and *unc-2,* we found that the average Grantham score of phenotype-causing mutations (insensitive MMP) is only slightly and not significantly higher than the average score of non-phenotype-causing mutations (sensitive MMP). However, the average Grantham score of previously identified missense alleles was significantly higher than that of non-phenotype-causing MMP missense alleles (Table 4-1). The clustering of previously identified and insensitive MMP missense alleles that we often observed suggests that the location of any given missense allele might be more predictive of effect than the specific nature of the amino acid substitution, but we would expect the Grantham score to be useful for predicting whether missense mutations in approximately the same region might be disruptive.

	Count (n)	Mean Grantham Score	P-value
Sensitive MMP	275	71	
Insensitive MMP	32	78	>0.05
Previously Identified Alleles	170	97	<0.001

Table 4-1: Mean Grantham scores of missense alleles in selected known touch genes. Set of selected known touch genes includes the 18 original touch genes plus *unc-2*. P-values indicate test statistic from Mann-Whitney-Wilcoxon test comparing mean Grantham scores between the indicated set of alleles and the set of sensitive MMP alleles.

mec-4

MEC-4 is the major subunit of the TRN mechanoreceptor channel (the channel can be formed by homotrimers of MEC-4 or heterotrimers of two MEC-4 subunits and one MEC-10 subunit). MEC-4 belongs to the degenerin epithelial sodium channel (DEG/ENaC) family and contains two membrane-spanning domains (MSDI and II), one of which contributes to the channel pore (MSDII) (Gessmann et al., 2010). The majority of the protein is situated on the extracellular side of the membrane between the two transmembrane domains and includes three cysteine-rich domains (CRDI, II, and III), which may interact with the extracellular matrix (Hong et al., 2000; Tavernarakis and Driscoll, 2000). Just before the start of MSDII, there is a degenerin (d)-site that can mutate to increase channel open probability and lead to necrotic cell death (Driscoll and Chalfie, 1991; Brown et al., 2008).

The most pronounced cluster of previously identified *mec-4* alleles occurs near the (d)-site and MSDII. However, no MMP alleles fall within the region covered by this tight cluster of previously identified alleles (Figure 4-1). Interestingly, in the region between CRDIII and MSDII, where a few previously identified alleles map to, only the MMP missense mutation with the lowest Grantham score out of three alleles caused touch insensitivity. This particular point mutation (*gk837870*) substitutes an isoleucine for a methionine and results in a strong insensitive

phenotype. The substitution should only result in a slight increase in hydrophobicity, and the residue is not strictly conserved across paralogous DEG/ENaC genes. However, a substitution two amino acids away in the homologous region of the DEG/ENaC UNC-8 disrupts touch sensitivity (Eastwood and Goodman, 2012). One MMP missense mutation identified as phenotype-causing occurs between CRDII and CRDIII and does not match locale with any previously identified missense alleles, but only caused a weak posterior response phenotype. Also of some note is the high Grantham score missense allele located near the very start of the protein coding sequence. In general this region is not conserved among DEG/ENaCs (Hong et al., 2000), so it is not surprising that the alteration caused no detectable phenotype.

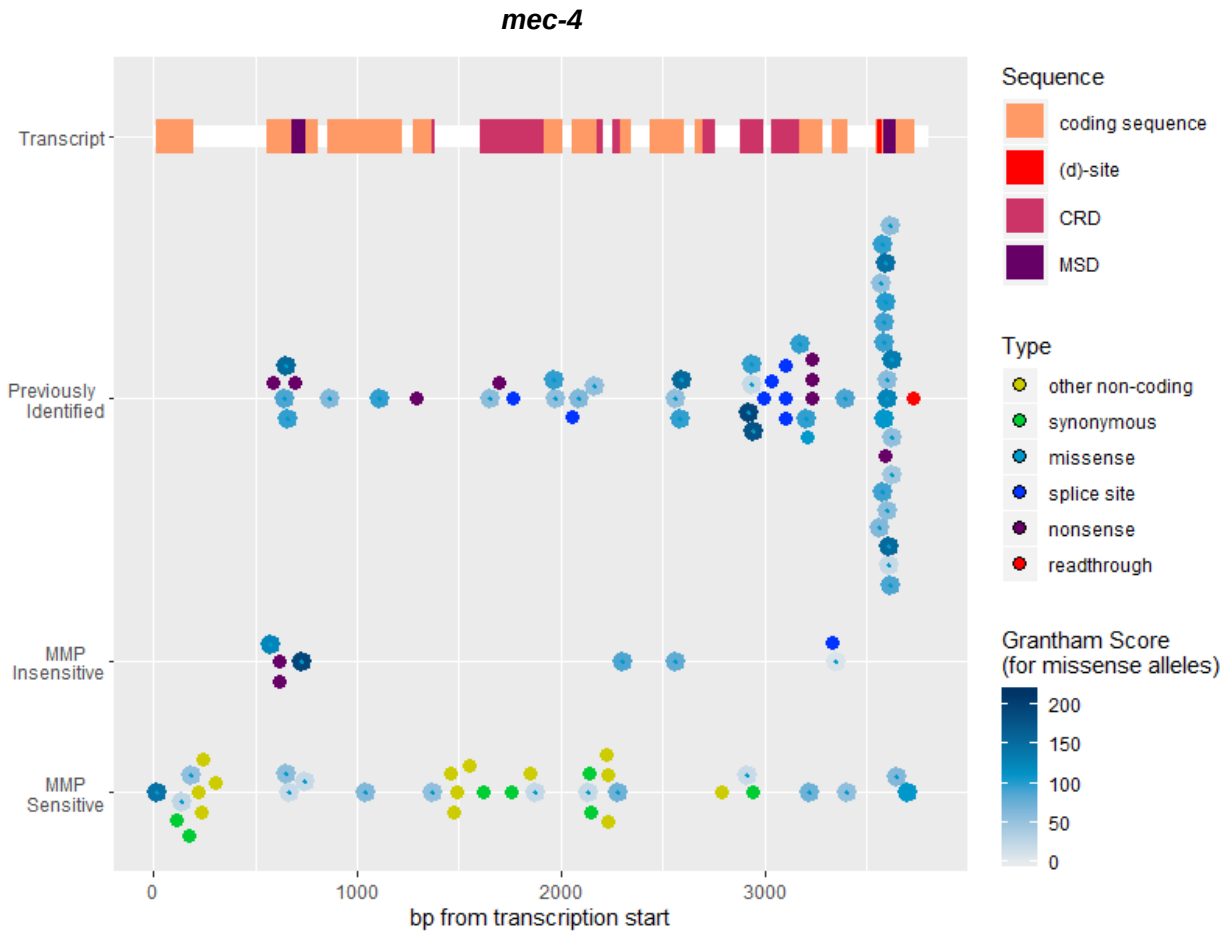

Figure 4-1: *mec-4* transcript and coding sequence plotted with previously identified alleles and MMP alleles grouped by associated phenotype**.** Other non-coding, synonymous, splice site, nonsense, and readthrough mutation alleles are represented by solid color dots. Missense mutations are represented by smaller dots surrounded by larger blue dots shaded according to the Grantham score of the amino acid substitution.

The lack of any MMP mutations occurring near the (d)-site despite the large number of previously identified alleles affecting the region demonstrates the bias towards identification of stronger phenotypes. Although the region is not large and is not significantly more prone to EMS-induced lesions than expected, the strong touch insensitive phenotypes associated with (d)-site mutations greatly increased their chances of being identified. While we expect that our identification of touch-insensitive MMP mutants was also biased towards stronger phenotypes,

their degree of overrepresentation does appear to be less than what we observe among the set of previously identified touch-insensitive mutants.

MMP missense mutations indicated on a 3D model of MEC-4 suggest that mutations affecting extracellular residues closer to the channel pore may be more likely to cause touch-insensitive phenotypes (Figure 4-2). However, not all of the MMP missense mutations that affect residues close to the channel pore were found to cause touch insensitivity, and it is not clear whether the phenotype-causing missense mutations that affect residues close to the channel pore actually affect the surface of the channel pore.

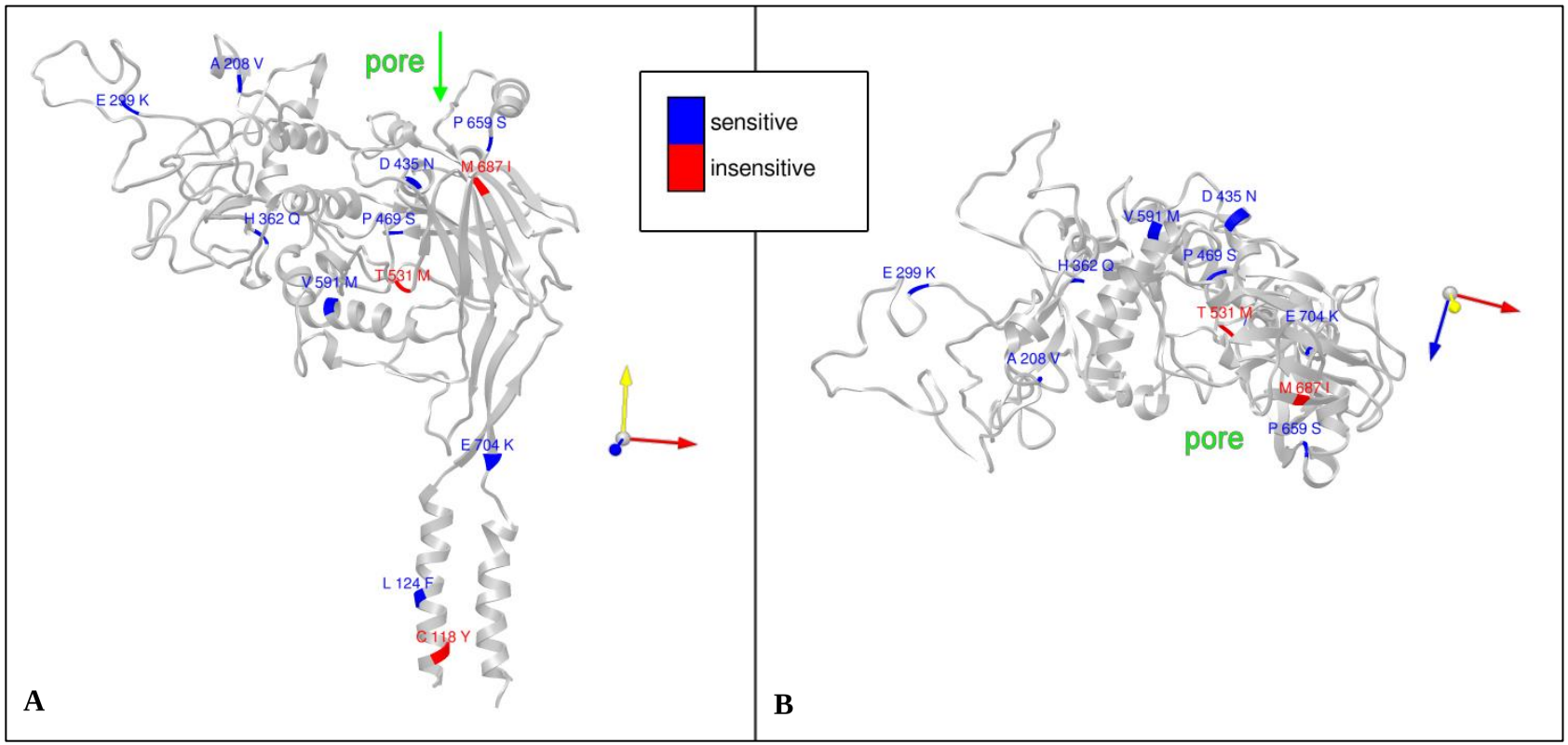

Figure 4-2: 3D model of MEC-4 with MMP missense mutations. Ribbon structure model includes MEC-4 aa 114 to 729 and is based on homology to human ENaC (Noreng et al., 2018). Residues affected by MMP missense mutations are labeled with WT aa one letter code, aa number, and mutant aa one letter code. Substitutions associated with touch sensitive phenotypes are indicated in blue and substitutions associated with touch insensitive phenotypes are indicated in red. The approximate location of the extracellular opening of the channel pore is indicated with green text/arrow. Relative X-Y-Z axes are indicated with red, yellow, and blue arrows, respectively. A) shows a side view of MEC-4 (extracellular regions are shown towards the top of the image and membrane-spanning domains are shown towards the bottom of the image). B) shows a top-down view of MEC-4 (extracellular regions are stacked in front of membrane-spanning domains) with labels for substitutions affecting membrane-spanning domains (L 124 F and C 118 Y) not shown.

mec-10

MEC-10 is a DEG/ENaC subunit of relatively lesser importance to gentle touch sensation as compared to MEC-4. However, MEC-10 and MEC-4 share the same general structure and topology and can both be mutated at the (d)-site to cause constitutive channel opening and necrotic cell death. MEC-10 MSDI was found to be critical for response to a particular type of mechanical stimulus (laminal sheer stress) in Xenopus oocytes, which was not also true for MEC-4. In the absence of MEC-10, the MEC-4 channel expressed in Xenopus oocytes did not respond to laminal sheer stress, and a chimeric MEC-10 channel with the MEC-4 MSDI did not enable response (Shi et al., 2016). Thus, the sequence of MSDI in MEC-10 may be particularly important for its activity.

The original screens for touch insensitive mutants only identified two *mec-10* loss-of-function mutations due to the relative weakness of *mec-10* loss-of-function and null phenotypes (Arnadottir et al., 2011). Additional *mec-10* alleles were identified from a screen for enhancers of neuronal death in *poml-1*; *mec-4*(d) mutants (mutations in *poml-1* suppress the TRN cell death phenotype in *mec-4*(d) mutants, and mutations in *mec-10* were found to increase cell death in *poml-1*; *mec-4*(d) mutants) (Chen et al., 2016b). Among the more recently identified *mec-10* alleles are two nonsense mutations and six splice site mutations, which we assume to result in loss-of-function phenotypes. However, in considering the previously identified *mec-10* mutations, I have separated the *mec-10* alleles identified from screens for touch insensitivity and from the screen for suppressed suppression (Figure 4-3).

We expected our screen of the MMP to be more sensitive to weak phenotypes as compared to previous screens and thus expected that we might detect relatively more *mec-10* loss-of-function alleles. However, we only confirmed two *mec-10* mutations to cause touch

insensitivity, and considering the set of MMP *mec-10* mutations, they were not the ones we would have naively predicted to be most likely to cause loss-of-function. There are two *mec-10* splice-site mutations that we would have expected to cause a phenotype. One of them is found in a strain that underwent one round of testing with a response rate under the 10th percentile (VC40582), but was not retested for confirmation of a weak touch insensitive phenotype based on our criteria (see Chapter 3). The other is carried in a strongly insensitive strain (VC40873) that complemented *mec-10* and did not appear to have an X-linked causative mutation (the *mec-10* gene is on X). We expect that the *mec-10* mutation in VC40582 may indeed cause a weak phenotype, but we would need to retest the strain to be certain. As for the *mec-10* mutation in VC40873, we wondered if the strong phenotype-causing mutation in a different gene caused us to disregard a weaker *mec-10* phenotype. We therefore considered the touch response of male progeny from VC40873 outcrosses, but did not find evidence of a weak X-linked phenotype (the male cross progeny responded to 90 and 93 out of 100 anterior and 100 posterior touches, respectively). Aside from the splice-site mutations, we would have also thought it likely for one or more of the missense mutations affecting the third cysteine-rich domain (CRDIII) to cause a phenotype, since missense alleles affecting the region were previously identified, but this did not prove to be the case (Figure 4-3).

One of the *mec-10* missense mutations we found to be phenotype-causing affects MSDI, the specific sequence of which is not believed to be critical for DEG/ENaC function in general (Hong and Driscoll, 1994), but which may play a relatively more important role in the function of MEC-10 (Shi et al., 2016). The second phenotype-causing mutation substitutes a residue directly adjacent to one mutated in a previously identified missense allele.

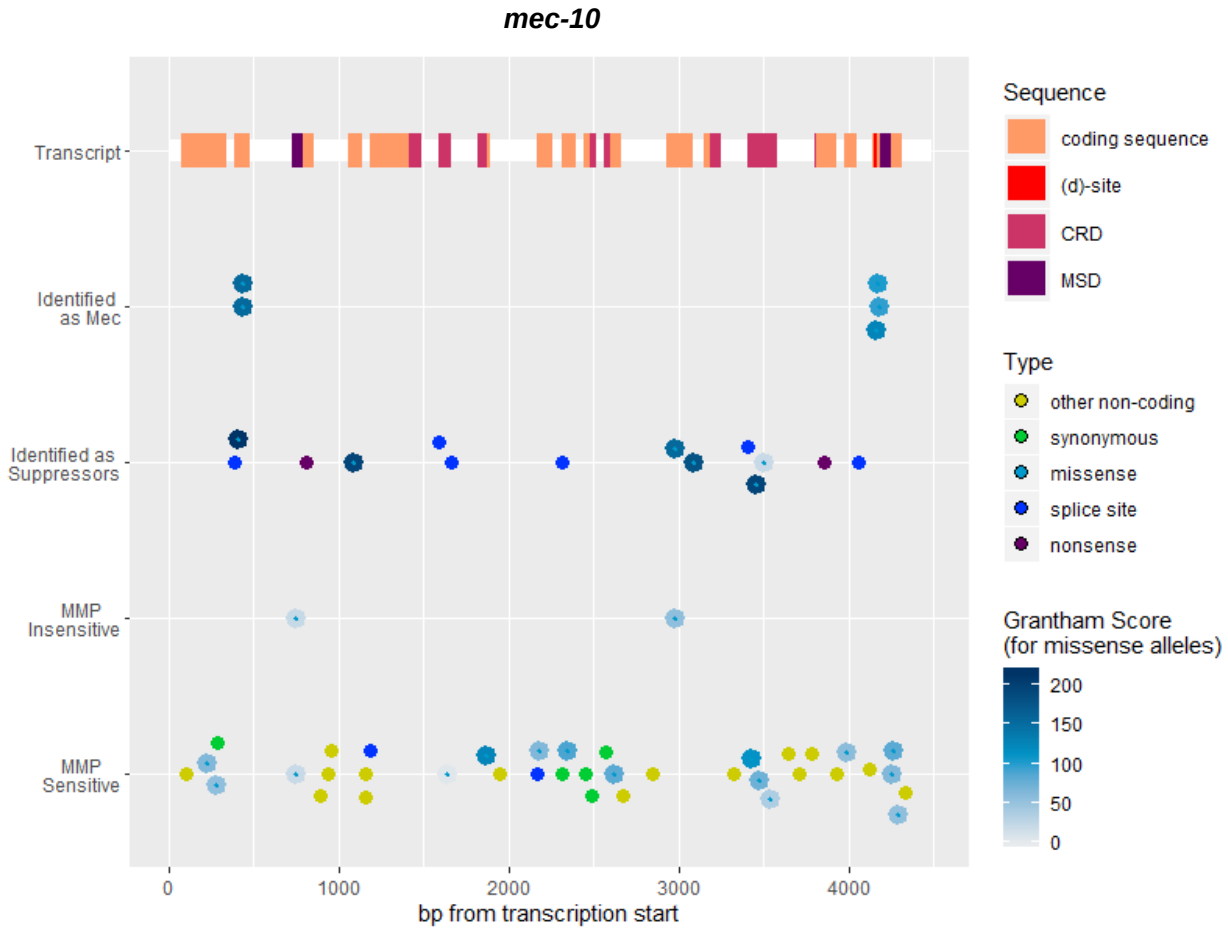

Figure 4-3: *mec-10* transcript and coding sequence plotted with previously identified alleles and MMP alleles grouped by associated phenotype. Other non-coding, synonymous, splice site, and nonsense mutation alleles are represented by solid color dots. Missense mutations are represented by smaller dots surrounded by larger blue dots shaded according to the Grantham score of the amino acid substitution.

As was the case with MEC-4, MMP missense mutations indicated on a 3D model of MEC-10 suggest that substitutions affecting extracellular residues closer to the channel pore are perhaps more likely to cause a phenotype (Figure 4-4). However, for the same reasons as given in the case of MEC-4, this conclusion is quite speculative.

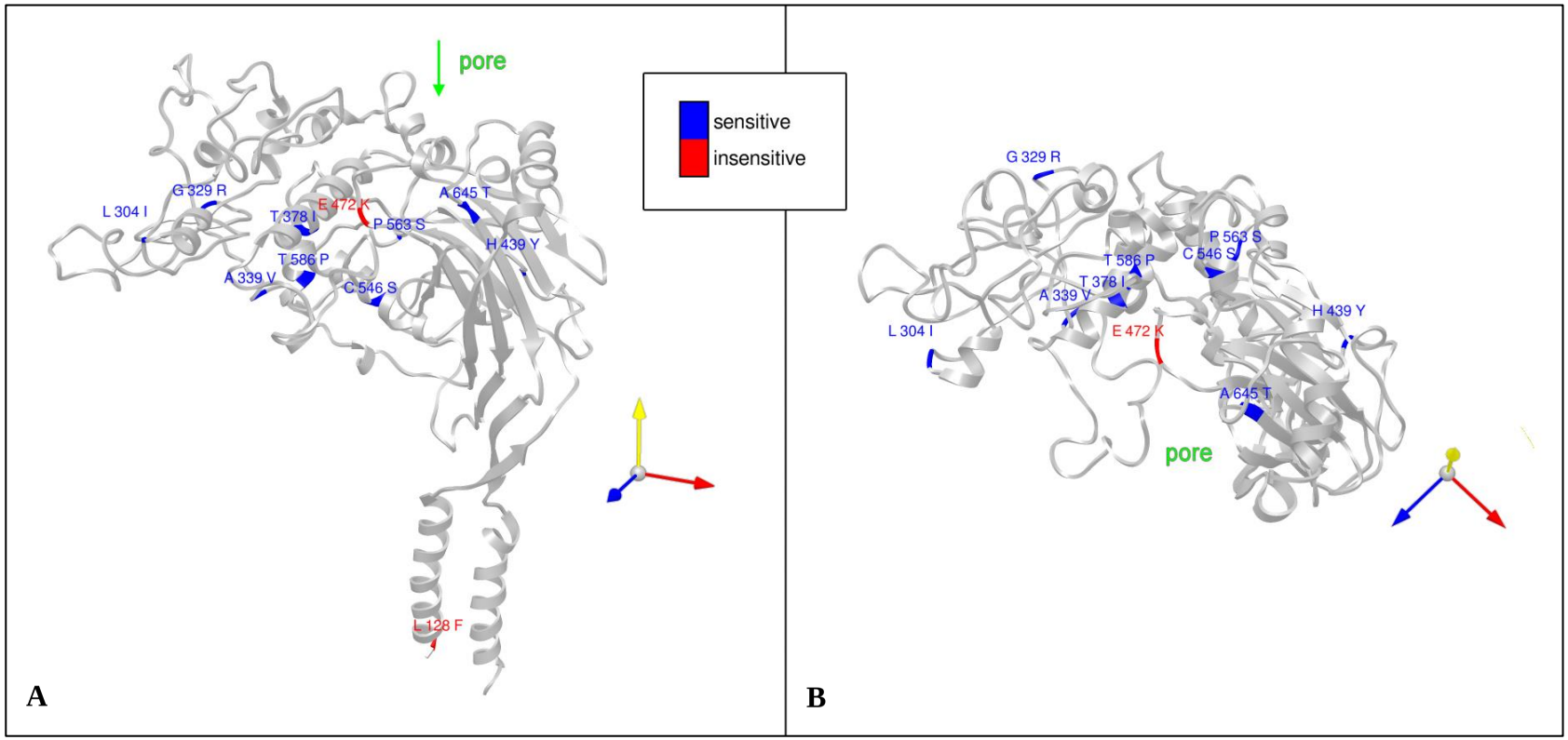

Figure 4-4: 3D model of MEC-10 with MMP missense mutations. Ribbon structure model includes MEC-10 aa 127 to 689 and is based on homology to human ENaC (Noreng et al., 2018). Residues affected by MMP missense mutations are labeled with WT aa, aa number, and mutant aa. Substitutions associated with touch sensitive phenotypes are indicated in blue and substitutions associated with touch insensitive phenotypes are indicated in red. The approximate location of the extracellular opening of the channel pore is indicated with green text/arrow. Relative X-Y-Z axes are indicated with red, yellow, and blue arrows, respectively. A) shows a side view of MEC-10 (extracellular regions are shown towards the top of the image and membrane-spanning domains are shown towards the bottom of the image). B) shows a top-down view of MEC-10 (extracellular regions are stacked in front of membrane-spanning domains) with the label for the substitution affecting MSDI not shown.

mec-2

MEC-2 is a cholesterol-binding protein embedded in the cytosolic surface of the plasma membrane. MEC-2 likely regulates mechanoreceptor channel activity, as is evidenced by the loss of TRN mechanoreceptor currents in *mec-2* mutants (O'Hagan et al., 2005) and by the striking increase in MEC-4(d) channel activity that occurs when MEC-2 and MEC-4(d) are coexpressed in Xenopus oocytes (Goodman et al., 2002). The stomatin-like prohibitin (PHB) domain of MEC-2 is of particular importance to its function. Mutations in the PHB domain can disrupt the normal punctate distribution of MEC-2 (Zhang et al., 2004) and prevent cholesterol binding (Huber et al., 2006).

The longest transcribed isoform of *mec-2* is relatively large, spanning over about 24,000 bp, and RNAseq reads have detected 17 different *mec-2* isoforms (Harris et al., 2019). Shorter isoforms appear to be more highly expressed (Harris et al., 2019), but mutations affecting only longer isoforms have been found to result in touch insensitivity. Previously identified *mec-2* alleles are enriched within and near the PHB domain (Figure 4-5). Other previously identified alleles affect splice junctions and a region just past the PHB domain. Most of the phenotype-causing *mec-2* alleles that we identified in the MMP set were similarly localized, except for one nonsense allele and two missense alleles. Given the large number of previously identified *mec-2* alleles, it is somewhat surprising that we identified any phenotype-causing MMP alleles outside of the regions covered by previously identified alleles. Both missense alleles caused weak phenotypes, which might explain the lack of similar previously identified alleles, but more strangely, none of the three unusual alleles affect the coding sequence of the *mec-2* isoform thought to be predominantly expressed in the TRNS (*mec-2*a) (Calixto et al., 2010b). The nonsense allele (*gk529960*) resulted in a strong phenotype and failed to complement a reference

mec-2 allele, suggesting that the isoforms it affects (d-g) play an important role in TRN function. However, considering that the coding sequence exclusive to isoforms d-g is rather long, it is very surprising that no other alleles have been mapped to the region (Figure 4-6).

A

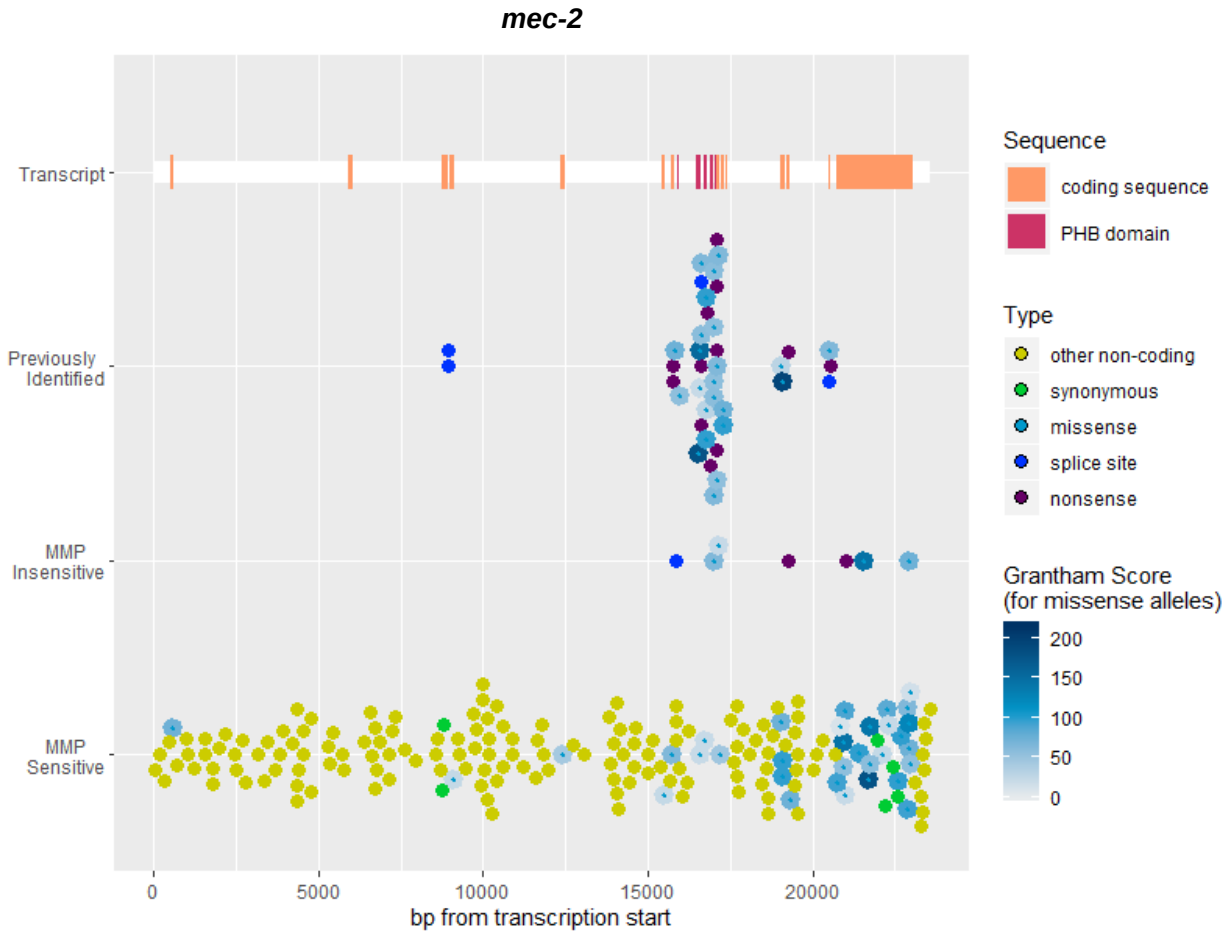
mec-2
Transcript
Previously Identified
MMP Insensitive
MMP Sensitive
0
5000
10000
15000
20000
bp from transcription start
Sequence
coding sequence
PHB domain
Type
other non-coding
synonymous
missense
splice site
nonsense
Grantham Score (for missense alleles)
200
150
100
50
0

B

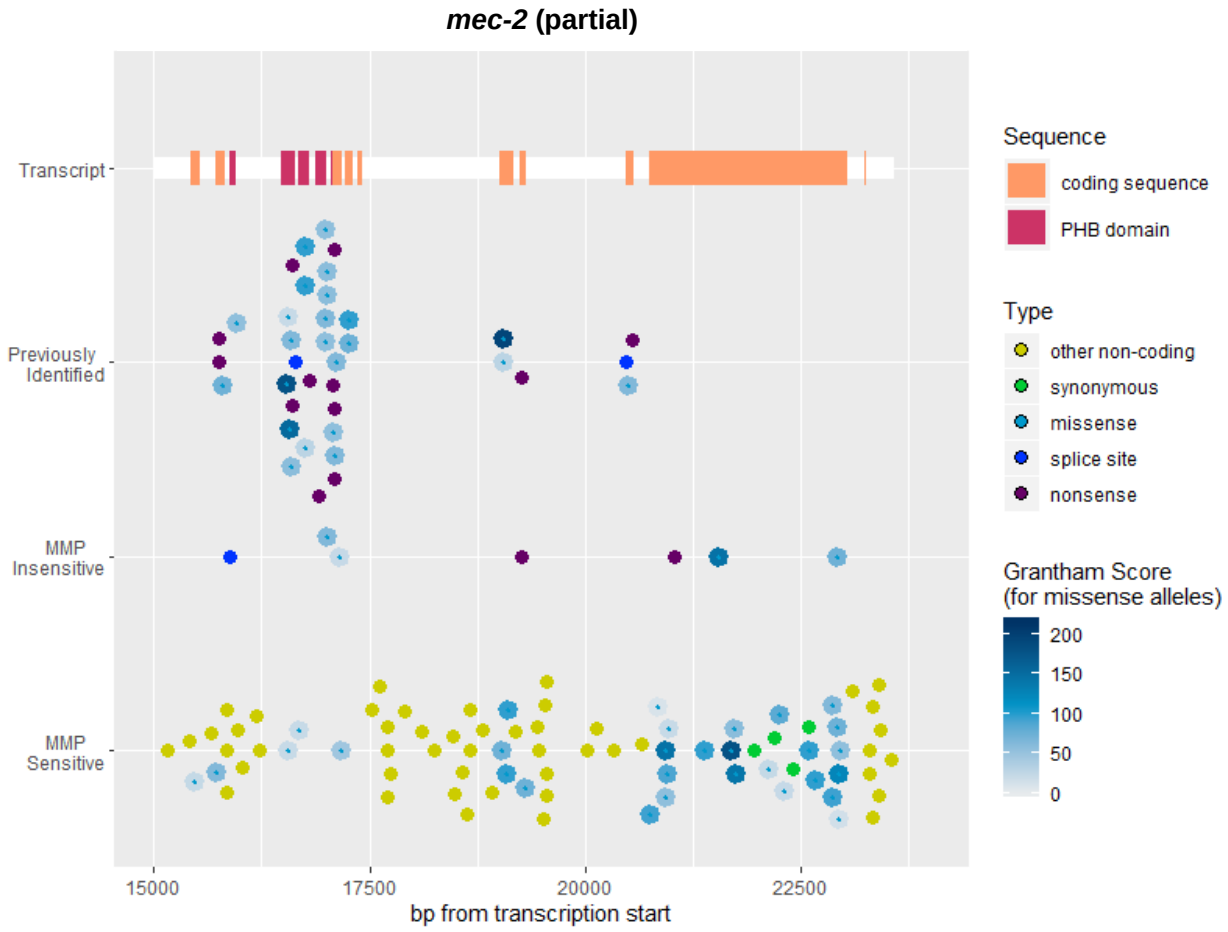

Figure 4-5: *mec-2* transcript and coding sequence plotted with previously identified alleles and MMP alleles grouped by associated phenotype. Other non-coding, synonymous, splice site, and nonsense mutation alleles are represented by solid color dots. Missense mutations are represented by smaller dots surrounded by larger blue dots shaded according to the Grantham score of the amino acid substitution. A) shows the entire *mec-2* gene. B) shows a partial view of the *mec-2* gene focused on a region richer in coding sequences.

A

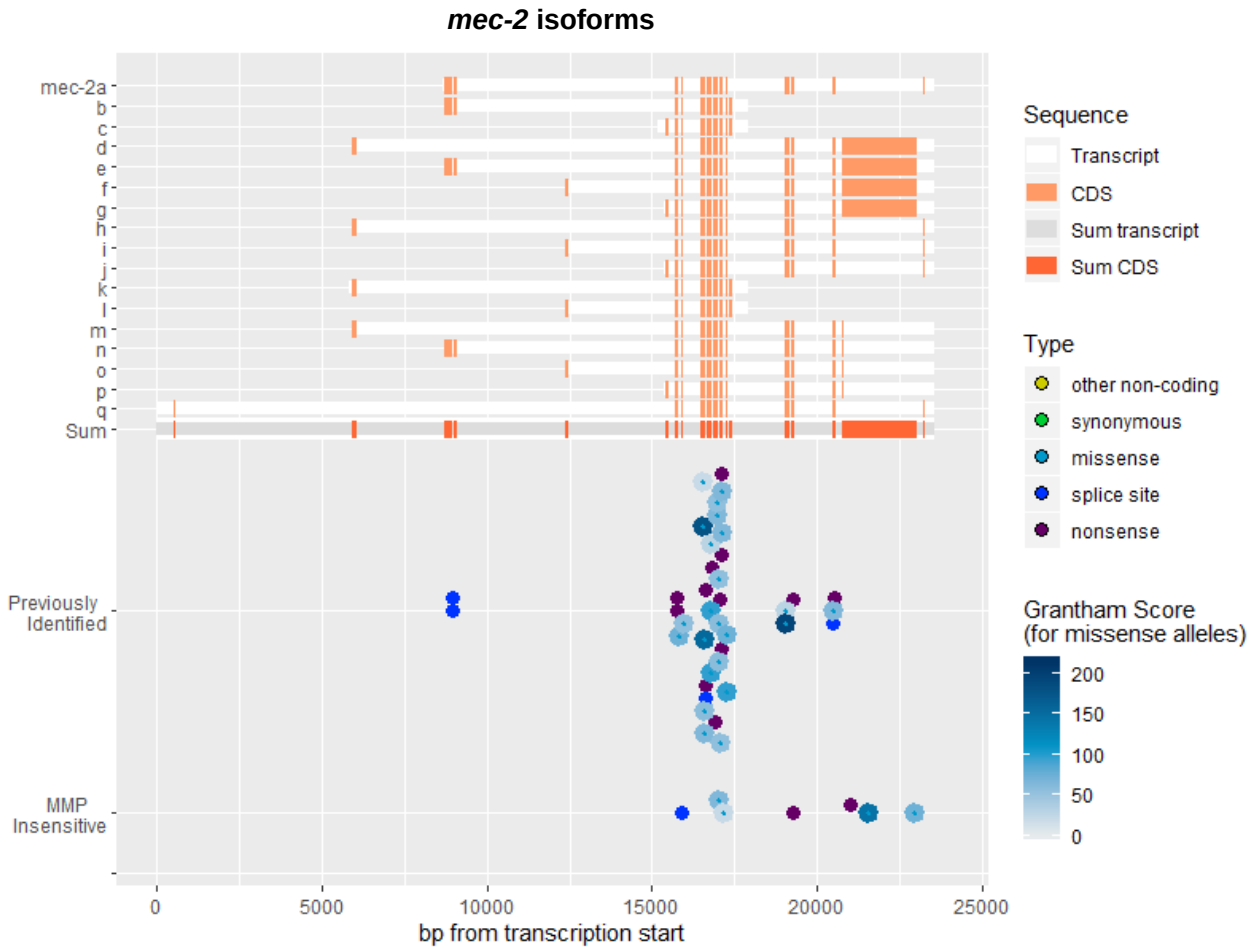
mec-2 isoforms
mec-2a
b
c
d
e
f
g
h
i
j
k
l
m
n
o
p
q
Sum
Previously Identified
MMP Insensitive
0
5000
10000
15000
20000
25000
bp from transcription start
Sequence
Transcript
CDS
Sum transcript
Sum CDS
Type
other non-coding
synonymous
missense
splice site
nonsense
Grantham Score (for missense alleles)
200
150
100
50
0

B

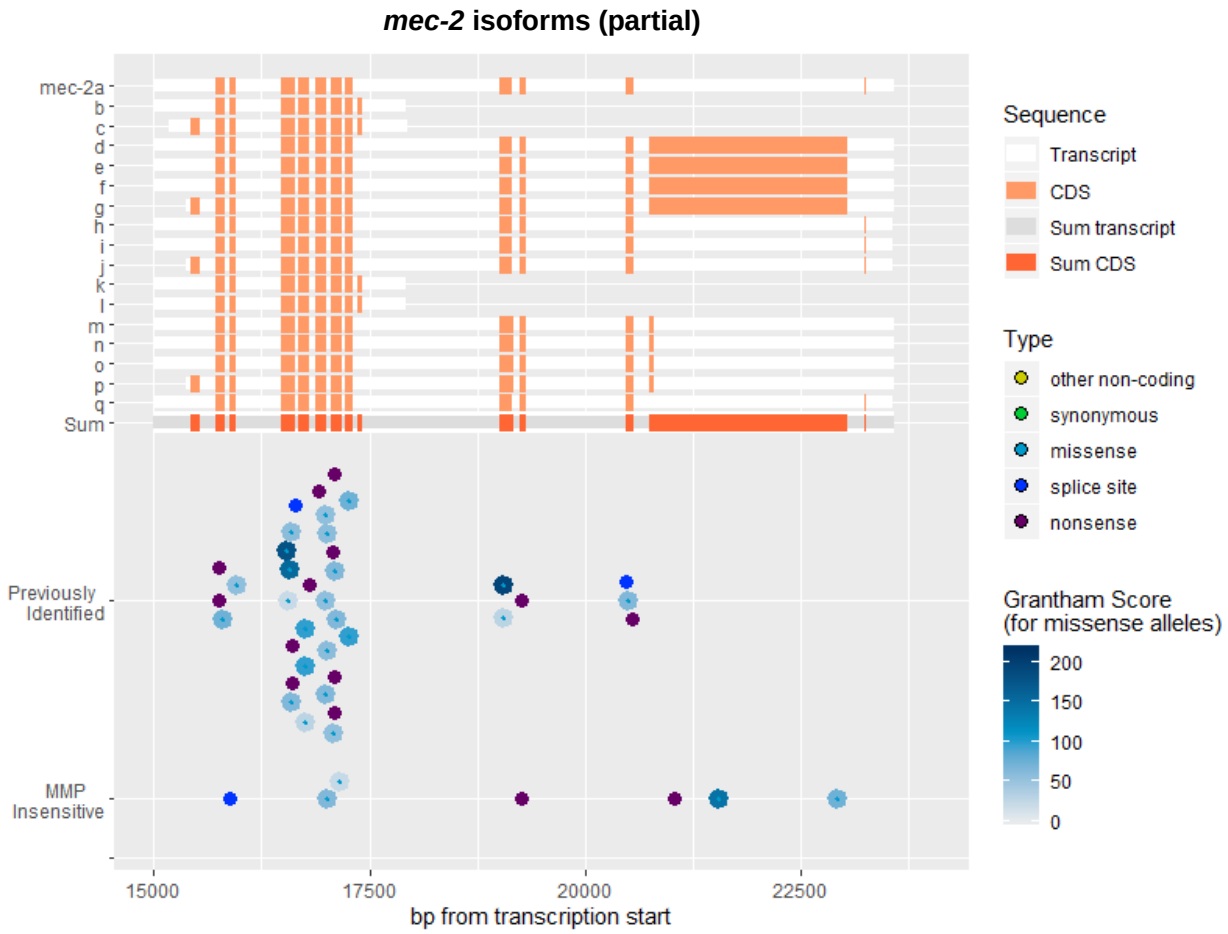

Figure 4-6: *mec-2* isoforms and summed coding sequences plotted with previously identified alleles and touch phenotype-causing MMP alleles. Other non-coding, synonymous, splice site, and nonsense mutation alleles are represented by solid color dots. Missense mutations are represented by smaller dots surrounded by larger blue dots shaded according to the Grantham score of the amino acid substitution. A) shows the entire *mec-2* gene. B) shows a partial view of the *mec-2* gene focused on a region richer in coding sequences.

mec-18

MEC-18 is likely an enzyme involved in lipid metabolism that modifies mechanoreceptor channel activity. Other than assumptions made based on its homology to CoA-synthase (Gu, 1998), little is known about the structure and function of MEC-18. All previously identified *mec-18* alleles are splice-site or nonsense mutations, but surprisingly, we identified a phenotype-causing MMP missense mutation. The mutation occurs close to the N-terminal start of the protein and does not affect any putative functional domains. 16 other MMP MEC-18 missense mutations did not prove to be phenotype-causing (Figure 4-7).

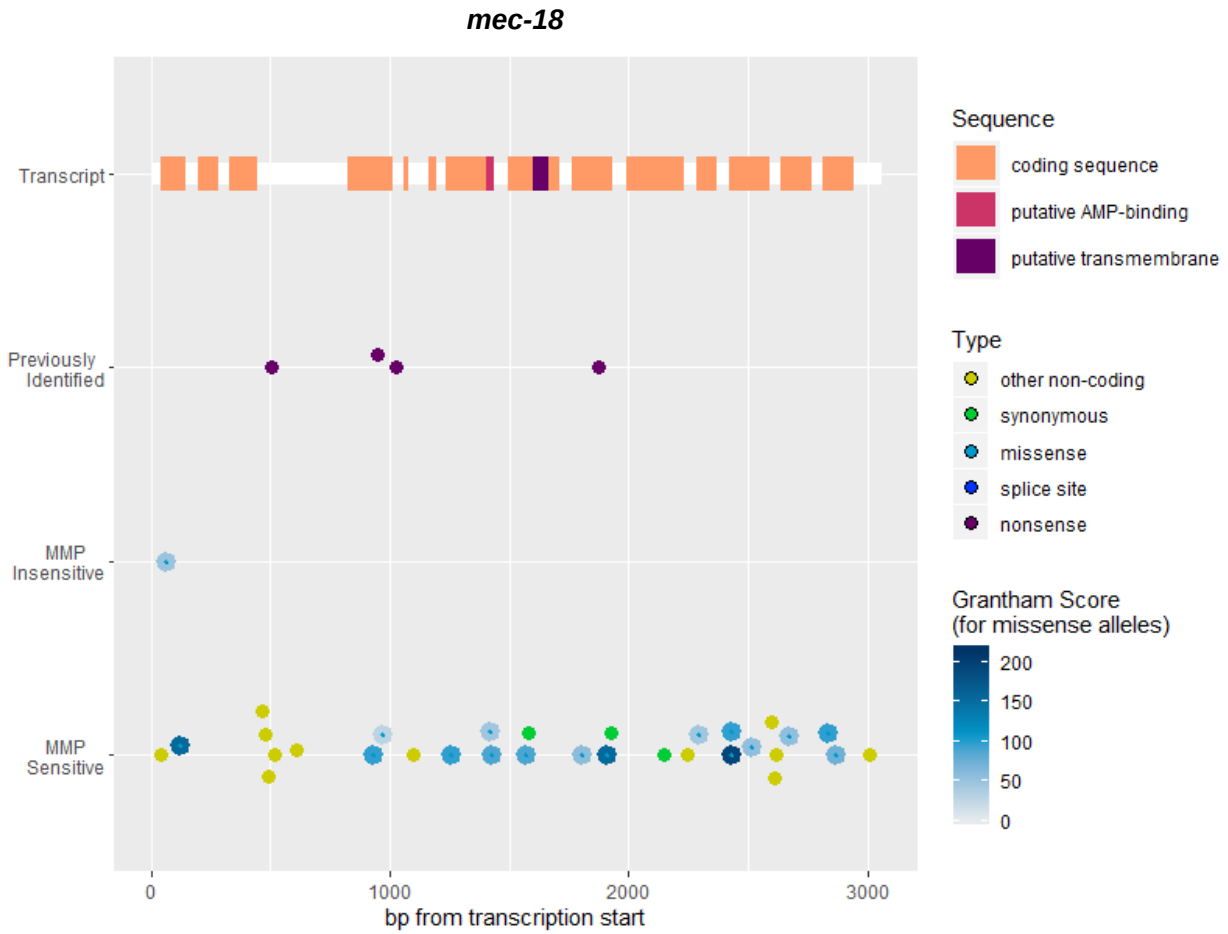

Figure 4-7: *mec-18* transcript and coding sequence plotted with previously identified alleles and MMP alleles grouped by associated phenotype. Other non-coding, synonymous, splice site, and nonsense mutation alleles are represented by solid color dots. Missense mutations are represented by smaller dots surrounded by larger blue dots shaded according to the Grantham score of the amino acid substitution.

mec-6

MEC-6 is a membrane-spanning ER resident chaperone involved in the maturation of DEG/ENaC proteins (Chen et al., 2016a). MEC-6 share similarities with mammalian paraoxonases, but it is unclear whether MEC-6 has any enzymatic activity (Brown et al., 2008). Although MEC-6 enzymatic activity has not been experimentally demonstrated, most previously identified *mec-6* missense mutations affect the domain with homology to arylesterases. The

MMP set included two missense alleles within either edge of this region, but we did not find either of them to cause touch insensitivity. The two phenotype-causing *mec-6* alleles found in our screen included one nonsense allele in the fourth exon and one missense allele affecting the C-terminal region of the protein (Figure 4-8). The importance of the MEC-6 C-terminal region is currently unclear.

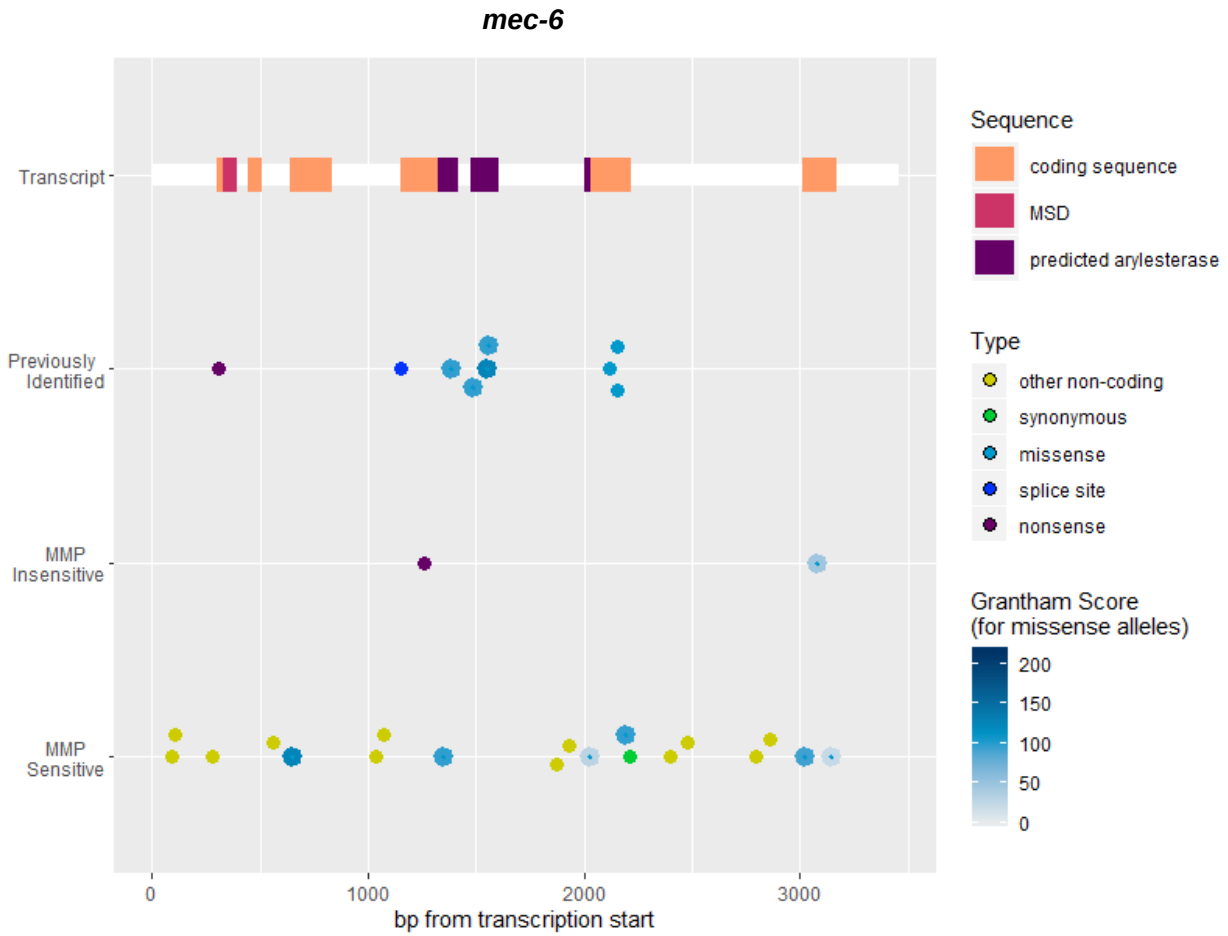

Figure 4-8: *mec-6* transcript and coding sequence plotted with previously identified alleles and MMP alleles grouped by associated phenotype. Other non-coding, synonymous, splice site, and nonsense mutation alleles are represented by solid color dots. Missense mutations are represented by smaller dots surrounded by larger blue dots shaded according to the Grantham score of the amino acid substitution.

mec-1

MEC-1 is a secreted constituent of the extracellular matrix (ECM) surrounding the TRN processes. The longest *mec-1* isoform, which is required for touch sensitivity, contains 15 Kunitz (Ku) domains and two EGF domains. It was previously shown that only the longest isoform of MEC-1 is sufficient for normal TRN function (Emtage et al., 2004). Of the fifteen Kunitz domain repeats in MEC-1, only the last three (Ku13-15) are absent from shorter isoforms. Kunitz and EGF domains are commonly found in ECM proteins, and are associated with high affinity protein-protein interactions (Emtage et al., 2004). Null mutations in *mec-1* disrupt the accumulation of the ECM surrounding the TRNs (Chalfie and Sulston, 1981). The *mec-1* missense alleles identified through the original set of screens for touch insensitivity only included two closely located alleles (Chalfie and Sulston, 1981; Chalfie and Au, 1989), suggesting that much of the MEC-1 protein sequence is redundant (Emtage et al., 2004). We identified three phenotype-causing *mec-1* missense alleles clustered to approximately the same region, although additional MMP *mec-1* missense alleles were numerous and spread somewhat evenly throughout the coding sequence (Figure 4-9).

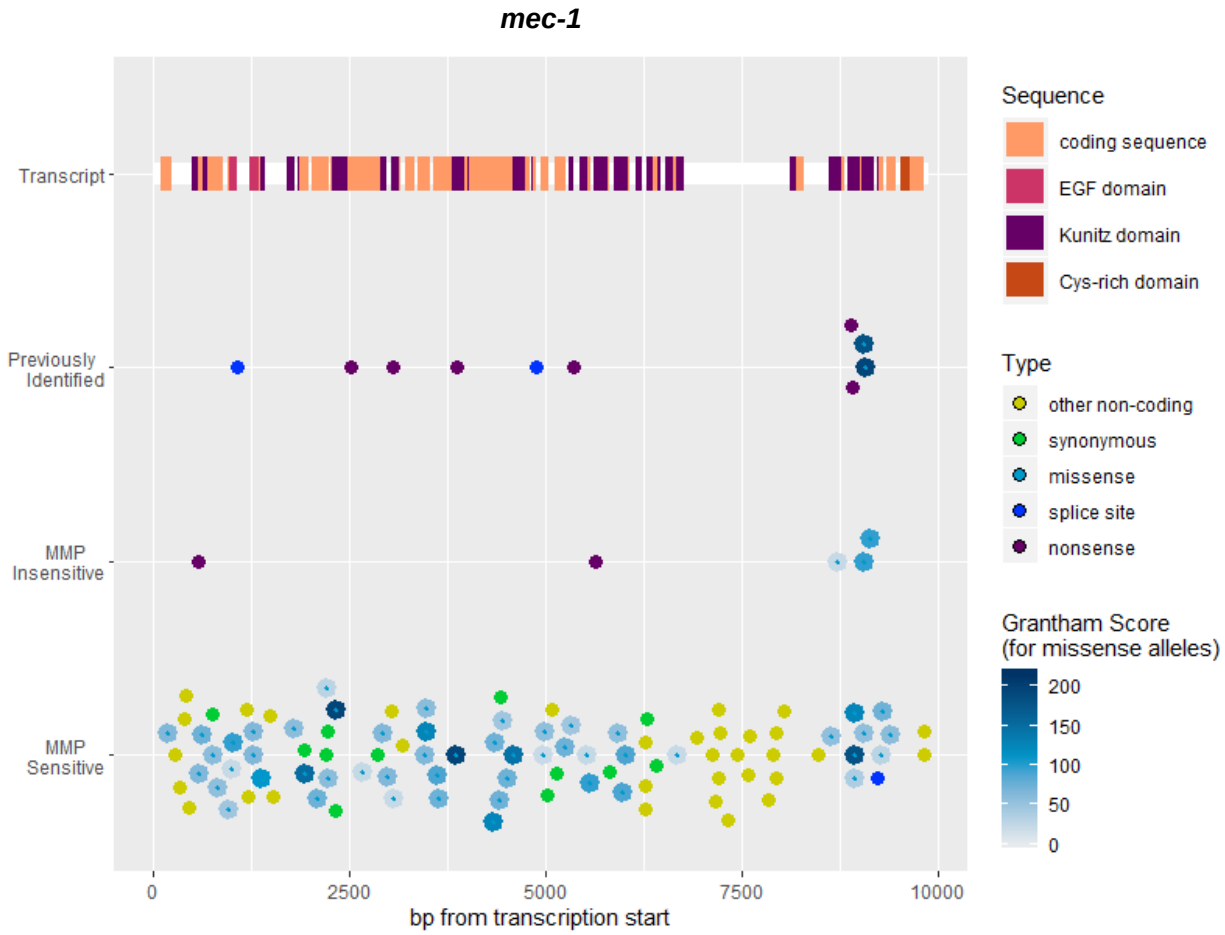

Figure 4-9: *mec-1* transcript and coding sequence plotted with previously identified alleles and MMP alleles grouped by associated phenotype. Other non-coding, synonymous, splice site, and nonsense mutation alleles are represented by solid color dots. Missense mutations are represented by smaller dots surrounded by larger blue dots shaded according to the Grantham score of the amino acid substitution.

The previously identified *mec-1* missense alleles (*e1526* and *u811*) cause substitutions affecting the 15th Kunitz domain repeat (Ku15). Two of the three MMP *mec-1* missense alleles which we determined to cause touch insensitivity also affect Ku15, but one allele results from a mutation affecting Ku13. Upon aligning the MEC-1 Kunitz domain repeats with reference to a Kunitz domain family consensus sequence (see section 4.4 Materials and Methods), we saw that the phenotype-causing mutation affecting Ku13 substitutes a highly conserved phenylalanine (Figure 4-10). Interestingly, one of the phenotype-causing mutations affecting Ku15 substitutes a

less conserved residue just adjacent to the homologous Ku15 phenylalanine. The second phenotype-causing mutation affecting Ku15 substitutes for a conserved glycine in between the two previously identified missense mutations. Another MMP missense allele affects the homologous glycine in Ku13 but was not found within a strain we considered touch insensitive (VC40782). However, VC40782 had initial anterior and posterior response rates that fell around the 8^{th} and 17^{th} percentile, respectively, suggesting that the strain could be weakly touch insensitive.

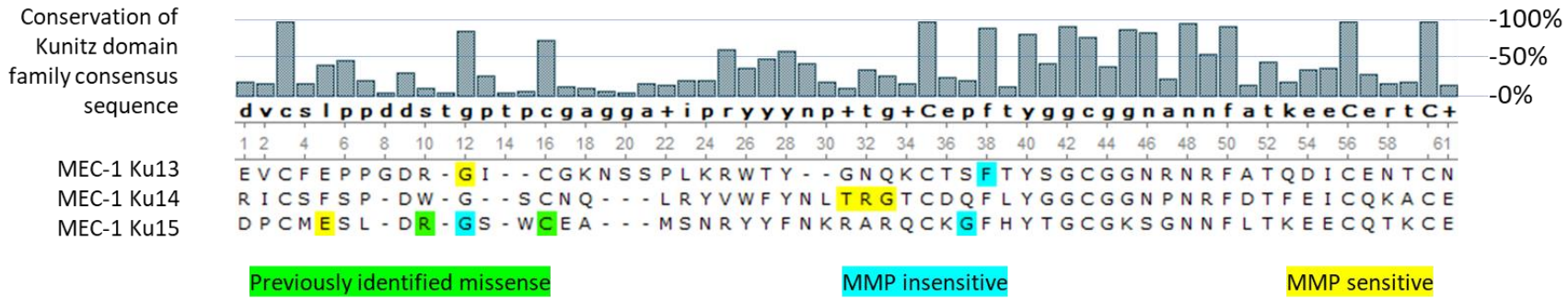

Figure 4-10: Aligned protein sequences for MEC-1 Kunitz domains 13-15. MEC-1 sequences (uppercase aa codes) were aligned along with 124 sequences from Kunitz domain SMART family alignment (see section 4.4 Materials and Methods) to determine consensus sequence (bold lowercase aa codes) and relative conservation levels (bar graph). MEC-1 residues affected by previously identified alleles and MMP alleles indicated. Green highlighting indicates previously identified mutations, blue highlighting indicates MMP mutations that were verified as phenotype-causing, and yellow highlighting indicates MMP mutations that did not appear to cause touch insensitivity.

mec-5

MEC-5 is a secreted collagen produced by the body wall muscle cells that contributes to the ECM surrounding the TRNs. A significant portion of the MEC-5 sequence encodes the collagen helix characterized by G-X-Y repeats (collagen repeats). Many of the previously identified *mec-5* alleles are temperature sensitive, causing touch insensitivity in animals raised at 25 but not 15°C. I conducted our screen of the MMP strains at 20°C, and may have overlooked *mec-5* mutations that caused decreased sensitivity at higher temperatures. However, the MMP *mec-5* alleles that we found to cause touch insensitivity occur in the same region of collagen repeats as other previously identified alleles, reinforcing its importance (Figure 4-11). It is interesting to note that most of the MMP missense alleles in this region did not cause touch insensitivity.

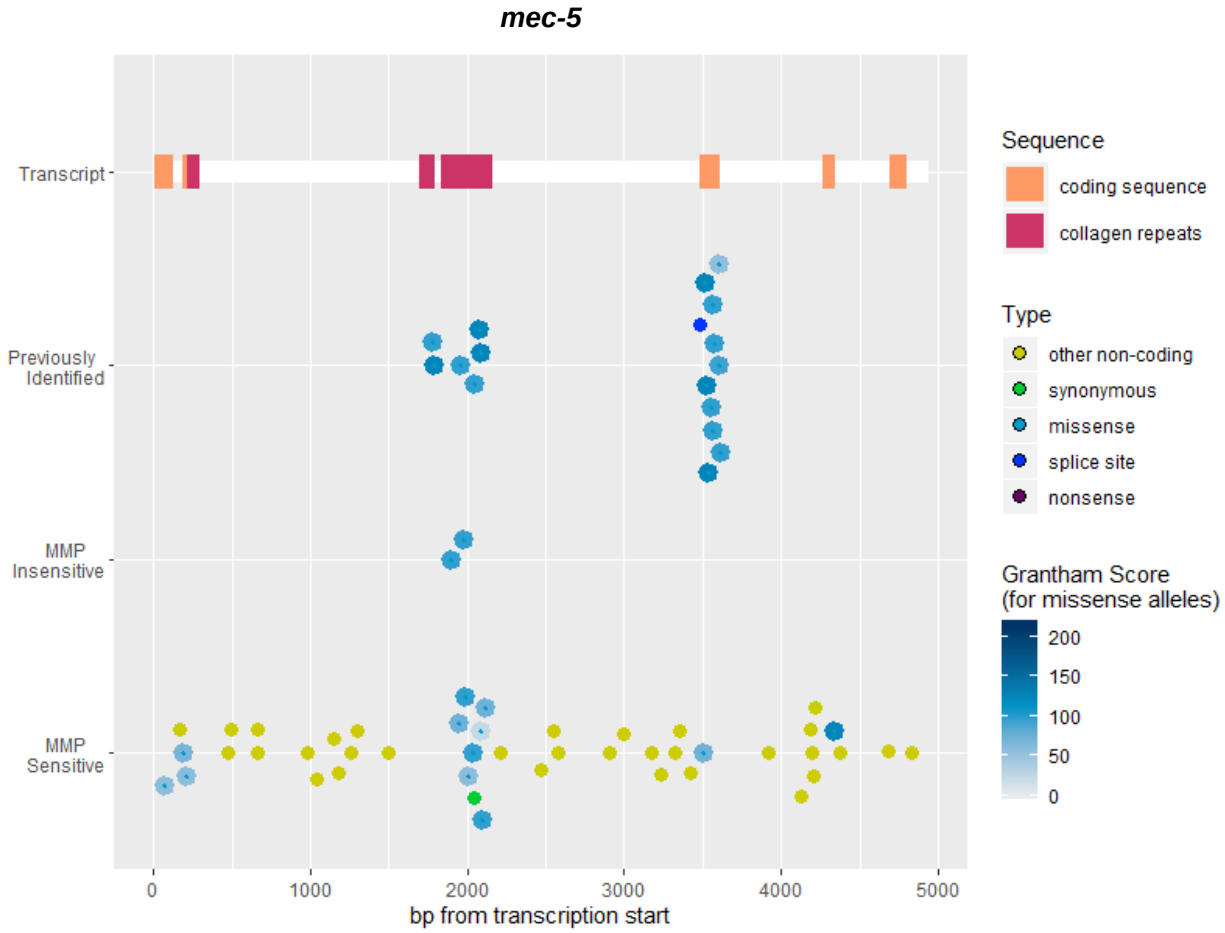

Figure 4-11: *mec-5* transcript and coding sequence plotted with previously identified alleles and MMP alleles grouped by associated phenotype. Other non-coding, synonymous, splice site, and nonsense mutation alleles are represented by solid color dots. Missense mutations are represented by smaller dots surrounded by larger blue dots shaded according to the Grantham score of the amino acid substitution.

Examining the sequence more closely, we observed that the two phenotype-causing MMP missense alleles both altered glycines, as did all of the previously identified *mec-5* alleles. Two of the non-phenotype-causing MMP alleles also altered glycines at the start of G-X-Y repeats (both of which were no less conserved than other G-X-Y glycines), but five affected one of the second two resides within the tripeptide repeats (which were generally less well conserved than G-X-Y glycines). The response rates of the sensitive strains carrying mutations in conserved

G-X-Y glycines fell within the bottom quartile of overall response rates (Figure 4-12). These could possibly represent temperature-sensitive alleles and should be retested at 25°C.

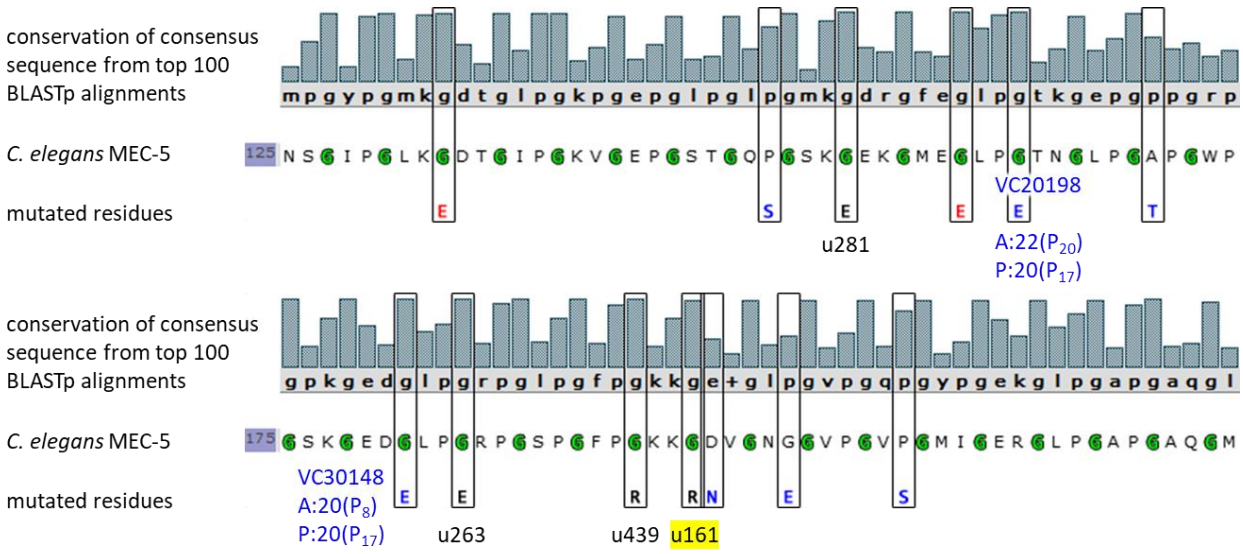

Figure 4-12: Resides mutated by MMP and previously identified *mec-5* missense alleles within amino acid residues 125-224 in *C. elegans* MEC-5. Bar charts indicate degree of conservation across top 100 BLASTp alignments, from 0 to 100%. Lower case amino acid sequences below bar charts indicate the consensus sequence from top 100 BLASTp alignments. Upper case amino acid sequences indicate *C. elegans* MEC-5 residues 125-224. Glycines in G-X-Y repeats of MEC-5 sequence are in green. Almost all G-X-Y glycines are highly conserved. Red mutated residues indicate phenotype-causing MMP mutations, blue mutated residues indicate non-phenotype-causing MMP mutations, and black mutated residues indicate previously identified alleles. Previously identified alleles are labeled with allele names in black, and the label for a temperature-sensitive previously identified allele is highlighted in yellow. Strains carrying *mec-5* mutations affecting conserved G-X-Y glycines that were not identified as being touch insensitive are identified along with anterior and posterior response rates (each out of 25) and percentile ranks.

mec-9

MEC-9 is another component of the TRN ECM. The shorter isoform of MEC-9, MEC-9S, is not required for touch sensitivity (Du et al., 1996). The longer isoform of MEC-9 (MEC-9L), which is necessary for touch sensitivity, contains 5 Kunitz domains and 7 EGF repeats. The

second and fourth EGF repeats (both of which are found in MEC-9L but not MEC-9S) are believed to have calcium-binding activity (Du et al., 1996).

All of the phenotype-causing *mec-9* mutations we identified in our screen were nonsense mutations. Notably, one of these nonsense mutations was located at the very C-terminal end of the protein, leaving out only 28 amino acid residues (Figure 4-13). And although there was one *mec-9* nonsense mutation that did not cause touch insensitivity, this was not surprising to us considering that the mutation only affects the coding sequence of MEC-9S. It has already been reported that mutations affecting MEC-9S but not MEC-9L do not result in touch insensitivity (Du et al., 1996). It was more surprising to see three high Grantham score missense alleles that did not cause a detectable phenotype. The three MEC-9 MMP missense mutations with the highest Grantham score were all C to Y substitutions. For each allele, I checked relative measures of conservation (GERP, phyloP, and phastCons scores). GERP and phyloP scores both measure evolutionary conservation by estimating the expected rate of substitutions at a given site between homologous alignments assuming neutral effects and then subtracting the observed rate of substitutions, but with different methods of statistical modeling (Cooper et al., 2005; Davydov et al., 2010). GERP scores can range from -12.3 (indicating faster than expected substitution rates) to 6.2 (indicating slower than expected substitution rates), and similarly, phyloP scores range from -11.7 to 6.4. PhastCons scores range from 0 to 1 and estimate the probability that a given sequence is conserved using a hidden Markov model that accounts for a window of bases (as opposed to GERP and phyloP which estimate values on a site-by-site basis) (Siepel et al., 2005). Looking at the conversation scores for MEC-9 C to Y substitutions, I found that each affected cysteine was moderately or highly conserved. Finally, I checked to see if the strains containing the mutations had lower than average touch response rates. All three strains had only

undergone one round of testing and did not have particularly low response rates (Table 4-2). Therefore, this appears to be another example of high Grantham score substitutions that do not have strong effects on protein function despite general conservation of the regions affected.

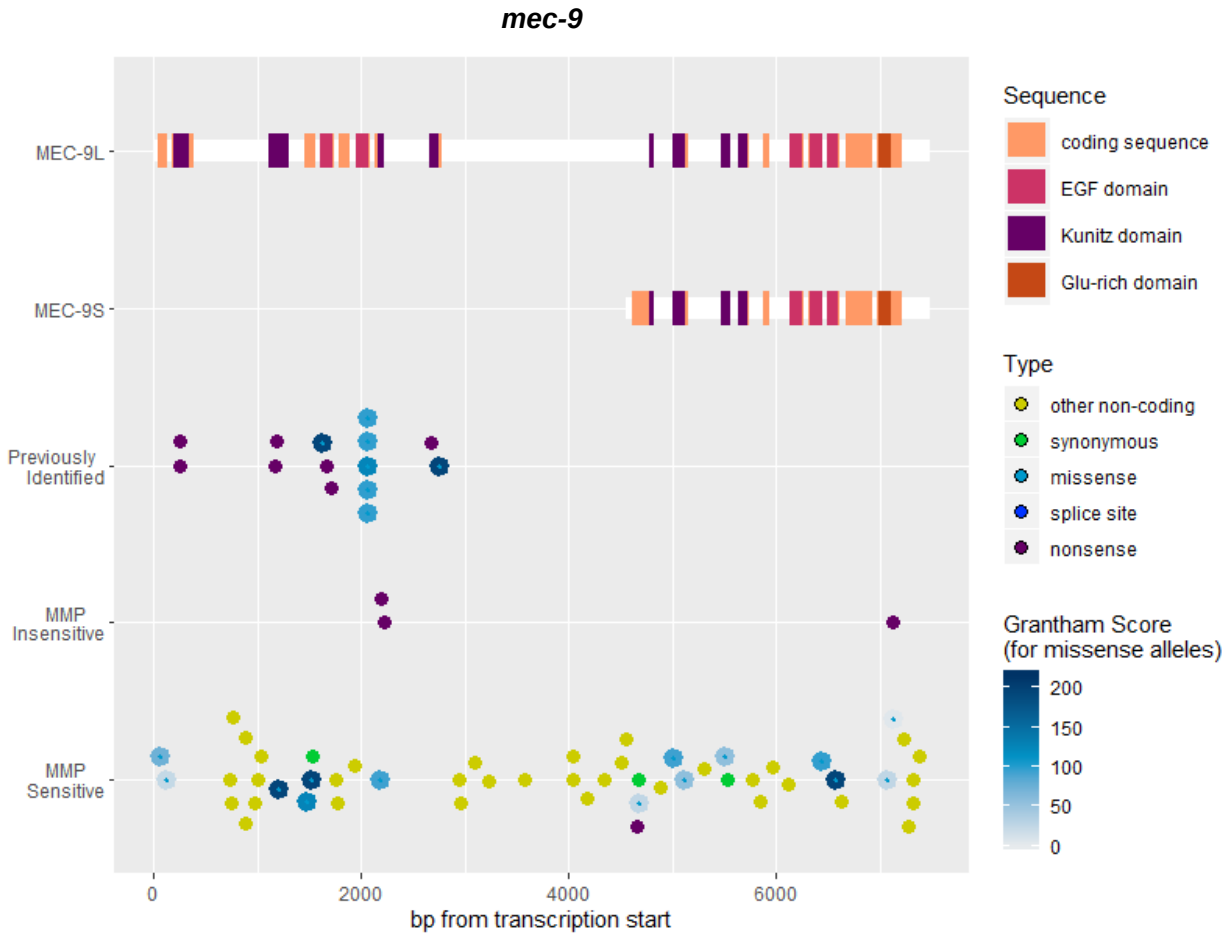

Figure 4-13: *mec-9* transcript and coding sequence plotted with previously identified alleles and MMP alleles grouped by associated phenotype. Other non-coding, synonymous, splice site, and nonsense mutation alleles are represented by solid color dots. Missense mutations are represented by smaller dots surrounded by larger blue dots shaded according to the Grantham score of the amino acid substitution.

Strain	Anterior	Posterior	Allele	Domain Affected	GERP	phyloP	phastCons
VC40071	23 (P_{30})	21 (P_{30})	gk452440	Kunitz	3.6	2.239	1
VC20650	24 (P_{60})	21 (P_{30})	gk244329		3.6	2.239	1
VC40120	22 (P_{20})	23 (P_{65})	gk472335	EGF	4.67	2.775	0.999

Table 4-2: MMP strains carrying *mec-9* missense mutations that did not result in touch insensitive phenotypes. Total anterior and posterior response rates are out of 25, and the approximate percentile rank of each response is noted. All three alleles represent C to Y substitutions with Grantham scores of 194. The functional domains affected by each mutation is given, along with GERP, phyloP, and phastCons scores.

mec-14

MEC-14 is a potential mechanoreceptor channel regulator. An oxidoreductase domain is predicted based on homology to shaker-type potassium channel β subunits (McCormack and McCormack, 1994), but enzymatic activity has not been demonstrated for MEC-14. I was only able to find the location of two previously identified *mec-14* point mutations, both of which are missense alleles (Gu et al., 1996). Our MMP screen identified three phenotype-causing missense mutations and one phenotype-causing non-coding mutation (Figure 4-14). The non-coding phenotype-causing *mec-14* mutation we found was not originally annotated as splice-site affecting, but noting that the mutation causes a substitution three bp from the exon-intron border, we consider it very likely that the touch insensitive phenotype is caused by abnormal splicing of *mec-14* and are therefore categorizing it as a splice-site mutation.

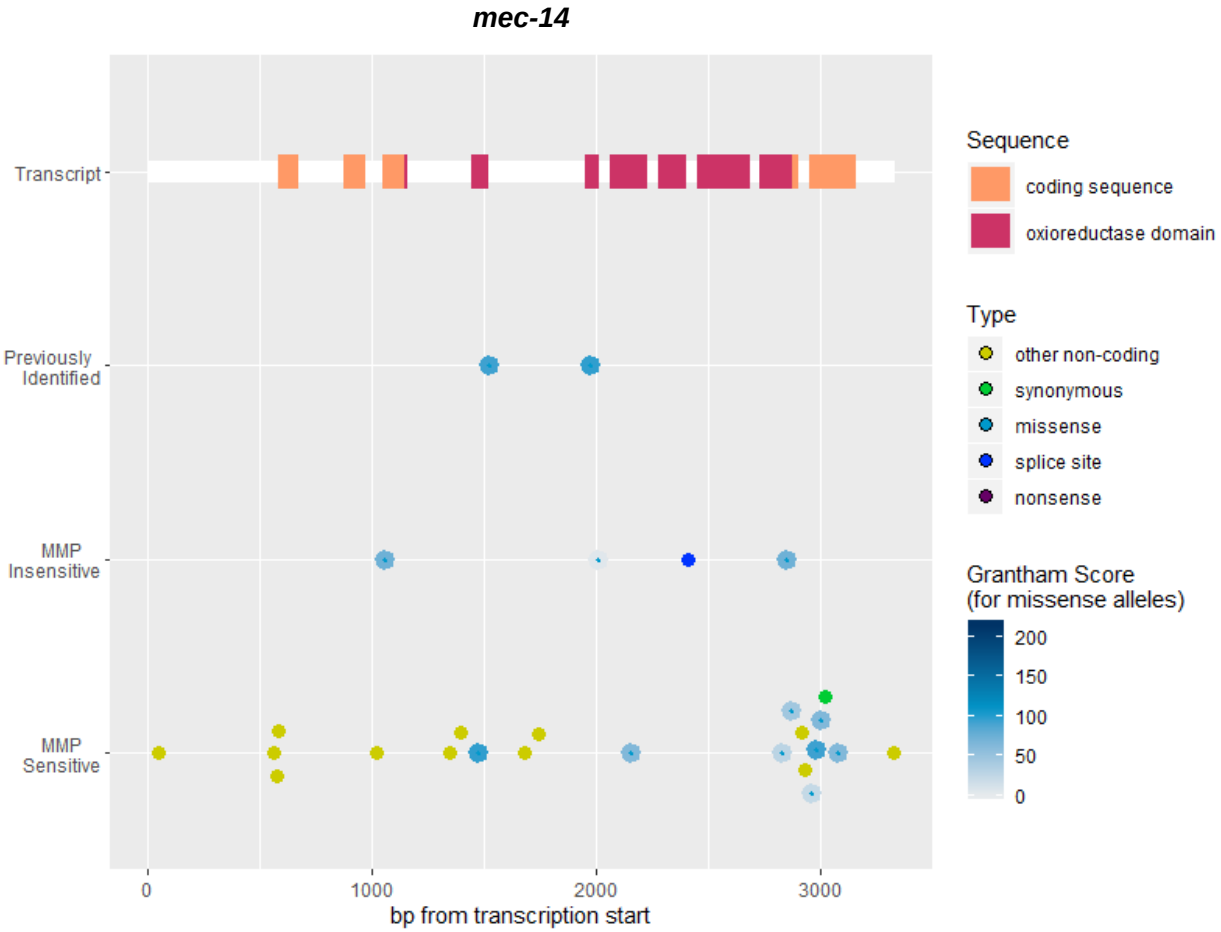

Figure 4-14: *mec-14* transcript and coding sequence plotted with previously identified alleles and MMP alleles grouped by associated phenotype. Other non-coding, synonymous, splice site, and nonsense mutation alleles are represented by solid color dots. Missense mutations are represented by smaller dots surrounded by larger blue dots shaded according to the Grantham score of the amino acid substitution.

I was intrigued by the very low Grantham score phenotype-causing *mec-14* missense mutation, so I checked to see how well conserved the altered residue was. I found that the residue was not significantly more or less conversed than other *mec-14* missense mutations and more surprisingly, I noticed that one of the phenotype-causing mutations we identified affected a residue that appeared to be poorly conserved. Furthermore, considering the Grantham, GERP, phyloP, and phastCons scores of all the *mec-14* missense alleles, there did not appear to be much of any correlation between the scores and touch insensitivity (Table 4-3).

AA position	WT	Mut	Grantham	GERP	phyloP	phastCons
67	P	S	74	3.78	2.393	0.974
104	A	T	58	3.78	2.333	0.987
110	G	E	98	3.78	2.333	1
145	I	L	5	3.78	1.812	0.895
179	A	V	64	3.78	2.393	0.999
359	V	I	29	3.78	2.333	0.998
366	S	P	74	0.341	0.147	0.668
373	D	E	45	-0.209	-0.068	0.948
388	D	N	23	3.78	2.333	0.995
394	G	D	94	3.78	2.333	0.998
401	A	V	64	3.78	2.393	0.994
427	A	V	64	3.78	2.393	0.997

Table 4-3: MEC-14 MMP missense mutations. Phenotype-causing mutations are highlighted in yellow.

mec-7

MEC-7 encodes the β-tubulin necessary for the formation of the unusual 15-protofilament (15-PF) TRN microtubules. A relatively large number of previously identified *mec-7* mutations are missense alleles, and they are spread somewhat evenly throughout the protein-coding sequence. This is not surprising considering the exceptionally high conservation of tubulin sequences (Erickson, 2007). Indeed, what is notable about the *mec-7* MMP alleles (in comparison to other *mec* genes) is the relatively large portion of missense mutations that resulted in a phenotype (Figure 4-15).

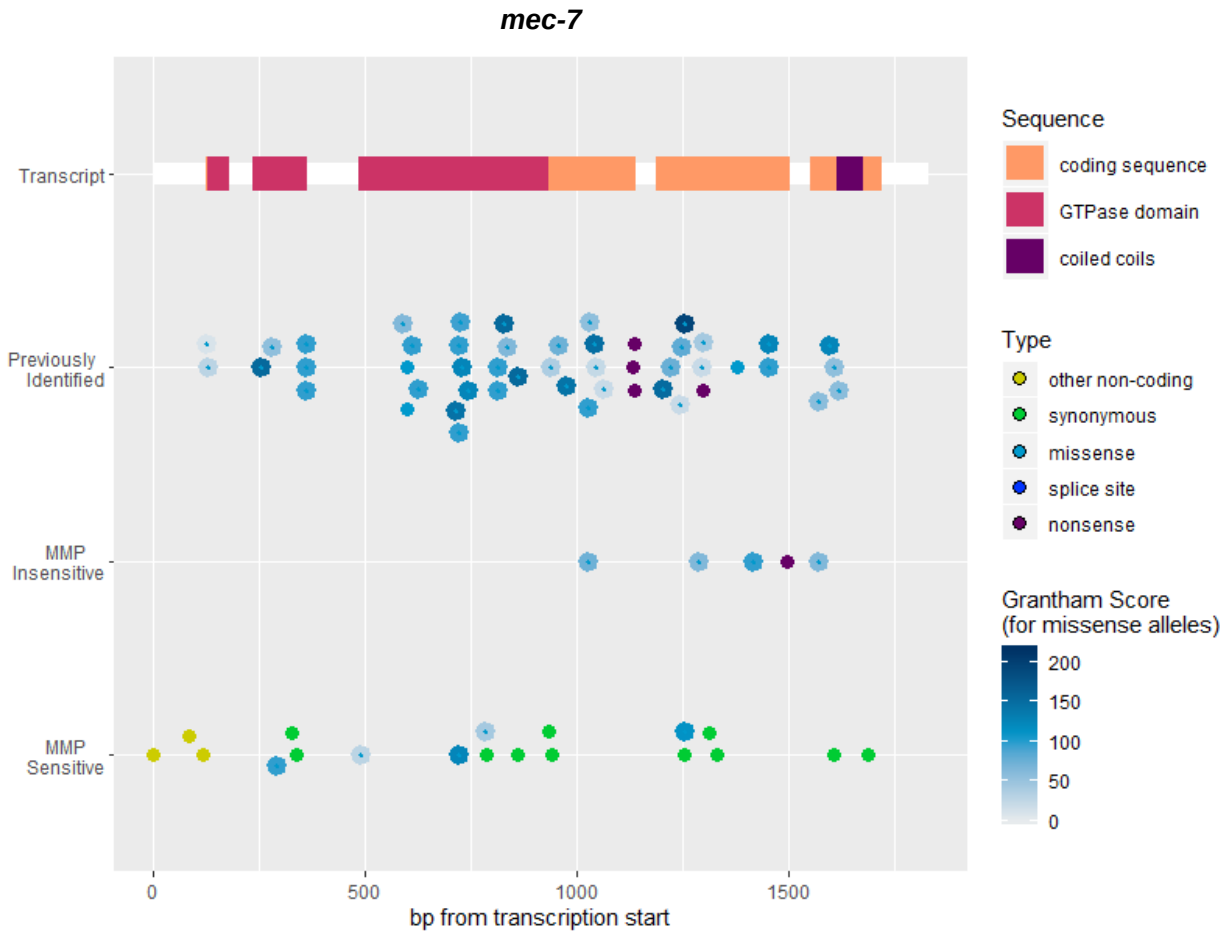

Figure 4-15: *mec-7* transcript and coding sequence plotted with previously identified alleles and MMP alleles grouped by associated phenotype. Other non-coding, synonymous, splice site, and nonsense mutation alleles are represented by solid color dots. Missense mutations are represented by smaller dots surrounded by larger blue dots shaded according to the Grantham score of the amino acid substitution.

mec-12

MEC-12 encodes the α-tubulin found in the 15-PF TRN microtubules. As we found to be true for *mec-7*, a relatively high proportion of *mec-12* MMP missense alleles were found to cause touch insensitivity, though to a slightly lesser extent (4 out of 9 *mec-7* missense alleles were phenotype-causing, whereas 3 out of 10 *mec-12* alleles were). Perhaps coincidentally, all of the phenotype-causing missense alleles we found are within 5 amino acid residues of previously identified alleles and cluster to approximately the same region of the protein (Figure 4-16). We

also found one non-coding mutation to cause insensitivity. The mutation causes a substitution about 100 bp away from the last exon of *mec-12*, so it is not immediately clear whether the phenotype results from a change in splicing or some other regulatory mechanism. ChIP-seq results suggest that the mutation occurs within an HPL-2 transcription factor binding region (Boyle et al. 2014), but HPL-2 has not been reported to be expressed in the TRNs or to affect mechanosensation. To our knowledge this is the first phenotype-causing *mec-12* mutation located outside of the coding sequence. Since it is so surprising that this mutation might cause a phenotype, it will be worthwhile to verify the location of the base change by sequencing of PCR products.

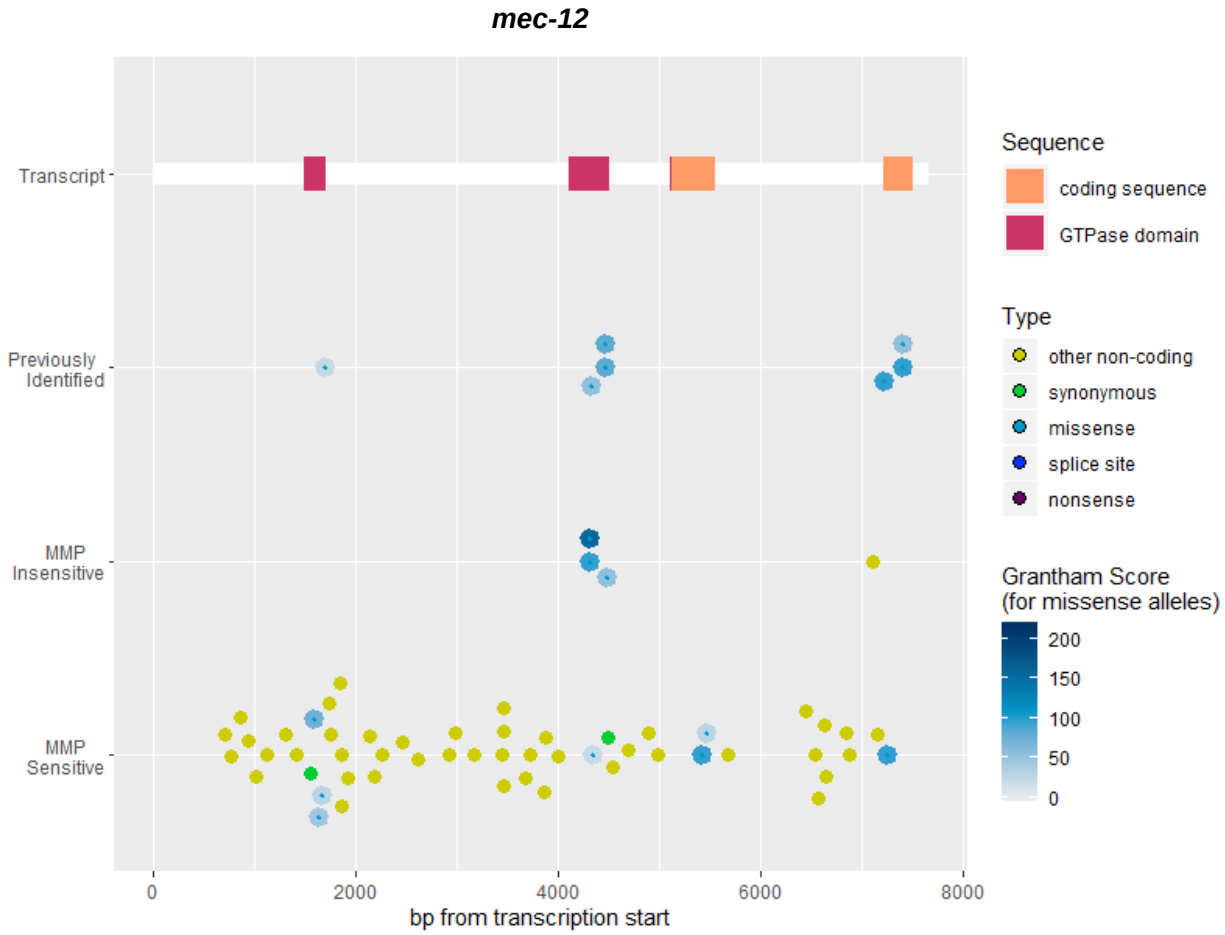

Figure 4-16: *mec-12* transcript and coding sequence plotted with previously identified alleles and MMP alleles grouped by associated phenotype. Other non-coding, synonymous, splice site, and nonsense mutation alleles are represented by solid color dots. Missense mutations are represented by smaller dots surrounded by larger blue dots shaded according to the Grantham score of the amino acid substitution.

mec-17

MEC-17 is an α-tubulin-acetyltransferase that acetylates MEC-12 lysine 40. The acetyltransferase activity of MEC-17 is not thought to be crucial for TRN function. Rather, MEC-17 appears to be in some sense a structural component of the 15-PF microtubules (Topalidou et al., 2012). It may affect microtubule stability by binding to tubulin at multiple sites (Howes et al., 2013), and may contribute to the material observed in the lumen of the TRN microtubules in EM images (Topalidou et al., 2012).

Considering the rarity of *mec-17* alleles discovered in previous mutagenesis screens, we were not expecting to find more than one phenotype-causing *mec-17* allele in the MMP set, if any. However, we found two (Figure 4-17). The phenotype-causing *mec-17* mutation outside the coding sequence (*gk206446*) was not originally annotated as splice-site affecting, but it occurs only five bp from the exon-intron border. It is notable that another MMP allele substitutes a base just two bp further into the intron but was not found to cause a phenotype. Tellingly, the base affected by *gk206446* is significantly more conserved across nematode species compared to the non-phenotype-causing allele (phyloP score of 1.0 vs. 0.3). Because *gk206446* causes touch insensitivity and is very close to the exon-border, we have reclassified it as a splice-site affecting mutation.

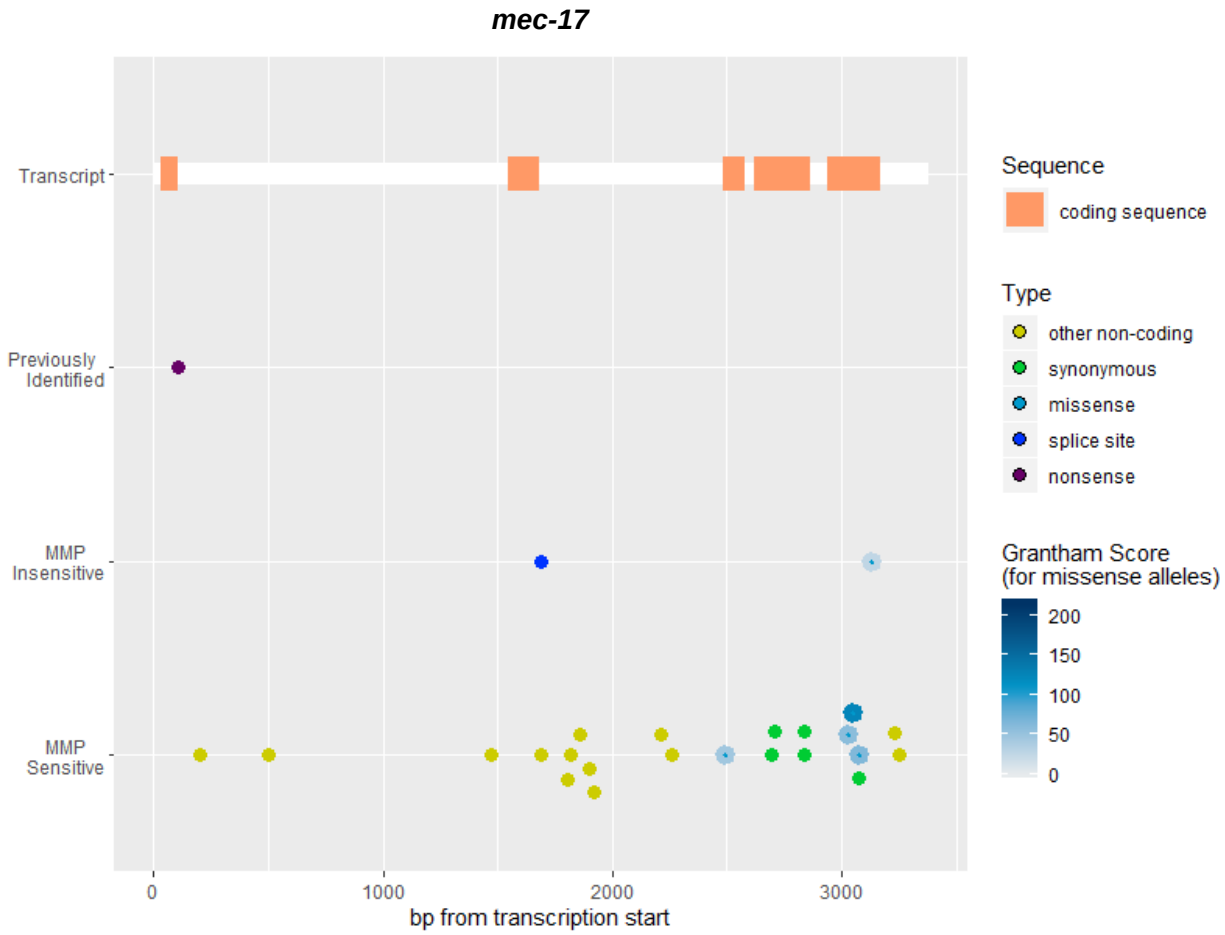

Figure 4-17: *mec-17* transcript and coding sequence plotted with previously identified alleles and MMP alleles grouped by associated phenotype. Other non-coding, synonymous, splice site, and nonsense mutation alleles are represented by solid color dots. Missense mutations are represented by smaller dots surrounded by larger blue dots shaded according to the Grantham score of the amino acid substitution.

We were somewhat surprised to find a missense mutation (*gk709949*) just 12 residues from the C-terminal end of MEC-17 that resulted in touch insensitivity. However, it should be noted that in our complementation tests using *mec-17* (*u265*) animals to verify the causative mutation, the *gk709949*/*u265* heterozygotes were weakly touch insensitive whereas the original MMP strain had been strongly touch insensitive. From this we concluded that *gk709949* had some effect on touch sensitivity, but that there must be another yet unknown factor at play making the MMP strain carrying *gk709949* more strongly touch insensitive.

mec-15

As is indicated by the presence of an F-box domain, MEC-15 is thought to form the substrate-recognition subunit of a ubiquitin-ligase complex. MEC-15 likely targets microtubule-destabilizing proteins for degradation and thus indirectly contributes to the stability of the TRN microtubules (Zheng et al., 2020). MEC-15 also contains WD40 repeats, which are common protein-protein interaction domains often found in F-box proteins (Kipreos and Pagano, 2000). Previously identified *mec-15* alleles include nonsense mutations and two missense mutations that do not affect either the F-box or WD40 repeat domains. Our MMP screen identified two *mec-15* nonsense alleles as being phenotype-causing, but none of 4 MMP *mec-15* missense alleles (Figure 4-18).

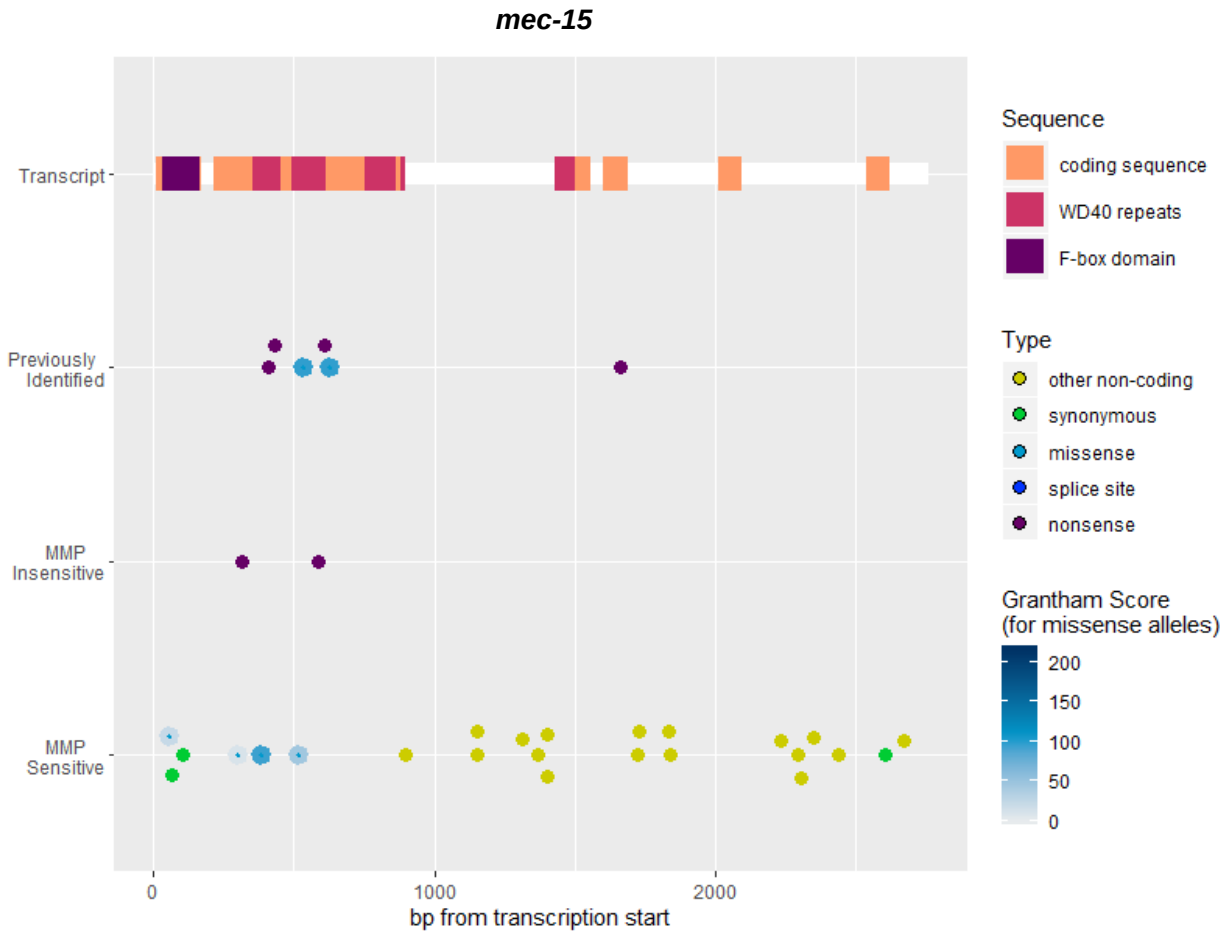

Figure 4-18: *mec-15* transcript and coding sequence plotted with previously identified alleles and MMP alleles grouped by associated phenotype. Other non-coding, synonymous, splice site, and nonsense mutation alleles are represented by solid color dots. Missense mutations are represented by smaller dots surrounded by larger blue dots shaded according to the Grantham score of the amino acid substitution.

unc-2

UNC-2 encodes a non-L-type voltage-gated calcium channel (VGCC) subunit. Although *unc-2* alleles were not reported as causing touch sensitivity along with the other original *mec* genes due to their pleiotropic effects (Chalfie and Sulston, 1981), our lab has known that *unc-2* mutants are gentle touch insensitive for *some* time (M. Chalfie, unpublished). UNC-2 is a large protein that includes four imperfectly repeated homologous domains joined by intracellular linkers. Each homologous domain contains six membrane-spanning α-helices (Mathews et al.,

2003). The fourth membrane-spanning helix is believed to be most important for the voltage-sensing properties of the channel, and the sixth membrane-spanning helix forms part of the channel pore (Pozdnyakov et al., 2018).

Previously identified *unc-2* mutations include five nonsense and two missense alleles. Similarly, our MMP screen identified four nonsense and two missense phenotype-causing mutations (Figure 4-19A). Since most of the UNC-2 coding sequence falls within $1/8^{th}$ of the longest *unc-2* transcript, I have also plotted mutations in a chart showing a partial region of *unc-2* (Figure 4-19B).

A

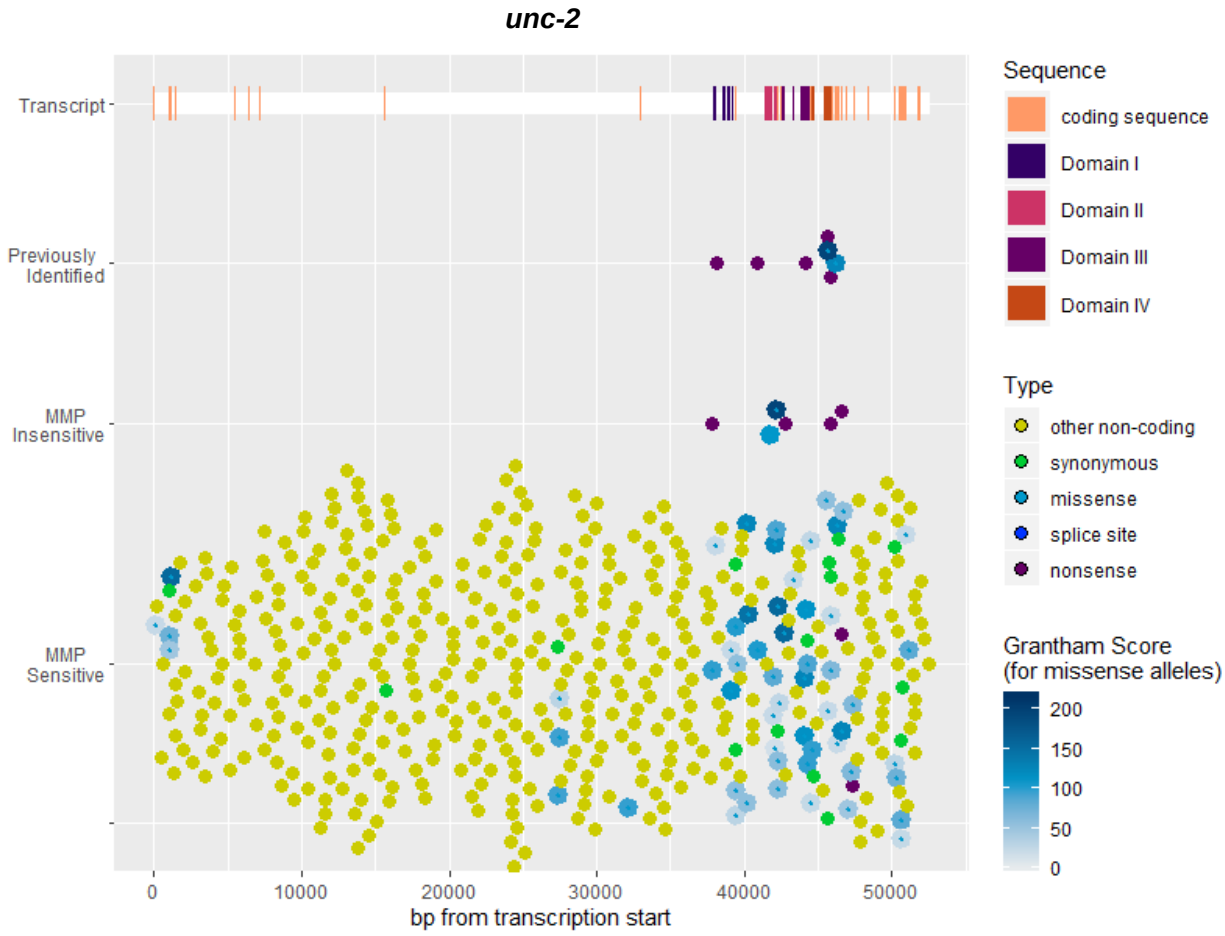
unc-2
Transcript
Previously Identified
MMP Insensitive
MMP Sensitive
0
10000
20000
30000
40000
50000
bp from transcription start
Sequence
coding sequence
Domain I
Domain II
Domain III
Domain IV
Type
other non-coding
synonymous
missense
splice site
nonsense
Grantham Score (for missense alleles)
200
150
100
50
0

B

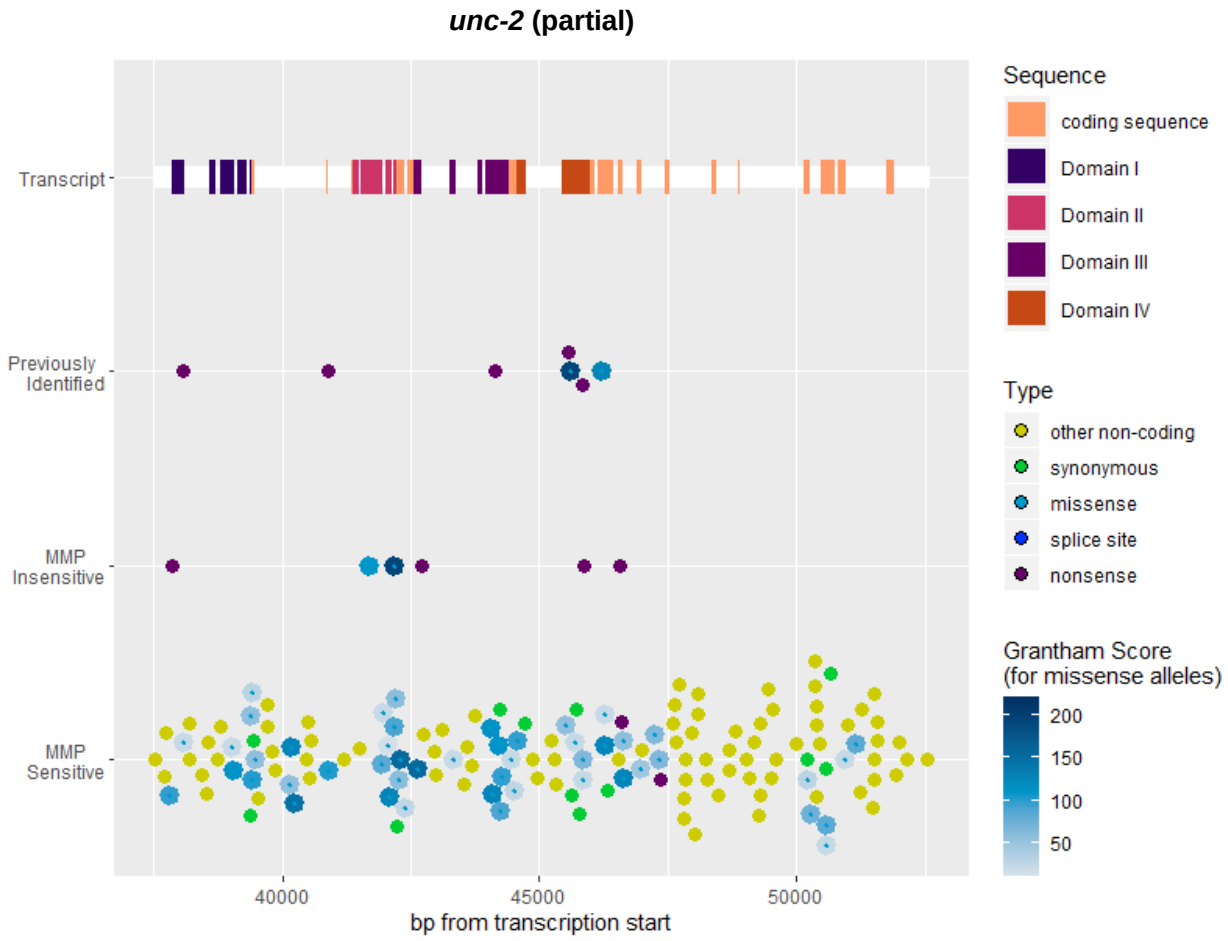

Figure 4-19: *unc-2* transcript and coding sequence plotted with previously identified alleles and MMP alleles grouped by associated phenotype. Other non-coding, synonymous, splice site, and nonsense mutation alleles are represented by solid color dots. Missense mutations are represented by smaller dots surrounded by larger blue dots shaded according to the Grantham score of the amino acid substitution. A) shows the entire *unc-2* gene. B) shows a partial view of the *unc-2* gene focused on a region richer in coding sequences.

Since UNC-2 is composed of four repeated homologous domains, I wondered if considering point mutations in the context of the aligned homologous protein sequences would prove more informative. Therefore, I aligned the protein sequences of the UNC-2 homologous domains and identified altered residues in previously identified and MMP missense mutations. I included both previously identified loss-of-function (LOF) mutations (the locations of which

were available on WormBase) and mutants found in a suppression screen for an UNC-2 gain-of-function (GOF) mutation (Huang et al., 2019) (Figure 4-20). The two phenotype-causing MMP missense mutations identified in our screen affected residues within transmembrane helices, and one previously identified LOF mutation affected a residue just adjacent to a transmembrane helix (the second LOF missense mutation charted with UNC-2 in Figure 4-17 affected a linker sequence between homologous domains). The GOF suppressor mutations identified by Huang et al. (2019) affected transmembrane helices and the linker sequence between S5 and S6. I noticed only one residue that was completely conserved across all four UNC-2 homologous domain sequences was affected by an MMP missense mutation (the tyrosine second within the S3 sequence), and that the mutation had not been identified as phenotype-causing in our screen. The MMP allele causes a Y to F substitution, but this exact substitution is also found in human and rabbit S3 sequences, so it is not surprising to find it has little or no effect.

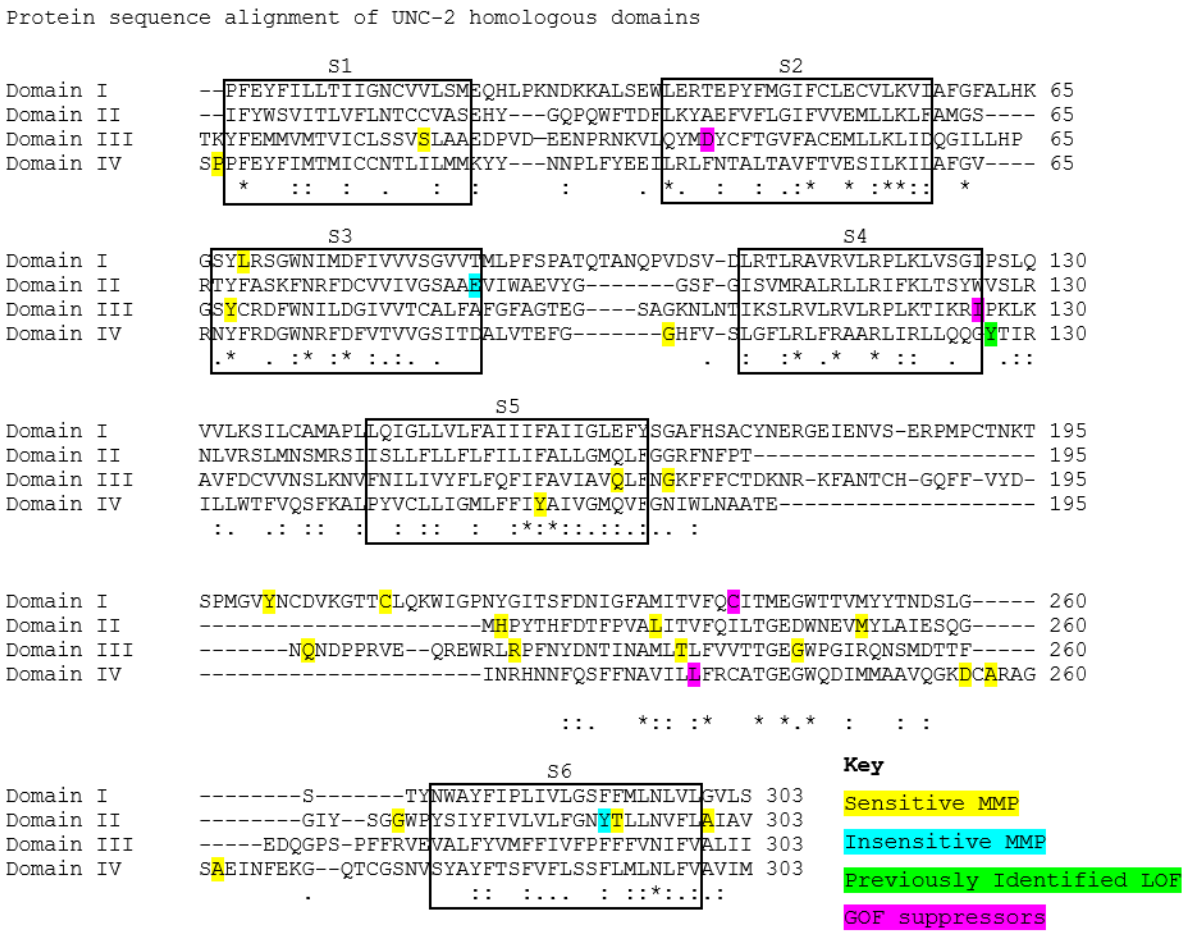

Figure 4-20: Alignment of UNC-2 homologous domains. Transmembrane helices are boxed, and missense mutations are identified within the sequence by highlighting. * indicates perfect conservation between aligned sequences, : indicates a site with strong amino acid similarities between aligned sequences, and . indicates a site with weak amino acid similarities between aligned sequences.

mec-8

MEC-8 is an RNA-processing factor that regulates the alternate splicing of the *mec-2* transcript. In the absence of MEC-8, longer MEC-2 isoforms necessary for TRN function are truncated, resulting in a touch-insensitive phenotype. Most of the previously identified *mec-8* alleles are nonsense mutations, but three missense alleles affecting the two MEC-8 RNA binding motifs have also been isolated (Figure 4-21).

A

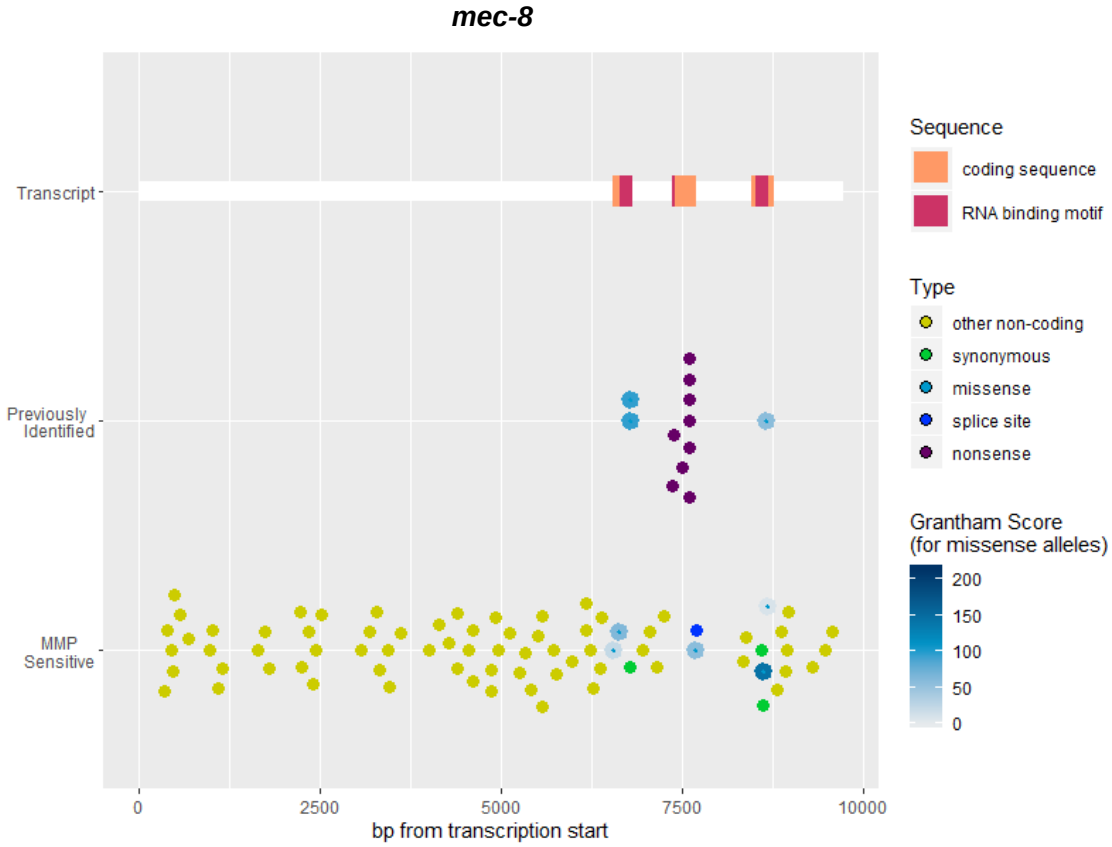
mec-8
Transcript
Previously Identified
MMP Sensitive
0
2500
5000
7500
10000
bp from transcription start
Sequence
coding sequence
RNA binding motif
Type
other non-coding
synonymous
missense
splice site
nonsense
Grantham Score (for missense alleles)
200
150
100
50
0

B

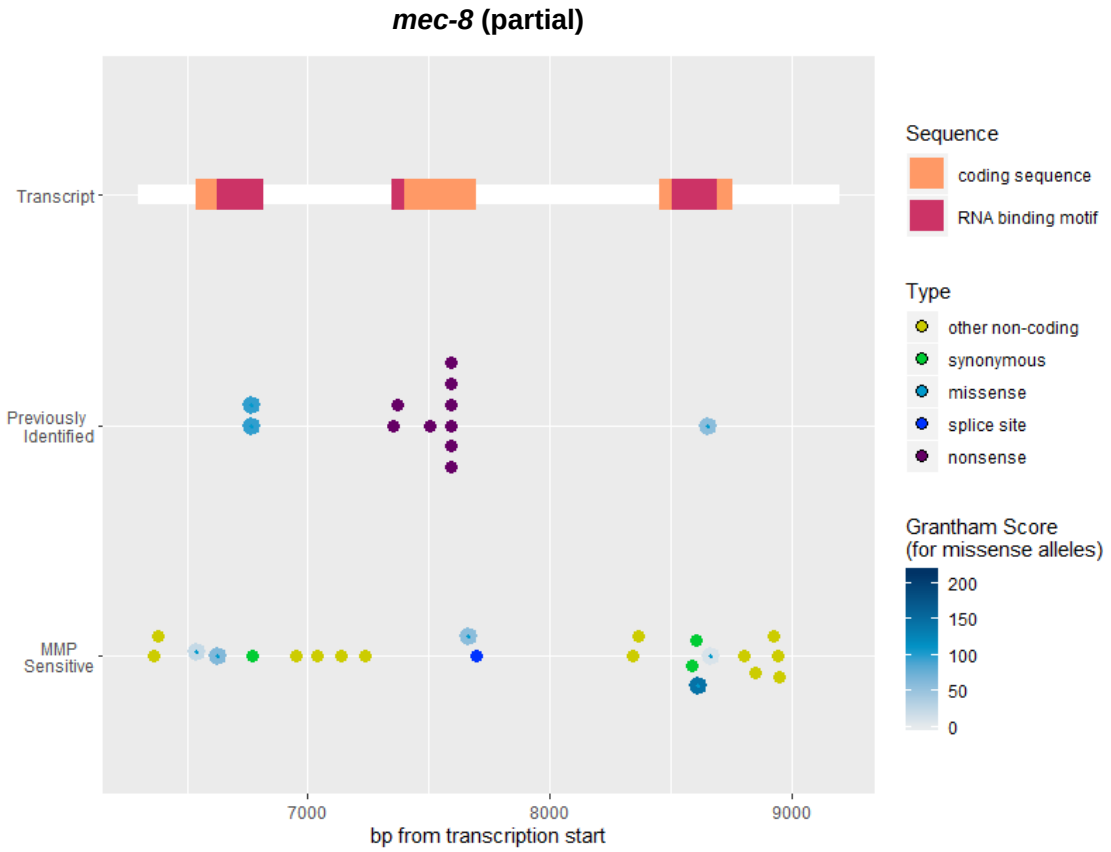

Figure 4-21: *mec-8* transcript and coding sequence plotted with previously identified alleles and MMP alleles. Other non-coding, synonymous, splice site, and nonsense mutation alleles are represented by solid color dots. Missense mutations are represented by smaller dots surrounded by larger blue dots shaded according to the Grantham score of the amino acid substitution. A) shows the entire *mec-8* gene. B) shows a partial view of the *mec-8* gene focused on a region richer in coding sequences.

Our screen did not identify any *mec-8* phenotype-causing alleles. The MMP set contains six protein-altering *mec-8* alleles, one of which is a splice-site mutation. The splice site mutation (*gk579727*) affects the splice junction at the end of the second exon, changing the highly conserved "GT" at the start of the intron to "AT." We would have expected this mutation to prevent production of wild-type MEC-8 and cause a touch insensitive phenotype, but we did not

find this to be the case. It may be that some amount of normal splicing still occurs in *gk579272* animals, since mutations of this sort have been found to allow residual amounts of wild-type splicing (Dassah et al., 2009), and *C. elegans* introns starting with "AT" have been detected under certain unusual conditions (Rushforth and Anderson, 1996). Previous studies have suggested that relatively low levels of MEC-8 are needed for its function (Calixto et al., 2010b), so *mec-2* mRNA processing may well not be disrupted by a sharp reduction in normal splicing of *mec-8*. It is also worth noting that the MMP strain carrying *gk579272* (VC40334) appeared to have slightly reduced average touch response ($<10^{th}$ percentile), but this was not confirmed by retesting according to our criteria. The strain may indeed have a weak touch insensitive phenotype, but we would need to retest it to be certain. Another somewhat surprising negative result is that the high Grantham score missense mutation in the third exon of *mec-8* did not cause a phenotype, considering that it falls within the RNA recognition motif and that a previously identified missense allele was identified nearby.

mec-3

MEC-3 is a transcription factor critical to TRN cell fate determination. The MEC-3 protein sequence includes three DNA-binding domains, including two LIM domains, each composed of two zinc finger domains, and a homeobox (HOX) domain. Interestingly, previously identified *mec-3* missense alleles affect sequences outside of the DNA-binding domains (Figure 4-22).

We did not identify any new phenotype-causing *mec-3* alleles in the MMP set. This is likely due to the complete lack of *mec-3* nonsense and splice site alleles, which make up the majority of previously identified *mec-3* alleles. The protein-altering MMP *mec-3* alleles consist

of five missense mutations that do not map to regions where previously identified missense mutations have been identified, and one missense mutation that is located close to previously identified missense mutations but has a low Grantham score. Therefore, although we were originally surprised to see that we had not found any phenotype-causing *mec-3* alleles in the MMP set, a closer inspection of the alleles we tested did not indicate any striking changes.

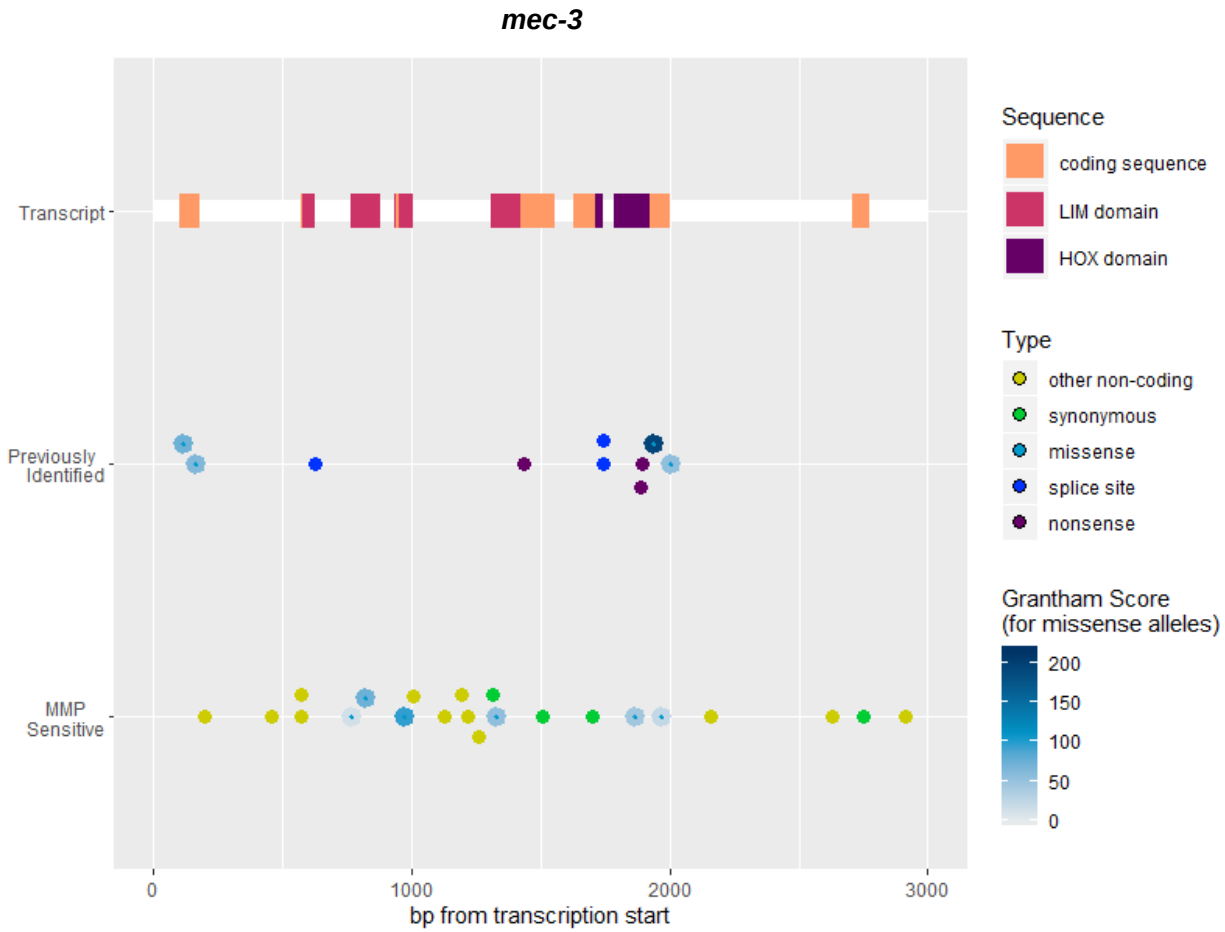

Figure 4-22: *mec-3* transcript and coding sequence plotted with previously identified alleles and MMP alleles. Other non-coding, synonymous, splice site, and nonsense mutation alleles are represented by solid color dots. Missense mutations are represented by smaller dots surrounded by larger blue dots shaded according to the Grantham score of the amino acid substitution.

unc-86

UNC-86 is a transcription factor that works in cooperation with MEC-3 to determine TRN cell fate. UNC-86 contains a HOX domain and an N-terminal transcriptional activation domain (Röckelein et al., 2000), as well as a POU domain is necessary for interaction with MEC-3 (Röhrig et al., 2000). Two of the previously identified missense alleles (*u5* and *u168*) are interesting in that they cause a similar touch insensitive phenotype as the *unc-86* splice site allele (*n846*), which is believed to be a null mutation, but do not have the effect of *n846* on egg-laying behavior. The difference is probably due to that *u5* and *u168* specifically interfere with MEC-3 binding without affecting the activity of UNC-86 in the motor neurons that control egg-laying (Röhrig et al., 2000). Coincidentally, the MMP *unc-86* missense mutation that we identified as phenotype-causing causes the very same substitution as *u5*. The identified MMP allele therefore tells us nothing new about UNC-86 but can be thought of as a positive control.

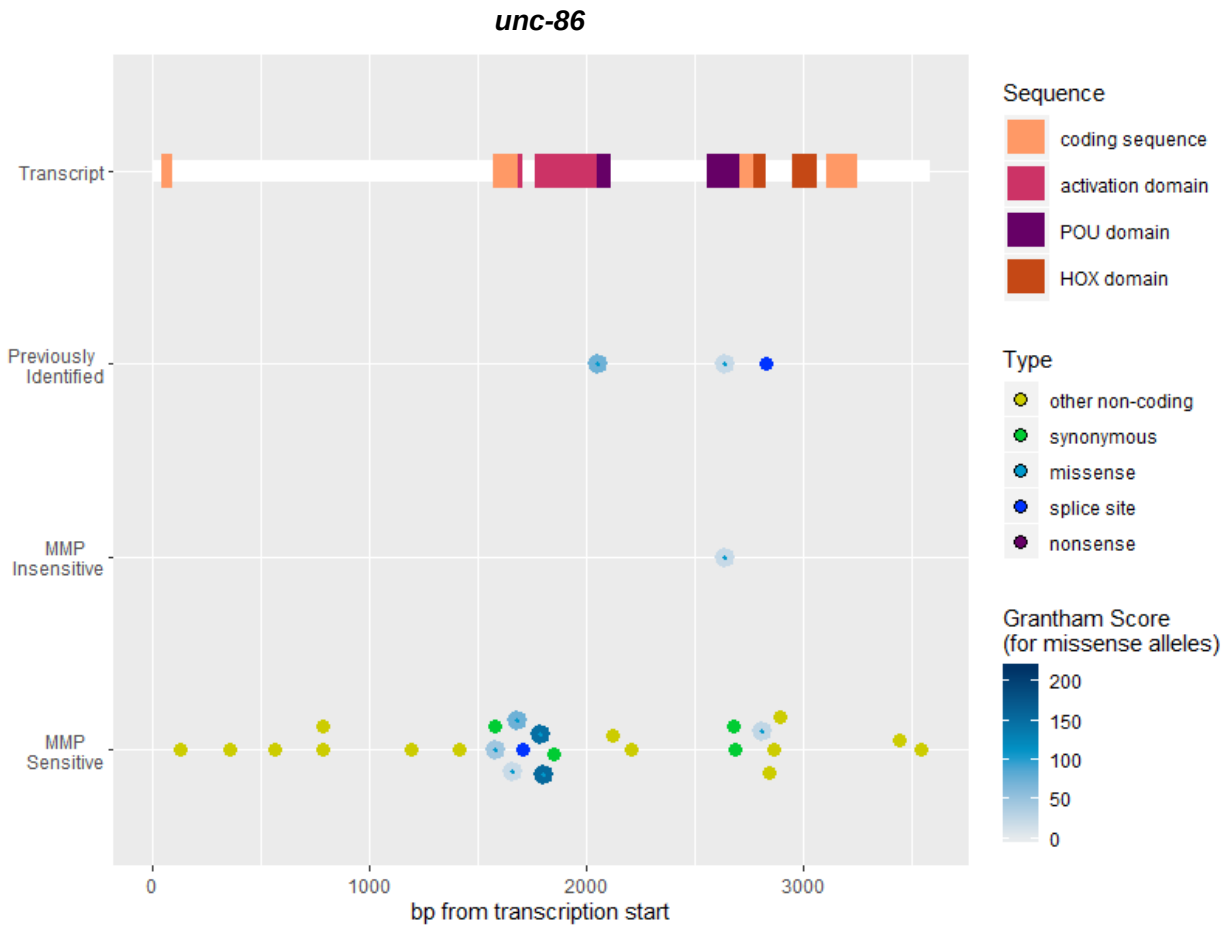

Figure 4-23: *unc-86* transcript and coding sequence plotted with previously identified alleles and MMP alleles grouped by associated phenotype. Other non-coding, synonymous, splice site, and nonsense mutation alleles are represented by solid color dots. Missense mutations are represented by smaller dots surrounded by larger blue dots shaded according to the Grantham score of the amino acid substitution.

egl-5

EGL-5 is a HOX domain containing protein that is necessary for the differentiation of the PLMs. There are only two previously identified point mutations, both of which result from the same base pair change. Our screen did not identify any phenotype-causing *egl-5* mutations, although the MMP set contained 8 *egl-5* missense alleles, one of which is a high Grantham score substitution (*gk565173*) located near the previously identified missense mutations. The MMP strain containing *gk565173* was tested twice by chance (we did not ever consider it a potentially

insensitive strain) and responded to 22 out of 25 posterior touches over both rounds of testing, confirming that it is not weakly posterior touch insensitive. The relatively small size of EGL-5 likely contributes to the relative paucity of previously identified *egl-5* point mutations, and based on our analysis of other *mec* genes we are not surprised to see the number of missense mutations that did not result in a detectable phenotype.

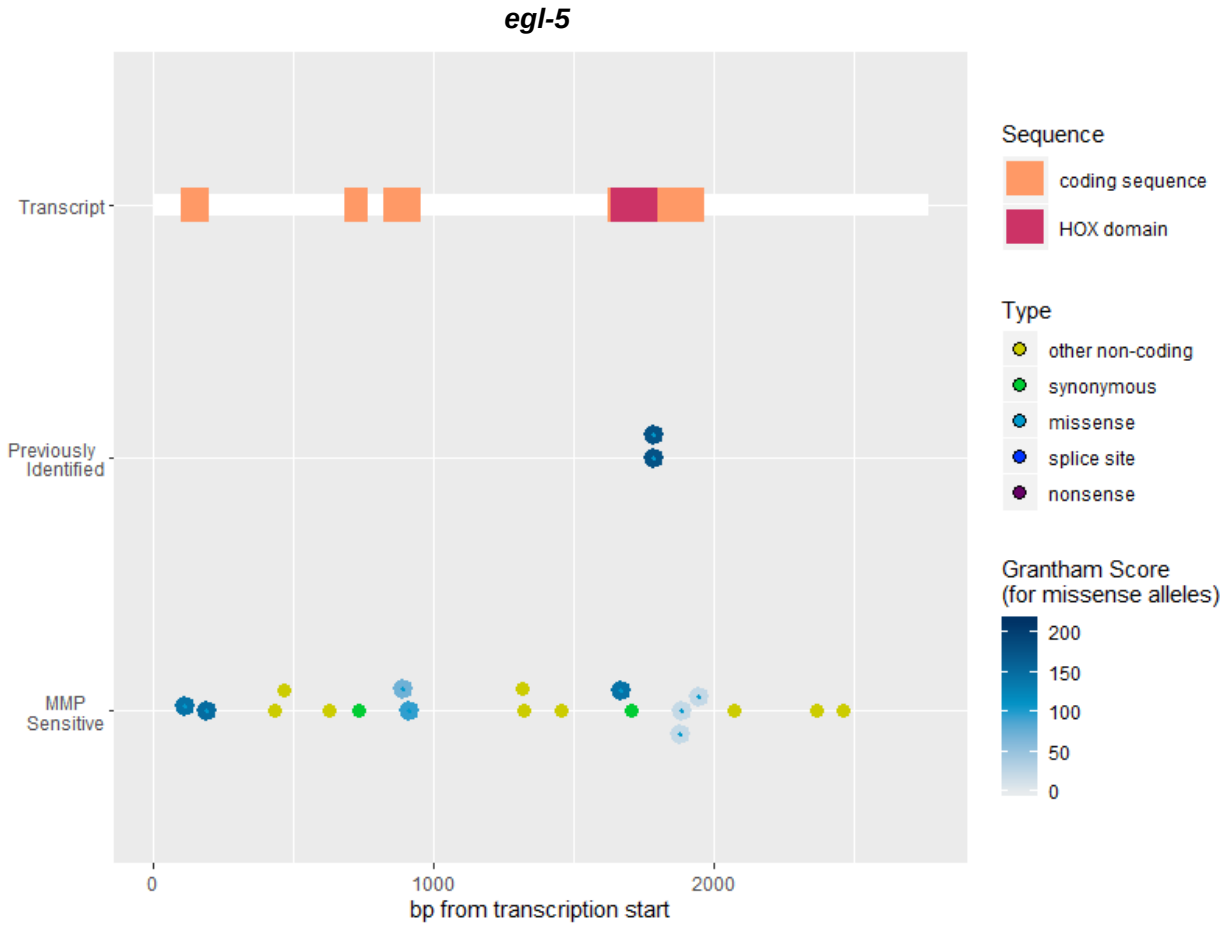

Figure 4-24: *egl-5* transcript and coding sequence plotted with previously identified alleles and MMP alleles. Other non-coding, synonymous, splice site, and nonsense mutation alleles are represented by solid color dots. Missense mutations are represented by smaller dots surrounded by larger blue dots shaded according to the Grantham score of the amino acid substitution.

lin-32

LIN-32 is a helix-loop-helix (HLH) domain containing transcription factor that is involved in the differentiation and migration of TRN precursor cells. Although LIN-32 is an even smaller protein than EGL-5, four nonsense and six missense alleles have been previously identified. The MMP set only contained three *lin-32* missense mutations, so we are not surprised not to have found any phenotype-causing *lin-32* MMP alleles. The locations of previously identified missense mutations suggest that the sequence of the LIN-32 HLH domain is most critical to its function, but there is only one MMP protein-altering mutation that affects the region, so the results of our screen provide little corroborating or challenging evidence (Figure 4-22).

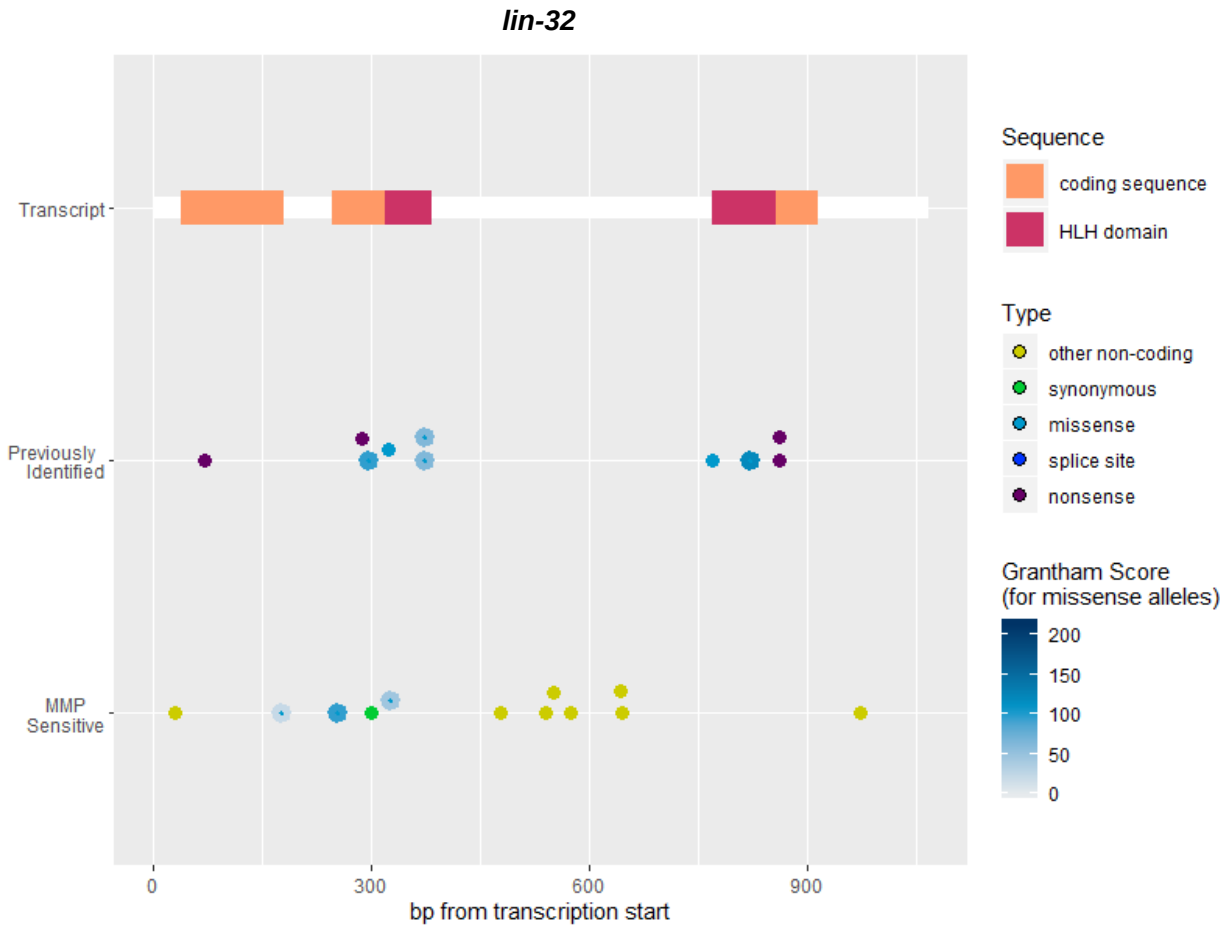

Figure 4-25: *lin-32* transcript and coding sequence plotted with previously identified alleles and MMP alleles. Other non-coding, synonymous, splice site, and nonsense mutation alleles are represented by solid color dots. Missense mutations are represented by smaller dots surrounded by larger blue dots shaded according to the Grantham score of the amino acid substitution.

4.3 Discussion

Our consideration of both phenotype-causing and non-phenotype-causing point mutations in known *mec* genes indicates the very limited types of mutations that result in strong touch insensitive phenotypes. Most of the missense *mec* mutations in the MMP set did not result in detectable touch phenotypes, even when substituted residues were highly evolutionarily conserved. Conservation of amino acid identities generally suggests that nonsynonymous substitutions cause phenotypes that are selected against, so our inability to detect touch response

phenotypes in strains with missense mutations in conserved residues highlights the difference between the sensitivities of our assays and relevant selective pressures. Alternatively or additionally, the missense mutations that we did not observe to cause touch insensitivity may result in other phenotypes that we were not testing for.

We are quite aware that our standard touch response assay is not particularly sensitive to small changes in touch sensitivity, especially since wild-type animals tend towards complete responsiveness. For this reason it has proven difficult to screen for factors that normally downregulate sensitivity, although we have done so with screens for suppressors of cell death in hyperactive mechanoreceptor channel mutants (Chen et al., 2016b). Furthermore, the low sensitivity of standard touch response assays is part of why saturated forward screens for touch insensitive mutants did not reveal every gene that can be mutated to cause reduced touch sensitivity.

Mechanized assays that deliver weaker stimuli represent one possible way towards touch assays greater sensitivity (Park et al., 2007). Mechanized assays that can be automated should also allow for more extensive data collection, which would help overcome the difficulty of detecting altered response rates among high variance data (Cho et al., 2017; McClanahan et al., 2017). However, the simplicity of our standard touch response assay has allowed us to phenotype animals with minimal upfront material cost using methods that can be easily be replicated in any *C. elegans* laboratory.

We also noticed that scores for chemical differences between amino acids (Grantham scores) and for evolutionary conservation of a given locus (GERP, PhyloP, and PhastCons scores) did not appear to lend to simple methods of predicting phenotype-causing changes. Although we found that phenotype-causing mutations consisted of higher Grantham score

substitutions on average (in comparing previously identified and non-phenotype-causing MMP alleles), we observed plenty of instances where low Grantham score mutations were phenotype-causing and high Grantham score mutations were not. I believe it would certainly be possible to construct an algorithm taking into account Grantham scores, evolutionary conservation, proximity to previously identified alleles, proximity to functional domains, and/or structural context that would be predictive of phenotype causing mutations.

Another general observation that we can draw from our comparisons of MMP alleles in known *mec* genes is that non-coding mutations within introns (not counting those near splice junctions) very rarely led to phenotypes (we only found one instance where this was the case out of 941 "other non-coding" mutations plotted above). Furthermore, we did not find any examples of phenotype-causing synonymous substitutions (out of 108 instances plotted above).

Although the information gathered from our screen of the MMP mostly served to confirm our existing hypotheses about the original *mec* genes, we also uncovered some evidence for phenomena that were not already part of our existing models. For one, we had not previously found any phenotype-causing *mec-2* alleles that affected the intron exclusively found in isoforms d-g. In fact, our own experimental evidence had not indicated that these isoforms are produced in the TRNs (Calixto et al., 2010b). Additionally, we identified missense mutations in regions that we did know to be affected by previously identified missense alleles in *mec-4*, *mec-10*, *mec-6*, *mec-1*, *mec-18*, and *mec-17*. Notably, the results of our screen more than doubled the number of phenotype-causing *mec-1* missense alleles we are aware of and have implicated a second *mec-1* Kunitz domain (Ku13) as being necessary for touch sensitivity.

4.4 Materials and Methods

Charts including coding sequences, previously identified alleles, and MMP alleles

Protein coding sequences for genes of interest were extracted from JBrowse Curated Genes track. Partially overlapping coding sequences were combined. Information on previously identified and MMP alleles was extracted from JBrowse Classical alleles and Million Mutation Project tracks. All alleles were filtered to include only small (1 or 2 bp change) substitutions, and MMP alleles were filtered to exclude potentially heterozygous variants (*gk962523* and up). MMP alleles considered candidate causative mutations that had not yet been or were unable to be verified were excluded. In cases where an insensitive MMP strain contained more than one mutation within a verified phenotype-causing gene but only one mutation was protein altering, intronic and synonymous mutations were excluded. In cases where previously known alleles were charted but not mapped on JBrowse, information was added relative to JBrowse coding sequence positioning. Protein domain information was either extracted from the JBrowse Protein motifs track or charted relative to JBrowse positions. Charts were created in R using ggplot2 and other packages.

Identification and alignment of MEC protein sequences

To align the MEC-1 C-terminal Kunitz domains, I input the protein sequences into Unipro UGENE (Okonechnikov et al., 2012) along with sequences from Kunitz domain SMART family alignment (Letunic and Bork, 2017), which consisted of 124 sequences selected by a hidden Markov model to optimally represent the divergence of the family. The sequences were aligned with T-COFFEE (Notredame et al., 2000).

For BLASTp of MEC-5, the MEC-5 protein sequence was queried against the UniProtKB database with default settings (Consortium, 2018; Sayers et al., 2018). The top 100 BLASTp results from query of the MEC-5 protein sequence were input into Unipro UGENE (Okonechnikov et al., 2012) and aligned with MUSCLE (Edgar, 2004).

For identification of the homologous domains of UNC-2, I referred to the boundaries applied by Huang et al. (2019). For identification of the membrane-spanning helices, I referred to the UniProtKB annotated sequence of the best human ortholog BLASTp hit (CACNA1C) for the UNC-2 protein sequence. The membrane-spanning helices of CACNA1C were defined in UniProtKB by sequence similarities to the solved structure of rabbit CACNA1S (Wu et al., 2016). I aligned the protein sequences of the UNC-2, CACNA1C, and CACNA1S homologous domains with T-Coffee (Notredame et al., 2000). In Figure 4-17, the human and rabbit sequences were removed following the alignment, and columns containing only gaps in UNC-2 protein sequence were removed.

Chapter 5: Million Mutation Project Strains with Unknown Phenotype-Causing Mutations

5.1 Introduction

Due to the apparent saturation of previous mutageneses for touch insensitive animals (Chalfie and Sulston, 1981; Chalfie and Au, 1989), we were not certain that we would find any touch insensitive Million Mutation Project (MMP) mutants with phenotype-causing mutations in previously unimplicated genes. However, after screening the set of MMP strains, we have identified a significant number of touch insensitive strains for which we do not have candidate causative mutations. It is possible that some or all of these strains have unreported *mec* gene mutations, but they might also have phenotype-causing mutations in genes that have not yet been linked to gentle touch sensitivity. Strains with weak phenotypes could be particularly likely to have mutations in yet unknown touch genes, since the previous forward screens for touch insensitive mutants only identified animals with relatively strong phenotypes. However, weak phenotypes are also more difficult to re-isolate following outcrosses. For this reason, we have chosen to first address finding causative mutations in strains with strong phenotypes.

There were a few strains we had identified as touch insensitive in our screen that upon closer inspection proved to have phenotypes that suggested against defects in gentle touch sensation. The phenotypic characterization of these strains was a necessary step in deprioritizing their genetic characterization, so I will discuss our observations regarding these strains here. Additionally, we identified one strain that in addition to being touch insensitive appeared to have a TRN differentiation phenotype. We have not yet completed genetic characterization of this strain, but I will present our phenotypic analysis.

5.2 Results

From our screen of 2006 Million Mutation Project (MMP) strains for touch insensitivity, we identified 38 touch insensitive strains for which we do not have candidate causative mutations. 24 of these strains were reported to have protein-altering mutations in genes known to mutate to cause touch insensitivity but they complemented reference alleles for their candidate phenotype-causing genes. 12 strains (including some of the 24 previously mentioned) were reported to have non-coding mutations in genes that were identified in forward screens for touch insensitive mutants (and therefore can be considered the most likely candidate genes for touch insensitive mutants identified in the MMP set), but also complemented reference alleles. We have not ruled out the possibilities of interallelic complementation having occurred or phenotype-causing non-coding mutations in genes that were not among the most likely candidates, but in the absence of additional evidence for these possibilities we are considering these strains to have touch phenotype-causing mutations in previously unidentified touch genes. Another 14 strains were not reported to have either type of mutation. Any of these strains might have acquired spontaneous mutations in known touch genes since the time of their sequencing, or may have carried low-frequency variants that were not called in the process of sequencing but increased in frequency through subsequent generations. Still, we consider it highly likely that at least some of the strains we do not have candidate mutations for will lead us to identify new touch genes.

For strains without candidate causative mutations, I have begun collecting more detailed phenotypic observations beyond the information collected during the screens. For the most part I have done this in parallel to genetic characterization to improve the likelihood of segregating out phenotypes caused by mutations other than those causing touch insensitivity. First, I will discuss

the phenotypes that might not be related to defects in touch insensitivity, and then I will describe the phenotypic characterization of a truly touch insensitive strain.

Uncoordinated mutants

Seven touch insensitive mutants without candidate causative mutations are clearly uncoordinated (Unc): VC20397, VC20714, VC20779, VC40338, VC40384, VC40558, and VC40737. For two of these strains, VC20779 and VC40338, I have determined that the Unc and touch insensitive phenotypes are genetically linked, suggesting that they might be caused by the same mutation. For both VC20779 and VC40338, all 29 and 20 touch insensitive animals, respectively, that were identified in the F2 generation from outcrossing (and produced similarly insensitive progeny) were Unc and produced Unc progeny. Since both strains and their touch-insensitive derivatives exhibit very poor movement, it is possible that their reduced responsiveness to touch does not reflect any defects in TRN function. These mutants should be further tested using assays for TRN function that do not rely on locomotory response.

Twitcher mutants

There are three MMP strains (VC20135, VC30130, and VC30218) that I have not included in my count of strains without candidate causative mutations on account of their exhibiting the twitcher phenotype, which generally interferes with assays for touch sensation. These strains were not reported as having any mutations in genes previously associated with the twitcher phenotype, but we do not consider their characterization a priority. However, I also identified a touch insensitive strain with no candidate causative mutations (VC40260) that I at first did not observe to exhibit the twitcher phenotype but later realized likely has either an

heterozygous recessive twitcher allele and/or a second mutation that suppresses the twitcher phenotype. I believe this strain may have two mutations that cause touch insensitivity, one that results in the twitcher phenotype, and one that is independent of the twitcher phenotype.

In the process of selecting touch insensitive animals from the F2 generation of an outcross of VC40260, I noticed that some insensitive animals twitched, whereas other insensitive animals did not. The ratio of F2 animals with the twitcher phenotype appeared to be much less than one in four but it was difficult to be certain without tracking offspring over a longer time period because the twitchers developed much more slowly and were therefore less visible. F2 animals that were twitchers produced only twitcher progeny (and were also notably less fecund) whereas about two thirds of animals that did not appear to be twitchers produced some twitcher progeny (n=36). The twitchers derived from VC40260 were indeed touch insensitive, but there were also many touch insensitive non-twitchers that did not produce any twitcher progeny. Furthermore, I mapped the non-twitcher phenotype-causing mutation to Chr. V and the twitcher phenotype-causing mutation to Chr. IV (see section on mapping).

VC40578

Within the context of our screen, VC40578 was scored as having a strong posterior insensitive phenotype. I later observed that VC40578 animals spent much more time in a backwards locomotory state than wild-type animals. I wondered if the strain might have a mutation affecting the interneurons that mediate the locomotory response to touch rather than a mutation affecting the TRNs. I then tested the posterior touch response of the animals using two different methods. For one set of trials, I used the same assay for posterior touch that I had utilized in the screen, first inciting backwards movement with an anterior stimulus, and then

observing the response to a posterior stimulus delivered shortly (about one second) afterwards. For another set of trials, I applied a posterior stimulus to animals that were already in a backwards locomotory state. The animals that were first touched anteriorly responded infrequently to posterior stimulus, but the animals that were only touched posteriorly had a significantly higher response rate (Figure 5-1). These results suggest that VC40578 animals are not defective in posterior gentle touch sensation, but rather have altered levels of interneuron activation. It may be that the interneurons promoting backwards movement are overactivated by anterior touch, preventing their inactivation by the interneurons that promote forwards movement, or that the interneurons that promote forwards movement are underactivated or are else less able to silence the interneurons that promote backwards movement.

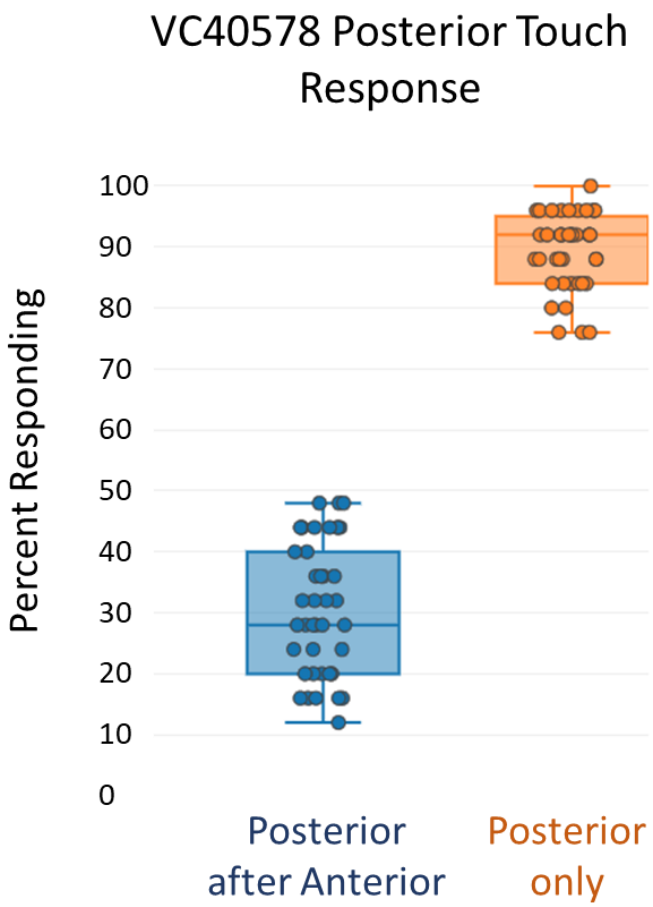

Figure 5-1: VC40578 posterior touch response. VC40578 animals infrequently responded to posterior stimulus applied shortly after anterior stimulus but responded frequently to posterior stimulus alone. Dots represent 38 biological replicates of 25 animals each tested with one posterior stimulus each.

Since the touch response phenotype observed in VC40578 animals suggests defects affecting the touch circuit interneurons, we are no longer categorizing it among the strains with unknown touch phenotype causing mutations.

VC20410

I observed that VC20410 animals had highly variable responses to anterior touch (Figure 5-2), and occasionally moved forwards in response to stimuli applied to the anterior half of the

animal. These phenotypes remained after two rounds of outcrossing. We wondered if the forward response to anterior touch might be caused by a morphological defect such as overgrowth of the PLM anterior process, so I derived a strain (TU6605) carrying the fluorescent TRN marker *Pmec-17::RFP* (*uIs115*). I observed that some animals did not have visible anterior TRNs. Since *mec-17* is highly expressed in cells that have adopted TRN cell fate and is also required for the maintenance of TRN protein expression (Way and Chalfie, 1989; Mitani et al., 1993), we believe the lack of marked TRNs is likely to indicate their complete absence. Furthermore, the defect does not appear to be associated with post-embryonic degeneration, because individual animals were observed to maintain a constant number of marked TRNs from L1 to adulthood.

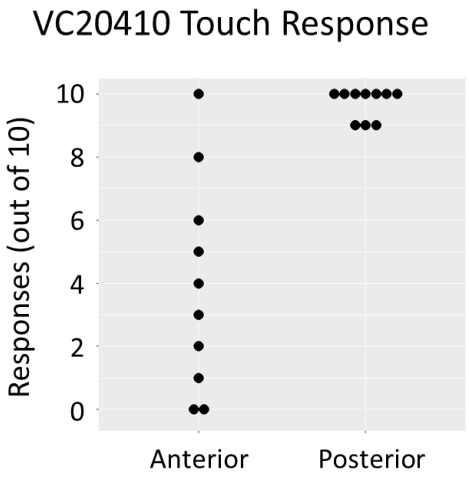

Figure 5-2: VC20410 touch response. Each point represents response data from one individual tested with either 10 anterior touches or 10 posterior touches. n = 10 each for anterior and posterior sets. Anterior response rates were highly variable between individuals while posterior response rates were consistently high.

Nearly all (>98%) TU6605 animals lacked a visible AVM. Most animals (>65%) lacked at least one visible ALM, while some (>17%) were lacking two (Table 5-1). The probability of missing either ALM appeared to be independent, since the proportion of animals missing two

ALMs was approximately equal to the product of the probabilities of missing ALML and ALMR. I did not see any animals that appeared to be missing PLMs or PVM.

The anterior TRN identity phenotype proved to be temperature-dependent, with a higher likelihood of missing ALMs at 20°C than at either 15°C or 25°C (Table 5-1). However, the animals were notably sicker and less fecund at increased temperatures. At 20°C, over half of individuals gave no progeny either due to lethality or sterility, and the proportion was even higher at 25°C. A relatively small proportion of animals appeared dumpy or paralyzed, but I did not find out if such phenotypes bred true because they were associated with further increased levels of lethality and sterility. Most TU6605 animals appeared to have normal body length and locomotion.

Temperature	Probability of Missing			Sample Size (animals)
	AVM	1 ALM	2 ALM	
15°C	98.4 ± 1.4%	64.7 ± 5.3%	18.9 ± 4.2%	317
20°C	99.0 ± 1.0%	79.5 ± 4.1%	36.2 ± 4.7%	381
25°C	98.7 ± 1.4%	68.3 ± 6.6%	18.2 ± 5.5%	192

Table 5-1: TRN identity phenotype in TU6605 at 15, 20, and 25°C. Animals are nearly equally likely to lack AVM across the range of temperatures, but are more likely to lack ALMs at 20°C. Margin of error represents 95% binomial proportion confidence interval.

In addition to the TRN identity defects observed, animals often exhibited defects in cell body migration and/or process extension. ALM cell bodies were often more anteriorly located than in wild-type animals, and ALM anterior processes exhibited overextension defects (Figure 5-3). PLM anterior process overextension defects were occasionally seen. Defects in cell body

migration and process extension appeared to be more frequent for animals raised at higher temperatures.

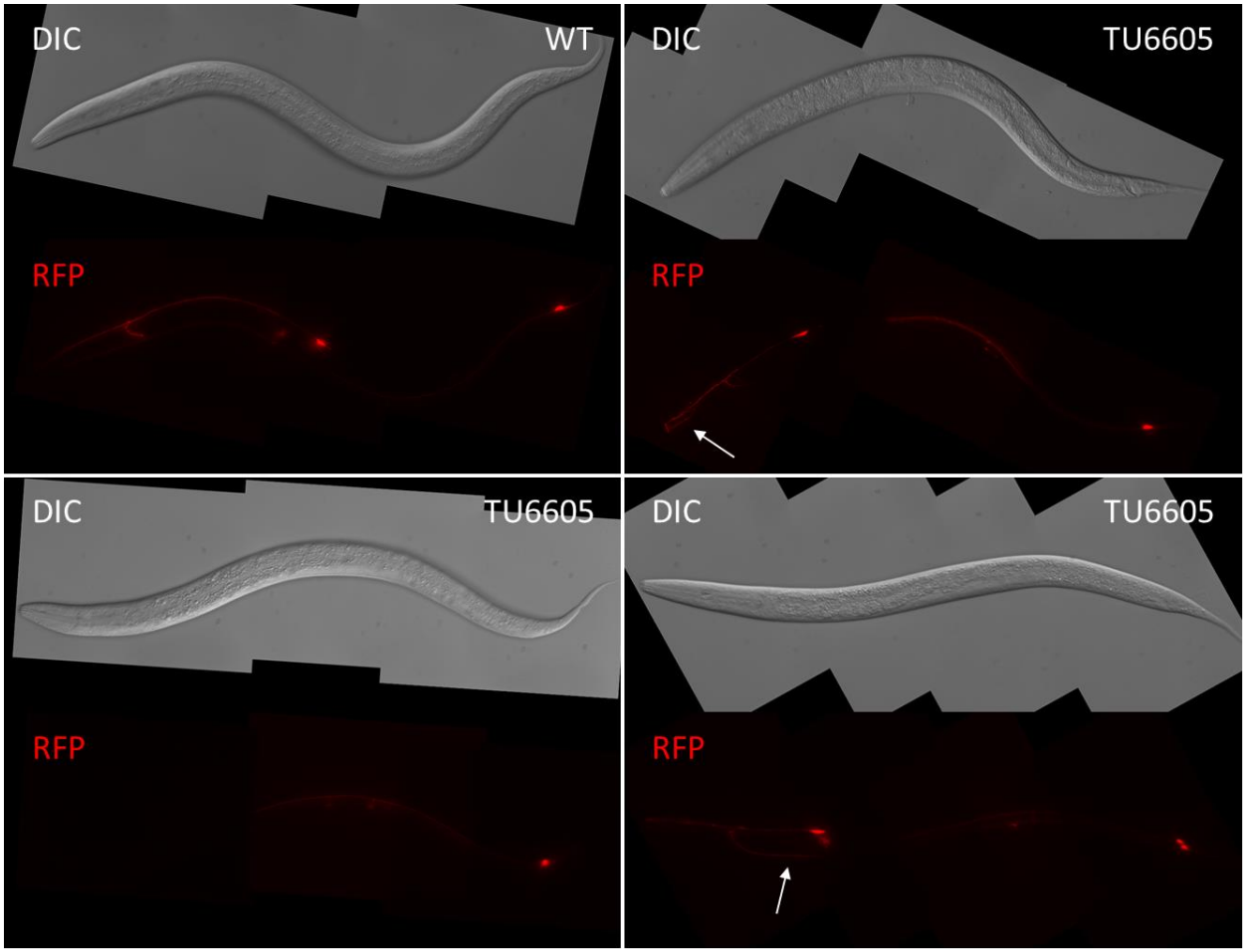

Figure 5-3: TU6605 anterior TRN defects. The top left quadrant shows Pmec-17::RFP (uIs115) expressed in a wild-type background (WT), and the other three quadrants show Pmec-17::RFP (uIs115) in a VC20410 derived background (TU6605). All animals shown were imaged at the L4 stage using a 40x objective lens. The bottom left quadrant shows a representative example of absent anterior TRNs, and the two right quadrants show representative examples of ALM migration and outgrowth defects. Arrows indicate overextended ALM branches.

These phenotypes are somewhat reminiscent of the ALM migration and axon outgrowth defects observed in *vab-15* and *lin-32* mutants, but do not include the same defects as those found in the posterior TRNs of *vab-15* and *lin-32* mutants (Du and Chalfie, 2001). However, the

similarities suggest that VC20410 animals carry defects in a gene affecting TRN precursor differentiation.

Mapping of unknown phenotype-causing mutations

Since the MMP strains have already been whole-genome sequenced, we decided to perform SNP-based genetic mapping to narrow down the list of candidate causative mutations in touch insensitive strains with unknown phenotype-causing mutations. This involved first mapping the phenotype-causing mutations to a chromosome and then mapping the mutations within the chromosome. In a number of cases, mapping successfully helped us identify a known touch gene phenotype-causing mutation that we did not originally consider. This was true for a strain carrying a phenotype-causing *mca-3* mutation (which I did not originally consider as a candidate gene due to associated lethal/sterile phenotypes (Bednarek et al., 2007)) and a strain carrying a phenotype-causing *mec-17* intronic mutation (which we later reclassified as a splice-site altering mutation due to its proximity to the intron-exon border), and several others.

We have been less successful in identifying unknown touch gene phenotype-causing mutations. For two strains, I mapped the phenotype-causing mutation to a particular region and then performed fosmid rescue experiments for candidate genes (genes containing protein-altering mutations within the mapped region), but did not find any evidence of phenotypic rescue (Table 5-2). For the strain we identified as having a TRN differentiation phenotype (VC20410), I mapped the phenotype-causing mutation and then PCR amplified and sequenced candidate causative mutations in outcrossed strains, only to find that none of the candidate alleles were homozygous mutant across all sequenced strains. We then sent the outcrossed strain for whole-genome resequencing.

Strain	Chr.	Approximate Mapped Region (cM)	Candidate Gene(s)	Fosmid Rescue Results
VC20029	X	+1 to +8	*pkn-1*	No rescue
VC20440	I	-4 to +3	ZK973.4	
			ZK973.8	
			W03G9.7	No rescue
			C32E12.1	No rescue
			dpy-14	
			lrp-1	No rescue
			F26A3.1	No rescue

Table 5-2: Fosmid rescue experiments for candidate genes in mapped strains. Blank cells in Fosmid Rescue Results column indicate that the experiment was not done.

After identifying several X-linked mutations, we also tested some X-linked strains for complementation against one another. VC40361 and VC40900 failed to complement one another and were mapped to the same approximate region of the X chromosome. However, based on the mutations reported for these strains in the MMP data set, they appeared to contain no overlapping protein-altering mutations. To check if the strains contained any unreported *mec* gene mutations, we complemented VC40361 and VC40900 to reference alleles of known *mec* genes that fell within the mapped region. Interestingly, VC40361 complemented *mec-7*, whereas VC40900 failed to complement *mec-7*. Additionally, VC40361 partially failed to complement *mec-2* (the heterozygous offspring were less sensitive than wild-type but more sensitive than either starting strain), whereas VC40900 complemented *mec-2*. Both strains will need to be further analyzed to address these confusing results.

We have also identified strains with mutations that do not appear to be linked to a single locus, due to that we have either not yet been able to isolate touch-insensitive mutants from outcrossed strains or else that we have re-isolated much fewer mutations than expected for a phenotype caused by a single gene. We expect we would be able to re-isolate more touch insensitive mutants and determine segregation frequencies by testing greater numbers of F2 cross-progeny, but for the time being we have chosen not to focus on such strains. For strains with unknown phenotype-causing mutations that have been successfully mapped, a summary is provided in Table 5-3.

Strain	Chr.	Approximate Mapped Region (cM)
VC20440	I	-4 to +3
VC40384	I	
VC20410	III	-2 to +5
VC20505	III	-3 to +10
VC40827	III	
VC40338	IV	
VC20779	V	
VC40260	V	
VC40873	V	
VC20029	X	
VC20135	X	
VC41015	X	

Table 5-3: Mapping of MMP strains with unknown causative mutations. Blank cells in Approximate Mapped Region column indicate that the chromosomal region has not been sufficiently narrowed down.

Whole-genome resequencing of outcrossed VC20410

After we discovered the TRN differentiation phenotype of VC20410, the strain could be outcrossed using the absence of fluorescent marked anterior TRNs to easily re-isolate the phenotype-causing mutation between rounds of outcrossing. After 8 rounds of outcrossing to an N2-derived strain from our laboratory (TU6718), we sent the outcrossed VC20410-derived strain (TU6765) and TU6718 for whole-genome resequencing.

To discover which variants were maintained in the outcrossed strain, I first mapped the WGS reads from TU6765 and TU6718 and subtracted the variant calls in TU6718 (WT) from those in TU6765 (TU6765 - TU6718). Then, I obtained the WGS reads of VC20410 from the NCBI Sequence Read Archive and mapped the reads using the same method as I had for TU6765, and extracted the intersection of variant calls from VC20410 and TU6765 (TU6765 ∩ VC20410). Finally, I extracted the intersection of (TU6765 - TU6718) and (TU6765 ∩ VC20410). However, the final intersection [(TU6765 - TU6718) ∩ (TU6765 ∩ VC20410)] contained very few variant calls, none of which were protein altering. I therefore looked at protein altering variant calls from (TU6765 - TU6718) and from (TU6765 ∩ VC20410) that were within the approximate region in which I had mapped the phenotype-causing mutation from VC20410 to (Table 5-4). I also checked to see whether the variant calls for VC20410 alone that I had obtained were similar to those in the dataset for the MMP. I found that there was incomplete overlap. 33 of the Chr. III variant calls from my data set of 112 calls matched those in the MMP data set of 45 calls. This could be due to my filtering criteria being less strict or from background mutations present in the strain VC20410 was mutagenized from, but it's unclear to me why 12 of the VC20410 Chr. III variant calls from the MMP data set were not output from my data processing pipeline.

Set	Position	Gene	Mutation	Gene Function	Known Phenotypes	Expression
TU6765 - TU6718	5208326	Syx-16	splice site	SNAP receptor and SNARE binding (Sato et al., 2011)	Axon guidance defects in ventral cord (Schmitz et al., 2007)	Transcript enriched in PVD, other neurons in embryonic and larval development (Smith et al., 2010; Spencer et al., 2011)
	7325159	F56C9.11	missense	Uncharacterized	Synthetic developmental defects with daf-2 and let-23 (Byrne et al., 2007)	Transcript enriched in germline (Grun et al., 2014)
	8539114	Ceh-23	missense	HOX protein (Forrester et al., 1998)	No obvious defects. Reduced expression of sra-11 in AIY (Altun-Gultekin et al., 2001), suppression of lifespan extension in isp-1 mutants (Walter et al., 2011)	AIY, ADF, ADL, AWC, AFD, PHA, PHB, CAN (Forrester et al., 1998; Altun-Gultekin et al., 2001)
	9552892	Unc-16	missense	Kinesin binding (Arimoto et al., 2011), receptor signaling complex adaptor (Byrd et al., 2001)	Locomotion variants (Yemini et al., 2013), axonal transport variants (Arimoto et al., 2011; Edwards et al., 2013; Noma et al., 2017), egg-laying defective, sluggish, weak coiler (Trent et al., 1983)	ALM (Edwards et al., 2013), broadly in the nervous system (Byrd et al., 2001)
	10498228	F43D9.1	missense	Transmembrane protein (Kwon et al., 2001)	Dumpy (Gonczy et al., 2000), low penetrance sterile/lethal (Rual et al., 2004)	Head neurons and muscle cells (Kwon et al., 2001)
TU6765 ∩ VC20410	8693701	B0303.7	missense	Proline-rich region binding activity (Shaye and Greenwald, 2011; Kim et al., 2018)		Enriched in intestine (Blazie et al., 2017), larval NSM, larval hypodermis (Spencer et al., 2011), nervous system (Watson et al., 2008; Kaletsky et al., 2016)

Table 5-4: Candidate genes on Chr. III [5.2 Mb-10.8 Mb] with protein-altering mutations in the set of variants called in TU6765 but not TU6718 and in the set of variants called in both TU6765 and VC20410. Candidate phenotype-causing mutations are consistent with EMS-induced transition mutations.

Of these genes, I consider *ceh-23* and *unc-16* to be the most likely candidate phenotype-causing genes due to *ceh-23* being a HOX protein (other HOX proteins have been found to cause similar partial-penetrance ALM differentiation defects (Zheng et al., 2015)) and *unc-16* being expressed in the ALMs. Null mutations for neither *ceh-23* nor *unc-16* are known to cause the ALM differentiation phenotypes I observed in VC20410-derived strains, but the *ceh-23* or *unc-16* missense mutations in TU6765 could be recessive gain-of-function. If so, we would still expect fosmid rescue to be possible.

5. 3 Discussion

Although we began our screen of the MMP with some hope for identifying new touch genes, we have not yet done so. Since three-factor mapping and subsequent fosmid rescue experiments with candidate genes has not proven to be particularly efficient, and since we have some evidence that mutations either not reported in the MMP datasets or that have spontaneously occurred can lead to touch phenotypes, it would probably be best to proceed using Hawaiian SNP mapping and WGS.

We have yet to try fosmid rescue experiments for the candidates we identified by WGS of a VC20410-derived strain, which is another logical next step. If either *ceh-23* or *unc-16* prove to contain gain-of-function phenotype-causing mutations, it will certainly be useful to incorporate knowledge of their role in ALM differentiation to what we already know about these genes. If one of the other candidates proves to be the phenotype-causing gene, it would be more

surprising but also potentially more informative since their functions are generally less well known.

We plan to continue complementing strains with unknown phenotype-causing mutations to known *mec* genes that fall within the regions that mutations have been mapped to, as we did with VC40900. It is quite possible that mutations not reported within the MMP data set are present within additional strains. If so, and if such mutations have led to the phenotypes in some of our strains lacking candidate mutations, it would help us have a better idea of the false negative rate for reported MMP mutations.

Although we have not yet determined previously unlinked genes to be involved in gentle touch sensation, we are excited by the number of MMP strains with touch insensitive phenotypes that we have identified. It seems to us that the MMP is a very good resource for performing forward genetic screens.

5.4 Materials and Methods

Microscopy

In vivo fluorescent images were captured using a Zeiss Axio Observer Z1 inverted microscope equipped with a Photometrics CoolSnap HQ2 camera. Captures were processed in Fiji (ImageJ) with use of the stitching plugin (Preibisch et al., 2009).

Genetic Mapping of Phenotype-Causing Mutant Alleles

Phenotype-causing mutant alleles were tested for X-linkage and dominance as described by Brenner (1974).

For strains with autosomal-linked mutations, mutant hermaphrodites were crossed to reference strain (either TU6770 or TU6771) males. For strains with X-linked mutations, mutant hermaphrodites were crossed to either TU6772 or TU6778 males. F1 cross-progeny were selected by the presence of a fluorescent marker, and touch-insensitive F2 progeny were singled out. F3 progeny were tested for touch sensitivity to verify the inheritance of the phenotype and then genotyped for single nucleotide variations (SNVs) present in the reference strains by allele-specific PCR.

Preparation of reference strains and primers for allele-specific PCR genotyping

VC20019 was selected as a source of marker SNVs based on the work by Mok et al. (2017). Reference strains for mapping of autosomal-linked mutations (TU6770 and TU6771) were generated by mating hermaphrodites from strains with X-linked fluorescent markers (CGC24 and OH13605) to VC20019 males, and then backcrossing into VC20019 an additional X times while selecting for retention of the fluorescent markers before isolating fluorescent marker homozygous self-progeny. Reference strains for mapping of X-linked mutations (TU6772 and TU6778) were generated by mating hermaphrodites from strains with autosomal-linked fluorescent markers (CGC18 and CGC54) to VC20019 males, and then backcrossing male cross progeny into VC20019 an additional two times before isolating fluorescent marker homozygous self-progeny.

VC20019 SNVs were evaluated for use as marker alleles by analyzing the 20 base-pair (bp) flanking sequences on either side of each variation. SNVs were considered candidate marker alleles if at least one 20 bp flank had a GC content between 30-60%, did not contain 4x mononucleotide or dinucleotide repeats, and was not predicted to self-anneal as determined by

use of the primer-dimer prediction generated by Thermo Scientific's Multiple Primer Analyzer tool with a dimer-detection sensitivity value of 4.

Allele-specific PCR primers were designed according to the principles described by (Liu et al., 2012). Primers paired with allele-specific primers were designed using Primer3. Primers for use in multi-product PCR were selected with consideration of product size (Δ > 75 bp), genetic position (for autosomal linkage assay, > -5 and < +5 cM; for intrachromosomal linkage assay, Δ > 5 cM), and the primer-dimer estimation generated by Thermo Scientific's Multiple Primer Analyzer tool. Table 5-5 lists primers used.

Chr.	Allele	Allele-specific Primer Sequence	Alternate Primer Sequence
I	gk110420	TTGTGAAAGTGAATCTGTTATT	AAACCCGTAGATACTACAAAGC
I	gk105830	TAATGGTGCTTTTGAGCCCTT	AACTATCATATTCTCGTCGCAC
I	gk117526	GGGTTACAACCTATTTTCTCACTA	TCAGCCTTTGTTTTGTTCAATC
I	gk122876	TTATCTTCTTGGGTGGCGCGAA	TTCAGCCGTCTACAAATACTTC
II	gk141093	GACCAGAGTGACAAATACA	AGTTCTTCTCTTCCAGTGTTTC
II	gk133320	ATAGGCATAGGCATAGAGT	TACTCAACGGTAGTATGCTTTG
II	gk134227	AAGAACTCCTTGGAGGAAT	CACTATCAATGACGGTAGGTAC
II	gk158973	GTCACGAGAGCTGGAATCAAGA	AACACATTAACATTGTCTTCGC
III	gk178605	TCTTCCTTGGATTTGTCTCGAT	TTGTAGAAGTTCAGACCCATTG
III	gk166049	ACTGTAGCACCGATTTTGGT	GGTATGGTGGTGGAAATGTC
III	gk171414	GTGACGGTAAGGAAGAGGTA	TTTCTAATGTGGTGGTCGTATG
III	gk187525	ACATGGTTAAGAACGTGTTA	AAGAGGACGACAAACAATAAGG
IV	gk198747	CATTAGCCCTTTCATAGTCCGT	TCTTTGACCTGACCTCAATTTC
IV	gk191256	ACTCCAGTTTCTTGTGCCTT	TCCCAAATAATGTTTGTATTGCC
IV	gk196460	CCATGTCTGTTATTGCTTAAATTTT	GGTGATGATTAGCCTATTACGG
IV	gk216503	GAACTGACGGAAGGTGGAT	AAATGGTAAACGAAGAAAGCAC
V	gk235636	CTCCGTTCACTTTACTCGGTT	ACTGATGTAGATTTGTGAGCTG
V	gk230207	AATGTGAGCTTCCAAAGACCTA	TCTACAAGTTATGAGCATTCCG
V	gk234414	GTGTAGATCAAATGAGTGCTTT	ATACTTTAATACCCTCTTGCCG
V	gk257182	CTTCCCTTTGCCCTTTACCA	TTCTTAATCCCTTACCTGTCAC
X	gk272703	TGTTATACCCTAGCAACACAA	GCTATCTGACAGTTGTTTCTTG
X	gk290261	CACCGACAATTCATCTCGGA	TCGAGAATGATTAATGGAGCAG
X	gk297348	GAGTTCGCAGTAAACAAATAT	TTTACGAGGAGAATAAGCGAAG

Table 5-5: Allele-specific primers used for mapping VC20019 SNVs.

Fosmid Rescue Experiments

Transgenic lines were generated by co-injecting 10 ng/µL of fosmid DNA, 5 ng/µL pCFJ104, 2.5ng /µL pCFJ90, and 82.5 ng/µL pBluescript II SK (+). Transgenic F2 and/or F3 animals were selected by the presence of fluorescent markers and tested for anterior and posterior touch sensitivity simultaneously. Touch sensitivity scores from transgenic lines were compared to those from the injected strain using a one-tailed Student's t-test with presumed equal variance.

Whole Genome Sequencing

Genomic DNA was extracted using the PureGene Genomic DNA Tissue Kit [QIAGEN (Valencia, CA) no. 158622]. Prepared DNA samples were sent to BGI. The samples were sequenced using paired reads on BGI's DNBSeq^{TM} platform with read length 150 for 2GB clean data per sample. The resulting data was processed in Galaxy. Fastq reads were cleaned with Trimmomatic using default settings and then mapped and processed using a protocol similar to that described by (Joseph et al., 2018).

Chapter 6: Conclusions

In this thesis, I have described screening the Million Mutation Project (MMP) strains for gentle touch sensitivity phenotypes. I was able to identify touch insensitive MMP mutants of varying phenotypic strength but found that the overall distribution of response rates was highly skewed towards full responsiveness. Most of the touch insensitive MMP mutants were reported to have mutations in genes already known to mutate to cause touch insensitivity, and I was able to verify the phenotype-causing mutations in most of such strains. For genes that were identified in previous mutageneses for touch insensitive mutants, I considered point mutations that both did and did not result in a phenotype. As such, I was able to determine that for most genes, the majority of missense mutations did not result in a phenotype. I also identified touch insensitive strains that were not reported to have mutations in genes previously implicated in touch sensitivity. More analysis will be necessary to determine the phenotype-causing mutations in these strains. I expect that in doing so, it will be possible to identify additional genes involved in touch receptor neuron function.

6.1 Future Experiments

There is remaining work to be done to wrap up our interrogation of the MMP set. We will want to perform further investigation of strains with unknown causative mutations and verify some specific cases involving the phenotypic effects of and nature of mutations in known *mec* genes. For the strains with unknown phenotype-causing mutations, we should continue genetic analysis of their touch-insensitive phenotypes. Our continuing genetic analysis should involve determining whether touch-insensitive phenotypes are genetically linked to additional

phenotypes and determining chromosomal linkage. As described in Chapter 5, these steps have already been completed for some touch insensitive strains with unknown causative mutations, but there are additional strains which we have yet to analyze. Figure 6-1 shows which steps in the analysis remain to be completed for each of the insensitive strains with unknown phenotype-causing mutations.

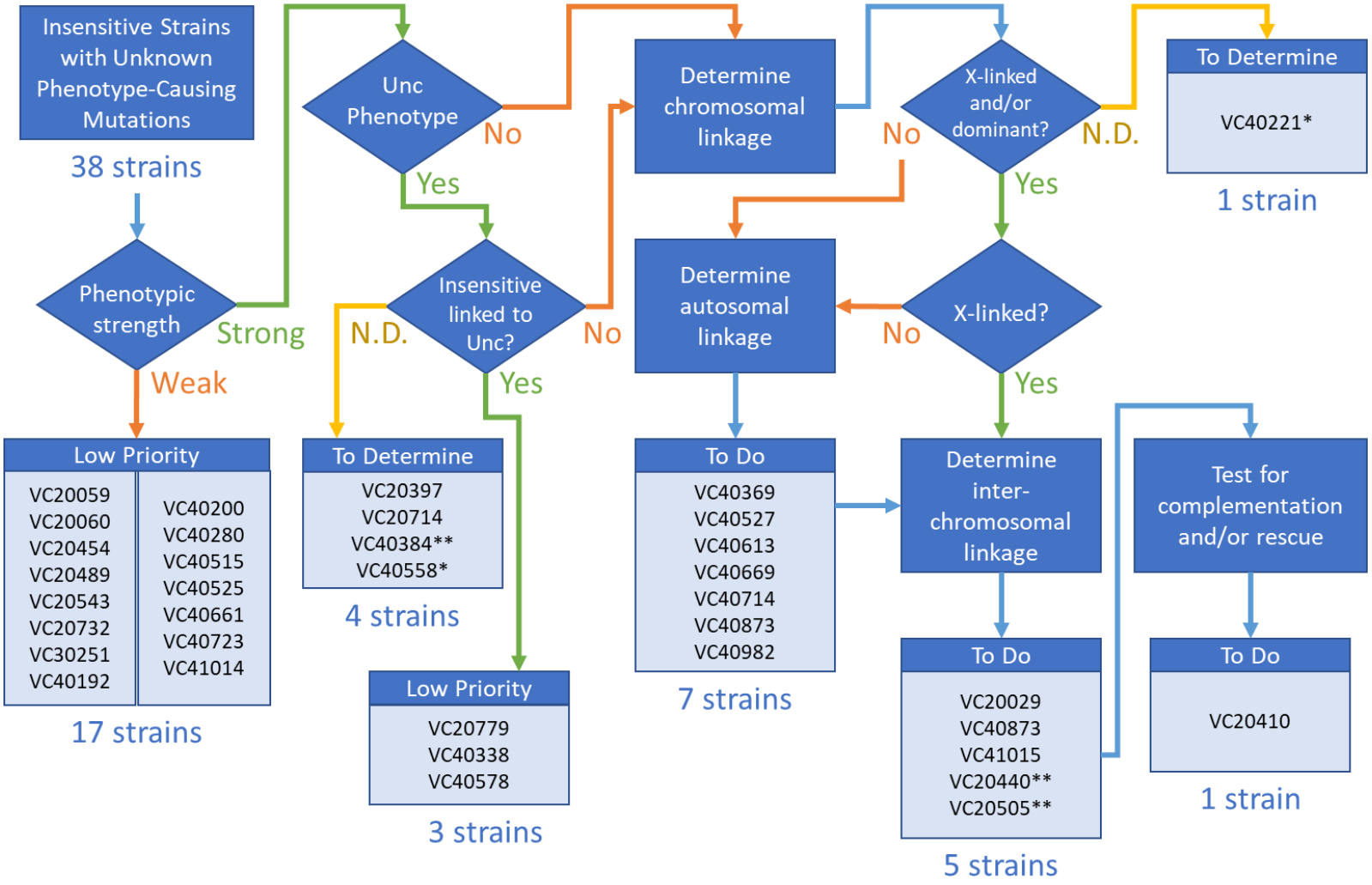

Figure 6-1: Flowchart for analysis of strains with unknown causative mutations. 38 strains are listed according to which steps of analysis have already been performed. Strains marked with * have proven to mate very poorly and may not be amenable to genetic analysis. Strains marked with ** have partially undergone the analysis step under which they are listed.

Experiments to complete analysis of MMP strains with mutations in known *mec* genes include complementation tests for insensitive strains with candidate causative mutations, retesting of potentially weakly insensitive or temperature-sensitive strains, and verification of the nature of certain mutations. Ten touch insensitive MMP strains have candidate causative mutations that have yet to be complemented to reference alleles (Table 6-1). Three strains that have protein altering mutations in known *mec* genes (excluding those with mutations in *mec-5*) and are suspected to have weak phenotypes should be retested (Table 6-2). 13 strains that have protein-altering mutations in *mec-5* should be tested for touch sensitivity at different temperatures to determine whether they exhibit temperature-sensitive phenotypes (Table 6-3). Finally, the phenotype-causing mutations in three strains should be verified by sequencing. The *mec-12* region should be amplified and sequenced from VC40359 due to the surprising nature of the reported change (a non-coding substitution not adjacent to an intron-exon border). The *mec-2* and *mec-7* regions should be amplified and sequenced from VC40361 and VC40900 due to the confusing complementation test results discussed in Chapter 5.

Strain	Phenotype	Candidate Causative Mutation(s)
VC20265	Weak Anterior	*unc-22*
VC20794	Weak Anterior	*mua-3*
VC40055	Weak Posterior	*lam-1*
VC40084	Weak Posterior	*lgc-37*
VC40195	Strong	*unc-2*
VC40277	Weak Posterior	*mec-8*
VC40366	Weak Posterior	*mec-4*
VC40458	Weak Posterior	*elo-1*
VC40507	Weak Anterior	*unc-2, unc-22, unc-31*
VC40739	Weak Anterior	*unc-31, mup-4*

Table 6-1: Remaining complementation tests

Strain	Mutated *mec* Gene	Initial Anterior Response Rate (out of 25)	Initial Posterior Response Rate (out of 25)
VC40782	*mec-1*	20	20
VC40334	*mec-8*	22	18
VC40582	*mec-10*	20	20

Table 6-2: Strains to retest for weak phenotypes.

Strain	Average Anterior Response at 20°C (out of 25)	Average Posterior Response at 20°C (out of 25)
VC20198	22	20
VC20354	22	21
VC20358	25	22
VC20367	22	20
VC20612	24	25
VC20665	23	22
VC30148	20	20
VC40275	22	20
VC40326	25	25
VC40344	22	18
VC40598	24	16
VC40675	24	23
VC40836	21	25

Table 6-3: Strains to test for temperature-sensitive phenotypes. Response rates are rounded to the nearest whole number.

Our screen also suggested some new information about known *mec* genes which should be further investigated. For one, the phenotypes of MMP strains with protein-altering mutations in *mec-2* suggest that *mec-2* isoforms d, e, f, and/or g are important for touch sensitivity. We had not previously found any phenotype-causing *mec-2* mutations that affected only these isoforms, and we had not previously found evidence that any of these isoforms were expressed in the touch receptor neurons. Since our lab has already collected RNA seq reads from cultured touch receptor neurons, we might first look to see if the data contain reads unique to isoforms d-g.

It was somewhat surprising to us that some of the touch-insensitive MMP strains with mutations in known *mec* genes exhibited different levels of anterior and posterior sensitivity,

since the majority of the *mec* mutants identified through mutageneses for touch insensitivity were not noted to have significant differences in anterior and posterior sensitivity (Chalfie and Sulston, 1981; Chalfie and Au, 1989). We might go on to investigate the MMP strains with differential levels of anterior and posterior touch sensitivity to see if the differences are due to the nature of specific *mec* gene mutations or else genetic background effects. Insensitive MMP strains with phenotype-causing mutations in original *mec* genes (genes identified in the initial mutageneses reported by Chalfie and Sulston (1981) and Chalfie and Au (1989)) that have differential anterior and posterior sensitivity are listed in Table 6-4. Additionally, since many of our lab's previous experiments on touch sensitivity used measures of the sum of anterior and posterior touch sensitivity, we might go back and test previously identified alleles for differential anterior and posterior touch sensitivity.

Strain	Phenotype-Causing Mutation	Phenotype	Average Anterior Response Rate (out of 25)	Average Posterior Response Rate (out of 25)
VC20738	*mec-2*	Strong Posterior	25	16
VC40096	*mec-2*	Strong Anterior	15	21
VC40344	*mec-5*	Weak Anterior	19	24
VC40598	*mec-5*	Strong Posterior	24	16
VC20186	*mec-7*	Strong Anterior	12	20
VC40378	*mec-9*	Strong Anterior	3	18
VC40243	*mec-14*	Strong Anterior	11	21
VC20213	*mec-15*	Strong Posterior	21	15
VC40469	*mec-15*	Strong Posterior	23	11
VC40592	*mec-17*	Strong Posterior	25	15
VC40619	*mec-18*	Strong Posterior	23	13

Table 6-4: Strains with differential anterior and posterior sensitivity. Only strains with verified phenotype-causing mutations in original *mec* genes are listed. Strains with relatively small differences between anterior and posterior response rates ($\Delta < 5$) are not included. Response rates are rounded to the nearest whole number.

The data from my screen may prove useful in making additional calculations and predictions, for example to train algorithms for predicting phenotype-causing mutations. Since I found that the majority of missense mutations in known *mec* genes did not cause a detectable phenotype (roughly 90%), we might further investigate the different features of phenotype-causing and non-phenotype-causing missense mutations. While there did not appear to be clear correlations between phenotypes and measures such as Grantham scores (indicating chemical differences between amino acid substitutions) and GERP scores (indicating evolutionary conservation of residues), some combination of such scores might be able to predict which missense mutations are more likely to be phenotype-causing.

6.2 Implications

Our screen demonstrated that the MMP set is a useful tool for discovery. We were able to find phenotypes unlike those identified through previous screens, namely a great number of weaker phenotypes and a relatively large number of strains with differential anterior and posterior sensitivity. We found phenotype-causing alleles unlike those previously identified, implicating new regions of significance in known *mec* genes. We are also likely to have found phenotype-causing mutations in genes not previously implicated in touch sensitivity, although more work will need to be done in order to verify the identity of such genes.

The MMP may be a particularly useful tool in studying phenotypes that tend to show incomplete penetrance. Such phenotypes might be difficult to pick out following mutagenesis, and the MMP should also make it easy to determine the penetrance of a given mutation.

As I showed for the original set of *mec* genes, phenotyping MMP strains can provide a structure-function analysis by identifying regions where mutations do and do not lead to detectable changes in protein function. This might be done in the context of a reverse screen, where MMP strains known to have mutations in a gene of interest are selected for phenotyping, or else following a forward screen, where phenotypes of MMP strains with mutations in a newly identified phenotype-causing gene are considered. Although other groups have already utilized the MMP in such ways (Mathew et al., 2016; Bulger et al., 2017; Chen et al., 2019), our screen provides the most extensive example yet reported.

6.3 Recommendations

Based on my experience of screening the MMP set for touch insensitive phenotypes, I have several recommendations for groups considering a similar screen. Here, I will start with

notes that are more technical in nature and conclude with those having more to do with experimental scope.

The MMP strains cover a wide range of growth and reproductive rates. Although I did not collect the data to verify this, I would very roughly approximate the population growth rates as a half-normal distribution, with the majority of the strains multiplying at approximately wild-type rates, few strains multiplying at slow rates, and fewer strains multiplying at very slow rates. The slowest growing strains must be maintained with caution, since transferring just a few animals from such strains to a new plate might fail to produce a subsequent generation. Less viable strains might also fail to reproduce at temperatures above 20°C. For this reason, I would not recommend attempting to screen the full MMP set at a 25°C cultivation temperature.

Many of the MMP strains have highly visible Unc (uncoordinated) phenotypes. In designing an MMP screen, one should consider whether such phenotypes might interfere with assessing the phenotype of interest and if strains with such phenotypes should be regarded differently. I would recommend making note of the obvious visible phenotypes associated with each strain during the process of data collection whether they are relevant to the phenotype of interest or not, since most of the MMP strains have not been assigned even highly visible phenotypes.

I believe the MMP set provides good opportunity to demonstrate range and nuance of phenotypes. I would recommend attempting to capture these features for the phenotype of interest in one's method of data collection. One might start with less nuanced judgements and then increase the descriptive level of data collection in stages since binary forms of classification are often much quicker to perform than more descriptive methods, but it might also be very interesting to consider higher resolution data for a larger set if feasible.

References

Akella, J.S., Wloga, D., Kim, J., Starostina, N.G., Lyons-Abbott, S., Morrissette, N.S., Dougan, S.T., Kipreos, E.T., and Gaertig, J. (2010). MEC-17 is an α-tubulin acetyltransferase. Nature *467*, 218-222.

Albeg, A., Smith, C.J., Chatzigeorgiou, M., Feitelson, D.G., Hall, D.H., Schafer, W.R., Miller, D.M., and Treinin, M. (2011). C. elegans multi-dendritic sensory neurons: Morphology and function. Molecular and Cellular Neuroscience *46*, 308-317.

Almedom, R.B., Liewald, J.F., Hernando, G., Schultheis, C., Rayes, D., Pan, J., Schedletzky, T., Hutter, H., Bouzat, C., and Gottschalk, A. (2009). An ER-resident membrane protein complex regulates nicotinic acetylcholine receptor subunit composition at the synapse. Embo j *28*, 2636-2649.

Altun-Gultekin, Z., Andachi, Y., Tsalik, E.L., Pilgrim, D., Kohara, Y., and Hobert, O. (2001). A regulatory cascade of three homeobox genes, ceh-10, ttx-3 and ceh-23, controls cell fate specification of a defined interneuron class in C. elegans. Development *128*, 1951-1969.

Aoyama, Y., Urushiyama, S., Yamada, M., Kato, C., Ide, H., Higuchi, S., Akiyama, T., and Shibuya, H. (2004). MFB-1, an F-box-type ubiquitin ligase, regulates TGF-β signalling. Genes to Cells *9*, 1093-1101.

Arimoto, M., Koushika, S.P., Choudhary, B.C., Li, C., Matsumoto, K., and Hisamoto, N. (2011). The Caenorhabditis elegans JIP3 protein UNC-16 functions as an adaptor to link kinesin-1 with cytoplasmic dynein. J Neurosci *31*, 2216-2224.

Arnadottir, J., O'Hagan, R., Chen, Y., Goodman, M.B., and Chalfie, M. (2011). The DEG/ENaC protein MEC-10 regulates the transduction channel complex in Caenorhabditis elegans touch receptor neurons. J Neurosci *31*, 12695-12704.

Auerbach, C., and Robson, J.M. (1946). Chemical production of mutations. Nature *157*, 302.

Avery, L. (1993). The genetics of feeding in Caenorhabditis elegans. Genetics *133*, 897-917.

Axäng, C., Rauthan, M., Hall, D.H., and Pilon, M. (2008). Developmental genetics of the C. eleganspharyngeal neurons NSML and NSMR. BMC Developmental Biology *8*, 38.

Barnes, T.M., Jin, Y., Horvitz, H.R., Ruvkun, G., and Hekimi, S. (1996). The Caenorhabditis elegans behavioral gene unc-24 encodes a novel bipartite protein similar to both erythrocyte band 7.2 (stomatin) and nonspecific lipid transfer protein. J Neurochem *67*, 46-57.

Bednarek, E.M., Schaheen, L., Gaubatz, J., Jorgensen, E.M., and Fares, H. (2007). The Plasma Membrane Calcium ATPase MCA-3 is Required for Clathrin-Mediated Endocytosis in Scavenger Cells of Caenorhabditis elegans. Traffic *8*, 543-553.

Bellanger, J.M., Cueva, J.G., Baran, R., Tang, G., Goodman, M.B., and Debant, A. (2012). The doublecortin-related gene zyg-8 is a microtubule organizer in Caenorhabditis elegans neurons. J Cell Sci *125*, 5417-5427.

Ben-Shahar, Y. (2011). 1 - Sensory Functions for Degenerin/Epithelial Sodium Channels (DEG/ENaC). In Advances in Genetics, T. Friedmann, J.C. Dunlap, and S.F. Goodwin, eds. (Academic Press), pp. 1-26.

Bessereau, J.L. (2006). Insertional mutagenesis in C. elegans using the Drosophila transposon Mos1: a method for the rapid identification of mutated genes. Methods Mol Biol *351*, 59-73.

Bianchi, L. (2007). Mechanotransduction: Touch and Feel at the Molecular Level as Modeled in Caenorhabditis elegans. Molecular Neurobiology *36*, 254-271.

Bianchi, L., Gerstbrein, B., Frøkjær-Jensen, C., Royal, D.C., Mukherjee, G., Royal, M.A., Xue, J., Schafer, W.R., and Driscoll, M. (2004). The neurotoxic MEC-4(d) DEG/ENaC sodium channel conducts calcium: implications for necrosis initiation. Nature Neuroscience *7*, 1337-1344.

Biemesderfer, D., Dekan, G., Aronson, P.S., and Farquhar, M.G. (1993). Biosynthesis of the gp330/44-kDa Heymann nephritis antigenic complex: assembly takes place in the ER. Am J Physiol *264*, F1011-1020.

Blazie, S.M., Geissel, H.C., Wilky, H., Joshi, R., Newbern, J., and Mangone, M. (2017). Alternative Polyadenylation Directs Tissue-Specific miRNA Targeting in Caenorhabditis elegans Somatic Tissues. Genetics *206*, 757-774.

Bodakuntla, S., Jijumon, A.S., Villablanca, C., Gonzalez-Billault, C., and Janke, C. (2019). Microtubule-Associated Proteins: Structuring the Cytoskeleton. Trends Cell Biol *29*, 804-819.

Borgen, M.A., Giles, A.C., Wang, D., and Grill, B. (2019). Synapse maintenance is impacted by ATAT-2 tubulin acetyltransferase activity and the RPM-1 signaling hub. Elife *8*.

Bounoutas, A., and Chalfie, M. (2007). Touch sensitivity in Caenorhabditis elegans. Pflugers Arch *454*, 691-702.

Bounoutas, A., Kratz, J., Emtage, L., Ma, C., Nguyen, K.C., and Chalfie, M. (2011). Microtubule depolymerization in Caenorhabditis elegans touch receptor neurons reduces gene expression through a p38 MAPK pathway. Proceedings of the National Academy of Sciences *108*, 3982-3987.

Bounoutas, A., O'Hagan, R., and Chalfie, M. (2009a). The multipurpose 15-protofilament microtubules in C. elegans have specific roles in mechanosensation. Curr Biol *19*, 1362-1367.

Bounoutas, A., Zheng, Q., Nonet, M.L., and Chalfie, M. (2009b). mec-15 Encodes an F-Box Protein Required for Touch Receptor Neuron Mechanosensation, Synapse Formation and Development. Genetics *183*, 607-617.

Brenner, S. (1974). The genetics of Caenorhabditis elegans. Genetics *77*, 71-94.

Brockie, P.J., Madsen, D.M., Zheng, Y., Mellem, J., and Maricq, A.V. (2001). Differential expression of glutamate receptor subunits in the nervous system of Caenorhabditis elegans and their regulation by the homeodomain protein UNC-42. J Neurosci *21*, 1510-1522.

Brown, A.L., Fernandez-Illescas, S.M., Liao, Z., and Goodman, M.B. (2007). Gain-of-Function Mutations in the MEC-4 DEG/ENaC Sensory Mechanotransduction Channel Alter Gating and Drug Blockade. The Journal of General Physiology *129*, 161-173.

Brown, A.L., Liao, Z., and Goodman, M.B. (2008). MEC-2 and MEC-6 in the Caenorhabditis elegans sensory mechanotransduction complex: auxiliary subunits that enable channel activity. J Gen Physiol *131*, 605-616.

Buddell, T., Friedman, V., Drozd, C.J., and Quinn, C.C. (2019). An autism-causing calcium channel variant functions with selective autophagy to alter axon targeting and behavior. PLoS Genet *15*, e1008488.

Bulger, D.A., Fukushige, T., Yun, S., Semple, R.K., Hanover, J.A., and Krause, M.W. (2017). Caenorhabditis elegans DAF-2 as a Model for Human Insulin Receptoropathies. G3 (Bethesda) *7*, 257-268.

Burgess, H.A., and Reiner, O. (2000). Doublecortin-like kinase is associated with microtubules in neuronal growth cones. Mol Cell Neurosci *16*, 529-541.

Butterworth, M.B., Edinger, R.S., Johnson, J.P., and Frizzell, R.A. (2005). Acute ENaC stimulation by cAMP in a kidney cell line is mediated by exocytic insertion from a recycling channel pool. J Gen Physiol *125*, 81-101.

Byrd, D.T., Kawasaki, M., Walcoff, M., Hisamoto, N., Matsumoto, K., and Jin, Y. (2001). UNC-16, a JNK-signaling scaffold protein, regulates vesicle transport in C. elegans. Neuron *32*, 787-800.

Byrne, A.B., Weirauch, M.T., Wong, V., Koeva, M., Dixon, S.J., Stuart, J.M., and Roy, P.J. (2007). A global analysis of genetic interactions in Caenorhabditis elegans. J Biol *6*, 8.

Cai, S.Q., Wang, Y., Park, K.H., Tong, X., Pan, Z., and Sesti, F. (2009). Auto-phosphorylation of a voltage-gated K+ channel controls non-associative learning. Embo j *28*, 1601-1611.

Calahorro, F., and Ruiz-Rubio, M. (2012). Functional phenotypic rescue of Caenorhabditis elegans neuroligin-deficient mutants by the human and rat NLGN1 genes. PLoS One *7*, e39277.

Calixto, A., Chelur, D., Topalidou, I., Chen, X., and Chalfie, M. (2010a). Enhanced neuronal RNAi in C. elegans using SID-1. Nature Methods *7*, 554-559.

Calixto, A., Ma, C., and Chalfie, M. (2010b). Conditional gene expression and RNAi using MEC-8-dependent splicing in C. elegans. Nat Methods *7*, 407-411.

Cassata, G., Rohrig, S., Kuhn, F., Hauri, H.P., Baumeister, R., and Burglin, T.R. (2000). The Caenorhabditis elegans Ldb/NLI/Clim orthologue ldb-1 is required for neuronal function. Dev Biol *226*, 45-56.

Caylor, R.C., Jin, Y., and Ackley, B.D. (2013). The Caenorhabditis elegans voltage-gated calcium channel subunits UNC-2 and UNC-36 and the calcium-dependent kinase UNC-43/CaMKII regulate neuromuscular junction morphology. Neural Development *8*, 10.

Chalfie, M., and Au, M. (1989). Genetic control of differentiation of the Caenorhabditis elegans touch receptor neurons. Science *243*, 1027-1033.

Chalfie, M., Hart, A.C., Rankin, C.H., and Goodman, M.B. (2014). Assaying mechanosensation. WormBook.

Chalfie, M., and Sulston, J. (1981). Developmental genetics of the mechanosensory neurons of Caenorhabditis elegans. Developmental Biology *82*, 358-370.

Chalfie, M., Sulston, J., White, J., Southgate, E., Thomson, J., and Brenner, S. (1985). The neural circuit for touch sensitivity in Caenorhabditis elegans. The Journal of Neuroscience *5*, 956-964.

Chalfie, M., and Thomson, J.N. (1979). Organization of neuronal microtubules in the nematode Caenorhabditis elegans. J Cell Biol *82*, 278-289.

Chalfie, M., and Thomson, J.N. (1982). Structural and functional diversity in the neuronal microtubules of Caenorhabditis elegans. J Cell Biol *93*, 15-23.

Chalfie, M., and Wolinsky, E. (1990). The identification and suppression of inherited neurodegeneration in Caenorhabditis elegans. Nature *345*, 410-416.

Chatzigeorgiou, M., Grundy, L., Kindt, K.S., Lee, W.-H., Driscoll, M., and Schafer, W.R. (2010a). Spatial Asymmetry in the Mechanosensory Phenotypes of the C. elegans DEG/ENaC Gene mec-10. Journal of Neurophysiology *104*, 3334-3344.

Chatzigeorgiou, M., and Schafer, William R. (2011). Lateral Facilitation between Primary Mechanosensory Neurons Controls Nose Touch Perception in C. elegans. Neuron *70*, 299-309.

Chatzigeorgiou, M., Yoo, S., Watson, J.D., Lee, W.-H., Spencer, W.C., Kindt, K.S., Hwang, S.W., Miller Iii, D.M., Treinin, M., Driscoll, M., *et al.* (2010b). Specific roles for DEG/ENaC and TRP channels in touch and thermosensation in C. elegans nociceptors. Nature Neuroscience *13*, 861-868.

Chelur, D.S., Ernstrom, G.G., Goodman, M.B., Yao, C.A., Chen, L., R, O.H., and Chalfie, M. (2002). The mechanosensory protein MEC-6 is a subunit of the C. elegans touch-cell degenerin channel. Nature *420*, 669-673.

Chen, C.-H., Lee, A., Liao, C.-P., Liu, Y.-W., and Pan, C.-L. (2014). RHGF-1/PDZ-RhoGEF and retrograde DLK-1 signaling drive neuronal remodeling on microtubule disassembly. Proceedings of the National Academy of Sciences *111*, 16568-16573.

Chen, X. (2013). Modulation of Touch Sensitivity in Caenorhabditis Elegans (Columbia University).

Chen, X., and Chalfie, M. (2014). Modulation of C. elegans touch sensitivity is integrated at multiple levels. J Neurosci *34*, 6522-6536.

Chen, X., and Chalfie, M. (2015). Regulation of mechanosensation in C. elegans through ubiquitination of the MEC-4 mechanotransduction channel. J Neurosci *35*, 2200-2212.

Chen, X., Cuadros, M.D., and Chalfie, M. (2015a). Identification of nonviable genes affecting touch sensitivity in Caenorhabditis elegans using neuronally enhanced feeding RNA interference. G3 (Bethesda) *5*, 467-475.

Chen, Y., Bharill, S., Altun, Z., O'Hagan, R., Coblitz, B., Isacoff, E.Y., and Chalfie, M. (2016a). Caenorhabditis elegans paraoxonase-like proteins control the functional expression of DEG/ENaC mechanosensory proteins. Mol Biol Cell *27*, 1272-1285.

Chen, Y., Bharill, S., Isacoff, E.Y., and Chalfie, M. (2015b). Subunit composition of a DEG/ENaC mechanosensory channel of Caenorhabditis elegans. Proc Natl Acad Sci U S A *112*, 11690-11695.

Chen, Y., Bharill, S., O'Hagan, R., Isacoff, E.Y., and Chalfie, M. (2016b). MEC-10 and MEC-19 Reduce the Neurotoxicity of the MEC-4(d) DEG/ENaC Channel in Caenorhabditis elegans. G3: Genes|Genomes|Genetics *6*, 1121.

Chen, Y.Z., Kloditz, K., Lee, E.S., Nguyen, D.P., Yuan, Q., Johnson, J., Lee-Yow, Y., Hall, A., Mitani, S., Xia, N.S., *et al.* (2019). Structure and function analysis of the C. elegans aminophospholipid translocase TAT-1. J Cell Sci *132*.

Chew, Y.L., Fan, X., Gotz, J., and Nicholas, H.R. (2013). PTL-1 regulates neuronal integrity and lifespan in C. elegans. J Cell Sci *126*, 2079-2091.

Cho, Y., Porto, D.A., Hwang, H., Grundy, L.J., Schafer, W.R., and Lu, H. (2017). Automated and controlled mechanical stimulation and functional imaging in vivo in C. elegans. Lab Chip *17*, 2609-2618.

Coblitz, B., Topalidou, I., and Chalfie, M. (2009). MEC-5 collagen expressed from muscle may link the extracellular matrix to the mechanotransduction channel complex responsible for gentle touch. Paper presented at: International Worm Meeting.

Cohen, Y., and Schuldiner, M. (2011). Advanced methods for high-throughput microscopy screening of genetically modified yeast libraries. Methods Mol Biol *781*, 127-159.

Consortium, T.U. (2018). UniProt: a worldwide hub of protein knowledge. Nucleic Acids Research *47*, D506-D515.

Cook, S.J., Jarrell, T.A., Brittin, C.A., Wang, Y., Bloniarz, A.E., Yakovlev, M.A., Nguyen, K.C.Q., Tang, L.T.H., Bayer, E.A., Duerr, J.S., *et al.* (2019). Whole-animal connectomes of both Caenorhabditis elegans sexes. Nature *571*, 63-71.

Cooper, G.M., Stone, E.A., Asimenos, G., Green, E.D., Batzoglou, S., and Sidow, A. (2005). Distribution and intensity of constraint in mammalian genomic sequence. Genome Res *15*, 901-913.

Corey, D.P., and Hudspeth, A.J. (1979). Response latency of vertebrate hair cells. Biophysical Journal *26*, 499-506.

Corsi, A.K., Wightman, B., and Chalfie, M. (2015). A Transparent Window into Biology: A Primer on Caenorhabditis elegans. Genetics *200*, 387-407.

Cueva, Juan G., Hsin, J., Huang, Kerwyn C., and Goodman, Miriam B. (2012). Posttranslational Acetylation of α-Tubulin Constrains Protofilament Number in Native Microtubules. Current Biology *22*, 1066-1074.

Cueva, J.G., Mulholland, A., and Goodman, M.B. (2007). Nanoscale Organization of the MEC-4 DEG/ENaC Sensory Mechanotransduction Channel in Caenorhabditis elegans Touch Receptor Neurons. The Journal of Neuroscience *27*, 14089-14098.

Dassah, M., Patzek, S., Hunt, V.M., Medina, P.E., and Zahler, A.M. (2009). A Genetic Screen for Suppressors of a Mutated 5′ Splice Site Identifies Factors Associated With Later Steps of Spliceosome Assembly. Genetics *182*, 725-734.

Davenport, A.M., Collins, L.N., Chiu, H., Minor, P.J., Sternberg, P.W., and Hoelz, A. (2014). Structural and Functional Characterization of the α-Tubulin Acetyltransferase MEC-17. Journal of Molecular Biology *426*, 2605-2616.

Davydov, E.V., Goode, D.L., Sirota, M., Cooper, G.M., Sidow, A., and Batzoglou, S. (2010). Identifying a high fraction of the human genome to be under selective constraint using GERP++. PLoS Comput Biol *6*, e1001025.

De Vore, D.M., Knobel, K.M., Nguyen, K.C.Q., Hall, D.H., and Barr, M.M. (2018). Extracellular matrix regulates morphogenesis and function of ciliated sensory organs in Caenorhabditis elegans. bioRxiv, 376152.

Desai, C., and Horvitz, H.R. (1989). Caenorhabditis elegans mutants defective in the functioning of the motor neurons responsible for egg laying. Genetics *121*, 703-721.

Dolphin, A.C. (2018). Voltage-gated calcium channels: their discovery, function and importance as drug targets. Brain Neurosci Adv *2*.

Doudna, J.A., and Charpentier, E. (2014). Genome editing. The new frontier of genome engineering with CRISPR-Cas9. Science *346*, 1258096.

Driscoll, M., and Chalfie, M. (1991). The mec-4 gene is a member of a family of Caenorhabditis elegans genes that can mutate to induce neuronal degeneration. Nature *349*, 588-593.

Du, H., and Chalfie, M. (2001). Genes Regulating Touch Cell Development in Caenorhabditis elegans. Genetics *158*, 197-207.

Du, H., Gu, G., William, C.M., and Chalfie, M. (1996). Extracellular Proteins Needed for C. elegans Mechanosensation. Neuron *16*, 183-194.

Duggan, A., Ma, C., and Chalfie, M. (1998). Regulation of touch receptor differentiation by the Caenorhabditis elegans mec-3 and unc-86 genes. Development *125*, 4107-4119.

Eastwood, A.L., and Goodman, M.B. (2012). Insight into DEG/ENaC Channel Gating from Genetics and Structure. Physiology *27*, 282-290.

Echeverri, C.J., Beachy, P.A., Baum, B., Boutros, M., Buchholz, F., Chanda, S.K., Downward, J., Ellenberg, J., Fraser, A.G., Hacohen, N., *et al.* (2006). Minimizing the risk of reporting false positives in large-scale RNAi screens. Nat Methods *3*, 777-779.

Edgar, R.C. (2004). MUSCLE: multiple sequence alignment with high accuracy and high throughput. Nucleic acids research *32*, 1792-1797.

Edwards, S.L., Charlie, N.K., Milfort, M.C., Brown, B.S., Gravlin, C.N., Knecht, J.E., and Miller, K.G. (2008). A novel molecular solution for ultraviolet light detection in Caenorhabditis elegans. PLoS Biol *6*, e198.

Edwards, S.L., Yu, S.C., Hoover, C.M., Phillips, B.C., Richmond, J.E., and Miller, K.G. (2013). An organelle gatekeeper function for Caenorhabditis elegans UNC-16 (JIP3) at the axon initial segment. Genetics *194*, 143-161.

Emtage, L., Gu, G., Hartwieg, E., and Chalfie, M. (2004). Extracellular Proteins Organize the Mechanosensory Channel Complex in C. elegans Touch Receptor Neurons. Neuron *44*, 795-807.

Erickson, H.P. (2007). Evolution of the cytoskeleton. Bioessays *29*, 668-677.

Eshun-Wilson, L., Zhang, R., Portran, D., Nachury, M.V., Toso, D.B., Löhr, T., Vendruscolo, M., Bonomi, M., Fraser, J.S., and Nogales, E. (2019). Effects of α-tubulin acetylation on

microtubule structure and stability. Proceedings of the National Academy of Sciences *116*, 10366-10371.

Finney, M., and Ruvkun, G. (1990). The unc-86 gene product couples cell lineage and cell identity in C. elegans. Cell *63*, 895-905.

Fire, A., Xu, S., Montgomery, M.K., Kostas, S.A., Driver, S.E., and Mello, C.C. (1998). Potent and specific genetic interference by double-stranded RNA in Caenorhabditis elegans. Nature *391*, 806-811.

Flibotte, S., Edgley, M.L., Chaudhry, I., Taylor, J., Neil, S.E., Rogula, A., Zapf, R., Hirst, M., Butterfield, Y., Jones, S.J., *et al.* (2010). Whole-genome profiling of mutagenesis in Caenorhabditis elegans. Genetics *185*, 431-441.

Forrester, W.C., Perens, E., Zallen, J.A., and Garriga, G. (1998). Identification of Caenorhabditis elegans genes required for neuronal differentiation and migration. Genetics *148*, 151-165.

Fraser, A.G., Kamath, R.S., Zipperlen, P., Martinez-Campos, M., Sohrmann, M., and Ahringer, J. (2000). Functional genomic analysis of C. elegans chromosome I by systematic RNA interference. Nature *408*, 325-330.

Fridolfsson, H.N., Roth, D.M., Insel, P.A., and Patel, H.H. (2014). Regulation of intracellular signaling and function by caveolin. Faseb j *28*, 3823-3831.

Frøkjær-Jensen, C., Kindt, K.S., Kerr, R.A., Suzuki, H., Melnik-Martinez, K., Gerstbreih, B., Driscol, M., and Schafer, W.R. (2006). Effects of voltage-gated calcium channel subunit genes on calcium influx in cultured C. elegans mechanosensory neurons. Journal of Neurobiology *66*, 1125-1139.

Fukushige, T., Siddiqui, Z.K., Chou, M., Culotti, J.G., Gogonea, C.B., Siddiqui, S.S., and Hamelin, M. (1999). MEC-12, an alpha-tubulin required for touch sensitivity in C. elegans. Journal of Cell Science *112*, 395-403.

Gamez-Del-Estal, M.M., Contreras, I., Prieto-Perez, R., and Ruiz-Rubio, M. (2014). Epigenetic effect of testosterone in the behavior of C. elegans. A clue to explain androgen-dependent autistic traits? Front Cell Neurosci *8*, 69.

Gao, S., Guan, S.A., Fouad, A.D., Meng, J., Kawano, T., Huang, Y.-C., Li, Y., Alcaire, S., Hung, W., Lu, Y., *et al.* (2018). Excitatory motor neurons are local oscillators for backward locomotion. eLife *7*, e29915.

Garcia-Anoveros, J., Ma, C., and Chalfie, M. (1995). Regulation of Caenorhabditis elegans degenerin proteins by a putative extracellular domain. Curr Biol *5*, 441-448.

Gessmann, R., Kourtis, N., Petratos, K., and Tavernarakis, N. (2010). Molecular Modeling of Mechanosensory Ion Channel Structural and Functional Features. PLOS ONE *5*, e12814.

Giles, A.C., Opperman, K.J., Rankin, C.H., and Grill, B. (2015). Developmental Function of the PHR Protein RPM-1 Is Required for Learning in Caenorhabditis elegans. G3 (Bethesda) *5*, 2745-2757.

Gittes, F., Mickey, B., Nettleton, J., and Howard, J. (1993). Flexural rigidity of microtubules and actin filaments measured from thermal fluctuations in shape. The Journal of Cell Biology *120*, 923-934.

Goedert, M., Baur, C.P., Ahringer, J., Jakes, R., Hasegawa, M., Spillantini, M.G., Smith, M.J., and Hill, F. (1996). PTL-1, a microtubule-associated protein with tau-like repeats from the nematode Caenorhabditis elegans. J Cell Sci *109 (Pt 11)*, 2661-2672.

Gönczy, P., Bellanger, J.-M., Kirkham, M., Pozniakowski, A., Baumer, K., Phillips, J.B., and Hyman, A.A. (2001). zyg-8, a Gene Required for Spindle Positioning in C. elegans, Encodes a Doublecortin-Related Kinase that Promotes Microtubule Assembly. Developmental Cell *1*, 363-375.

Gonczy, P., Echeverri, C., Oegema, K., Coulson, A., Jones, S.J., Copley, R.R., Duperon, J., Oegema, J., Brehm, M., Cassin, E., *et al.* (2000). Functional genomic analysis of cell division in C. elegans using RNAi of genes on chromosome III. Nature *408*, 331-336.

Goodman, M.B., Ernstrom, G.G., Chelur, D.S., O'Hagan, R., Yao, C.A., and Chalfie, M. (2002). MEC-2 regulates C. elegans DEG/ENaC channels needed for mechanosensation. Nature *415*, 1039-1042.

Goodson, H.V., and Jonasson, E.M. (2018). Microtubules and Microtubule-Associated Proteins. Cold Spring Harb Perspect Biol *10*.

Gordon, P., Hingula, L., Krasny, M.L., Swienckowski, J.L., Pokrywka, N.J., and Raley-Susman, K.M. (2008). The invertebrate microtubule-associated protein PTL-1 functions in mechanosensation and development in Caenorhabditis elegans. Development Genes and Evolution *218*, 541-551.

Gordon, Patricia M., and Hobert, O. (2015). A Competition Mechanism for a Homeotic Neuron Identity Transformation in C. elegans. Developmental Cell *34*, 206-219.

Grantham, R. (1974). Amino acid difference formula to help explain protein evolution. Science *185*, 862-864.

Grill, B., Murphey, R.K., and Borgen, M.A. (2016). The PHR proteins: intracellular signaling hubs in neuronal development and axon degeneration. Neural Dev *11*, 8.

Grun, D., Kirchner, M., Thierfelder, N., Stoeckius, M., Selbach, M., and Rajewsky, N. (2014). Conservation of mRNA and protein expression during development of C. elegans. Cell Rep *6*, 565-577.

Gründer, S., Fowler Jaeger, N., Gautschi, I., Schild, L., and Rossier, B.C. (1999). Identification of a highly conserved sequence at the N-terminus of the epithelial Na+ channel α subunit involved in gating. Pflügers Archiv *438*, 709-715.

Gu, G. (1998). A molecular model for mechanosensory transduction in Caenorhabditis elegans. In Biological Sciences (New York, New York: Columbia University).

Gu, G., Caldwell, G.A., and Chalfie, M. (1996). Genetic interactions affecting touch sensitivity in Caenorhabditis elegans. Proc Natl Acad Sci U S A *93*, 6577-6582.

Hamelin, M., Scott, I.M., Way, J.C., and Culotti, J.G. (1992). The mec-7 beta-tubulin gene of Caenorhabditis elegans is expressed primarily in the touch receptor neurons. Embo j *11*, 2885-2893.

Hanukoglu, I., and Hanukoglu, A. (2016). Epithelial sodium channel (ENaC) family: Phylogeny, structure-function, tissue distribution, and associated inherited diseases. Gene *579*, 95-132.

Harris, T., Arnaboldi, V., Cain, S., Chan, J., Chen, W., Cho, J., Davis, P., Gao, S., Grove, C., Kishore, R., *et al.* (2019). WormBase: a modern Model Organism Information Resource. Nucleic acids research *48*.

Hedgecock, E.M., Culotti, J.G., Hall, D.H., and Stern, B.D. (1987). Genetics of cell and axon migrations in Caenorhabditis elegans. Development *100*, 365-382.

Hegedűs, L., Zámbó, B., Pászty, K., Padányi, R., Varga, K., Penniston, J.T., and Enyedi, Á. (2020). Molecular Diversity of Plasma Membrane Ca2+ Transporting ATPases: Their Function Under Normal and Pathological Conditions. In Calcium Signaling, M.S. Islam, ed. (Cham: Springer International Publishing), pp. 93-129.

Hobert, O., Moerman, D.G., Clark, K.A., Beckerle, M.C., and Ruvkun, G. (1999). A conserved LIM protein that affects muscular adherens junction integrity and mechanosensory function in Caenorhabditis elegans. J Cell Biol *144*, 45-57.

Hong, K., and Driscoll, M. (1994). A transmembrane domain of the putative channel subunit MEC-4 influences mechanotransduction and neurodegeneration in C. elegans. Nature *367*, 470-473.

Hong, K., Mano, I., and Driscoll, M. (2000). In vivo structure-function analyses of Caenorhabditis elegans MEC-4, a candidate mechanosensory ion channel subunit. J Neurosci *20*, 2575-2588.

Horke, S., Witte, I., Wilgenbus, P., Kruger, M., Strand, D., and Forstermann, U. (2007). Paraoxonase-2 reduces oxidative stress in vascular cells and decreases endoplasmic reticulum stress-induced caspase activation. Circulation *115*, 2055-2064.

Horvitz, H.R., and Sulston, J.E. (1980). Isolation and genetic characterization of cell-lineage mutants of the nematode Caenorhabditis elegans. Genetics *96*, 435-454.

Howes, S.C., Alushin, G.M., Shida, T., Nachury, M.V., and Nogales, E. (2013). Effects of tubulin acetylation and tubulin acetyltransferase binding on microtubule structure. Molecular Biology of the Cell *25*, 257-266.

Hsu, J.-M., Chen, C.-H., Chen, Y.-C., McDonald, K.L., Gurling, M., Lee, A., Garriga, G., and Pan, C.-L. (2014). Genetic Analysis of a Novel Tubulin Mutation That Redirects Synaptic Vesicle Targeting and Causes Neurite Degeneration in C. elegans. PLOS Genetics *10*, e1004715.

Huang, M., and Chalfie, M. (1994). Gene interactions affecting mechanosensory transduction in Caenorhabditis elegans. Nature *367*, 467-470.

Huang, M., Gu, G., Ferguson, E.L., and Chalfie, M. (1995). A stomatin-like protein necessary for mechanosensation in C. elegans. Nature *378*, 292-295.

Huang, Y.-C., Pirri, J.K., Rayes, D., Gao, S., Mulcahy, B., Grant, J., Saheki, Y., Francis, M.M., Zhen, M., and Alkema, M.J. (2019). Gain-of-function mutations in the UNC-2/CaV2α channel lead to excitation-dominant synaptic transmission in Caenorhabditis elegans. eLife *8*, e45905.

Huber, T.B., Schermer, B., Müller, R.U., Höhne, M., Bartram, M., Calixto, A., Hagmann, H., Reinhardt, C., Koos, F., Kunzelmann, K., *et al.* (2006). Podocin and MEC-2 bind cholesterol to regulate the activity of associated ion channels. Proceedings of the National Academy of Sciences *103*, 17079.

Hueston, J.L., Herren, G.P., Cueva, J.G., Buechner, M., Lundquist, E.A., Goodman, M.B., and Suprenant, K.A. (2008). The C. elegans EMAP-like protein, ELP-1 is required for touch sensation and associates with microtubules and adhesion complexes. BMC Developmental Biology *8*, 110.

Hunt-Newbury, R., Viveiros, R., Johnsen, R., Mah, A., Anastas, D., Fang, L., Halfnight, E., Lee, D., Lin, J., Lorch, A., *et al.* (2007). High-throughput in vivo analysis of gene expression in Caenorhabditis elegans. PLoS Biol *5*, e237.

Hurd, D.D. (2018). Tubulins in C. elegans. WormBook *2018*, 1-32.

Jarrell, T.A., Wang, Y., Bloniarz, A.E., Brittin, C.A., Xu, M., Thomson, J.N., Albertson, D.G., Hall, D.H., and Emmons, S.W. (2012). The Connectome of a Decision-Making Neural Network. Science *337*, 437-444.

Jasti, J., Furukawa, H., Gonzales, E.B., and Gouaux, E. (2007). Structure of acid-sensing ion channel 1 at 1.9 Å resolution and low pH. Nature *449*, 316-323.

Jia, Y., Xie, G., and Aamodt, E. (1996). pag-3, a Caenorhabditis elegans gene involved in touch neuron gene expression and coordinated movement. Genetics *142*, 141-147.

Jinek, M., Chylinski, K., Fonfara, I., Hauer, M., Doudna, J.A., and Charpentier, E. (2012). A programmable dual-RNA-guided DNA endonuclease in adaptive bacterial immunity. Science *337*, 816-821.

Jones, R.N. (2005). McClintock's controlling elements: the full story. Cytogenet Genome Res *109*, 90-103.

Jorgensen, E.M., and Mango, S.E. (2002). The art and design of genetic screens: caenorhabditis elegans. Nat Rev Genet *3*, 356-369.

Joseph, B.B., Blouin, N.A., and Fay, D.S. (2018). Use of a Sibling Subtraction Method for Identifying Causal Mutations in Caenorhabditis elegans by Whole-Genome Sequencing. G3: Genes|Genomes|Genetics *8*, 669-678.

Jurgens, G., Wieschaus, E., Nusslein-Volhard, C., and Kluding, H. (1984). Mutations affecting the pattern of the larval cuticle inDrosophila melanogaster : II. Zygotic loci on the third chromosome. Wilehm Roux Arch Dev Biol *193*, 283-295.

Kalebic, N., Martinez, C., Perlas, E., Hublitz, P., Bilbao-Cortes, D., Fiedorczuk, K., Andolfo, A., and Heppenstall, P.A. (2013). Tubulin Acetyltransferase αTAT1 Destabilizes Microtubules Independently of Its Acetylation Activity. Molecular and Cellular Biology *33*, 1114-1123.

Kaletsky, R., Lakhina, V., Arey, R., Williams, A., Landis, J., Ashraf, J., and Murphy, C.T. (2016). The C. elegans adult neuronal IIS/FOXO transcriptome reveals adult phenotype regulators. Nature *529*, 92-96.

Kamat, S., Yeola, S., Zhang, W., Bianchi, L., and Driscoll, M. (2014). NRA-2, a Nicalin Homolog, Regulates Neuronal Death by Controlling Surface Localization of Toxic Caenorhabditis elegans DEG/ENaC Channels. Journal of Biological Chemistry *289*, 11916-11926.

Kass, J., Jacob, T.C., Kim, P., and Kaplan, J.M. (2001). The EGL-3 proprotein convertase regulates mechanosensory responses of Caenorhabditis elegans. J Neurosci *21*, 9265-9272.

Kelley, M., Yochem, J., Krieg, M., Calixto, A., Heiman, M.G., Kuzmanov, A., Meli, V., Chalfie, M., Goodman, M.B., Shaham, S., *et al.* (2015). FBN-1, a fibrillin-related protein, is required for resistance of the epidermis to mechanical deformation during C. elegans embryogenesis. Elife *4*.

Kim, W., Underwood, R.S., Greenwald, I., and Shaye, D.D. (2018). OrthoList 2: A New Comparative Genomic Analysis of Human and Caenorhabditis elegans Genes. Genetics *210*, 445-461.

Kindt, K.S., Quast, K.B., Giles, A.C., De, S., Hendrey, D., Nicastro, I., Rankin, Catharine H., and Schafer, W.R. (2007). Dopamine Mediates Context-Dependent Modulation of Sensory Plasticity in C. elegans. Neuron *55*, 662-676.

Kindt, K.S., Tam, T., Whiteman, S., and Schafer, W.R. (2002). Serotonin Promotes Go-Dependent Neuronal Migration in Caenorhabditis elegans. Current Biology *12*, 1738-1747.

Kipreos, E.T., and Pagano, M. (2000). The F-box protein family. Genome Biol *1*, Reviews3002.

Kirszenblat, L., Neumann, B., Coakley, S., and Hilliard, M.A. (2012). A dominant mutation in mec-7/β-tubulin affects axon development and regeneration in Caenorhabditis elegans neurons. Molecular Biology of the Cell *24*, 285-296.

Kleckner, N., Roth, J., and Botstein, D. (1977). Genetic engineering in Vivo using translocatable drug-resistance elements: New methods in bacterial genetics. Journal of Molecular Biology *116*, 125-159.

Koornneef, M., and Meinke, D. (2010). The development of Arabidopsis as a model plant. The Plant Journal *61*, 909-921.

Krieg, M., Dunn, A.R., and Goodman, M.B. (2014). Mechanical control of the sense of touch by β-spectrin. Nature Cell Biology *16*, 224-233.

Krieg, M., Dunn, A.R., and Goodman, M.B. (2015). Mechanical systems biology of C. elegans touch sensation. Bioessays *37*, 335-344.

Krieg, M., Stühmer, J., Cueva, J.G., Fetter, R., Spilker, K., Cremers, D., Shen, K., Dunn, A.R., and Goodman, M.B. (2017). Genetic defects in β-spectrin and tau sensitize C. elegans axons to movement-induced damage via torque-tension coupling. eLife *6*, e20172.

Kutscher, L.M., and Shaham, S. (2014). Forward and reverse mutagenesis in C. elegans. WormBook : the online review of C elegans biology, 1-26.

Kwon, S., Song, W.K., Park, C.S., and Ahnn, J. (2001). Characterization of a novel gene expressed in neuromuscular tissues and centrosomes in Caenorhabditis elegans. Cell Biochem Funct *19*, 79-88.

Lai, C.C., Hong, K., Kinnell, M., Chalfie, M., and Driscoll, M. (1996). Sequence and transmembrane topology of MEC-4, an ion channel subunit required for mechanotransduction in Caenorhabditis elegans. J Cell Biol *133*, 1071-1081.

Lainé, V., Frøkjær-Jensen, C., Couchoux, H., and Jospin, M. (2011). The α1 Subunit EGL-19, the α2/δ Subunit UNC-36, and the β Subunit CCB-1 Underlie Voltage-dependent Calcium Currents in Caenorhabditis elegans Striated Muscle. Journal of Biological Chemistry *286*, 36180-36187.

LeBoeuf, B., Gruninger, T.R., and Garcia, L.R. (2007). Food deprivation attenuates seizures through CaMKII and EAG K+ channels. PLoS Genet *3*, 1622-1632.

Lee, D., Singaravelu, G., Park, B.-J., and Ahnn, J. (2007). Differential Requirement of Unfolded Protein Response Pathway for Calreticulin Expression in Caenorhabditis elegans. Journal of Molecular Biology *372*, 331-340.

Lee, R.Y., Lobel, L., Hengartner, M., Horvitz, H.R., and Avery, L. (1997). Mutations in the alpha1 subunit of an L-type voltage-activated Ca2+ channel cause myotonia in Caenorhabditis elegans. Embo j *16*, 6066-6076.

Letunic, I., and Bork, P. (2017). 20 years of the SMART protein domain annotation resource. Nucleic Acids Research *46*, D493-D496.

Lewis, J.A., and Hodgkin, J.A. (1977). Specific neuroanatomical changes in chemosensory mutants of the nematode Caenorhabditis elegans. Journal of Comparative Neurology *172*, 489-510.

Lewis, J.A., Wu, C.H., Berg, H., and Levine, J.H. (1980). The genetics of levamisole resistance in the nematode Caenorhabditis elegans. Genetics *95*, 905-928.

Li, W., Kang, L., Piggott, B.J., Feng, Z., and Xu, X.Z.S. (2011). The neural circuits and sensory channels mediating harsh touch sensation in Caenorhabditis elegans. Nature Communications *2*, 315.

Li, Y., Um, S.Y., and McDonald, T.V. (2006). Voltage-gated potassium channels: regulation by accessory subunits. Neuroscientist *12*, 199-210.

Liu, J., Huang, S., Sun, M., Liu, S., Liu, Y., Wang, W., Zhang, X., Wang, H., and Hua, W. (2012). An improved allele-specific PCR primer design method for SNP marker analysis and its application. Plant Methods *8*, 34.

Liu, P., Ge, Q., Chen, B., Salkoff, L., Kotlikoff, M.I., and Wang, Z.W. (2011). Genetic dissection of ion currents underlying all-or-none action potentials in C. elegans body-wall muscle cells. J Physiol *589*, 101-117.

Lundquist, E.A., and Herman, R.K. (1994). The mec-8 gene of Caenorhabditis elegans affects muscle and sensory neuron function and interacts with three other genes: unc-52, smu-1 and smu-2. Genetics *138*, 83.

Lundquist, E.A., Herman, R.K., Rogalski, T.M., Mullen, G.P., Moerman, D.G., and Shaw, J.E. (1996). The mec-8 gene of C. elegans encodes a protein with two RNA recognition motifs and regulates alternative splicing of unc-52 transcripts. Development *122*, 1601-1610.

Mackay, T.F.C. (2014). Epistasis and quantitative traits: using model organisms to study gene–gene interactions. Nature Reviews Genetics *15*, 22-33.

Mackereth, C.D. (2015). Splicing factor SUP-12 and the molecular complexity of apparent cooperativity. Worm *3*, e991240-e991240.

Mathew, M.D., Mathew, N.D., Miller, A., Simpson, M., Au, V., Garland, S., Gestin, M., Edgley, M.L., Flibotte, S., Balgi, A., *et al.* (2016). Using C. elegans Forward and Reverse Genetics to Identify New Compounds with Anthelmintic Activity. PLOS Neglected Tropical Diseases *10*, e0005058.

Mathews, E.A., Garcia, E., Santi, C.M., Mullen, G.P., Thacker, C., Moerman, D.G., and Snutch, T.P. (2003). Critical residues of the Caenorhabditis elegans unc-2 voltage-gated calcium channel that affect behavioral and physiological properties. J Neurosci *23*, 6537-6545.

Matthewman, C., Johnson, C.K., Miller, D.M., and Bianchi, L. (2018). Functional features of the "finger" domain of the DEG/ENaC channels MEC-4 and UNC-8. American Journal of Physiology-Cell Physiology *315*, C155-C163.

Matthewman, C., Miller-Fleming, T.W., Miller, D.M., and Bianchi, L. (2016). Ca2+ permeability and Na+ conductance in cellular toxicity caused by hyperactive DEG/ENaC channels. American Journal of Physiology-Cell Physiology *311*, C920-C930.

McClanahan, P.D., Xu, J.H., and Fang-Yen, C. (2017). Comparing Caenorhabditis elegans gentle and harsh touch response behavior using a multiplexed hydraulic microfluidic device. Integr Biol (Camb) *9*, 800-809.

McClintock, B. (1950). The origin and behavior of mutable loci in maize. Proc Natl Acad Sci U S A *36*, 344-355.

McCormack, T., and McCormack, K. (1994). Shaker K+ channel beta subunits belong to an NAD(P)H-dependent oxidoreductase superfamily. Cell *79*, 1133-1135.

McKay, S.J., Johnsen, R., Khattra, J., Asano, J., Baillie, D.L., Chan, S., Dube, N., Fang, L., Goszczynski, B., Ha, E., *et al.* (2003). Gene expression profiling of cells, tissues, and developmental stages of the nematode C. elegans. Cold Spring Harb Symp Quant Biol *68*, 159-169.

Meyerowitz, E.M. (2001). Prehistory and history of Arabidopsis research. Plant Physiol *125*, 15-19.

Michalak, M., Groenendyk, J., Szabo, E., Gold, L.I., and Opas, M. (2009). Calreticulin, a multi-process calcium-buffering chaperone of the endoplasmic reticulum. Biochem J *417*, 651-666.

Mitani, S., Du, H., Hall, D.H., Driscoll, M., and Chalfie, M. (1993). Combinatorial control of touch receptor neuron expression in Caenorhabditis elegans. Development *119*, 773-783.

Moerman, D.G., and Baillie, D.L. (1979). Genetic Organization in CAENORHABDITIS ELEGANS: Fine-Structure Analysis of the unc-22 Gene. Genetics *91*, 95-103.

Moerman, D.G., and Baillie, D.L. (1981). Formaldehyde mutagenesis in the nematode Caenorhabditis elegans. Mutat Res *80*, 273-279.

Mohr, S.E., Smith, J.A., Shamu, C.E., Neumuller, R.A., and Perrimon, N. (2014). RNAi screening comes of age: improved techniques and complementary approaches. Nat Rev Mol Cell Biol *15*, 591-600.

Mok, C.A., Au, V., Thompson, O.A., Edgley, M.L., Gevirtzman, L., Yochem, J., Lowry, J., Memar, N., Wallenfang, M.R., Rasoloson, D., *et al.* (2017). MIP-MAP: High-Throughput Mapping of Caenorhabditis elegans Temperature-Sensitive Mutants via Molecular Inversion Probes. Genetics *207*, 447-463.

Moresco, E.M., Li, X., and Beutler, B. (2013). Going forward with genetics: recent technological advances and forward genetics in mice. Am J Pathol *182*, 1462-1473.

Morley, S.J., Qi, Y., Iovino, L., Andolfi, L., Guo, D., Kalebic, N., Castaldi, L., Tischer, C., Portulano, C., Bolasco, G., *et al.* (2016). Acetylated tubulin is essential for touch sensation in mice. eLife *5*, e20813.

Morris, M., Maeda, S., Vossel, K., and Mucke, L. (2011). The Many Faces of Tau. Neuron *70*, 410-426.

Muller, H.J. (1927). Artificial Transmutation of the Gene. Science *66*, 84-87.

Nagamine, T., Shimomura, S., Sueyoshi, N., and Kameshita, I. (2011). Influence of Ser/Pro-rich domain and kinase domain of double cortin-like protein kinase on microtubule-binding activity. J Biochem *149*, 619-627.

Nakano, S., Ikeda, M., Tsukada, Y., Fei, X., Suzuki, T., Niino, Y., Ahluwalia, R., Sano, A., Kondo, R., Ihara, K., *et al.* (2020). Presynaptic MAST kinase controls opposing postsynaptic responses to convey stimulus valence in Caenorhabditis elegans. Proceedings of the National Academy of Sciences *117*, 1638-1647.

Neumann, B., and Hilliard, Massimo A. (2014). Loss of MEC-17 Leads to Microtubule Instability and Axonal Degeneration. Cell Reports *6*, 93-103.

Noma, K., Goncharov, A., Ellisman, M.H., and Jin, Y. (2017). Microtubule-dependent ribosome localization in C. elegans neurons. eLife *6*, e26376.

Noreng, S., Bharadwaj, A., Posert, R., Yoshioka, C., and Baconguis, I. (2018). Structure of the human epithelial sodium channel by cryo-electron microscopy. Elife *7*.

Notredame, C., Higgins, D.G., and Heringa, J. (2000). T-Coffee: A novel method for fast and accurate multiple sequence alignment. J Mol Biol *302*, 205-217.

Nusslein-Volhard, C., and Wieschaus, E. (1980). Mutations affecting segment number and polarity in Drosophila. Nature *287*, 795-801.

Nusslein-Volhard, C., Wieschaus, E., and Kluding, H. (1984). Mutations affecting the pattern of the larval cuticle inDrosophila melanogaster : I. Zygotic loci on the second chromosome. Wilehm Roux Arch Dev Biol *193*, 267-282.

O'Hagan, R., Chalfie, M., and Goodman, M.B. (2005). The MEC-4 DEG/ENaC channel of Caenorhabditis elegans touch receptor neurons transduces mechanical signals. Nature Neuroscience *8*, 43-50.

Oh, E., Akopian, D., and Rape, M. (2018). Principles of Ubiquitin-Dependent Signaling. Annu Rev Cell Dev Biol *34*, 137-162.

Okonechnikov, K., Golosova, O., Fursov, M., and the, U.t. (2012). Unipro UGENE: a unified bioinformatics toolkit. Bioinformatics *28*, 1166-1167.

Page, D.R., and Grossniklaus, U. (2002). The art and design of genetic screens: Arabidopsis thaliana. Nat Rev Genet *3*, 124-136.

Pan, C.-L., Peng, C.-Y., Chen, C.-H., and McIntire, S. (2011). Genetic analysis of age-dependent defects of the Caenorhabditis elegans touch receptor neurons. Proceedings of the National Academy of Sciences *108*, 9274-9279.

Pan, J.A., Fan, Y., Gandhirajan, R.K., Madesh, M., and Zong, W.X. (2013). Hyperactivation of the mammalian degenerin MDEG promotes caspase-8 activation and apoptosis. J Biol Chem *288*, 2952-2963.

Park, B.J., Lee, D.G., Yu, J.R., Jung, S.K., Choi, K., Lee, J., Lee, J., Kim, Y.S., Lee, J.I., Kwon, J.Y., *et al.* (2001). Calreticulin, a calcium-binding molecular chaperone, is required for stress response and fertility in Caenorhabditis elegans. Mol Biol Cell *12*, 2835-2845.

Park, E.C., Glodowski, D.R., and Rongo, C. (2009). The ubiquitin ligase RPM-1 and the p38 MAPK PMK-3 regulate AMPA receptor trafficking. PLoS One *4*, e4284.

Park, S.J., Goodman, M.B., and Pruitt, B.L. (2007). Analysis of nematode mechanics by piezoresistive displacement clamp. Proc Natl Acad Sci U S A *104*, 17376-17381.

Perkins, L.A., Hedgecock, E.M., Thomson, J.N., and Culotti, J.G. (1986). Mutant sensory cilia in the nematode Caenorhabditis elegans. Developmental Biology *117*, 456-487.

Portran, D., Schaedel, L., Xu, Z., Théry, M., and Nachury, Maxence V. (2017). Tubulin acetylation protects long-lived microtubules against mechanical ageing. Nature Cell Biology *19*, 391-398.

Pozdnyakov, I., Matantseva, O., and Skarlato, S. (2018). Diversity and evolution of four-domain voltage-gated cation channels of eukaryotes and their ancestral functional determinants. Scientific Reports *8*, 3539.

Précourt, L.-P., Amre, D., Denis, M.-C., Lavoie, J.-C., Delvin, E., Seidman, E., and Levy, E. (2011). The three-gene paraoxonase family: Physiologic roles, actions and regulation. Atherosclerosis *214*, 20-36.

Preibisch, S., Saalfeld, S., and Tomancak, P. (2009). Globally optimal stitching of tiled 3D microscopic image acquisitions. Bioinformatics (Oxford, England) *25*, 1463-1465.

Probst, F.J., and Justice, M.J. (2010). Mouse mutagenesis with the chemical supermutagen ENU. Methods Enzymol *477*, 297-312.

Ranasinghe, S., and McManus, D.P. (2013). Structure and function of invertebrate Kunitz serine protease inhibitors. Dev Comp Immunol *39*, 219-227.

Rankin, C.H., and Wicks, S.R. (2000). Mutations of the caenorhabditis elegans brain-specific inorganic phosphate transporter eat-4 affect habituation of the tap-withdrawal response without affecting the response itself. J Neurosci *20*, 4337-4344.

Rapoport, I. (1946). Carbonyl compounds and the chemical mechanism of mutations. Compt Rend Acad Sci *54*, 65-67.

Roca-Lapirot, O., Radwani, H., Aby, F., Nagy, F., Landry, M., and Fossat, P. (2018). Calcium signalling through L-type calcium channels: role in pathophysiology of spinal nociceptive transmission. British Journal of Pharmacology *175*, 2362-2374.

Röckelein, I., Röhrig, S., Donhauser, R., Eimer, S., and Baumeister, R. (2000). Identification of amino acid residues in the Caenorhabditis elegans POU protein UNC-86 that mediate UNC-86-MEC-3-DNA ternary complex formation. Molecular and cellular biology *20*, 4806-4813.

Röhrig, S., Röckelein, I., Donhauser, R., and Baumeister, R. (2000). Protein interaction surface of the POU transcription factor UNC-86 selectively used in touch neurons. The EMBO journal *19*, 3694-3703.

Royal, D.C., Bianchi, L., Royal, M.A., Lizzio, M., Mukherjee, G., Nunez, Y.O., and Driscoll, M. (2005). Temperature-sensitive Mutant of the Caenorhabditis elegans Neurotoxic MEC-4(d) DEG/ENaC Channel Identifies a Site Required for Trafficking or Surface Maintenance. Journal of Biological Chemistry *280*, 41976-41986.

Rual, J.F., Ceron, J., Koreth, J., Hao, T., Nicot, A.S., Hirozane-Kishikawa, T., Vandenhaute, J., Orkin, S.H., Hill, D.E., van den Heuvel, S., *et al.* (2004). Toward improving Caenorhabditis elegans phenome mapping with an ORFeome-based RNAi library. Genome Res *14*, 2162-2168.

Rushforth, A.M., and Anderson, P. (1996). Splicing removes the Caenorhabditis elegans transposon Tc1 from most mutant pre-mRNAs. Mol Cell Biol *16*, 422-429.

Sagnol, S., Yang, Y., Bessin, Y., Allemand, F., Hapkova, I., Notarnicola, C., Guichou, J.-F., Faure, S., Labesse, G., and Santa Barbara, P.d. (2014). Homodimerization of RBPMS2 through a new RRM-interaction motif is necessary to control smooth muscle plasticity. Nucleic Acids Research *42*, 10173-10184.

Sanyal, S., Wintle, R.F., Kindt, K.S., Nuttley, W.M., Arvan, R., Fitzmaurice, P., Bigras, E., Merz, D.C., Hebert, T.E., van der Kooy, D., *et al.* (2004). Dopamine modulates the plasticity of mechanosensory responses in Caenorhabditis elegans. Embo j *23*, 473-482.

Sarasija, S., Laboy, J.T., Ashkavand, Z., Bonner, J., Tang, Y., and Norman, K.R. (2018). Presenilin mutations deregulate mitochondrial Ca2+ homeostasis and metabolic activity causing neurodegeneration in Caenorhabditis elegans. eLife *7*, e33052.

Sato, M., Saegusa, K., Sato, K., Hara, T., Harada, A., and Sato, K. (2011). Caenorhabditis elegans SNAP-29 is required for organellar integrity of the endomembrane system and general exocytosis in intestinal epithelial cells. Molecular biology of the cell *22*, 2579-2587.

Savage, C., Hamelin, M., Culotti, J.G., Coulson, A., Albertson, D.G., and Chalfie, M. (1989). mec-7 is a beta-tubulin gene required for the production of 15-protofilament microtubules in Caenorhabditis elegans. Genes Dev *3*, 870-881.

Savage, C., Xue, Y., Mitani, S., Hall, D., Zakhary, R., and Chalfie, M. (1994). Mutations in the Caenorhabditis elegans beta-tubulin gene mec-7: effects on microtubule assembly and stability and on tubulin autoregulation. Journal of Cell Science *107*, 2165-2175.

Sayers, E.W., Agarwala, R., Bolton, E.E., Brister, J R., Canese, K., Clark, K., Connor, R., Fiorini, N., Funk, K., Hefferon, T., *et al.* (2018). Database resources of the National Center for Biotechnology Information. Nucleic Acids Research *47*, D23-D28.

Schafer, W.R., and Kenyon, C.J. (1995). A calcium-channel homologue required for adaptation to dopamine and serotonin in Caenorhabditis elegans. Nature *375*, 73-78.

Schafer, W.R., Sanchez, B.M., and Kenyon, C.J. (1996). Genes Affecting Sensitivity to Serotonin in Caenorhabditis elegans. Genetics *143*, 1219-1230.

Schmitz, C., Kinge, P., and Hutter, H. (2007). Axon guidance genes identified in a large-scale RNAi screen using the RNAi-hypersensitive Caenorhabditis elegans strain nre-1(hd20) lin-15b(hd126). Proc Natl Acad Sci U S A *104*, 834-839.

Schumacher, J.A., Hsieh, Y.W., Chen, S., Pirri, J.K., Alkema, M.J., Li, W.H., Chang, C., and Chuang, C.F. (2012). Intercellular calcium signaling in a gap junction-coupled cell network establishes asymmetric neuronal fates in C. elegans. Development *139*, 4191-4201.

Schwarz, K., Simons, M., Reiser, J., Saleem, M.A., Faul, C., Kriz, W., Shaw, A.S., Holzman, L.B., and Mundel, P. (2001). Podocin, a raft-associated component of the glomerular slit diaphragm, interacts with CD2AP and nephrin. J Clin Invest *108*, 1621-1629.

Sedensky, M.M., Siefker, J.M., Koh, J.Y., Miller, D.M., 3rd, and Morgan, P.G. (2004). A stomatin and a degenerin interact in lipid rafts of the nervous system of Caenorhabditis elegans. Am J Physiol Cell Physiol *287*, C468-474.

Shaye, D.D., and Greenwald, I. (2011). OrthoList: a compendium of C. elegans genes with human orthologs. PLoS One *6*, e20085.

Shi, S., Buck, T.M., Kinlough, C.L., Marciszyn, A.L., Hughey, R.P., Chalfie, M., Brodsky, J.L., and Kleyman, T.R. (2017). Regulation of the epithelial Na+ channel by paraoxonase-2. Journal of Biological Chemistry *292*, 15927-15938.

Shi, S., Luke, C.J., Miedel, M.T., Silverman, G.A., and Kleyman, T.R. (2016). Activation of the Caenorhabditis elegans Degenerin Channel by Shear Stress Requires the MEC-10 Subunit. Journal of Biological Chemistry *291*, 14012-14022.

Shi, S., Mutchler, S.M., Blobner, B.M., Kashlan, O.B., and Kleyman, T.R. (2018). Pore-lining residues of MEC-4 and MEC-10 channel subunits tune the Caenorhabditis elegans degenerin channel's response to shear stress. Journal of Biological Chemistry *293*, 10757-10766.

Shida, T., Cueva, J.G., Xu, Z., Goodman, M.B., and Nachury, M.V. (2010). The major α-tubulin K40 acetyltransferase αTAT1 promotes rapid ciliogenesis and efficient mechanosensation. Proceedings of the National Academy of Sciences *107*, 21517-21522.

Shreffler, W., Magardino, T., Shekdar, K., and Wolinsky, E. (1995). The unc-8 and sup-40 genes regulate ion channel function in Caenorhabditis elegans motorneurons. Genetics *139*, 1261-1272.

Siepel, A., Bejerano, G., Pedersen, J.S., Hinrichs, A.S., Hou, M., Rosenbloom, K., Clawson, H., Spieth, J., Hillier, L.W., Richards, S., *et al.* (2005). Evolutionarily conserved elements in vertebrate, insect, worm, and yeast genomes. Genome Res *15*, 1034-1050.

Smith, Cody J., O'Brien, T., Chatzigeorgiou, M., Spencer, W.C., Feingold-Link, E., Husson, Steven J., Hori, S., Mitani, S., Gottschalk, A., Schafer, William R., *et al.* (2013). Sensory Neuron Fates Are Distinguished by a Transcriptional Switch that Regulates Dendrite Branch Stabilization. Neuron *79*, 266-280.

Smith, C.J., Watson, J.D., Spencer, W.C., O'Brien, T., Cha, B., Albeg, A., Treinin, M., and Miller, D.M., 3rd (2010). Time-lapse imaging and cell-specific expression profiling reveal dynamic branching and molecular determinants of a multi-dendritic nociceptor in C. elegans. Dev Biol *345*, 18-33.

Snyers, L., Umlauf, E., and Prohaska, R. (1999). Association of stomatin with lipid-protein complexes in the plasma membrane and the endocytic compartment. Eur J Cell Biol *78*, 802-812.

Solinger, J.A., Paolinelli, R., Klöß, H., Scorza, F.B., Marchesi, S., Sauder, U., Mitsushima, D., Capuani, F., Stürzenbaum, S.R., and Cassata, G. (2010). The Caenorhabditis elegans Elongator Complex Regulates Neuronal α-tubulin Acetylation. PLOS Genetics *6*, e1000820.

Soufari, H., and Mackereth, C.D. (2017). Conserved binding of GCAC motifs by MEC-8, couch potato, and the RBPMS protein family. RNA *23*, 308-316.

Spencer, W.C., Zeller, G., Watson, J.D., Henz, S.R., Watkins, K.L., McWhirter, R.D., Petersen, S., Sreedharan, V.T., Widmer, C., Jo, J., *et al.* (2011). A spatial and temporal map of C. elegans gene expression. Genome research *21*, 325-341.

Spike, C.A., Davies, A.G., Shaw, J.E., and Herman, R.K. (2002). MEC-8 regulates alternative splicing of unc-52 transcripts in C. elegans hypodermal cells. Development *129*, 4999.

St Johnston, D. (2002). The art and design of genetic screens: Drosophila melanogaster. Nature Reviews Genetics *3*, 176-188.

Sulston, J.E. (1983). Neuronal cell lineages in the nematode Caenorhabditis elegans. Cold Spring Harb Symp Quant Biol *48 Pt 2*, 443-452.

Sulston, J.E., and Horvitz, H.R. (1981). Abnormal cell lineages in mutants of the nematode Caenorhabditis elegans. Dev Biol *82*, 41-55.

Suzuki, C.K., Bonifacino, J.S., Lin, A.Y., Davis, M.M., and Klausner, R.D. (1991). Regulating the retention of T-cell receptor alpha chain variants within the endoplasmic reticulum: Ca(2+)-dependent association with BiP. J Cell Biol *114*, 189-205.

Suzuki, H., Kerr, R., Bianchi, L., Frøkjær-Jensen, C., Slone, D., Xue, J., Gerstbrein, B., Driscoll, M., and Schafer, W.R. (2003). In Vivo Imaging of C. elegans Mechanosensory Neurons Demonstrates a Specific Role for the MEC-4 Channel in the Process of Gentle Touch Sensation. Neuron *39*, 1005-1017.

Sze, J.Y., Liu, Y., and Ruvkun, G. (1997). VP16-activation of the C. elegans neural specification transcription factor UNC-86 suppresses mutations in downstream genes and causes defects in neural migration and axon outgrowth. Development *124*, 1159-1168.

Tam, T., Mathews, E., Snutch, T.P., and Schafer, W.R. (2000). Voltage-Gated Calcium Channels Direct Neuronal Migration in Caenorhabditis elegans. Developmental Biology *226*, 104-117.

Tao, L., Porto, D., Li, Z., Fechner, S., Lee, S.A., Goodman, M.B., Xu, X.Z.S., Lu, H., and Shen, K. (2019). Parallel Processing of Two Mechanosensory Modalities by a Single Neuron in C. elegans. Developmental Cell *51*, 617-631.e613.

Tavernarakis, N., and Driscoll, M. (2000). Caenorhabditis elegans degenerins and vertebrate ENaC ion channels contain an extracellular domain related to venom neurotoxins. J Neurogenet *13*, 257-264.

Teplova, M., Farazi, T.A., Tuschl, T., and Patel, D.J. (2016). Structural basis underlying CAC RNA recognition by the RRM domain of dimeric RNA-binding protein RBPMS. Quarterly Reviews of Biophysics *49*, e1.

Thompson, O., Edgley, M., Strasbourger, P., Flibotte, S., Ewing, B., Adair, R., Au, V., Chaudhry, I., Fernando, L., Hutter, H., *et al.* (2013). The million mutation project: a new approach to genetics in Caenorhabditis elegans. Genome Res *23*, 1749-1762.

Timbers, T.A., Garland, S.J., Mohan, S., Flibotte, S., Edgley, M., Muncaster, Q., Au, V., Li-Leger, E., Rosell, F.I., Cai, J., *et al.* (2016). Accelerating Gene Discovery by Phenotyping Whole-Genome Sequenced Multi-mutation Strains and Using the Sequence Kernel Association Test (SKAT). PLoS Genet *12*, e1006235.

Toba, G., and White, K. (2008). The third RNA recognition motif of Drosophila ELAV protein has a role in multimerization. Nucleic Acids Res *36*, 1390-1399.

Toker, A.S., Teng, Y., Ferreira, H.B., Emmons, S.W., and Chalfie, M. (2003). The Caenorhabditis elegans spalt-like gene sem-4 restricts touch cell fate by repressing the selector Hox gene egl-5 and the effector gene mec-3. Development *130*, 3831-3840.

Topalidou, I., and Chalfie, M. (2011). Shared gene expression in distinct neurons expressing common selector genes. Proceedings of the National Academy of Sciences *108*, 19258.

Topalidou, I., Keller, C., Kalebic, N., Nguyen, Ken C.Q., Somhegyi, H., Politi, Kristin A., Heppenstall, P., Hall, David H., and Chalfie, M. (2012). Genetically Separable Functions of the MEC-17 Tubulin Acetyltransferase Affect Microtubule Organization. Current Biology *22*, 1057-1065.

Treinin, M., and Chalfie, M. (1995). A mutated acetylcholine receptor subunit causes neuronal degeneration in C. elegans. Neuron *14*, 871-877.

Trent, C., Tsuing, N., and Horvitz, H.R. (1983). Egg-laying defective mutants of the nematode Caenorhabditis elegans. Genetics *104*, 619-647.

Vasquez, V., Krieg, M., Lockhead, D., and Goodman, M.B. (2014). Phospholipids that contain polyunsaturated fatty acids enhance neuronal cell mechanics and touch sensation. Cell Rep *6*, 70-80.

Venken, K.J., and Bellen, H.J. (2014). Chemical mutagens, transposons, and transgenes to interrogate gene function in Drosophila melanogaster. Methods *68*, 15-28.

Villanueva, A., Lozano, J., Morales, A., Lin, X., Deng, X., Hengartner, M.O., and Kolesnick, R.N. (2001). jkk-1 and mek-1 regulate body movement coordination and response to heavy metals through jnk-1 in Caenorhabditis elegans. Embo j *20*, 5114-5128.

Vogel, B.E., and Hedgecock, E.M. (2001). Hemicentin, a conserved extracellular member of the immunoglobulin superfamily, organizes epithelial and other cell attachments into oriented line-shaped junctions. Development *128*, 883.

Walter, L., Baruah, A., Chang, H.W., Pace, H.M., and Lee, S.S. (2011). The homeobox protein CEH-23 mediates prolonged longevity in response to impaired mitochondrial electron transport chain in C. elegans. PLoS Biol *9*, e1001084.

Wang, X., Liu, J., Zhu, Z., and Ou, G. (2015). The heparan sulfate-modifying enzyme glucuronyl C5-epimerase HSE-5 controls Caenorhabditis elegans Q neuroblast polarization during migration. Developmental Biology *399*, 306-314.

Wang, Z., and Sherwood, D.R. (2011). Chapter 5 - Dissection of Genetic Pathways in C. elegans. In Methods in Cell Biology, J.H. Rothman, and A. Singson, eds. (Academic Press), pp. 113-157.

Watson, J.D., Wang, S., Von Stetina, S.E., Spencer, W.C., Levy, S., Dexheimer, P.J., Kurn, N., Heath, J.D., and Miller, D.M., 3rd (2008). Complementary RNA amplification methods enhance microarray identification of transcripts expressed in the C. elegans nervous system. BMC Genomics *9*, 84.

Way, J.C., and Chalfie, M. (1988). mec-3, a homeobox-containing gene that specifies differentiation of the touch receptor neurons in C. elegans. Cell *54*, 5-16.

Way, J.C., and Chalfie, M. (1989). The mec-3 gene of Caenorhabditis elegans requires its own product for maintained expression and is expressed in three neuronal cell types. Genes Dev *3*, 1823-1833.

White, J.G., Southgate, E., Thomson, J.N., and Brenner, S. (1986). The structure of the nervous system of the nematode Caenorhabditis elegans. Philos Trans R Soc Lond B Biol Sci *314*, 1-340.

Wieschaus, E., and Nüsslein-Volhard, C. (2016). The Heidelberg Screen for Pattern Mutants of Drosophila: A Personal Account. Annual Review of Cell and Developmental Biology *32*, 1-46.

Wieschaus, E., Nusslein-Volhard, C., and Jurgens, G. (1984). Mutations affecting the pattern of the larval cuticle inDrosophila melanogaster : III. Zygotic loci on the X-chromosome and fourth chromosome. Wilehm Roux Arch Dev Biol *193*, 296-307.

Wood, W.B., Hecht, R., Carr, S., Vanderslice, R., Wolf, N., and Hirsh, D. (1980). Parental effects and phenotypic characterization of mutations that affect early development in Caenorhabditis elegans. Dev Biol *74*, 446-469.

Wouters, M.A., Rigoutsos, I., Chu, C.K., Feng, L.L., Sparrow, D.B., and Dunwoodie, S.L. (2005). Evolution of distinct EGF domains with specific functions. Protein Sci *14*, 1091-1103.

Wu, J., Duggan, A., and Chalfie, M. (2001). Inhibition of touch cell fate by egl-44 and egl-46 in C. elegans. Genes Dev *15*, 789-802.

Wu, J., Yan, Z., Li, Z., Qian, X., Lu, S., Dong, M., Zhou, Q., and Yan, N. (2016). Structure of the voltage-gated calcium channel Ca(v)1.1 at 3.6 A resolution. Nature *537*, 191-196.

Wu, M.C., Lee, S., Cai, T., Li, Y., Boehnke, M., and Lin, X. (2011). Rare-variant association testing for sequencing data with the sequence kernel association test. Am J Hum Genet *89*, 82-93.

Xiong, Z.G., Zhu, X.M., Chu, X.P., Minami, M., Hey, J., Wei, W.L., MacDonald, J.F., Wemmie, J.A., Price, M.P., Welsh, M.J., *et al.* (2004). Neuroprotection in ischemia: blocking calcium-permeable acid-sensing ion channels. Cell *118*, 687-698.

Xu, K., Tavernarakis, N., and Driscoll, M. (2001). Necrotic Cell Death in C. elegans Requires the Function of Calreticulin and Regulators of Ca2+ Release from the Endoplasmic Reticulum. Neuron *31*, 957-971.

Xue, D., Finney, M., Ruvkun, G., and Chalfie, M. (1992). Regulation of the mec-3 gene by the C.elegans homeoproteins UNC-86 and MEC-3. Embo j *11*, 4969-4979.

Xue, D., Tu, Y., and Chalfie, M. (1993). Cooperative interactions between the Caenorhabditis elegans homeoproteins UNC-86 and MEC-3. Science *261*, 1324-1328.

Yan, C., Wang, F., Peng, Y., Williams, C.R., Jenkins, B., Wildonger, J., Kim, H.-J., Perr, J.B., Vaughan, J.C., Kern, M.E., *et al.* (2018). Microtubule Acetylation Is Required for Mechanosensation in Drosophila. Cell Reports *25*, 1051-1065.e1056.

Yang, W., Guo, X., Thein, S., Xu, F., Sugii, S., Baas, Peter W., Radda, George K., and Han, W. (2013). Regulation of adipogenesis by cytoskeleton remodelling is facilitated by acetyltransferase MEC-17-dependent acetylation of α-tubulin. Biochemical Journal *449*, 605-612.

Yemini, E., Jucikas, T., Grundy, L.J., Brown, A.E., and Schafer, W.R. (2013). A database of Caenorhabditis elegans behavioral phenotypes. Nat Methods *10*, 877-879.

Yermolaieva, O., Leonard, A.S., Schnizler, M.K., Abboud, F.M., and Welsh, M.J. (2004). Extracellular acidosis increases neuronal cell calcium by activating acid-sensing ion channel 1a. Proceedings of the National Academy of Sciences of the United States of America *101*, 6752.

Zhang, S., Arnadottir, J., Keller, C., Caldwell, G.A., Yao, C.A., and Chalfie, M. (2004). MEC-2 Is Recruited to the Putative Mechanosensory Complex in C. elegans Touch Receptor Neurons through Its Stomatin-like Domain. Current Biology *14*, 1888-1896.

Zhang, W., Bianchi, L., Lee, W.H., Wang, Y., Israel, S., and Driscoll, M. (2008). Intersubunit interactions between mutant DEG/ENaCs induce synthetic neurotoxicity. Cell Death & Differentiation *15*, 1794-1803.

Zhang, Y., Ma, C., Delohery, T., Nasipak, B., Foat, B.C., Bounoutas, A., Bussemaker, H.J., Kim, S.K., and Chalfie, M. (2002). Identification of genes expressed in C. elegans touch receptor neurons. Nature *418*, 331-335.

Zhao, D., Chen, S., Horie, T., Gao, Y., Bao, H., and Liu, X. (2020). Comparison of differentiation gene batteries for migratory mechanosensory neurons across bilaterians. Evol Dev.

Zhen, M., Huang, X., Bamber, B., and Jin, Y. (2000). Regulation of presynaptic terminal organization by C. elegans RPM-1, a putative guanine nucleotide exchanger with a RING-H2 finger domain. Neuron *26*, 331-343.

Zheng, C., Atlas, E., Lee, H.M.T., Jao, S.L.J., Sayegh, N.Y., Nguyen, K.C.Q., Hall, D.H., and Chalfie, M. (2020). F-box protein MEC-15 promotes microtubule stability and neurite growth by antagonizing the activity of the HSP90 chaperone network in Caenorhabditis elegans T.U.o.H. Kong, C. University, and A.E.C.o. Medicine, eds.

Zheng, C., Diaz-Cuadros, M., Nguyen, K.C.Q., Hall, D.H., and Chalfie, M. (2017). Distinct effects of tubulin isotype mutations on neurite growth in Caenorhabditis elegans. Mol Biol Cell *28*, 2786-2801.

Zheng, C., Jin, F.Q., and Chalfie, M. (2015). Hox Proteins Act as Transcriptional Guarantors to Ensure Terminal Differentiation. Cell Reports *13*, 1343-1352.

Zheng, C., Jin, F.Q., Trippe, B.L., Wu, J., and Chalfie, M. (2018). Inhibition of cell fate repressors secures the differentiation of the touch receptor neurons of Caenorhabditis elegans. Development *145*.

Appendix I: List of Additional *C. elegans* Strains Used

Strain Name	Genotype
BP75	eff-1 (hy21)
CA388	pch-2 (tm1458)
CB1108	unc-54 (e1108)
CB1253	che-3 (e1253)
CB130	dpy-8 (e130)
CB1336	mec-1 (e1336)
CB1338	mec-3 (e1338)
CB14	dpy-6 (e14)
CB1416	unc-86 (e1416)
CB1421	unc-52 (e1421)
CB1472	mec-6 (e1342)
CB1605	mec-12 (e1605)
CB251	unc-36 (e251)
CB3270	mec-7 (e1506) lon-2 (e678)
CB3273	mec-2 (e1084) lon-2 (e678)
CB3274	mec-4 (e1497) lon-2 (e678)
CB3275	lon-2 (e678) mec-5 (e1504)
CB398	mec-8 (e398)
CB419	unc-42 (e419)
CB47	unc-11 (e47)
CB66	unc-22 (e66)
CB698	vab-10 (e698)
CB928	unc-31 (e923)
CZ2485	ahr-1 (ju145)
CZ401	vab-19 (e1036)
DR1942	daf-2 (e979)
EM305	efn-4 (bx80); him-5 (e1490)
ET137	C30G12.1 (ok910)
FX19163	mca-3 (tm6395)/tmIn11
GL302	cid-1 (rf34)
HA1857	osm-7 (tm2256)
JC55	flr-1 (ut11)
JT9609	pdk-1 (sa680)
KG2730	clu-1 (ok2)
KP4	glr-1 (n2461)
KR1319	dpy-5 (e61) nars-1 (h680) unc-13 (e450); sDp2
KR1374	dpy-5(e61) let-502(h733) unc-13(e450) ; sDp2

LX999	kcc-2 (vs132)
MT10661	tdc-1 (n3420)
MT4818	unc-70 (n493)
MT6308	eat-4 (ky5)
OT136	mua-3 (rh195)
PK172	ptc-1 (ok122) unc-4 (e120)/mnC1 [dpy-10 (e128) unc-52 (e444)]
RB1138	F08G2.7 (ok1161)
RB1333	hrp-2 (ok1278)
RB1480	nra-2 (ok2871)
RB1500	ulp-1 (ok1768)
RB1534	npp-16 (ok1839)
RB1728	tra-3 (ok2207)
RB1748	eat-4 & ZK512.7 (ok2233)
RB1814	R151.1 & R151.4 (ok2347)
RB1869	atat-2 (ok2415)
RB1925	mec-19 (ok2504)
RB2119	acr-23 (ok2804)
RB630	rpm-1 (ok364)
RB751	eps-8 (ok539)
RB759	akt-1 (ok525)
RB762	alr-1 (ok545)
RB785	dop-5 (ok568)
RB793	pbo-4 (ok583)
RB804	T07F10.1 (ok608)
RW3538	myo-3 (st386)/sqt-3 (e24)
RW3600	pat-3 (st564)/qC1 [dpy-19 (e1259) glp-1 (q339)]
RW3609	unc-112 (st581)/unc-39 (e257)
RW3625	let-805 (st456)/qC1 [dpy-19 (e1259) glp-1 (q339)]
SP1205	dyf-1 (mn335)
TJ1052	age-1 (hx546)
TU1108	unc-2 (e55) lon-2 (e678)
TU1109	mec-18 (u452) lon-2 (e678)
TU1366	deg-1 (u506)
TU2362	vab-15 (u781)
TU265	mec-17 (u265)
TU5776	mec-5 (e1340); dpy-5 (e61)
TU6467	mec-9 (u42) ; uIs88
TU6605	u1183; uIs115 [Pmec-17::RFP]
TU6718	WT
TU6765	u1183; uIs115 [Pmec-17::RFP]
TU6770	umnIs13 [myo-2p::GFP + NeoR]
TU6771	otIs619 [unc-11(prom8)::2xNLS::TagRFP]

TU6772	umnIs7 [myo-2p::GFP + NeoR]
TU6774	mec-10 (ok1104); dpy-5 (e61)
TU6778	umnIs44 [myo-2p::mKate2 + NeoR]
TU75	mec-15 (u75)
TU82	mec-14 (u82)
VC146	cln-3.3 (gk118)
VC1720	rpn-1 (ok2259) /nT1 [qIs51]
VC1785	F08A8.1 (ok2257)
VC1990	mup-4 (ok2321)/mT1 [dpy-10 (e128)] ; +/mT1
VC1992	egas-2 & Y69H2.3 (ok2651)
VC2122	glr-23 (ok2849)
VC2203	taf-9 (ok2871)
VC2226	cgt-3 (ok2877)/mIn1 [mIs14 dpy-10 (e128)]
VC26	pgp-12 (gk19)
VC2787	knl-1 (ok3457)/mT1 [dpy-10 (e128)] ; +/mT1
VC437	nhr-233 (gk223)
VC641	parg-2 (ok980)
VC724	mog-5 (ok1101)/mIn1 [mIs14 dpy-10 (e128)]
VC955	mps-1 (ok1376)
WH170	eff-1 (oj55)
ZB1029	crt-1 (bz30)
ZZ1	lev-11 (x1)

Some strains were provided by the CGC, which is funded by NIH Office of Research Infrastructure Programs (P40 OD010440).

Appendix II: *twk-10* Encodes a Potassium Channel That Inhibits Gentle Touch Sensitivity

(The following describes an additional discovery I made in the course of my graduate work)

Introduction

Two-pore K+ (TWK) channels are non-gated potassium channels thought to be involved in setting the resting membrane potential of neurons. In *C. elegans* there are over 40 *twk* genes, most of which are expressed in a relatively small subset of neurons. It is hypothesized that the different TWK channel variants serve to "fine tune" the excitability of different sets of neurons (Salkoff et al., 2001), but there is little experimental evidence regarding the function of all but a few *twk* genes. A major barrier to the study of *twk* gene function is the apparent lack of obvious phenotypes produced by isolated loss-of-function (LOF) *twk* mutations. Most of the *twk* mutations identified through forward screens have been determined to cause gain-of-function (GOF) phenotypes which likely increase channel activity (Kunkel et al., 2000; de la Cruz et al., 2003). The lack of obvious null *twk* phenotypes may be due to a large degree of redundant activity between channel types, and/or because individual channel types only have subtle effects. There is still much to discover about *C. elegans twk* genes, so upon finding that three *twk* genes (*twk-10*, *twk-28*, and *twk-43*) may be overexpressed in the *C. elegans* gentle touch receptor neurons (TRNs) as evidenced by microarray analysis of mRNA from cultured neurons, we took advantage of the opportunity to find if these genes played a functional role in our system of study (Zhang et al., 2002; Topalidou and Chalfie, 2011).

Results

To confirm the TRN expression of *twk-10*, *twk-28*, and *twk-43* in vivo, we used CRISPR/Cas-9 to engineer transcriptional reporters and N- and C-terminal tagged proteins from the native genetic loci. Fluorescent signal from the *twk-10* N-terminal transcriptional reporter and tagged protein was observed in the six TRNs (Figure 1). For *twk-28*, fluorescent signals from the N-terminal transcriptional reporter and tagged protein suggest that *twk-28* is primarily expressed in the body wall muscle and not in the TRNs (Figure 2). For *twk-43*, we observed expression of the C-terminal tagged protein in an unidentified head neuron but not in the TRNs (Figure 3).

To further investigate the functional role of *twk-10* in the TRNs, we assayed the anterior touch response of *twk-10* presumed LOF and GOF mutants. To check for temperature-dependent phenotypic effects, we performed the assays on animals raised at 15, 20, and 25°C (Figure 4). The LOF *twk-10* mutants appeared to be slightly more responsive than wild-type (WT) animals. Our results indicated a statistically significant difference between the anterior touch sensitivity of *twk-10* LOF mutants and WT animals at 15°C, but not at 20 and 25°C. However, because the *twk-10* LOF and WT response rates did not appear to be strongly affected by temperature, the statistical significance of comparisons at different temperatures may have arisen from sampling error. *twk-10* GOF mutants were significantly less sensitive than WT animals at all three temperatures, but appeared to be most sensitive when cultivated at 20°C and least sensitive when cultivated at 25°C. These differences indicate temperature-dependent effects on the GOF mutant protein and hint that the WT protein might also be temperature-sensitive.

As an alternative approach to determining the effects of *twk-10* on gentle touch sensitivity, we considered the phenotypic effects of the *twk-10* LOF mutation in a sensitized

mec-4 background. MEC-4 is an essential component of the TRN mechanoreceptor channel. We previously identified a temperature sensitive (ts) *mec-4* allele with near normal activity at 20°C but significantly inhibited activity at 25°C (Gu et al., 1996). We hypothesized that the *twk-10* LOF mutation might lead to a more significant increase in touch sensitivity in the *mec-4* ts background as compared to in the WT background. Indeed, this proved to be the case (Figure 5).

Our results suggest that *twk-10* functions in the TRNs to inhibit touch sensitivity. We showed that *twk-10* is expressed in the TRNs and that the loss of *twk-10* causes increased touch sensitivity. Furthermore, we showed that a *twk-10* mutation which likely causes increased channel activity results in significantly decreased touch sensitivity.

Figures

A

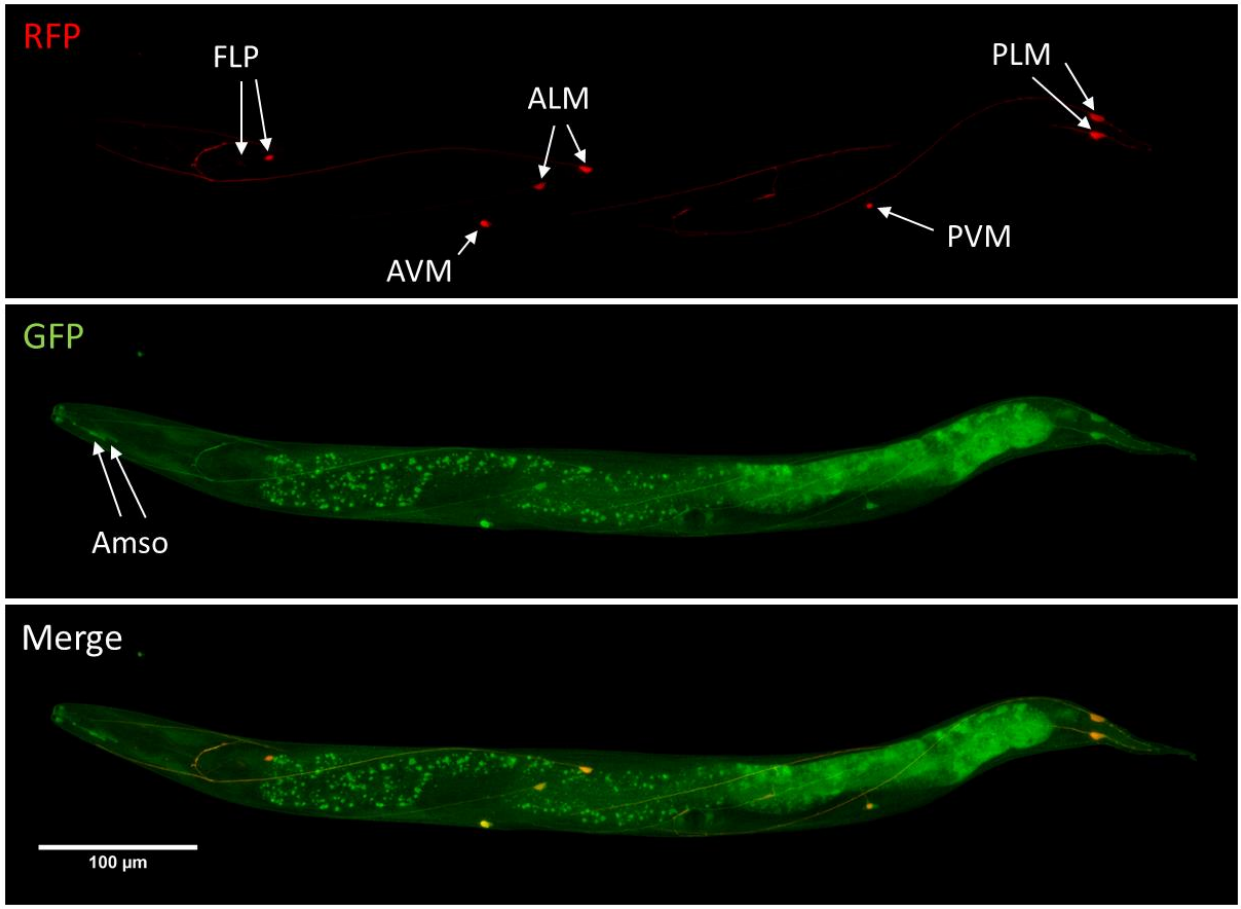

B

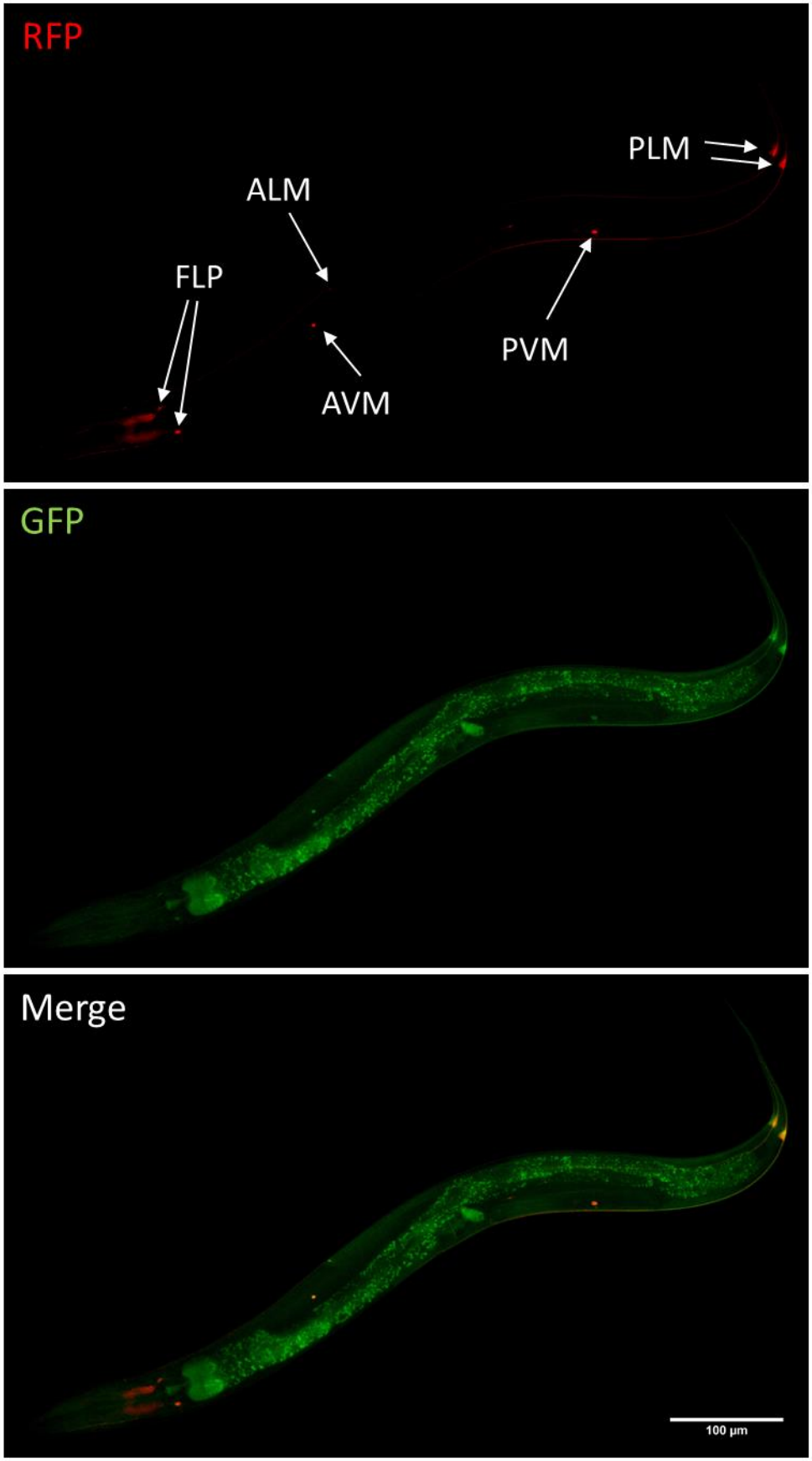

Figure 1: *twk-10* transcriptional and protein fusion reporters. Confocal images of fluorescence from a TRN and FLP marker (Pmec-3::RFP, A and B RFP) and a *twk-10* transcriptional reporter (mNeonGreen::SEC::twk-10, A GFP) or N-terminal tagged TWK-10 (mNeonGreen::twk-10, B GFP). Both reporters indicate *twk-10* expression in the six TRNs. Images were created from stitching maximum-intensity Z-projections from Z-slices acquired with a 40x objective lens. Scale bars show a length of 100 μM. In the A and B RFP frames, the TRNs (ALMs, AVM, PLMs, and PVM) and FLPs are indicated by white arrows. In the A GFP frame, fluorescent signal from amphid sheath cells is indicated with white arrows.

A

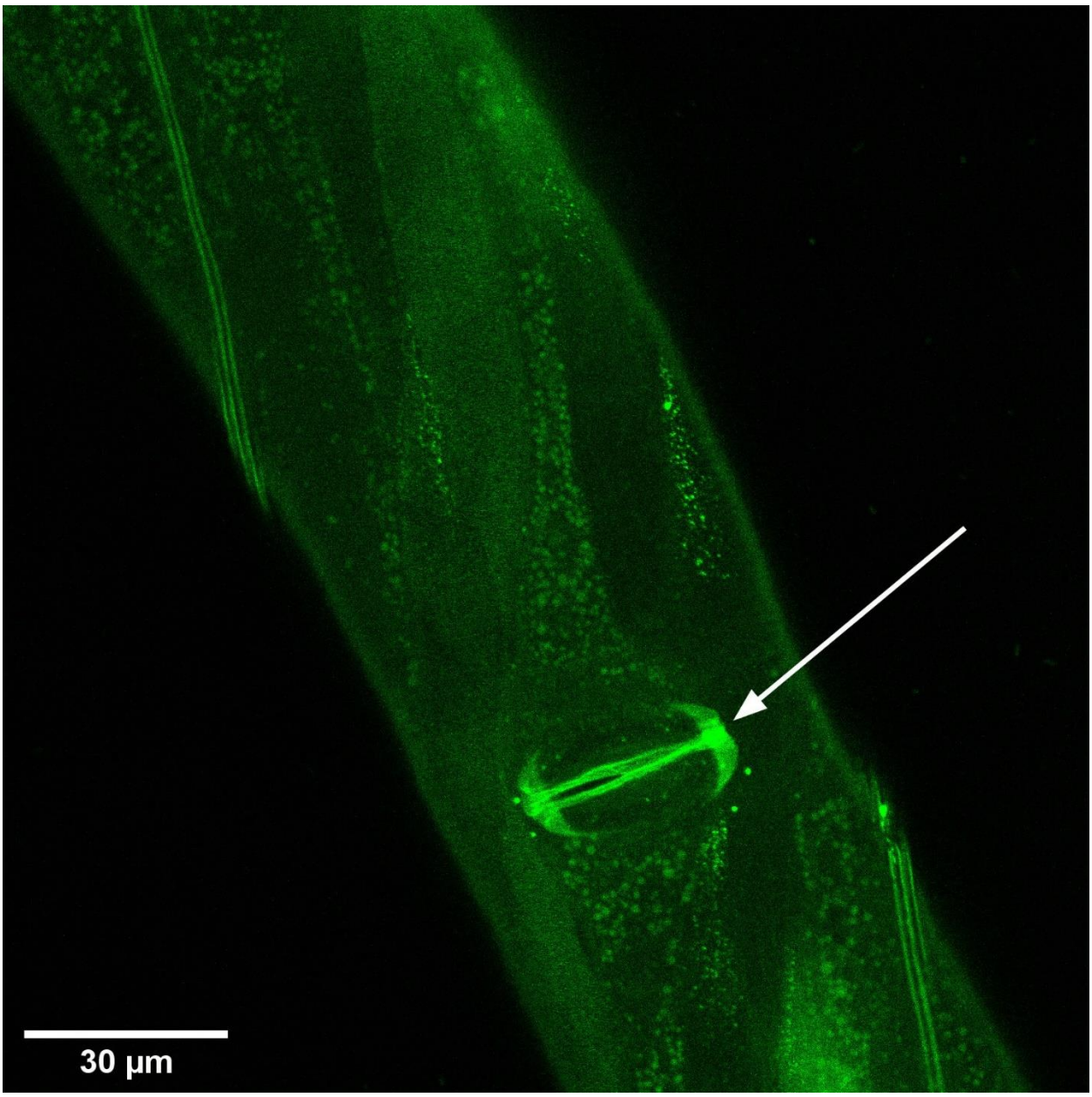

B

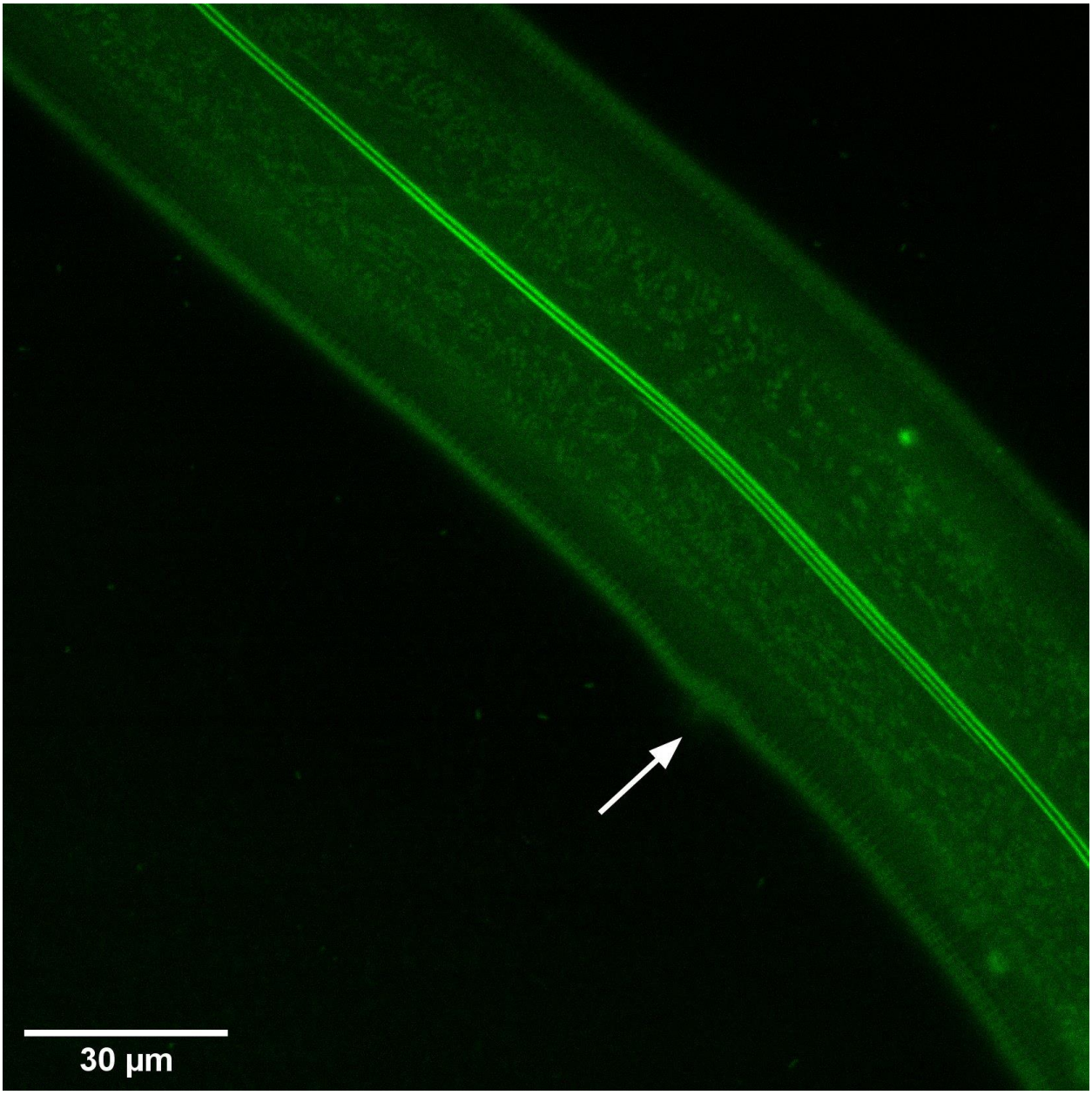

Figure 2: *twk-28* transcriptional and protein fusion reporters. A) shows a *twk-28* transcriptional reporter (mNeonGreen::SEC::twk-28) and B) shows N-terminal tagged TWK-28 (mNeonGreen::twk-28). Both reporters indicate *twk-28* expression in the body wall muscle. White arrows indicate the position of the vulva, and scale bars show a length of 30 µM. Images were acquired by confocal with a 40x objective lens.

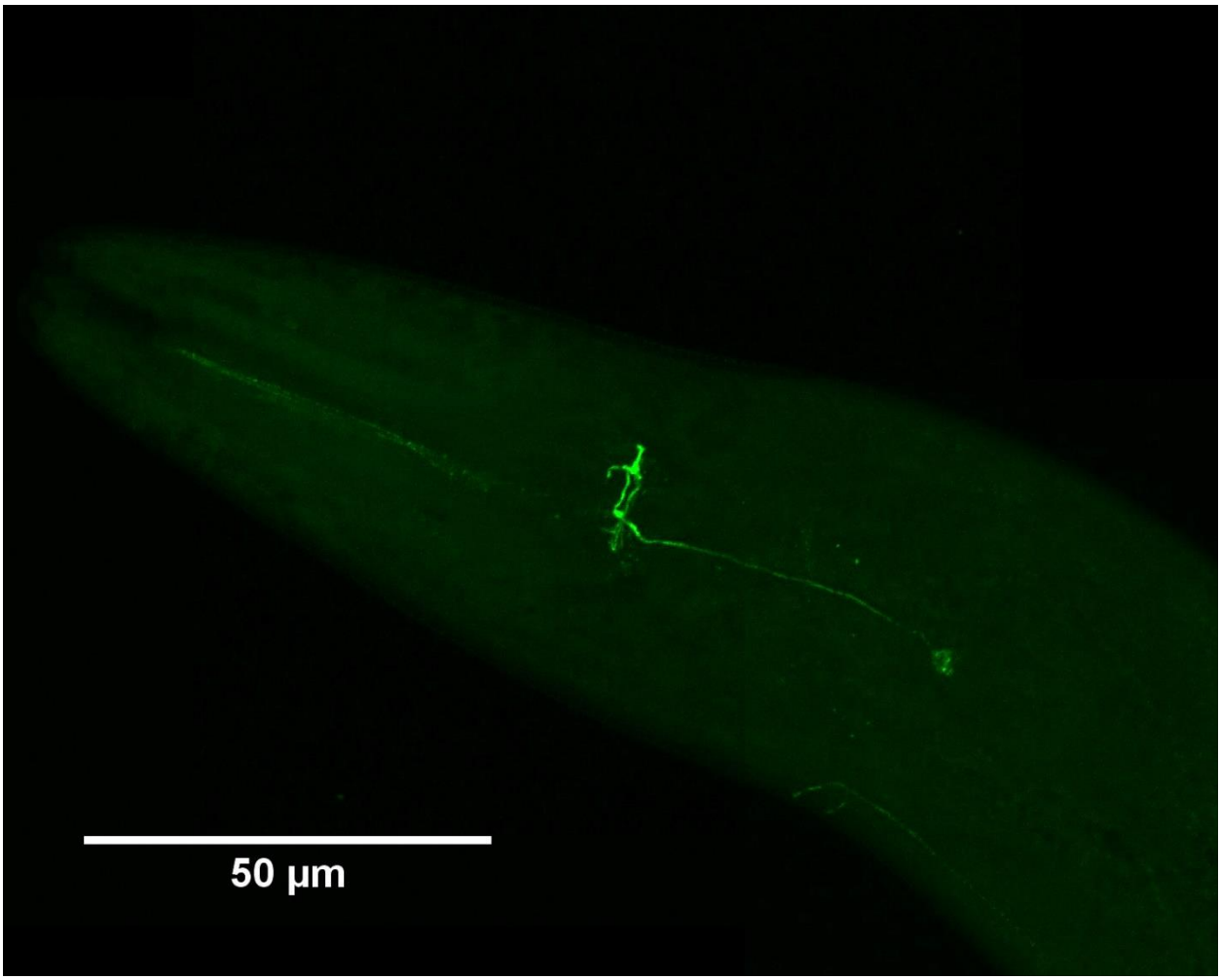

Figure 3: *twk-43* C-terminal protein fusion reporter. Fluorescence detected via confocal imaging from twk-43::mNeonGreen shows signal in an unidentified head neuron. Image was created from stitching maximum-intensity Z-projections from Z-slices acquired with a 40x objective lens.

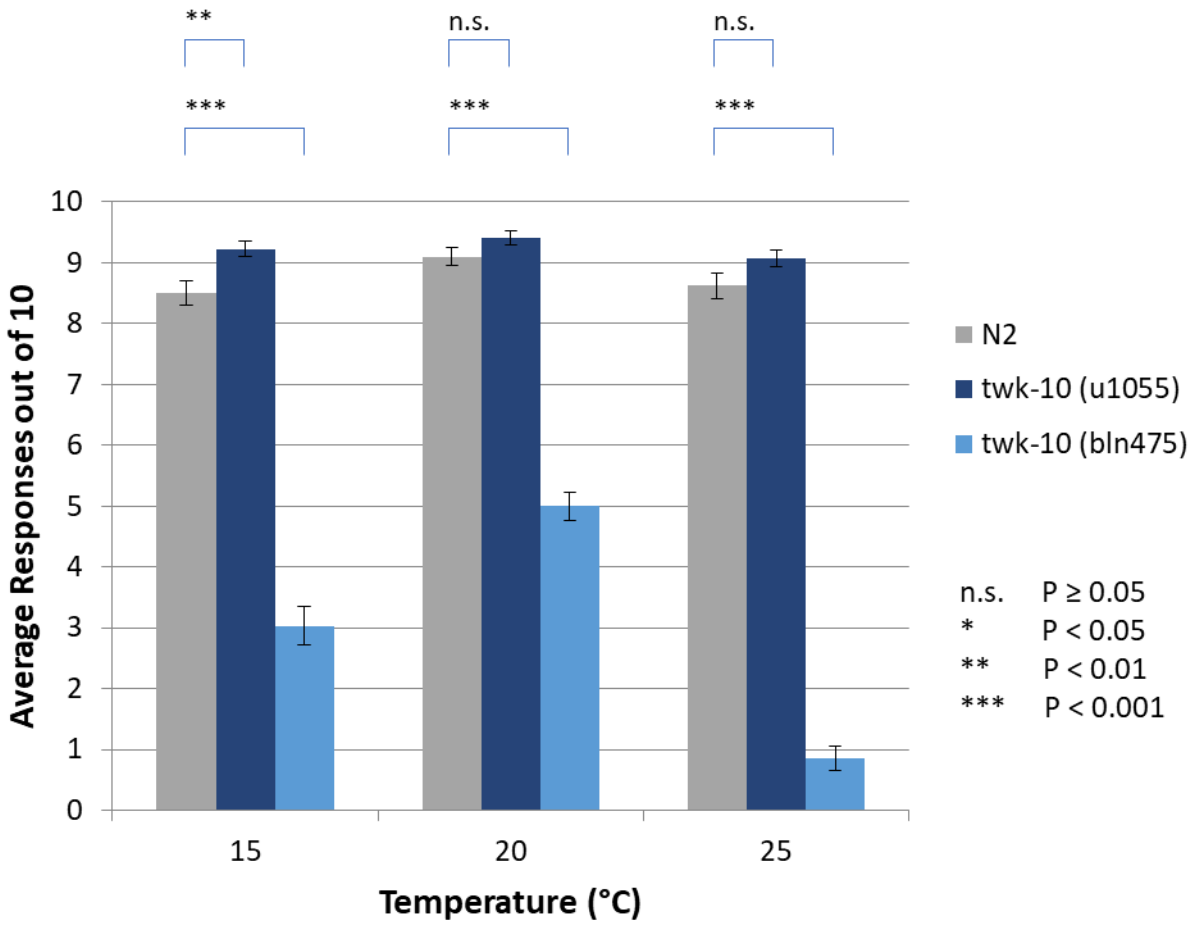

Figure 4: Anterior Touch Sensitivity in *twk-10* mutants. *twk-10* (*u1055*) is a putative LOF mutation, and *twk-10* (*bln475*) is a putative GOF mutation. *twk-10* LOF mutants appeared to be slightly but not necessarily significantly more anterior touch sensitive than WT animals across temperatures. *twk-10* GOF mutants were significantly less sensitive than WT animals across temperatures but appeared to be most sensitive at 20°C and least sensitive at 25°C. Error bars show standard error of the mean. P-values were calculated using a two-tailed t-test with unequal variance. Each bar represents two biological replicates with 20 animals each.

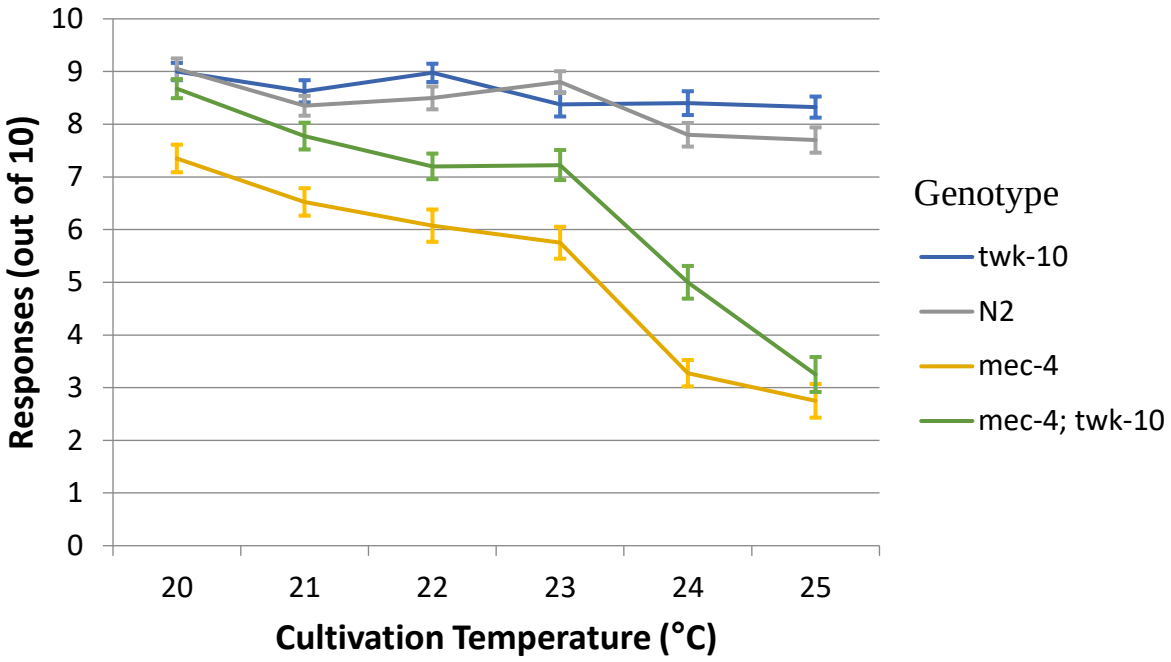

Figure 5: Gentle touch response of *twk-10* mutants in a sensitized background. Anterior and posterior responses were summed for each animal tested. Summed responses are plotted as to average responses per genotype and cultivation temperature. Each point represents four biological replicates of 10 animals each. Error bars show standard error of the mean. Genotypes indicate *twk-10* (*u1055*) and *mec-4* (*u45*) alleles.

Materials and Methods

C. elegans strains were maintained at 20°C (unless otherwise noted) as described by Brenner (1974). Fluorescent tagged proteins were engineered based on the process described by Dickinson et al. (2015). The *twk-10* presumed LOF mutant strain was obtained during the process of engineering the tagged protein and was derived from animals carrying injection markers and unstable transgenic arrays but lacking genomic insertions. The *twk-10* region was amplified by PCR and sequenced to identify a 7 bp frame-shift deletion within exon 5. The *twk-10* GOF mutant strain was a gift from the Boulin lab.

Confocal images were acquired using a Confocal ZEISS LSM700 and processed using ImageJ with use of the stitching plugin (Preibisch et al., 2009).

Anterior touch response alone was assessed by touching each animal ten times anteriorly, with at least a three second gap between stimuli with additional pause if necessary until the animal ceased backing, turning, or coiling behavior. Anterior and posterior touch response together was assessed by touching each animal five times anteriorly and five times posteriorly in alternation (Hobert et al., 1999). All touch response assays were performed blind to genotype.

C. elegans strains

Strain	Genotype
JIP1169	twk-10 (bln475)
TU45	mec-4 (u45)
TU5184	twk-28 (u1047) [mNeonGreen::SEC::twk-28]
TU5187	twk-28 (u1049) [mNeonGreen::twk-28]
TU5215	twk-10 (u1055)
TU5611	mec-4 (u45); twk-10 (u1055)
TU5619	twk-43 (u1066) [twk-43::mNeonGreen]
TU6012	twk-10 (u1051) [mNeonGreen::twk-10]; uIs152 [Pmec-3::RFP]
TU6846	twk-10 (u1078) [mNeonGreen::SEC::twk-10]; uIs152 [Pmec-3::RFP]

References

Brenner, S. (1974). The genetics of Caenorhabditis elegans. Genetics *77*, 71-94.

de la Cruz, I.P., Levin, J.Z., Cummins, C., Anderson, P., and Horvitz, H.R. (2003). sup-9, sup-10, and unc-93 may encode components of a two-pore K+ channel that coordinates muscle contraction in Caenorhabditis elegans. J Neurosci *23*, 9133-9145.

Dickinson, D.J., Pani, A.M., Heppert, J.K., Higgins, C.D., and Goldstein, B. (2015). Streamlined Genome Engineering with a Self-Excising Drug Selection Cassette. Genetics *200*, 1035-1049.

Gu, G., Caldwell, G.A., and Chalfie, M. (1996). Genetic interactions affecting touch sensitivity in Caenorhabditis elegans. Proc Natl Acad Sci U S A *93*, 6577-6582.

Hobert, O., Moerman, D.G., Clark, K.A., Beckerle, M.C., and Ruvkun, G. (1999). A conserved LIM protein that affects muscular adherens junction integrity and mechanosensory function in Caenorhabditis elegans. J Cell Biol *144*, 45-57.

Kunkel, M.T., Johnstone, D.B., Thomas, J.H., and Salkoff, L. (2000). Mutants of a Temperature-Sensitive Two-P Domain Potassium Channel. The Journal of Neuroscience *20*, 7517-7524.

Preibisch, S., Saalfeld, S., and Tomancak, P. (2009). Globally optimal stitching of tiled 3D microscopic image acquisitions. Bioinformatics (Oxford, England) *25*, 1463-1465.

Salkoff, L., Butler, A., Fawcett, G., Kunkel, M., McArdle, C., Paz-y-Mino, G., Nonet, M., Walton, N., Wang, Z.W., Yuan, A., *et al.* (2001). Evolution tunes the excitability of individual neurons. Neuroscience *103*, 853-859.

Topalidou, I., and Chalfie, M. (2011). Shared gene expression in distinct neurons expressing common selector genes. Proceedings of the National Academy of Sciences *108*, 19258.

Zhang, Y., Ma, C., Delohery, T., Nasipak, B., Foat, B.C., Bounoutas, A., Bussemaker, H.J., Kim, S.K., and Chalfie, M. (2002). Identification of genes expressed in C. elegans touch receptor neurons. Nature *418*, 331-335.